University of São Paulo
Luiz de Queiroz College of Agriculture

Identification, characterization, and evolutionary features of *Brevipalpus*-transmitted viruses causing citrus leprosis disease

Camila Chabi de Jesus

Thesis presented to obtain the degree of Doctor in Science.
Area: Agricultural Microbiology

Piracicaba
2021

Camila Chabi de Jesus
Biology

Identification, characterization, and evolutionary features of *Brevipalpus*-transmitted viruses causing citrus leprosis disease

versão revisada de acordo com a resolução CoPGr 6018 de 2011

Advisor: Dr. **JULIANA FREITAS-ASTÚA**
Co-advisor: Dr. **PEDRO LUIS RAMOS GONZÁLEZ**

Thesis presented to obtain the degree of Doctor in Science.
Area: Agricultural Microbiology

Piracicaba
2021

Dados Internacionais de Catalogação na Publicação
DIVISÃO DE BIBLIOTECA – DIBD/ESALQ/USP

Jesus, Camila Chabi de

Identification, characterization, and evolutionary features of *Brevipalpus*-transmitted viruses causing citrus leprosis disease / Camila Chabi de Jesus. - - versão revisada de acordo com a resolução CoPGr 6018 de 2011. - - Piracicaba, 2021.

193 p.

Tese (Doutorado) - - USP / Escola Superior de Agricultura “Luiz de Queiroz”.

1. *Cilevirus* 2. *Dichorhavirus* 3. CiLV-C 4. CiLV-N 5. CiCSV 6. CiBSV 7. Ácaros tenuipalpídeos I. Título

I dedicate my doctoral thesis to all professors and researchers who contributed to the generation of information and knowledge that allowed me to get here.

ACKNOWLEDGEMENTS

I thank the Lord, for my life and my health;

To my advisors, Drs. Juliana Freitas-Astúa and Pedro Luis Ramos-González, for the opportunity, guidance, support, teachings, trust, and all the contribution in this study;

To the citrus leprosis research group, especially to Prof. Elliot W. Kitajima, Drs. Gabriela D. Arena and Aline D. Tassi, MS. Thais E. Sinico, Matheus B. Postclam, Mariane C. Rodrigues and Isabela Leão, for their support and contributions to this work;

To Luiz de Queiroz College of Agriculture (ESALQ, Piracicaba, SP) and Graduate program in Agricultural Microbiology, for the opportunity to complete the course and for the academic growth absorbed in this Institution;

To Biological Institute (IB, SP), for the availability of infrastructure, resources, and scientific support, especially to Dr. Ricardo Harakava;

To Dr. Varsani's research group, especially Drs. Arvind Varsani and Rafaela Fontenele, for the opportunity and contribution to this work;

To the São Paulo Research Foundation (FAPESP), for the concession of the scholarship, for support and resources;

To the Fund for Citrus Protection (Fundecitrus), in particular to Dr. Renato B. Bassanezi, for his support and contribution in this work;

To Embrapa Cassava and Fruits, in particular to Dr. Alecio S. Moreira, for his support and contribution to this work;

To Dr. Eduardo Seiti Gomide Mizubuti, for the suggestions of research and collaborators for this work;

To the several other collaborators belonging to the institutions: Embrapa, CCSM, Unesp, UFPI, UFPR, and Epagri, for making available several samples used in this work;

To my friends, for their supporting friendship and for making my days more fun;

To my husband Diego Barbosa, for the support, love, encouragement, understanding, and friendship;

To my parents and brothers, for their love, support, and understanding;

To everyone, who in some way, contributed to the realization of this work.

SUMMARY

RESUMO

Identificação, caracterização e aspectos evolutivos dos vírus transmitidos por *Brevipalpus* que causam a leprose dos citros

A leprose dos citros (LC) é uma doença não sistêmica que afeta os pomares de citros principalmente na América Latina. Transmitida por ácaros *Brevipalpus*, a doença é causada por um grupo heterogêneo de vírus dos gêneros *Cilevirus* (família *Kitaviridae*) e *Dichorhavirus* (família *Rhabdoviridae*), conhecidos coletivamente como vírus transmitidos por *Brevipalpus* (VTBs). Descrita pela primeira vez na Flórida/EUA, no final do século 19, a LC foi detectada na década de 1930 no Brasil, Argentina e Paraguai e mais recentemente em diversos países latino-americanos. A LC prevalente é causada pelo cilevirus citrus leprosis virus C (CiLV-C) e em menor extensão por outros VTBs cuja diversidade molecular ainda não foi bem compreendida. O presente estudo teve como objetivo descrever detalhadamente a população de CiLV-C e caracterizar três novos dichorhavirus que causam a LC. Para as análises da população de CiLV-C, examinamos um conjunto de 425 amostras sintomáticas de citrus coletadas na América Latina no período de 1932-2019, incluindo oito amostras herborizadas conservadas por mais de 80 anos. Análises de diversidade e filogenia indicaram que a população do CiLV-C é subdividida em três linhagens, denominadas CRD, SJP e ASU, cujos membros apresentam sinais de processos de recombinação interclados. Membros do clado CRD foram identificados amplamente no subcontinente desde 1932, enquanto os do clado SJP foram restritos a pomares comerciais no cinturão citrícola de São Paulo-Minas Gerais, em amostras coletadas após 2015. A linhagem ASU é representada por apenas um isolado coletado em Assunção, Paraguai, em 1937, e a diversidade e distribuição dos atuais membros, se houver, ainda são desconhecidas. O ancestral comum mais recente das três linhagens provavelmente originou-se em contato com a vegetação nativa em um ecossistema selvagem da América do Sul, antes da introdução dos citros na América. As subpopulações atuais de CiLV-C são geneticamente bem diferenciadas, apresentam diversidade genética muito baixa, onde quase todos os haplótipos são únicos, e sob purificação. Três novas espécies de dichorhavirus foram identificadas em amostras de laranjeiras doce (*Citrus sinensis*) coletadas em pomares não comerciais ou em pequenos pomares de regiões distantes e climaticamente distintas do Brasil. Enquanto o citrus leprosis virus N (CiLV-N) e o citrus bright spot virus (CiBSV) foram detectados nas regiões Sul e Sudeste, o citrus chlorotic spot virus (CiCSV) foi encontrado na região Nordeste. Além de laranja doce, o CiCSV infecta naturalmente plantas das espécies *Taliparitiliaceum* e *Agave desmettiana*. O CiLV-N é transmitido por ácaros da espécie *Brevipalpus phoenicis* s.s., que também provavelmente é o vetor do CiBSV. Por sua vez, o CiCSV é transmitido por *B. yothersi*, a espécie mais abundante em pomares de citros no Brasil e o principal vetor do CiLV-C, enquanto *B.* aff. *yothersi*, provavelmente uma nova espécie, também é capaz de transmiti-lo. Além de revelar a estrutura e as forças evolutivas que impulsionam a população de CiLV-C, este trabalho revela novos VTBs causadores da LC. Ademais, expõe um fragmento do cenário desafiador para o desenvolvimento da citricultura frente ao risco de saturação em áreas cultiváveis pelos vírus prevalentes e a ameaça dos supostos emergentes.

Palavras-chave: *Cilevirus*, *Dichorhavirus*, CiLV-C, CiLV-N, CiCSV, CiBSV, Ácaros tenuipalpídeos

ABSTRACT

Identification, characterization, and evolutionary features of *Brevipalpus*-transmitted viruses causing citrus leprosis disease

Citrus leprosis (CL) is a non-systemic disease affecting citrus orchards mainly in Latin America. Vectored by mites of the genus *Brevipalpus*, the disease is caused by a heterogeneous group of viruses of the genera *Cilevirus* (family *Kitaviridae*) and *Dichorhavirus* (family *Rhabdoviridae*), which are collectively known as *Brevipalpus*-transmitted viruses (BTVs). Originally described in Florida, USA, at the end of the 19th century, CL was detected in the 1930s in Brazil, Argentina, and Paraguay and, more recently, in several countries in Latin America. Citrus leprosis is caused mainly by the cilevirus citrus leprosis virus C (CiLV-C) and, in less extension, by BTVs whose molecular diversity has been poorly understood. The current study aimed to deeply describe the CiLV-C population and to characterize three new dichorhaviruses causing CL. To address the CiLV-C variability, we examined a cohort of 425 symptomatic samples collected over Latin America in the period 1932-2019, including eight herborized samples conserved for more than 80 years. Diversity and phylogenetic evaluation indicated that the CiLV-C population is subdivided into three lineages, named CRD, SJP, and ASU, whose members show signs of inter-clade recombination processes. Members of the clade CRD were identified widespread in the subcontinent in samples collected as early as 1932, while those of the clade SJP were restricted to commercial orchards in the citrus belt of *São Paulo−Minas Gerais*, in samples collected after 2015. The lineage ASU is represented by a single isolate collected in Asunción, Paraguay, in 1937, and the diversity and distribution of current members, if any, are still unknown. The most recent common ancestor of viruses of the three lineages likely originated in contact with native vegetation in a wild ecosystem of South America before the citrus introduction in America. Current subpopulations of CiLV-C are genetically well-differentiated, show a very low genetic diversity where almost every haplotype is unique, and, as a whole, are under purifying selection. Three new species of dichorhaviruses were identified in samples of sweet oranges (*Citrus sinensis*) collected in non-commercial or small orchards of distant and climatically distinct regions in Brazil. While citrus leprosis virus N (CiLV-N) and citrus bright spot virus (CiBSV) were detected in the Southern and Southeastern regions, citrus chlorotic spot virus (CiCSV) was found in the Northeast of the country. Besides sweet oranges, CiCSV naturally infects plants of the species *Taliparitiliaceum*, and *Agave desmettiana*. CiLV-N is transmitted by mites of the species *Brevipalpus phoenicis* s.s., which also likely vector CiBSV. In contrast, CiCSV is transmitted by *B. yothersi*, the most abundant *Brevipalpus* spp. in citrus orchards in Brazil, and the primary vector of CiLV-C, whereas *B.* aff. *yothersi* mites, probably a new species, might also transmit it. In addition to disclosing the structure and the evolutionary forces driving the population of CiLV-C, this work reveals new CL-causing BTVs. Altogether, it exposes a fragment of the challenging scenario for the development of the citrus industry facing the latent risk of crop saturation by the prevalent viruses and the threat of the putative emergent ones.

Keywords: *Cilevirus*, *Dichorhavirus*, CiLV-C, CiLV-N, CiCSV, CiBSV, Tenuipalpid mites

1. INTRODUCTION

Agribusiness leads the international trade of Brazil and underpins its economic development. Brazilian citriculture accounts for more than 30% of the world's orange production and more than 80% of the sweet orange juice in the global market (Bassanezi et al., 2019; Passos et al., 2019). The citrus belt of Brazil, comprising the Central-northern area of the state of São Paulo and Triângulo Mineiro, in Minas Gerais, responds for 80% of the national citrus production (Andrade et al., 2018; Bassanezi et al., 2019). However, despite its global leadership, the Brazilian citriculture has not reached its full production potential yet, mainly constrained by pests and diseases (Bassanezi et al., 2019; Carvalho et al., 2019).

Among the citrus-affecting diseases, citrus leprosis disease (CL) is considered the main disorder of viral etiology that impact citrus production in Brazil (Freitas-Astúa et al., 2018). This disease causes local chlorotic and/or necrotic lesions in leaves and fruits, and can provoke branch dieback, premature drops of leaves and fruits, and sometimes the death of the plants (Ramos-González et al., 2018a).

Management of CL primarily includes the chemical control of the viral vectors, mites of the genus *Brevipalpus*, and less often the pruning of the affected branches (Bassanezi et al., 2019). When large areas of the canopy are infected, pruning becomes ineffective due to the complex and costly handling, and because of its burden to the tree development (Laranjeira et al., 2015; Andrade et al., 2018; Bassanezi et al., 2019). Control of mites in the citrus belt of Brazil has been estimated at more than US$ 54 million, which represents around 5% of the total cost of the orchard management (Bassanezi et al., 2019). Besides the costs, it is believed that the low availability of molecules with acaricidal activity and the high application intensity in citrus orchards of the commercially available chemicals has resulted in the selection of resistant mite populations which consequently make more difficult the control of CL (Maia and Oliveira, 2004; Andrade et al., 2018).

Citrus leprosis disease is caused by a heterogeneous group of ssRNA viruses (Dietzgen et al., 2018; Freitas-Astúa et al., 2018). These viruses belong to different taxonomic groups; nevertheless, they are all strictly transmitted by mites of the genus *Brevipalpus* and, therefore, are recognized as BTVs (*Brevipalpus*-transmitted viruses) (Kitajima et al., 2003; Bastianel et al., 2010; Freitas-Astúa et al., 2018). In addition to the vector, BTVs have segmented ssRNA genomes, induce localized symptoms, and, except for the BTV that infects orchids, they are mostly restricted to America (Kitajima et al., 2003; Arena et al., 2016; Dietzgen et al., 2018; Freitas-Astúa et al., 2018; Arena et al., 2020; Quito-Avila et al., 2020).

Phylogenetically, BTVs are classified into the genera *Cilevirus* [ss(+)RNA genome; family *Kitaviridae*] and *Dichorhavirus* [ss(-)RNA genome; family *Rhabdoviridae*] (Locali-Fabris et al., 2012; Dietzgen et al., 2014; Freitas-Astúa et al., 2018). Citrus leprosis virus C (CiLV-C) is the type member of the genus *Cilevirus* and the first kitavirus having its genome completely sequenced (Locali et al., 2003; Locali-Fabris et al., 2006). Besides CiLV-C, citrus leprosis virus C2 (CiLV-C2) and passion fruit green spot virus (tentative species) are members of the genus (Melzer et al., 2013; Ramos-González et al., 2020). Orchid fleck virus (OFV), the type member of the genus *Dichorhavirus*, and coffee ringspot virus (CoRSV) were the only dichorhaviruses characterized until 2015 (Kondo et al., 2006; Ramalho et al., 2014). In 2018, *Clerodendrum chlorotic spot dichorhavirus* was included in the genus (Ramos-González et al., 2018b) and, in this work, three new dichorhaviruses were identified and characterized: the *Citrus leprosis N dichorhavirus* and *Citrus chlorotic spot dichorhavirus* and the tentative citrus bright spot virus.

CiLV-C is the prevalent virus associated with CL in Latin America, although CiLV-C2 and OFV_cit have been also associated with CL in Colombia and Mexico, respectively (Roy et al., 2015). In Brazil, CL associated with dichorhaviruses have been reported since 1970s, however, the diversity of these viruses were unknown for over 40 years (Bastianel et al., 2010; Freitas-Astúa et al., 2018). Out of America, OFV causes CL-like symptoms in South Africa (Cook et al., 2019).

Brevipalpus yothersi is the primary vector of cileviruses, however, it has recently been shown that *B. papayensis* can vector the CiLV-C as well (Ramos-González et al., 2016; Nunes et al., 2018). Biological parameters of the transmission and electron microscopy suggest that *B. yothersi* transmits CiLV-C in a circulative manner (Kitajima et al., 2008; Rodrigues and Childers, 2013; Tassi et al., 2017); whereas non-conclusive molecular assays suggest the propagation of the virus in the vector cells (Roy et al., 2015). Dichorhaviruses are persistently transmitted by different mite species but it seems that viruses belonging to the same lineage are transmitted by the same mite species (Chabi-Jesus et al., 2018; Freitas-Astúa et al., 2018).

It has been suggested that BTVs likely originated from non-segmented RNA arthropod viruses in South America and have recently adapted to infect plants (Dietzgen et al., 2018; Freitas-Astúa et al., 2018; Arena et al., 2020; Ramos-González et al., 2020). This hypothesis is based on plant-virus interaction studies which propose that symptoms of BTV infection are the result of an incompatible interaction, South America is the BTV center of diversity because holds all known viruses of the group, and Brazil accounts for more than 90%, BTV and some arthropod viruses keep an almost similar virion morphology and particle size, and the genomic

synteny (Dietzgen et al., 2018; Quito-Avila et al., 2020). However, information about the diversity, phylogeny, and co-evolution of BTVs and their host plant species and vectors are still scarce (Freitas-Astúa et al., 2018). Evolutionary studies of dichorhaviruses have been limited to OFV and CoRSV and have indicated the existence of genomic reassortment and low genetic variability (Ramalho et al., 2015; Dietzgen et al., 2018). Within the genus *Cilevirus*, after the characterization of three species, it was demonstrated the existence of two clades inside the population of CiLV-C, and the high diversity structure of the 5 'region of their RNA2, which have been considered a recombination hotspot in CiLV-C (Ramos-González et al., 2016, 2020).

Considering South America as the center of origin and diversification of BTVs, this study aimed to identify, characterize, and estimate the diversity and phylogeny of viruses associated with citrus leprosis disease in that region. A particular objective was to obtain an in-depth study on the distribution, diversity, and phylodynamics of CiLV-C. To address this, different detection techniques [transmission electron microscopy (MET), RT-PCR, and dot blot], identification methods [Sanger and high throughput sequencing (HTS)], biological characterization (experimental transmission, identification of host and vector ranges), and bioinformatic analyses (diversity estimation, genetic differentiation, origin, and evolution) were carried out.

REFERENCES

Andrade, D. J., Lorençon, J. R., Siqueira, D. S., Novelli, V. M., and Bassanezi, R. B. (2018). Space–time variability of citrus leprosis as strategic planning for crop management. *Pest Manag. Sci.* 74, 1798–1803. doi:10.1002/ps.4877.

Arena, G. D., Ramos-González, P. L., Falk, B. W., Clare, L., Ramos-González, P. L., Freitas-astúa, J., et al. (2020). Plant immune system activation upon citrus leprosis virus C infection is mimicked by the ectopic expression of the P61 viral protein. *Front. Microbiol.* 11, 0–24. doi:10.3389/fpls.2020.01188.

Arena, G. D., Ramos-González, P. L., Nunes, M. A., Alves, M. R., Camargo, L. E. A., Kitajima, E. W., et al. (2016). Citrus leprosis virus C infection results in hypersensitive-like response, suppression of the JA/ET plant defense pathway and promotion of the colonization of its mite vector. *Front. Plant Sci.* 7, 1757. doi:10.3389/FPLS.2016.01757.

Bassanezi, R. B., Czermainski, A. B. C., Laranjeira, F. F., Moreira, A. S., Ribeiro, P. J., Krainski, E. T., et al. (2019). Spatial patterns of the Citrus leprosis virus and its associated mite vector in systems without intervention. *Plant Pathol.* doi:10.1111/ppa.12930.

Bastianel, M., Novelli, V. M., Kitajima, E. W., Kubo, K. S., Bassanezi, R. B., Machado, M. A., et al. (2010). Citrus Leprosis: Centennial of an unusual mite–virus pathosystem. *Plant Dis.* 94, 284–292. doi:10.1094/PDIS-94-3-0284.

Carvalho, S. A., Girardi, E. A., Filho, F. de A. A. M., Ferrarezi, R. S., and Filho, H. D. C. (2019). *Advances in citrus propagation in Brazil*. doi:10.1590/0100-29452019422.

Chabi-Jesus, C., Ramos-González, P. L., Guerra-Peraza, O., Kitajima, E. W., Harakava, R., Beserra Jr., J. E. A., et al. (2018). Identification and characterization of citrus chlorotic spot virus, a new dichorhavirus associated with citrus leprosis-like symptoms. *Plant Dis.* 102, 1588–1598. doi:10.1094/PDIS-09-17-1425-RE.

Cook, G., Kirkman, W., Clase, R., Steyn, C., Basson, E., Fourie, P. H., et al. (2019). Orchid fleck virus associated with the first case of Citrus Leprosis-N in South Africa. *Plant Pathol.* 155, 1373–1379.

Dietzgen, R. G., Kuhn, J. H., Clawson, A. N., Freitas-Astúa, J., Goodin, M. M., Kitajima, E. W., et al. (2014). Dichorhavirus: a proposed new genus for *Brevipalpus* mite-transmitted, nuclear, bacilliform, bipartite, negative-strand RNA plant viruses. *Arch. Virol.* 159, 607–19. doi:10.1007/s00705-013-1834-0.

Dietzgen, R. G. R. G., Freitas-Astúa, J., Chabi-Jesus, C., Ramos-González, P. L. P. L., Goodin, M. M. M. M., Kondo, H., et al. (2018). Dichorhaviruses in their host plants and mite vectors. *Adv. Virus Res.* 102, 119–148. doi:10.1016/bs.aivir.2018.06.001.

Freitas-Astúa, J., Ramos-González, P. L., Arena, G. D., Tassi, A. D., and Kitajima, E. W. (2018). *Brevipalpus*-transmitted viruses: parallelism beyond a common vector or convergent evolution of distantly related pathogens? *Curr. Opin. Virol.* 33, 66–73. doi:10.1016/j.coviro.2018.07.010.

Kitajima, E. W., Chagas, C. M., and Rodrigues, J. C. V (2003). *Brevipalpus*-transmitted plant virus and virus-like diseases: cytopathology and some recent cases. *Exp. Appl. Acarol.* 30, 135–60.

Kitajima, E. W., Kubo, K. S., Ferreira, P. de T. O., Alcântara, B. K. de, Boari, A. J., Gomes, R. T., et al. (2008). Chlorotic spots on Clerodendrum, a disease caused by a nuclear type of Brevipalpus (Acari:Tenuipalpidae) transmitted virus. *Sci. Agric.* 65, 36–49. doi:10.1590/S0103-90162008000100006.

Kondo, H., Maeda, T., Shirako, Y., and Tamada, T. (2006). Orchid fleck virus is a rhabdovirus with an unusual bipartite genome. *J. Gen. Virol.* 87, 2413–2421. doi:10.1099/vir.0.81811-0.

Laranjeira, F. F., Silva, S. X. de B., de Andrade, E. C., Almeida, D. de O., da Silva, T. S. M., Soares, A. C. F., et al. (2015). Infestation dynamics of *Brevipalpus phoenicis* (Geijskes) (Acari: Tenuipalpidae) in citrus orchards as affected by edaphic and climatic variables. *Exp. Appl. Acarol.* 66. doi:10.1007/s10493-015-9921-4.

Locali-Fabris, E. C., Freitas-Astúa, J., and Machado, M. A. (2012). "Genus *Cilevirus*. International Committee on Taxonomy of Viruses," in *Virus Taxonomy*, eds. A. King, M. Adams, E. Carstens, and E. Lefkowitz (London, United Kingdom: Elsevier/Avademic Press), 1139–1142.

Locali-Fabris, E. C., Freitas-Astúa, J., Souza, A. A., Takita, M. A., Astúa-Monge, G., Antonioli-Luizon, R., et al. (2006). Complete nucleotide sequence, genomic organization and phylogenetic analysis of citrus leprosis virus cytoplasmic type. *J. Gen. Virol.* 87, 2721–9. doi:10.1099/vir.0.82038-0.

Locali, E. C., Freitas-Astua, J., de Souza, A. A., Takita, M. A., Astua-Monge, G., Antonioli, R., et al. (2003). Development of a molecular tool for the diagnosis of leprosis, a major threat to citrus production in the Americas. *Plant Dis.* 87, 1317–1321. doi:10.1094/PDIS.2003.87.11.1317.

Maia, O. M. A., and Oliveira, C. A. L. (2004). Capacidade de colonização de *Brevipalpus phoenicis* (Geijskes) (Acari: Tenuipalpidae) em cercas-vivas, quebra-ventos e plantas invasoras. *Neotrop. Entomol.* 33, 625–629. doi:10.1590/s1519-566x2004000500013.

Melzer, M. J., Simbajon, N., Carillo, J., Borth, W. B., Freitas-Astúa, J., Kitajima, E. W., et al. (2013). A cilevirus infects ornamental hibiscus in Hawaii. *Arch. Virol.* doi:10.1007/s00705-013-1745-0.

Nunes, M. A., de Carvalho Mineiro, J. L., Rogerio, L. A., Ferreira, L. M., Tassi, A., Novelli, V. M., et al. (2018). First Report of *Brevipalpus papayensis* as vector of *Coffee ringspot virus* and *Citrus leprosis virus C*. *Plant Dis.* 102, 1046–1046. doi:10.1094/PDIS-07-17-1000-PDN.

Passos, O. S., Souza, J. S., Bastos, D. C., Girardi, E. A., Gurgel, F. de L., Garcia, M. V. B., et al. (2019). "Citrus Industry in Brazil with Emphasis on Tropical Areas," in *Citrus - Health Benefits and Production Technology* (IntechOpen). doi:10.5772/intechopen.80213.

Quito-Avila, D. F., Freitas-Astúa, J., and Melzer, M. J. (2020). Bluner-, Cile-, and Higreviruses (*Kitaviridae*). *Ref. Modul. Life Sci.*, 1–5. doi:10.1016/b978-0-12-809633-8.21248-x.

Ramalho, T. O., Figueira, A. R., Sotero, A. J., Wang, R., Geraldino Duarte, P. S., Farman, M., et al. (2014). Characterization of Coffee ringspot virus-Lavras: a model for an emerging threat to coffee production and quality. *Virology* 464–465, 385–96. doi:10.1016/j.virol.2014.07.031.

Ramos-González, P. L., Chabi-Jesus, C., Arena, G. D., Tassi, A. D., Kitajima, E. W., Freitas-Astúa, J., et al. (2018a). Citrus leprosis: a unique multietiologic disease. *Cítricos en las Américas* 1, 1–9.

Ramos-González, P. L., Chabi-Jesus, C., Guerra-Peraza, O., Breton, M. C., Arena, G. D. G. D. G. D., Nunes, M. A. M. A., et al. (2016). Phylogenetic and molecular variability studies reveal a new genetic clade of Citrus leprosis virus C. *Viruses* 8, 153. doi:10.3390/v8060153.

Ramos-González, P. L. P. L., Chabi-Jesus, C., Banguela-Castillo, A., Tassi, A. D. A. D., Rodrigues, M. C. M. da C., Kitajima, E. W. E. W., et al. (2018b). Unveiling the complete genome sequence of clerodendrum chlorotic spot virus, a putative dichorhavirus infecting ornamental plants. *Arch. Virol.* 163, 2519–2524. doi:10.1007/s00705-018-3857-z.

Ramos-González, P. L., Santos, G. F. dos, Chabi-Jesus, C., Harakava, R., Kitajima, E. W., and Freitas-Astúa, J. (2020). Passion fruit green spot virus genome harbors a new orphan ORF and highlights the flexibility of the 5′-end of the RNA2 segment across cileviruses. *Front. Microbiol.* 11, 206. doi:10.3389/fmicb.2020.00206.

Rodrigues, J. C. V., and Childers, C. C. (2013). *Brevipalpus* mites (Acari: Tenuipalpidae): vectors of invasive, non-systemic cytoplasmic and nuclear viruses in plants. *Exp. Appl. Acarol.* 59, 165–75. doi:10.1007/s10493-012-9632-z.

Roy, A., Hartung, J. S., Schneider, W. L., Shao, J., Leon M, G., Melzer, M. J., et al. (2015). Role bending: Complex relationships between viruses, hosts, and vectors related to citrus leprosis, an emerging disease. *Phytopathology* 105, 872–884. doi:10.1094/PHYTO-12-14-0375-FI.

Tassi, A. D., Garita-Salazar, L. C., Amorim, L., Novelli, V. M., Freitas-Astúa, J., Childers, C. C., et al. (2017). Virus-vector relationship in the Citrus leprosis pathosystem. *Exp. Appl. Acarol.* 71, 227–241. doi:10.1007/s10493-017-0123-0.

2 BIBLIOGRAPHIC REVIEW

2.1 Biology, diversity and taxonomy of *Brevipalpus* mites

Genus *Brevipalpus,* family *Tenuipalpidae* encompasses around 300 species distributed worldwide; from which less than 10 have been confirmed as vectors of plant viruses (Beard et al., 2013, 2015). *Brevipalpus* mites are polyphagous and have a wide host range, being capable of colonizing more than 928 species of plants, distributed in 513 genera and 139 families in subtropical and tropical regions (Navia et al., 2013; Rodrigues and Childers, 2013). This range includes cultivated plants (citrus, coffee, and passion fruit) and weeds (Childers et al., 2003a; Maia and Oliveira, 2004). *B. yothersi,* reported in more than 486 species of plants distributed worldwide, is the most studied species given its economic importance (Maia and Oliveira, 2004; Tassi et al., 2017; Nunes et al., 2020).

Brevipalpus mites have only two chromosomes and their adults are haploids (Helle and Bolland, 1972). The predominant presence of the symbiotic bacterium *Cardinium* sp. causes the feminization of eggs, resulting in thelytokous parthenogenesis (females generating females) (Weeks et al., 2001). Thus, in the wild, females correspond to more than 99% of the population, which in favorable conditions survive for more than 30 days and oviposit around 50 eggs throughout their live span (Haramoto, 1966; Teodoro and Reis, 2006).

Recognition of *Brevipalpus* species is difficult due to large intraspecies morphological variations (Navia et al., 2013; Dos Santos Alves et al., 2019). Recent studies have revealed inconsistencies between the conventional morphological descriptions used for the mite classification and the molecular-based phylogenetic characterization based on molecular markers of the mitochondrial DNA cytochrome oxidase I (COI) gene, and even further, they have discovered the presence of cryptic species (Beard et al., 2013, 2015; Navia et al., 2013; Tassi et al., 2017). Regarding this, some *Brevipalpus* species were reclassified (Beard et al., 2015), and, particularly, species of *Brevipalpus* vectors transmitting viruses are divided into three groups: (1) *B. phoenicis*, subdivided into seven morphological groups, including *B. phoenicis* sensu stricto, *B. yothersi*, and *B. papayensis* (Beard et al., 2013, 2015); (2) *B. californicus*, subdivided into morphological groups; and (3) *B. obovatus*, still without a defined identity for the extant morphological groups (Beard et al., 2013, 2015; Navia et al., 2013; Tassi, 2018).

B. yothersi is the predominant species in commercial citrus orchards in Brazil and some other American countries such as Colombia, Mexico, and Paraguay (Sánchez-Velázquez et al., 2015; Bassanezi et al., 2019). The control of these mites is mainly based on the use of acaricides (Andrade et al., 2018; Bassanezi et al., 2019). The very low diversity of active ingredients and

the frequent use of the extant acaricides may be one of the factors causing the inefficient control of these mites in crop fields, where it is believed that resistant *B. yothersi* populations already exist (Maia and Oliveira, 2004; Bassanezi et al., 2019). However, information on the dynamics of resistance, susceptibility, and cross-resistance, as well as the influence of the population diversity of *Brevipalpus* spp. over these factors, is still scarce.

Preliminary studies on *Brevipalpus* mites diversity in Mexico and Brazil revealed great genetic variability in the populations of *B. yothersi* (Sánchez-Velázquez et al., 2015; Salinas-Vargas et al., 2016), which suggest that the inter- and intra- diversity of circulating *Brevipalpus* spp. is unknown and raise many questions about how this diversity affects the transmission of phytopathogens in commercial orchards. In parallel, other studies demonstrate that the infection by CiLV-C increases *B. yothersi* oviposition and enhances its colonization (Arena et al., 2016). This beneficial interaction could be mediated by the rewiring of the plant hormonal pathways by the virus and/or the protection of eggs laid on structures created as a consequence of the CL lesions in leaves, fruits, and branches.

2.2 *Brevipalpus* mite-transmitted viruses

Brevipalpus mite-transmitted viruses (BTVs) are subdivided into the genera *Dichorhavirus,* family *Rhabdoviridae*, order *Mononegavirales,* and *Cilevirus*, family *Kitaviridae,* order *Martellivirales* (Koonin et al., 2020; Quito-Avila et al., 2020). Since the transmission by *Brevipalpus* mite of Hibiscus green spot virus 2, genus *Higrevirus*, family *Kitaviridae,* has not been confirmed yet, the virus is going to be unconsidered in this section (Melzer et al., 2013a).

BTVs replicate in different subcellular compartments in their host cells, accordingly, they are generically classified as BTV-C or BTV-N, when replicates in the cytoplasm or nucleus, respectively (Kitajima et al., 2003).

The genus *Cilevirus* includes BTV-C which has bisegmented ss(+)RNA genomes (Locali-Fabris et al., 2012; Freitas-Astúa et al., 2018). Virions are short bacilliform particles of 60-70 nm wide and 120-150 nm long, which in the infected cells are found isolated or grouped in the lumen of the endoplasmic reticulum, and their viroplasms occur as dense and vacuolated electron cytoplasmic inclusions of varying shapes and dimensions (Kitajima et al., 2003). RNA1 of cileviruses (~8Kb) harbors two ORFs (*RdRp* and *p29*), encoding the *RNA-dependent RNA polymerase* (*RdRp*) and the tentative coat protein (*p29*). RNA2 (~ 4.9 Kb) contains four ORFs (*p15, p61, mp,* and *p24*) as well as a ~ 1 kb intergenic region (IR) situated between the *p15* and *p61* cistrons (Figure 1) (Locali-Fabris et al., 2012; Ramos-González et al., 2016).

Generally, the IR contains small orphan ORFs in each species of cileviruses. The *mp* gene encodes the movement protein (MP), which belongs to the superfamily 30K (Melcher, 2000). Based on the lack of similarity of the sequences and structure of the proteins with all the others available in the public domain, the proteins P15, P61, and P24 of cileviruses have unknown functions (Freitas-Astúa et al., 2018; Quito-Avila et al., 2020), although both P61 and P15 are suggested as possible RNA silencing suppressors (Leastro et al., 2020). Sub-cellular localization assays have shown that these proteins associate with the endoplasmic reticulum (ER) (Leastro et al., 2018). The expression of P61 in *Nicotiana benthamiana* plants induces cell death and genes involved in both ER stress and defense responses, suggesting that this protein might trigger a hypersensitive-like response in infected plants due to an unmitigated ER stress (Arena et al., 2020).

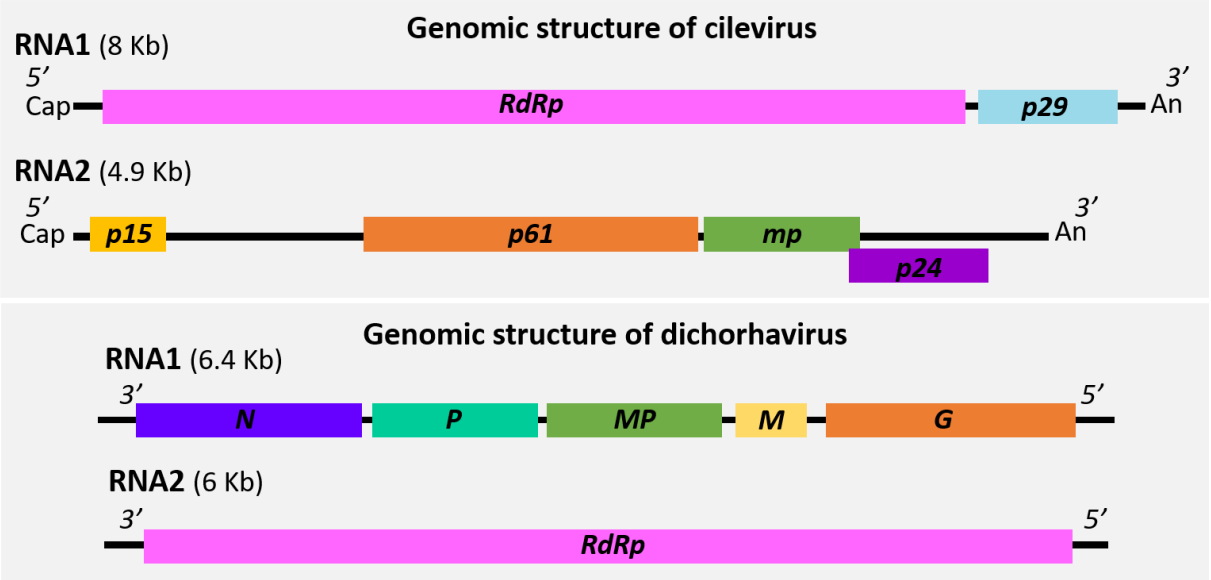

Figure 1. Genomic organization of cileviruses (family *Kitaviridae*) and dichorhaviruses (family *Rhabdoviridae*). Cileviruses have a bisegmented genome of ss(+)RNA, which encode six ORFs (indicated by rectangles): *RdRp*- RNA-dependent RNA polymerase; *p29*- tentative coat protein; *mp*- movement protein; *p15*, *p61* and *p24* with no known function yet. Dichorhaviruses have a bisegmented genome of ss(-)RNA, which also encode six ORFs: *N*-nucleocapsid; *MP*- movement protein; *M*- matrix; *G*- glycoprotein and *L*-RNA-dependent RNA polymerase.

Citrus leprosis virus C (CiLV-C), citrus leprosis virus C2 (CiLV-C2), and passion fruit green spot virus (PfGSV) are the best-characterized accepted or tentative members of the genus *Cilevirus* (Locali-Fabris et al., 2006; Melzer et al., 2013b; Roy et al., 2013b; Ramos-González et al., 2020). CiLV-C, the type member of the genus, occurs in most Latin American countries including Mexico; all Central American countries; Argentina, Bolivia, Brazil, Colombia, Paraguay, and Venezuela (Ramos-González et al., 2018a). CiLV-C2 has been detected in

hibiscus in Hawaii and Florida and in citrus in Colombia, while PfGSV has been reported only in Brazil (Ramos-González et al., 2018a, 2020).

The genus *Dichorhavirus* groups the BTV-N, which presents bisegmented ss(-)RNA genomes (Dietzgen et al., 2014, 2018b). Dichorhavirus particles accumulate in the nucleus and cytoplasm of the infected cells, where they can be found forming typical structures in form of spoke wheel (Dietzgen et al., 2018b). Virions are non-enveloped bacilliform particles with 40-50 nm in width and 100-110 nm in length, which represents about the half size of a "classic" non-segmented plant rhabdovirus suggesting that RNA1 and RNA2 are separately packaged (Kitajima et al., 1972; Kondo et al., 2006; Kitajima et al., 2011a; Dietzgen et al., 2014, 2018b). RNA1 of these viruses (~ 6.4 Kb) has five ORFs (*N*, *P*, *MP*, *M* and *G*) and its RNA2 (~ 6 Kb) has only one gene that codes for the RNA-dependent RNA polymerase (*RdRp*), also known as L protein (Figure 1) (Dietzgen et al., 2014).

Orchid fleck virus, OFV, the type member of genus *Dichorhavirus*, is the most studied dichorhavirus. It is distributed worldwide due to the presence of its mite vector and mainly as a consequence of the international trade of orchids (Kondo et al., 2017; Dietzgen et al., 2018b). The virus was reported for the first time in Japan infecting *Cymbidium* plants (Doi et al., 1969), and later in Australia, Brazil, Denmark, Germany, Korea and USA, in many plants of the family Orchidaceae (Blanchfield et al., 2001; Kitajima et al., 2001). Coffee ring spot virus (CoRSV), and the ornamental-infecting clerodendrum chlorotic spot virus (ClCSV) (Annex I) are present in several Brazilian states (Kitajima et al., 2008, 2010; Ramalho et al., 2014, 2015; Ramos-González et al., 2018b). CiLV-N0 is the only tentative dicorhavirus that was found only in a herborized sample, and possibly no longer exists in nature (Kondo et al., 2006; Ramalho et al., 2014; Hartung et al., 2015; Ramos-González et al., 2018b). Its partial sequences were obtained from herbarium conserved *Citrus sinensis* tissues, and revealed different to those of OFV, suggesting a putative new species (Hartung et al., 2015). In addition to these dichorhaviruses, in this work we characterize viruses from three new species, two of them were recently recognized as new species by the International Committee on Taxonomy of Viruses (ICTV) (chapter 2 and 3) and one tentative new species not yet submitted to the ICTV appreciation (chapter 4).

Dichorhaviruses are persistently transmitted by *Brevipalpus* of several species. OFV is transmitted by *B. californicus*, CoRSV by *B. papayensis* and *B. yothersi*, and ClCSV can be transmitted by *B. yothersi* (Kondo et al., 2003; Ramos-González et al., 2016; Nunes et al., 2018a; Ramos-González et al., 2018b). Cileviruses are transmitted by *B. yothersi*, although CiLV-C can also be transmitted less efficiently by *B. papayensis* (Roy et al., 2015; Ramos-

González et al., 2016, 2020; Nunes et al., 2018b). Cileviruses transmission by *B. yothersi* has not been fully characterized. Even though the replication of CiLV-C in the mite vector has been proposed (Roy et al., 2015), the absence of viroplasms and virions inside cells of viruliferous mites, among other features, suggest a circulative virus transmission (Tassi et al., 2017; Freitas-Astúa et al., 2018).

According to the ICTV, two dichorhaviruses are considered members of different species when they show less than 80% nucleotide sequence identity comparing their RNA1 and the *L* gene (RNA2) (Dietzgen et al., 2018b). In the case of cileviruses, isolates with more than 85% nucleotide sequence identity in their complete genomes are considered members of the same species (Freitas-Astúa et al., 2018). However, the different strains of CiLV-C recently discovered are within this limit of the demarcation criteria, developed based on only two species. Further studies on the biological, ecological, genetic and evolutionary characteristics of these viruses are required to evaluate the accuracy of the current demarcation rules.

2.3 Populational diversity and phylodynamic of *Brevipalpus* mites-transmitted viruses

Data from the co-evolution of BTVs and their host plant species and vectors are, in general, scarce. Variability studies, although at different depth and extension, have been carried out with CiLV-C, CoRSV, while host range diversity of CiLV-C2 and PfGSV have been partially revealed (Melzer et al., 2013b; Roy et al., 2015; Ramos-González et al., 2016, 2020) (Ramalho et al., 2015; Kondo et al., 2017).

CiLV-C isolates are distributed in two lineages (Ramos-González et al., 2016). Members of the lineage CRD (in reference to the municipality Cordeirópolis, collection site) are distributed throughout the Brazilian territory, and those of the lineage SJP (in reference to the municipality São José do Rio Preto, collection site) were found only in three municipalities of the state of São Paulo (Ramos-González et al., 2016). Preliminary studies using partial sequences (*p29*, *p15*, IR and *mp*) of 51 CiLV-C isolates demonstrated that the CRD and SJP subpopulations are phylogenetically distinct, with low genetic diversity (π = ~ 0.07) and under high negative selection pressure (ω = <0.5). As a practical consequence of that study, viruses from both lineages are easily detected using primers that specifically detect the *p29* genes of members of each clade (Ramos-González et al., 2016). Viruses in the clades CRD and SJP share about 85% identity, except for the 5 'region of RNA2 (*p15*-IR), where they have 98% nucleotide sequence identity. This region was likely involved in interclade recombination processes (Ramos-González et al., 2016).

The 5 'region of RNA2 (*p15*-IR) is highly diverse among members of the genus *Cilevirus* and is considered a recombination hotspot (Ramos-González et al., 2016, 2020). The IR of cileviruses shows small and non-homologous orphans ORFs, as observed, for instance, among the PfGSV strains (Ramos-González et al., 2020). Although more pieces of evidence need to be gathered, it is suggested that the region *p15*-IR in the RNA2 is prone to inter- and intra-cileviruses recombination events and may be associated with some type of adaptive advantage.

Besides CiLV-C, CiLV-C2 isolates show a relatively large diversity among isolates (Melzer et al., 2013b; Roy et al., 2013a). CiLV-C2_Co (Colombia) and CiLV-C2_Hw (Hawaii) share about 85% nucleotide identity and are originally found naturally infecting *Citrus* spp. and *Hibiscus sinensis*, respectively. Viruses from both strains have been found in mixed infections in citrus plants in Colombia (Roy et al., 2018), whereas an isolate of CiLV-C2_Hw was identified in hibiscus in Florida (Roy et al., 2019). Passion fruit green spot virus (PfGSV), a tentative member of the genus *Cilevirus*, is the only cilevirus naturally infecting native plants of South America, including species of the families *Passifloraceae*, *Solanaceae*, *Orchidaceae*, *Oleaceae*, *Malvaceae*, *Caprifoliaceae*, *Araliaceae*, *Fabaceae*, *Lamiaceae*, *Acanthaceae*, *Amaranthaceae*, and *Araceae* (Saito, 2020).

Compared with *Cilevirus*, the genus *Dichorhavirus* comprises a larger number of species but details of the population of any of its members are rather scarce (Dietzgen et al., 2018b; Freitas-Astúa et al., 2018). Preliminary studies based on the *N* gene of 20 CoRSV isolates demonstrated a low genetic diversity and that the viral population was under high negative selection pressure ($\omega = < 0.03$) (Ramalho et al., 2015). Studies on the phylogeny of OFV suggest that reassortment events may be involved between RNA1 and RNA2 of some isolates in orchids (Kondo et al., 2017) and citrus (Roy et al., 2020). Besides the impacts on orchids, OFV has become one of the most studied BTV due to the high risk that some OFV-citrus strains pose to citrus orchards worldwide. OFV-orchid and OFV-citrus share up to 97% nucleotide identity and have been identified in Mexico, Colombia, and South Africa (Kondo et al., 2006; Roy et al., 2013c, 2014, 2020; Cruz-Jaramillo et al., 2014; Afonso et al., 2016; Cook et al., 2019). Interestingly, OFV-citrus from South Africa shares about 99% identity with OFV that infect orchids and about 86% with OFV-citrus from Mexico and Colombia, suggesting a recent spillover of orchids for citrus in this region. Moreover, OFV has also been reported naturally infecting other ornamental plants, like ti plant (*Cordyline terminalis*) and lilyturf (*Liriope spicata*) in Australia (Mei et al., 2016; Dietzgen et al., 2018a).

In general terms, BTVs are considered atypical in comparison with other plant infecting viruses. As a group, they are phylogenetically distinct but are vectored by mites of the same genus, and are unable to move systemically in all their host plants, under natural conditions (Freitas-Astúa et al., 2018). Probably, cileviruses and dichorhaviruses are descendants of arthropod viruses having plants as replicative intermediates or vectors (Dietzgen et al., 2018b; Freitas-Astúa et al., 2018). Regarding the prevalence and diversity, the most likely center of origin of BTV is South America. Except for OFV, which has a worldwide distribution, all BTVs have a restricted distribution to the American continent (Dietzgen et al., 2018b; Freitas-Astúa et al., 2018).

2.4 Cileviruses and dichorhaviruses associated with citrus leprosis disease

Citrus leprosis (CL) is considered the main viral disorder affecting the Brazilian citriculture (Ramos-González et al., 2018a). It causes local chlorotic and necrotic lesions, always around the feeding site of the mite vector (Kitajima et al., 2003). The disease produces premature fruit drop, decreases the tree life-span and the quality of the fruits, increasing the production costs of citrus groves (Ramos-González et al., 2016). Management of CL is mainly based on the chemical control of the mite vector, although the high cost of acaricides associated with the emergence of resistant *Brevipalpus* populations has hindered the control of the disease, especially in the states of São Paulo and Minas Gerais (Andrade et al., 2018; Bassanezi et al., 2019).

Different viral species belonging to the genera *Dichorhavirus* (BTV-N) and *Cilevirus* (BTV-C) causes symptoms associated with CL (Kitajima et al., 1972, 2003; Freitas-Astúa et al., 2018). Viroplasms of such BTVs occur in either the cytoplasm (BTV-C) or the nucleus (BTV-N) of the infected plant cells, resulting in the wonted subclassification of CL in the types CL-cytoplasmic (CL-C) and CL-nuclear (CL-N) (Figure 2) (Kitajima et al., 1972, 2003). Globally, , the CL is present in most countries in South America (Argentina, Brazil, Bolivia, Colombia, Paraguay, and Venezuela), throughout Central America, and in some regions of North America (Mexico) (Dietzgen et al., 2018b; Freitas-Astúa et al., 2018). In 2019, the disease was reported for the first time outside the American continent, in South Africa (Cook et al., 2019).

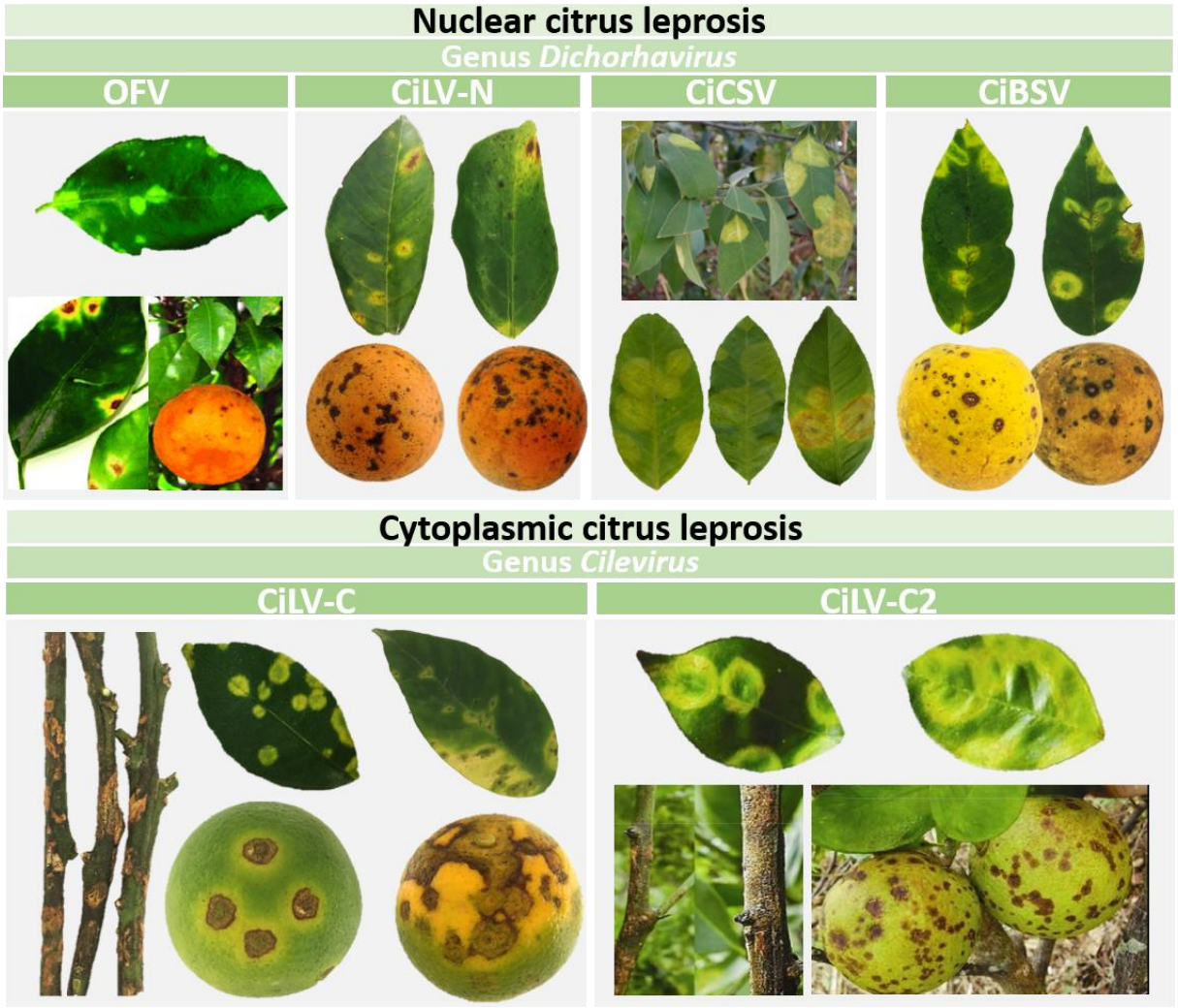

Figure 2. *Brevipalpus* mites-transmitted viruses associated with citrus leprosis disease. Nuclear citrus leprosis-causing dichorhaviruses (genus *Dichorhavirus*). Sample identification: Orchid fleck virus (OFV)-infected *Citrus* sp., collected in Mexico, 2014 (Roy et al., 2015); Citrus leprosis virus N (CiLV-N)-infected *Citrus sinensis*, collected in São Paulo, Brazil (Ramos-González et al., 2017); Citrus chlorotic spot virus (CiCSV)-infected *C. sinensis*, collected in Teresina, Piauí, Brazil (Chabi-Jesus et al., 2018; 2019); Citrus bright spot virus (CiBSV)-infected *C. sinensis*, collected in Santa Catarina and Rio Grande do Sul, Brazil, 2016 and 2019. Cytoplasmic citrus leprosis-causing cileviruses (genus *Cilevirus*). Sample identification: Citrus leprosis virus C (CiLV-C)-infected *C. sinensis*, collected in São Paulo, Brazil, 2018; Citrus leprosis virus C2 (CiLV-C2)-infected *C. sinensis*, collected in Colombia, 2013 (Melzer et al., 2013a);

CL was first reported in Florida in 1907; where disappeared after 60 years (Fawcett, 1909; Childers et al., 2003b). Possibly, the intense use of sulfur and the successive frosts eliminated the viruliferous *Brevipalpus* populations (Kitajima et al., 2011b; Hartung et al., 2015). Although it is impossible to know the diversity of BTVs associated with CL in Florida in the 1900-1960s (Kitajima et al., 2011b; Hartung et al., 2015). Studies with an herbarium sample of sweet orange collected in 1948 demonstrated the presence of a putative new species of dichorhavirus, named CiLV-N0, which probably no longer exists in nature (Hartung et al.,

2015). There are recent reports of CL-N in Mexico, Colombia, South Africa, Brazil, and Panama. In the first three countries, CL-N is caused by OFV-citrus (Figure 2) (Freitas-Astúa et al., 2018). Although OFV is present in orchids in Brazil since the 1970s (Kitajima et al., 1974, 2001), infection by this virus has not been reported in citrus. It is hypothesized that the *B. californicus,* the known vector of OFV, is not able to properly colonize sweet oranges in Brazil. Indeed, there is a report of *B. californicus* infecting *Citrus sinensis* in the state of Amazonas, Brazil, but its incidence was lower than 0.1% of the total phytophagous mites found in citrus orchards (Bobot et al., 2011). The morphological complex of *B. californicus* is likely formed by more than three species of mites, which can vary in transmission efficiency. In addition, they probably have differential capacity to colonize citrus (Tassi, 2018). Apparently, these tentative species are unequally distributed in citrus-producing countries, which may explain the absence of OFV in citrus in Brazil. Nevertheless, other dichorhaviruses associated with CL-N have been reported since the 1970s in Brazil, but the information of these BTV-N was restricted to the detection of viral particles by transmission electron microscopy (Kitajima et al., 1972; Freitas-Astúa et al., 2018). After almost 50 years, three new dichorhaviruses (CiLV-N, CiCSV and CiBSV) associated with CL-N in Brazil were identified (Figure 2), the complete description of the identification and characterization of these viruses are described in Chapters 2, 3 and 4.

Cytoplasmic leprosis caused by CiLV-C is the prevalent type of CL (Freitas-Astúa et al., 2018), except in some Colombian regions, where the disease is mainly caused by CiLV-C2 (Figure 2) (Melzer et al., 2013b; Roy et al., 2013a, 2015). Sweet oranges are highly susceptible to the CiLV-C, while tangerines exhibit intermediate resistance, and lemons and limes are immune (Bastianel et al., 2018). CiLV-C isolates of the clade CRD are detected from Mexico to Argentina, but CiLV-C isolates of the clade SJP are found in the citrus belt SP-MG (Ramos-González et al., 2016).

Plant-CiLV-C interaction studies indicate that CL symptoms resulting from a hypersensitive-like response (Arena et al., 2016, 2020). From an evolutionary point of view, this incompatibility might indicate a recent interaction between BTVs and its host plants. Citrus leprosis disease, although relatively easy to control, has become one of the main concerns for citrus growers in the citrus belt of Brazil (Andrade et al., 2018; Bassanezi et al., 2019). Understanding the diversity of viruses and their vectors, as well as the adaptive characteristics of each CiLV-C strain, is essential for the development of efficient molecular detection methods and for the generation of information necessary to devise the best management and control strategies of the disease.

REFERENCES

Afonso, C. L., Amarasinghe, G. K., Bányai, K., Bào, Y., Basler, C. F., Bavari, S., et al. (2016). Taxonomy of the order *Mononegavirales*: update 2016. *Arch. Virol.* 161, 2351–60. doi:10.1007/s00705-016-2880-1.

Andrade, D. J., Lorençon, J. R., Siqueira, D. S., Novelli, V. M., and Bassanezi, R. B. (2018). Space–time variability of citrus leprosis as strategic planning for crop management. *Pest Manag. Sci.* 74, 1798–1803. doi:10.1002/ps.4877.

Arena, G. D., Ramos-González, P. L., Falk, B. W., Clare, L., Ramos-González, P. L., Freitas-astúa, J., et al. (2020). Plant immune system activation upon citrus leprosis virus C infection is mimicked by the ectopic expression of the P61 viral protein. *Front. Microbiol.* 11, 0–24. doi:10.3389/fpls.2020.01188.

Arena, G. D., Ramos-González, P. L., Nunes, M. A., Alves, M. R., Camargo, L. E. A., Kitajima, E. W., et al. (2016). Citrus leprosis virus C infection results in hypersensitive-like response, suppression of the JA/ET plant defense pathway and promotion of the colonization of its mite vector. *Front. Plant Sci.* 7, 1757. doi:10.3389/FPLS.2016.01757.

Bassanezi, R. B., Czermainski, A. B. C., Laranjeira, F. F., Moreira, A. S., Ribeiro, P. J., Krainski, E. T., et al. (2019). Spatial patterns of the Citrus leprosis virus and its associated mite vector in systems without intervention. *Plant Pathol.* doi:10.1111/ppa.12930.

Bastianel, M., Pereira-Martin, J. A., Novelli, V. M., Freitas-Astúa, J., and Nunes, M. A. (2018). Citrus leprosis resistance within the citrus group. *VirusDisease*, 1–8. doi:10.1007/s13337-018-0489-6.

Beard, J. J., Ochoa, R., Braswell, W. E., and Bauchan, G. R. (2015). *Brevipalpus phoenicis* (Geijskes) species complex (Acari: Tenuipalpidae)-a closer look. *Zootaxa* 3944, 1–67. Available at: http://www.ncbi.nlm.nih.gov/pubmed/25947538 [Accessed June 30, 2015].

Beard, J., Ochoa, R., Bauchan, G., Trice, T., Redford, A., Walters, T., et al. (2013). Flat mites of the world. http://idtools.org/id/mites/flatmites/.

Blanchfield, A. L., Mackenzie, A. M., Gibbs, A., Kondo, H., Tamada, T., and Wilson, C. R. (2001). Identification of orchid fleck virus by reverse transcriptase-polymerase chain reaction and analysis of isolate relationships. *J. Phytopathol.* 149, 713–718. doi:10.1046/j.1439-0434.2001.00702.x.

Bobot, T. da E., Franklin, E., Navia, D., Gasnier, T. R. J., Lofego, A. C., and Oliveira, B. M. de (2011). Mites (Arachnida, Acari) on *Citrus sinensis* L. Osbeck orange trees in the state of Amazonas, Northern Brazil. *Acta Amaz.* 41, 557–566. doi:10.1590/S0044-59672011000400013.

Childers, C. C., Rodrigues, J. C. V., and Welbourn, W. C. (2003a). Host plants of *Brevipalpus californicus*, *B. obovatus*, and *B. phoenicis* (Acari: Tenuipalpidae) and their potential involvement in the spread of viral diseases vectored by these mites. *Exp. Appl. Acarol.* 30, 29–105. doi:10.1023/B:APPA.0000006544.10072.01.

Childers, C. C., Rodrigues, J. C. V, Derrick, K. S., Achor, D. S., French, J. V, Welbourn, W. C., et al. (2003b). Citrus leprosis and its status in Florida and Texas: past and present. *Exp. Appl. Acarol.* 30, 181–202.

Cook, G., Kirkman, W., Clase, R., Steyn, C., Basson, E., Fourie, P. H., et al. (2019). Orchid fleck virus associated with the first case of Citrus Leprosis-N in South Africa. *Plant Pathol.* 155, 1373–1379.

Cruz-Jaramillo, J. L., Ruiz-Medrano, R., Rojas-Morales, L., López-Buenfil, J. A., Morales-Galván, O., Chavarín-Palacio, C., et al. (2014). Characterization of a proposed dichorhavirus associated with the citrus leprosis disease and analysis of the host response. *Viruses* 6, 2602–22. doi:10.3390/v6072602.

Dietzgen, R. G., Freitas-Astúa, J., Salaroli, R. B., and Kitajima, E. W. (2018a). Tomato spotted wilt virus infects spider lily plants in Australia. *Australas. Plant Dis. Notes* 13, 2–4. doi:10.1007/s13314-018-0310-9.

Dietzgen, R. G., Kuhn, J. H., Clawson, A. N., Freitas-Astúa, J., Goodin, M. M., Kitajima, E. W., et al. (2014). Dichorhavirus: a proposed new genus for *Brevipalpus* mite-transmitted, nuclear, bacilliform, bipartite, negative-strand RNA plant viruses. *Arch. Virol.* 159, 607–19. doi:10.1007/s00705-013-1834-0.

Dietzgen, R. G. R. G., Freitas-Astúa, J., Chabi-Jesus, C., Ramos-González, P. L. P. L., Goodin, M. M. M. M., Kondo, H., et al. (2018b). Dichorhaviruses in their host plants and mite vectors. *Adv. Virus Res.* 102, 119–148. doi:10.1016/bs.aivir.2018.06.001.

Dos Santos Alves, J. L., Ferragut, F., Mendonça, R. S., Tassi, A. D., and Navia, D. (2019). A new species of *Brevipalpus* (Acari: Tenuipalpidae) from the Azores Islands, with remarks on the *B. cuneatu*s species group. *Syst. Appl. Acarol.* 24, 2184–2208. doi:10.11158/saa.24.11.10.

Fawcett, H. S. (1909). "Scarly bark of citrus," in *Florida Agricultural Experimental Station Annual Report*, ed. P. H. Rolfs (Gainesville Fla: Pepper Pub and Ptg. Co.), 75–80.

Freitas-Astúa, J., Ramos-González, P. L., Arena, G. D., Tassi, A. D., and Kitajima, E. W. (2018). *Brevipalpus*-transmitted viruses: parallelism beyond a common vector or convergent evolution of distantly related pathogens? *Curr. Opin. Virol.* 33, 66–73. doi:10.1016/j.coviro.2018.07.010.

Haramoto, F. H. (1966). Biology and control of *Brevipalpus phoenicis* (Geijskes) (Acarina: Tenuipalpidae). *Univ. Hawiaii*.

Hartung, J. S., Roy, A., Fu, S., Shao, J., Schneider, W. L., and Brlansky, R. H. (2015). History and diversity of citrus leprosis virus recorded in herbarium specimens. *Phytopathology* 105, 1277–84. doi:10.1094/PHYTO-03-15-0064-R.

Helle, W., and Bolland, H. . (1972). Artificial induction of males in a thelytokous mite species by means of X-rays. *Entomol. Exp. Appl.* 15, 395–396. Available at: https://agris.fao.org/agris-search/search.do?recordID=US201302334613 [Accessed September 10, 2020].

Kitajima, E. W., Blumenschein, A., and Costa, A. S. (1974). Rodlike particles associated with ringspot symptoms in several orchid species in Brazil. *J. Phytopathol.* 81, 280–286. doi:10.1111/j.1439-0434.1974.tb02801.x.

Kitajima, E. W., Chagas, C. M., Braghini, M. T., Fazuoli, L. C., Locali-Fabris, E. C., and Salaroli, R. B. (2011a). Natural infection of several *Coffea* species and hybrids and *Psilanthus ebracteolatus* by the coffee ringspot virus (CoRSV). *Sci. Agric.* 68, 503–507. doi:10.1590/S0103-90162011000400017.

Kitajima, E. W., Chagas, C. M., Harakava, R., Calegario, R. F., Freitas-Astúa, J., Rodrigues, J. C. V., et al. (2011b). Citrus leprosis in Florida, USA, appears to have been caused by the Nuclear type of citrus leprosis virus (CiLV-N). *VIRUS Rev. Res.* 16, 4. doi:10.17525/vrr.v16i1-2.51.

Kitajima, E. W., Chagas, C. M., and Rodrigues, J. C. V (2003). *Brevipalpus*-transmitted plant

virus and virus-like diseases: cytopathology and some recent cases. *Exp. Appl. Acarol.* 30, 135–60.

Kitajima, E. W., Kondo, H., Mackenzie, A., Rezende, J. A. M., Gioria, R., Gibbs, A., et al. (2001). Comparative cytopathology and immunocytochemistry of japanese, australian and Brazilian isolates of orchid fleck virus. *J. Gen. Plant Pathol.* 67, 231–237. doi:10.1007/PL00013018.

Kitajima, E. W., Kubo, K. S., Ferreira, P. de T. O., Alcântara, B. K. de, Boari, A. J., Gomes, R. T., et al. (2008). Chlorotic spots on Clerodendrum, a disease caused by a nuclear type of *Brevipalpus* (Acari:Tenuipalpidae) transmitted virus. *Sci. Agric.* 65, 36–49. doi:10.1590/S0103-90162008000100006.

Kitajima, E. W., Müller, G. W., Costa, A. S., and Yuki, W. (1972). Short, rod-like particles associated with Citrus leprosis. *Virology* 50, 254–8.

Kitajima, E. W., Rodrigues, J. C. V., and Freitas-Astua, J. (2010). An annotated list of ornamentals naturally found infected by *Brevipalpus* mite-transmitted viruses. *Sci. Agric.* 67, 348–371. doi:10.1590/S0103-90162010000300014.

Kondo, H., Hirota, K., Maruyama, K., Andika, I. B., and Suzuki, N. (2017). A possible occurrence of genome reassortment among bipartite rhabdoviruses. *Virology* 508, 18–25. doi:10.1016/j.virol.2017.04.027.

Kondo, H., Maeda, T., Shirako, Y., and Tamada, T. (2006). Orchid fleck virus is a rhabdovirus with an unusual bipartite genome. *J. Gen. Virol.* 87, 2413–2421. doi:10.1099/vir.0.81811-0.

Kondo, H., Maeda, T., and Tamada, T. (2003). Orchid fleck virus: *Brevipalpus californicus* mite transmission, biological properties and genome structure. *Exp. Appl. Acarol.* 30, 215–223. Available at: http://www.ncbi.nlm.nih.gov/pubmed/14756418 [Accessed July 25, 2016].

Koonin, E. V., Dolja, V. V., Krupovic, M., Varsani, A., Wolf, Y. I., Yutin, N., et al. (2020). Global organization and proposed megataxonomy of the virus world. 84, 1–33. doi:10.1128/MMBR.00061-19CE.

Leastro, M. O., Kitajima, E. W., Silva, M. S., Resende, R. O., and Freitas-Astúa, J. (2018). Dissecting the Subcellular localization, intracellular trafficking, interactions, membrane association, and topology of citrus leprosis virus c proteins. *Front. Plant Sci.* 9, 1299. doi:10.3389/fpls.2018.01299.

Locali-Fabris, E. C., Freitas-Astúa, J., and Machado, M. A. (2012). "Genus *Cilevirus*. International Committee on Taxonomy of Viruses," in *Virus Taxonomy*, eds. A. King, M. Adams, E. Carstens, and E. Lefkowitz (London, United Kingdom: Elsevier/Avademic Press), 1139–1142.

Locali-Fabris, E. C., Freitas-Astúa, J., Souza, A. A., Takita, M. A., Astúa-Monge, G., Antonioli-Luizon, R., et al. (2006). Complete nucleotide sequence, genomic organization and phylogenetic analysis of citrus leprosis virus cytoplasmic type. *J. Gen. Virol.* 87, 2721–9. doi:10.1099/vir.0.82038-0.

Maia, O. M. A., and Oliveira, C. A. L. (2004). Capacidade de colonização de *Brevipalpus phoenicis* (Geijskes) (Acari: Tenuipalpidae) em cercas-vivas, quebra-ventos e plantas invasoras. *Neotrop. Entomol.* 33, 625–629. doi:10.1590/s1519-566x2004000500013.

Mei, Y., Bejerman, N., Crew, K. S., McCaffrey, N., and Dietzgen, R. G. (2016). First report of orchid fleck virus in lilyturf (*Liriope spicat*a) in Australia. *Plant Dis.* 100, 1028.

doi:10.1094/PDIS-10-15-1205-PDN.

Melcher, U. (2000). The “30K” superfamily of viral movement proteins. *J. Gen. Virol.* 81, 257–266. doi:10.1099/0022-1317-81-1-257.

Melzer, M. J., Sether, D. M., Borth, W. B., and Hu, J. S. (2013a). Characterization of a virus infecting *Citrus volkameriana* with citrus leprosis-like symptoms. *Phytopathology* 102, 122–7. doi:10.1094/PHYTO-01-11-0013.

Melzer, M. J., Simbajon, N., Carillo, J., Borth, W. B., Freitas-Astúa, J., Kitajima, E. W., et al. (2013b). A cilevirus infects ornamental hibiscus in Hawaii. *Arch. Virol.* doi:10.1007/s00705-013-1745-0.

Navia, D., Mendonça, R. S., Ferragut, F., Miranda, L. C., Trincado, R. C., Michaux, J., et al. (2013). Cryptic diversity in *Brevipalpus* mites (Tenuipalpidae). *Zool. Scr.* 42, 406–426. doi:10.1111/zsc.12013.

Nunes, M. A., de Carvalho Mineiro, J. L., Rogerio, L. A., Ferreira, L. M., Tassi, A., Novelli, V. M., et al. (2018a). First Report of *Brevipalpus papayensis* as vector of *Coffee ringspot virus* and *Citrus leprosis virus C*. *Plant Dis.* 102, 1046–1046. doi:10.1094/PDIS-07-17-1000-PDN.

Nunes, M. A., de Carvalho Mineiro, J. L., Rogero, L. A., Ferreira, L. M., Tassi, A. D., Novelli, V. M., et al. (2018b). First report of *Brevipalpus papayensis* Baker (Acari: Tenuipalpidae) as vector of Coffee ringspot virus and Citrus leprosis virus C. *Plant Dis.* doi:10.1094/PDIS-07-17-1000-PDN.

Nunes, M. A., Novelli, V. M., da Cunha, B. A., Soares, A. J., de Mineiro, J. L. C., Freitas-Astúa, J., et al. (2020). Survey of the citrus leprosis vector (*Brevipalpus yothersi*) and phytoseiids in spontaneous plants of an organic citrus orchard. *Exp. Appl. Acarol.* doi:10.1007/s10493-020-00543-w.

Quito-Avila, D. F., Freitas-Astúa, J., and Melzer, M. J. (2020). Bluner-, Cile-, and Higreviruses (*Kitaviridae*). *Ref. Modul. Life Sci.*, 1–5. doi:10.1016/b978-0-12-809633-8.21248-x.

Ramalho, T. O., Figueira, A. R., Sotero, A. J., Wang, R., Geraldino Duarte, P. S., Farman, M., et al. (2014). Characterization of Coffee ringspot virus-Lavras: a model for an emerging threat to coffee production and quality. *Virology* 464–465, 385–96. doi:10.1016/j.virol.2014.07.031.

Ramalho, T. O., Figueira, A. R., Wang, R., Jones, O., Harris, L. E., Goodin, M. M., et al. (2015). Detection and survey of coffee ringspot virus in Brazil. *Arch. Virol.* 161, 335–343. doi:10.1007/s00705-015-2663-0.

Ramos-González, P. L., Chabi-Jesus, C., Arena, G. D., Tassi, A. D., Kitajima, E. W., Freitas-Astúa, J., et al. (2018a). Citrus leprosis: a unique multietiologic disease. *Cítricos en las Américas* 1, 1–9.

Ramos-González, P. L., Chabi-Jesus, C., Guerra-Peraza, O., Breton, M. C., Arena, G. D. G. D. G. D., Nunes, M. A. M. A., et al. (2016). Phylogenetic and molecular variability studies reveal a new genetic clade of Citrus leprosis virus C. *Viruses* 8, 153. doi:10.3390/v8060153.

Ramos-González, P. L. P. L., Chabi-Jesus, C., Banguela-Castillo, A., Tassi, A. D. A. D., Rodrigues, M. C. M. da C., Kitajima, E. W. E. W., et al. (2018b). Unveiling the complete genome sequence of clerodendrum chlorotic spot virus, a putative dichorhavirus infecting ornamental plants. *Arch. Virol.* 163, 2519–2524. doi:10.1007/s00705-018-3857-z.

Ramos-González, P. L., Santos, G. F. dos, Chabi-Jesus, C., Harakava, R., Kitajima, E. W., and Freitas-Astúa, J. (2020). Passion fruit green spot virus genome harbors a new orphan ORF and highlights the flexibility of the 5′-end of the RNA2 segment across cileviruses. *Front. Microbiol.* 11, 206. doi:10.3389/fmicb.2020.00206.

Rodrigues, J. C. V., and Childers, C. C. (2013). *Brevipalpus* mites (Acari: Tenuipalpidae): vectors of invasive, non-systemic cytoplasmic and nuclear viruses in plants. *Exp. Appl. Acarol.* 59, 165–75. doi:10.1007/s10493-012-9632-z.

Roy, A., Choudhary, N., Guillermo, L. M., Shao, J., Govindarajulu, A., Achor, D., et al. (2013a). A novel virus of the genus *Cilevirus* causing symptoms similar to citrus leprosis. *Phytopathology* 103, 488–500. doi:10.1094/PHYTO-07-12-0177-R.

Roy, A., Hartung, J. S., Schneider, W. L., Shao, J., Leon M, G., Melzer, M. J., et al. (2015). Role bending: Complex relationships between viruses, hosts, and vectors related to citrus leprosis, an emerging disease. *Phytopathology* 105, 872–884. doi:10.1094/PHYTO-12-14-0375-FI.

Roy, A., Leon, M. G., Stone, A. L., Schneider, W. L., Hartung, J., and Brlansky, R. H. (2014). First report of citrus leprosis virus nuclear type in sweet orange in Colombia. *Plant Dis.* 98, 1162. doi:10.1094/PDIS-02-14-0117-PDN.

Roy, A., Shao, J., Hartung, J. S., Schneider, W., and Brlansky, R. (2013b). A case study on discovery of novel citrus leprosis virus cytoplasmic type 2 utilizing small rna libraries by next generation sequencing and bioinformatic analyses. *J. Datamining Genomics Proteomics* 4.

Roy, A., Stone, A. L., León Martínez, G., Hartung, J. S., Wei, G., Mavrodieva, V. A., et al. (2018). First report of Hibiscus-infecting cilevirus in citrus sinensis in Meta and Casanare, Colombia. *Plant Dis.* 102, 1675. doi:10.1094/PDIS-01-18-0150-PDN.

Roy, A., Stone, A. L., Melzer, M. J., Shao, J., Hartung, J. S., Mavrodieva, V., et al. (2019). Complete nucleotide sequence of a novel hibiscus-infecting cilevirus from Florida and its relationship with closely associated cileviruses. *Genome Announc.* 6, 1–2. doi:10.1128/genomeA.01521-17.

Roy, A., Stone, A. L., Otero-Colina, G., Wei, G., Brlansky, R. H., Ochoa, R., et al. (2020). Reassortment of genome segments creates stable lineages among strains of orchid fleck virus infecting citrus in Mexico. *Phytopathology* 110, 106–120. doi:10.1094/PHYTO-07-19-0253-FI.

Roy, A., Stone, A., Otero-Colina, G., Wei, G., Choudhary, N., Achor, D., et al. (2013c). Genome assembly of citrus leprosis virus nuclear type reveals a close association with orchid fleck virus. *Genome Announc.* 1, e00519-13-e00519-13. doi:10.1128/genomeA.00519-13.

Saito, M. S. G. (2020). O vírus da pinta verde do maracujazeiro (passion fruit green spot virus - PfGSV), isolado de ligustro: suas relações com o ácaro vetor Brevipalpus.

Salinas-Vargas, D., Santillán-Galicia, M. T., Guzmán-Franco, A. W., Hernández-López, A., Ortega-Arenas, L. D., and Mora-Aguilera, G. (2016). Analysis of genetic variation in *Brevipalpus yothersi* (Acari: Tenuipalpidae) populations from four species of citrus host plants. *PLoS One* 11, 1–11. doi:10.1371/journal.pone.0164552.

Sánchez-Velázquez, E. J., Santillán-Galicia, M. T., Novelli, V. M., Nunes, M. A., Mora-Aguilera, G., Valdez-Carrasco, J. M., et al. (2015). Diversity and genetic variation among *Brevipalpus* populations from Brazil and Mexico. *PLoS One* 10, e0133861.

doi:10.1371/journal.pone.0133861.

Tassi, A. D. (2018). Diversidade morfológica e genética de diferentes espécies de *Brevipalpus* (Acari: Tenuipalpidae) e suas competências como vetores de vírus. 263. Available at: http://www.teses.usp.br/teses/disponiveis/11/11135/tde-17072018-160552/pt-br.php.

Tassi, A. D., Garita-Salazar, L. C., Amorim, L., Novelli, V. M., Freitas-Astúa, J., Childers, C. C., et al. (2017). Virus-vector relationship in the Citrus leprosis pathosystem. *Exp. Appl. Acarol.* 71, 227–241. doi:10.1007/s10493-017-0123-0.

Teodoro, A. V., and Reis, P. R. (2006). Reproductive performance of the mite *Brevipalpus phoenicis* (Geijskes, 1939) on citrus and coffee, using life table parameters. *Brazilian J. Biol.* 66, 899–905. doi:10.1590/S1519-69842006000500016.

Weeks, A. R., Marec, F., and Breeuwer, J. A. (2001). A mite species that consists entirely of haploid females. *Science* 292, 2479–82. doi:10.1126/science.1060411.

APPENDIX I

Ramos-González, P. L. P. L., Chabi-Jesus, C., Banguela-Castillo, A., Tassi, A. D. A. D., Rodrigues, M. C. M. C., Kitajima, E. W. E. W., et al. (2018). Unveiling the complete genome sequence of clerodendrum chlorotic spot virus, a putative dichorhavirus infecting ornamental plants. **Archives of Virology** 163, 2519–2524. doi:10.1007/s00705-018-3857-z.

3. CHAPTER 1

GENETIC ESTRUCTURE AND EVOLUTION OF CITRUS LEPROSIS VIRUS C

ABSTRACT

Despite their importance as agents of emerging diseases, genetic and evolutionary processes affecting the ecology of viral strains/variants are not fully understood. To get insight into this topic, we assessed the population and spatial dynamic parameters of citrus leprosis virus C (CiLV-C) (genus *Cilevirus*, family *Kitaviridae*). This virus is limited to Latin America, where it causes citrus leprosis (CL) disease, a non-systemic infection considered the main viral disorder affecting citrus orchards in Brazil. Overall, the nucleotide sequences (nts) of (*i*) 14 complete viral genomes; (*ii*) 123 putative coat protein (*cp*) open reading frame (ORF) *p29* (792 nts); and (*iii*) 204 movement protein (*mp*) partial ORF (288 nts) were obtained from the analyses of 425 infected *Citrus* spp. samples collected between 1932 and 2019. The comprehensive examination of phylogenetic and genetic diversity data suggest that the CiLV-C population is mainly made up by the two unevenly-distributed lineages CRD and SJP, whilst a third one, whose current spread and circulation are unknown, is epitomized by an isolate identified in a herbarium sample formerly collected in Asuncion, Paraguay, in 1937. Viruses from different lineages share about 85% nucleotide sequence identity and show signs of inter-clade recombination processes. Members of the lineage CRD were identified both in commercial and non-commercial citrus orchards, but those of the lineages SJP, were exclusively identified in samples collected after 2015 and in the citrus belt of São Paulo and Triângulo/Southwest of Minas Gerais, the leading Brazilian citrus production region. The most recent common ancestor of viruses of the three lineages was estimated at approximately 500 A.D. (PP= 1; HPD 95%= 94–858 A.D). Since *Citrus* spp. plants were introduced in the Americas by the Portuguese around 1520s, the Bayesian phylodynamic analysis suggests that CiLV-C lineage ancestors likely originated in contact with native vegetation in a wild ecosystem of South America. Intensive expansion of CRD and SJP lineages started as of 1870, probably linked to the beginning of the citrus industry in Brazil. The high prevalence of CiLV-C in the citrus belt of Brazil, likely ensues the intensive connectivity between orchards, which represents a potential risk toward the pathogen saturation across the region.

Keywords: Citrus leprosis disease; *Cilevirus*; *Kitaviridae*; *Brevipalpus* mites.

3.1 INTRODUCTION

Brazil is the leading sweet orange producer in the world. With almost 197.7 million of the sweet orange (*Citrus sinensis*) trees[1], the citrus belt of São Paulo (SP) and Triângulo/Southwest of Minas Gerais (MG) is the largest citrus cultivation area in South America and accounts for more than 80% of the national sweet orange production (Bassanezi et al., 2019). Citrus orchard yields may be impacted by citrus leprosis (CL) disease , ranked first among the viral diseases affecting this crop in Brazil (Ramos-González et al., 2018a). Control of CL reaches up to US$ 54 million/year, a value representing about 5% of the management cost of orchards in the main Brazilian citrus belt (Bassanezi et al., 2019).

Despite the multi-etiological character of CL, citrus leprosis virus C (CiLV-C) is, by far, the prevalent causal agent in Brazil (Ramos-González et al., 2016, 2018a). The virus infects several species within the genus *Citrus*, although with different degrees of severity. While sweet oranges (*C. sinensis*) show high susceptibility, mandarins (*C. reshni*, *C. reticulata,* and *C. deliciosa*) are moderately resistant, while lemons (*C. limon*) and limes (*C. aurantifolia*) are considered resistant (Bastianel et al., 2018). CiLV-C also naturally infects *Commelina benghalensis* and *Swinglea glutinosa* and can be experimentally transmitted to plants of 28 families (León et al., 2008; Nunes et al., 2012; Arena et al., 2013; Garita et al., 2014).

CiLV-C does not systemically infect its host plants, it only causes local chlorotic and/or necrotic lesions (Figure 1), which may result from an incompatible interaction spearheaded by a hypersensitivity-like response (Arena et al. 2016, 2020). The viral spread, even to different points in infected plants, is exclusively mediated by viruliferous mites of, mainly, the species *Brevipalpus yothersi* (Ramos-González et al., 2016), and to a lower extent by the species *B. papayensis* (Nunes et al., 2018b). Nonetheless, the CiLV-C/*Brevipalpus* spp. interaction has not been fully characterized yet. While biological and electron microscopy data suggest a circulative transmission (Kitajima et al., 2003, 2008; Tassi et al., 2017), non-conclusive molecular assays suggest the viral multiplication in the *Brevipalpus* cells (Roy et al., 2015a).

Citrus leprosis virus C is the type species of the genus *Cilevirus*, family *Kitaviridae* (Locali-Fabris et al., 2012b; Freitas-Astúa et al., 2018). In addition to cileviruses, the family also includes members of the genera *Higrevirus* and *Blunervirus* (Melzer et al., 2013a; Quito-Avila et al., 2013). Kitaviruses have bacilliform or spherical virions that shelter segmented positive single-stranded RNA genomes (Quito-Avila et al., 2020a), and share common

[1] https://www.fundecitrus.com.br/

ancestors with arthropod infecting-viruses of the group negevirus and other nege-like viruses (Kondo et al., 2020; Ramos-González et al., 2020).

Aside from CiLV-C, the genus *Cilevirus* also includes citrus leprosis virus C2 and tentatively passion fruit green spot virus (PfGSV) (Roy et al., 2013a; Ramos-González et al., 2020). The canonical cilevirus genome comprises of six open reading frames (ORFs) across two molecules, RNA1 and 2. RNA1 is ~ 9.0 kb in length and encodes two ORFs, the RNA-dependent RNA polymerase (*RdRp*) and the putative coat protein (*p29*) genes. RNA2 is ~4.9 kb in length and encodes four ORFs (*p15, p61, mp,* and *p24* genes). In CiLV-C, the RNA2 also contains an intergenic region (IR) of ~1 kb located between the *p15* and *p61* cistrons. P15, P61, and P24 are proteins without definitive associated functions, although the first two seem to be involved in silencing suppression mechanisms (Leastro et al., 2020) and the latter is conserved among cileviruses, higreviruses, and members of the insect-specific negevirus group (Ramos-González et al., 2020). The *mp* encodes a putative movement protein (MP) of the 30K superfamily (Mushegian and Elena, 2015).

Preliminary studies have revealed that the CiLV-C population has a low genetic variability ($\pi < 0.01$) and is subdivided into the clades CRD and SJP (Ramos-González et al., 2016). Type viruses of each lineage share ~85% genome nucleotide identity, except for the region spanning the *p15*-IR of their RNA2. High uniformity in this genomic segment, ~ 98% nucleotide sequence identity, is likely a consequence of a natural recombination process (Ramos-González et al., 2016). The strain CRD is prevalent throughout Latin America, whereas, until 2015, the strain SJP was only detected in three counties in the northwestern region of the state of São Paulo (Ramos-González et al., 2016). However, most aspects concerning diversity, distribution, transmissibility, and virulence of these strains remain largely unknown.

Here, we delve into the distribution, dynamic and evolutionary parameters of the CiLV-C population through the analysis of 425 samples comprising fresh and herborized tissues of CL-affected plants collected from commercial and non-commercial citrus orchards between 1932 and 2019. We also reconstruct the evolutionary history of CiLV-C based on concatenates of the *p29* and *mp* genes from 127 isolates and contextualize it with the origin and expansion of citrus crops in the Americas.

3.2 MATERIALS AND METHODS

3.2.1 Citrus samples

A total of 425 individual or mixed lesions from leaves, fruits, or branches collected from 299 citrus plants showing typical chlorotic and/or necrotic lesions of CL were analyzed (Table 1, Supplementary Table 1, Annex I). The RNA extracts were obtained from: i) sweet orange (*Citrus sinensis*) herborized samples stored at the Herbarium of Instituto Biológico, São Paulo, collected from 1932 to 1975, in Brazil (n=6), Argentina (n=1), and Paraguay (n=1); ii) 41 leaf samples of *Citrus* spp. stored in -80ºC freezer collected from 2003 to 2015, in Brazil (n=32), Argentina (n=6), Bolivia (n=1), Paraguay (n=1), and Colombia (n=1); iii) 37 sweet orange fruit samples collected from commercial citrus orchards in São Paulo and Triângulo Mineiro of Minas Gerais from 2015 and 2016; iv) 17 leaf samples of *Citrus* spp. collected from non-commercial citrus orchards in Brazil (n=9), Argentina (n=7), and Paraguay (n=1) in the period 2015-2019; v) 322 fruit lesions from 196 sweet orange samples collected from commercial citrus orchards in São Paulo and Triângulo Mineiro of Minas Gerais from 2017-2019.

Table 1. Summary of *Citrus* spp. samples showing symptoms associated with Citrus leprosis disease used in this work.

Collection site	Orchard type	Collection year	Total individual or mixed lesions analyzed
Brazil			
SP and MG	commercial	2003-2016	55
SP and MG	commercial	2017-2019	322
SP and MG	non-commercial	1932-2019	19
Other states	non-commercial	1937-2018	10
Other countries			
Argentina	non-commercial	1937-2019	14
Colombia	non-commercial	2008	1
Bolivia	non-commercial	2003	1
Paraguay	Unknown (n=1) and non-commercial (n=2)	1937, 2010 and 2019	3
			Total = 425

3.2.2 RNA isolation

RNA extraction was performed either from fresh or herborized plant tissues. For fresh samples, about 100 mg of leaf lesions were ground in liquid nitrogen and the total RNA was extracted using Trizol® according to the manufacturer's recommendation (Thermo Fisher Scientific, Waltham, MA, USA). For herborized samples, in addition to the treatment with 0.01% diethylpyrocarbonate (DEPC) solution and 120°C sterilization, mortars and pestles were kept in an oven at 200°C for 48 hours before the extractions. Approximately 600 mg of dry symptomatic tissues were ground in liquid nitrogen and processed following the Trizol®

procedure. Regardless of the origin of samples, RNA solutions were precipitated using 0.1 volume of sodium acetate 3M and 2.5 volume of isopropanol, kept at -80°C for 12 hours, and centrifuged at 10.000xg for 10 min at 4°C. The concentration and integrity of the RNA extracts were assessed by NanoDrop ND 8000 spectrophotometer (Thermo Fisher Scientific, Waltham, MA, USA) and 1.2% agarose gel stained with ethidium bromide (10mg/mL). For samples collected in commercial citrus orchards from 2017 to 2019, the total RNA was extracted from individual lesions found on the affected fruits.

3.2.3 Generic and specific detection of CiLV-C strains by RT-PCR

Five hundred nanograms of total RNA was used for cDNA synthesis using the RevertAid H Minus First-Strand cDNA Synthesis Kit (Thermo Fisher Scientific, Waltham, MA, USA). The presence of CL-associated viruses was assessed by PCR using cDNA as template (3 µL), specific primer pairs (Table 2), and GoTaq G2 Master Mix Green kit (Promega, Madison, WI, USA). For CiLV-C, in addition to primers for the detection of p29 (Ramos-González et al., 2016) and mp genes (Locali et al., 2003), a set of specific and degenerate primers for the detection of viral strains were developed based on the sequence of the p24 gene (CiLV-C SJP and CRD GenBank accession numbers are KP336747 and DQ352195, respectively). CiLV-C genomic sequences were aligned using MUSCLE implemented in MEGA version 7.0.21 (Kumar et al., 2016), and specific primers for each of the strains CRD and SJP were designed using Geneious (Kearse et al., 2012) (Table 2). The thermal cycles were as follows: 94°C, 3 min; 35 cycles of 94°C, 30 sec; 54°C, 30 sec; 72°C, 30 sec; and a final extension at 72°C for 5 min. To confirm primer specificity, the amplicons were resolved on a 1% agarose gel, excised, purified, and Sanger sequenced. The putative presence of the cilevirus citrus leprosis virus C2 (CiLV-C2) and the dichorhaviruses citrus leprosis virus N (CiLV-N), citrus chlorotic spot virus (CiCSV), and orchid fleck virus (OFV) were screened by PCR using primers previously described (Kubo et al., 2009; Roy et al., 2013a, 2014; Ramos-González et al., 2017; Chabi-Jesus et al., 2018) (Table 2).

Table 2. Primers list used for the detection of viruses associated with citrus leprosis disease by RT-PCR

BTV[1]		**Region**	**Tm (°C)**	**Size (bp)**	**Reference**
genus	**virus**				
Cilevirus	CiLV-C	*mp*	56	339	(Locali et al., 2003)
		p29[2]	56	1000	(Ramos-González et al., 2016)
		p15	56	667	
		p24	54	322	**This study** (sequence: 5'-3')
					F: CGCAGTTTCCTAATAACACC

					R: GCTTTATGCTGAACTCCC
	CiLV-C CRD	*p29*	56	330	(Ramos-González et al., 2016)
		p24	54	522	**This study** (sequence: 5'-3')
					F: ATGTTGGCAACGGAAAGTT
					R: GTGAACAGGGTTGAAAAAGTT
	CiLV-C SJP	*p29*	56	456	(Ramos-González et al., 2016)
		p24	54	393	**This study** (sequence: 5'-3')
					F: CTCATGATATCCTTGATGACC
					R: GACTAATAAGGTTGAGAAGGTTG
	CiLV-C2	*p29*	56	795	(Roy et al., 2013b)
Dichorhavirus	OFV+CiLV-N	*L*	54	362	(Ramos-González et al., 2017b)
	CiCSV	*G*	54	500	(Chabi-Jesus et al., 2018)

[1]Name abbreviation: *Brevipalpus* mites-transmitted viruses; [2]These primers were used to validate the CiLV-C_BR_SP_SJP01 genome, sequences: F: ACCGTGAATTTGTATTTTGTCA and R: CAGCTGGAAGAGACTAGAAA.

3.2.4 Partial sequences of CiLV-C isolates

The complete sequence of the *p29* (795 nt) and partial sequence of the *mp* (288 nt) genes in the RNA1 and RNA2, respectively, of CiLV-C isolates, were obtained using described primers (Locali et al., 2003; Ramos-González et al., 2016) (Table 2). Amplicons were obtained from 26 samples collected in non-commercial citrus regions in Brazil and Argentina, from 2006 to 2019, and 31 from commercial citrus orchards inside the Brazilian citrus belt, in the period 2017 – 2019 (Supplementary Table 1). After RT-PCR, amplicons were purified using Wizard SV Gel and PCR Clean-Up System (Promega, Madison, WI, USA), and cloned into pGEM-T-Easy (Promega, Madison, WI, USA). Plasmids were transformed into *Escherichia coli* DH10β competent cells by electroporation, and 5 to 10 recombinant clones derived from each sample were sequenced by the Sanger method. Amplicons from some samples collected in non-commercial orchards were directly sequenced after their purification (Supplementary Table 1, Annex I).

3.2.5 Complete genome sequence of selected CiLV-C isolates by high throughput sequencing

Small RNA (sRNA) from herborized samples were sequenced on an Illumina HiSeq 2500 Sequencer either at Genewiz (South Plainfield, NJ, USA) or BGI (Shenzhen, Guangdong, China) (Table 3). RNA from non-herborized samples were sequenced using the Illumina GA IIX technology at the Laboratory of Animal Biotechnology of the University of São Paulo (Piracicaba, SP, Brazil). For all, the ribosomal RNA depletion and libraries construction were performed using recommended Illumina products (Illumina, San Diego, CA, USA). The quality

of reads were checked using FastQC (Andrews, 2010) (Table 3) and the adaptor sequences were removed using the Trimmomatic (Bolger et al., 2014). Reads from both types of libraries were assembled with SPAdes (Bankevich et al., 2012) although using different subsequences lengths: for sRNA libraries, the k-mer values were 21,25,33, whereas for mRNA libraries the k-mer were 33, 43, 55. Viral contigs were identified using Basic Local Alignment Search Tool (BLASTx and/or BLASTn) against a viral database. After the identification and when necessary, reads were mapped to the reference genomes using Bowtie2 or BBMap to fill gaps and find the end sequences of viral genomes (Langmead and Salzberg, 2012; Bushnell, 2014).

Besides those from citrus infected plants, a sRNA library from CiLV-C-infected Arabidopsis thaliana plant was processed (Table 3). This sample was the result of a previous study that allowed, for the first time, confirming the transmission of CiLV-C by B. yothersi (Ramos-González et al., 2016).

Table 3. List of *Citrus* spp. and *Arabidopsis thaliana* samples sequenced by high through sequencing.

Host	Local	Year	Sequencing Company	HTS library	Nº reads	Reads and Contigs concerning CiLV-C					
						RNA	Reads		Contigs		
							Nº (%)	Coverage (%)	Nº	Length(nt)	Coverage (%)
Herbarium samples											
Citrus sinensis	Jacarei, SP	1932	Genewiz, USA	ssRNA	59,435,658	1	0.01	99,3	15	150-1423	82.7
						2	0.01	99,6	9	148-2116	92.2
C. sinensis	Piracicaba, SP	1932	Genewiz, USA	ssRNA	71,037,882	1	0.01	100	6	121-4168	98.4
						2	0.01	100	3	1478-1916	96.8
C. sinensis	Uruguaiana, RS	1937	BGI, China	ssRNA	63,116,147	1	2.1	100	3	235-7026	100
						2	1.1	100	2	24499-2317	97
C. sinensis	Asuncion, PY	1937	BGI, China	ssRNA	61,507,832	1	20.2	100	6	403-3709	98.8
						2	14.6	100	4	1085-3781	97.7
C. sinensis	Santa'Ana, AR	1937	BGI, China	ssRNA	62,116,588	1	6.5	100	2	427-8144	97.5
						2	4.3	100	1	4785	95.8
C. sinensis	Limeira, SP,	1939	Genewiz, USA	ssRNA	74,407,978	1	0.02	100	6	187-7577	99.5
						2	0.01	100	4	4850-4858	97.6
C. sinensis	Sao, Paulo, SP	1941	BGI, China	ssRNA	59,404,138	1	0.05	100	19	147-988	65.2
						2	0.05	100	9	144-707	68.7
Citrus sp.	Jaboticabal, SP	1975	Genewiz, USA	ssRNA	56,790,128	1	16.4	100	22	117-4750	97.70
						2	7.7	100	19	125-4428	96.50
Stored at - 80ºC											
C. sinensis	Argentina	2006	Esalq, USP, Brazil	mRNA	14,872,149	1	14.2	100	23	154-8724	100
						2	2.5	100	5	162-5276	100
Fresh tissue											
Arabidopsis thaliaina	Experimental transmission (CiLV-C_SJP-infected *Brevipalpus*)	2015	Fasteris, Switzerland	ssRNA	10,689,576	1	7.7	100	1	8675	98.6
						2	7.6	100	5	361-1568	91.3
C. sinensis	Piracicaba, SP	2016	Esalq, USP, Brazil	mRNA	15,553,431	1	5.5	100	2	630-8147	100
						2	1.2	100	1	4963	100
C. sinensis	Corrientes, AR	2017	Esalq, USP, Brazil	mRNA	14,410,186	1	1.6	100	1	8747	99.9
						2	1.4	100	2	292-4742	100
C. reticulata	Piracicaba, SP	2018	Esalq, USP, Brazil	mRNA	15,165,394	1	0.9	100	3	416-8755	100
						2	0.2	100	1	4975	100
C. sinensis	Vitoria, ES	2018	Esalq, USP, Brazil	mRNA	13,111,075	1	6.7	100	8	181-7800	100
						2	1.6	100	1	4968	100

3.2.6 Recombination and reassortment analyses

Recombination events were assessed using seven methods (RDP, GENECONV, Bootscan, Maxchi, Chimaera, SiScan, and Topal) implemented in the RDP version 5.5 (Martin et al., 2015) and GARD software (Kosakovsky Pond et al., 2006). Sequences were aligned using the MUSCLE, MAFFT, and Clustal software, implemented in Geneious package (Kearse et al., 2012). Recombination events detected by more than three programs implemented in the RDP version 5.5 were considered as presumed recombinants. The regions detected with recombination events were excluded from phylogenetic and diversity analyses. Due to the length heterogeneity of sequences available, three independent analyses were carried out, *i.e.*, complete sequences of each CiLV-C genome, *p29* (RNA1) and *mp* (RNA2) genes sequences, and a partial RNA2 concatenate [complete *p15* gene (393 nt) - intergenic region (934 nt, upstream the *p61* gene) - partial *mp* gene (288)]. The reassortment events were analyzed from the topology of the phylogenetic trees.

3.2.7 Phylogenetic analyses based on complete genome and genes of CiLV-C

All CiLV-C sequences available at the GenBank were retrieved and incorporated into the analyses. Nucleotide or amino acid alignments were performed using MUSCLE implemented in MEGA version 7.0.21 (Kumar et al., 2016). Best-fit models for nucleotide or amino acid substitutions, determined according to Maximum Likelihood statistic method implemented in c, were as follow: HKY+G+I for RNA1 (n=18), HKY+G for the RNA2 (n=18), the partial RNA2 concatenate (*p15*-IR-*mp*, n=51) and the *p29* (n=185) and *mp* (n=265) genes sequences, and JTT for the amino acid sequences alignments of P29 (n=185) and MP (n=265). Phylogenetic trees were generated by Bayesian inference using a variant of Markov chain Monte Carlo with MrBayes, implemented in Geneious (Huelsenbeck and Ronquist, 2001; Kearse et al., 2012), with 6,000,000 generations and cognate sequences from CiLV-C2_Colombia (NC038848 and NC038849) as outgroup. The regions detected with recombination events were excluded the phylogenetic and diversity analyses. Phylogenetic trees were viewed and edited using iTOL (Letunic and Bork, 2007). Nucleotide distances within and between clades were calculated using MEGA version 7.0.21.

3.2.8 Spatial-temporal phylogenetic analyses of CiLV-C populations

Assessment of the time of the most recent common ancestor (tMRCA) of CiLV-C isolates was based on concatenates of the complete *p29* (795 nt) and partial *mp* (288 nt) gene nucleotide sequences from 127 isolates using BEAST software version 1.10.04 (Suchard et al.,

2018). Fifteen samples of *C. sinensis* collected in commercial orchards gave rise to different numbers of clones for *p29* and *mp* genes sequences (Supplementary Table 2, Annex I). These samples share less than 0.007 nucleotide diversity; in short, only different haplotypes representing each sample were selected for the concatenate (Supplementary Table 2, Annex I). All combinations were included in the alignments. In parallel, phylogenetic trees were constructed using all the haplotypes in independent analysis by each gene (*p29*: n= 165; *mp*: n= 265). Initially, "non-clock" maximum likelihood phylogenetic trees were reconstructed with the best evolutionary model (TN93+G) using IQtree software version 1.5.5 (Nguyen et al., 2015). Then, the temporal signal was evaluated from the concatenate and each tree (*p29* and *mp*) using TempEst version 1.5.3 software (Rambaut et al., 2016).

BEAST version 1.10.4 was used to get the Bayesian Markov Chain Monte Carlo (MCMC) to analyze growth history of CiLV-C populations. The best model of nucleotide substitution for *p29* and *mp* and concatenate sequences TN93+G were selected. The Bayesian skygrid model (number of parameters = 20; time of last transition point = 87) was selected as the tree coalescent model and using the strict clock. The MCMC analyses were performed with 100 million generations, sampling a tree every 1000 steps. MCMC convergence and the effective sample sizes (ESS) estimates (200) were verified using Tracer version 1.7 (Rambaut et al., 2018). The Maximum clade credibility (MCC) tree was created by discarding the initial 10% of the chains and summarized in TreeAnnotator version 1.10.4. The phylogenetic tree was viewed using IcyTree (Vaughan, 2017).

3.2.9 Population genetic and selection tests

Population genetic parameters, *i.e.* diversity of nucleotide (π) and haplotype (Hd), the number of polymorphic sites (s), nucleotide differences (k), mutations (θ) and haplotypes (H); and the ratio of non-synonymous (dN) to synonymous (dS) nucleotide substitutions (ω =dN/dS) were calculated using DnaSP v. 6.12.03 (Rozas et al., 2017). Selection in polymorphic sites of the CiLV-C genes was calculated using Fast Unconstrained Bayesian AppRoximation for Inferring Selection (FUBAR), Fixed Effects Likelihood (FEL), and Mixed Effects Model of Evolution (MEME) methods with the GTR model, implemented in Datamonkey 2.0 (Weaver et al., 2018). For the identification of the amino acids under selection and its involvement in the protein structure, predicted secondary structures of deduced amino acid sequences of the P29 and MP proteins from definitive and tentative members of the genus *Cilevirus*: CiLV-C CRD (DQ352194 and DQ352195), CiLV-C SJP (KP336746 and KP336747), CiLV-C2_Colombia (NC038848 and NC038849), CiLV-C2_Hawaii (MG253805 and MG253804) and

PfGSV_Snp1 (MK804171 and MK804172) were obtained using PROMALS (PROfile Multiple Alignment with Local Structure) (Pei and Grishin, 2007).

3.2.10 Neutrality and differentiation tests in the CiLV-C population

CiLV-C population expansion was evaluated by three statistical tests: Tajima's D (Tajima, 1989), Fu and Li's F and D (Fu and Li, 1993), and Fu's FS (Fu, 1997) implemented in DnaSP v. 6.12.03 package (Rozas et al., 2017). These estimates the difference between two measures of genetic diversity: the mean number of pairwise differences and the number of segregating sites. Negative values indicate populations in expansion or after a recent bottleneck, whereas positive values indicate a decrease in population size and/or balancing selection.

Demographic expansions of CiLV-C subpopulations assessed by mismatch distributions (distribution of pairwise nucleotide differences) were performed based on the sum of squared deviation (SSD) and Harpending's Raggedness index (HRI) using Arlequin v. 3.5.2.2 (Excoffier and Lischer, 2010). The HRI test determines whether an observed mismatch distribution is drawn from an expanded (small raggedness index or non-significative) or a stationary population (large raggedness index), while the SSD quantifies the smoothness of the observed mismatch distribution and a non-significant result indicates an expanding population (Rogers and Harpending, 1992; Harpend et al., 1994).

Genetic subdivision of the CiLV-C population was assessed using the nearest-neighbor statistic (*Snn*) (Hudson, 2000), Hudson's test statistics [*Hst* (haplotype-based statistics), Kst (nucleotide-based statistics)], *Fst*, and *Nm* (Hudson et al., 1992) tests using DnaSP v. 6.12.03 and Arlequin v. 3.5.2.2. The *Snn* is a measure of how often the nearest neighbors of sequences are found in the same locality (Hudson, 2000). *Snn* values range from 0.5 to 1, being the lowest indexes an indicative of that isolates from both locations are part of the same population, and the highest one that the populations in the two locations are highly differentiated. *Hst* and *Kst* statistics calculate the level of differentiation based on haplotypes and nucleotides, respectively, and values close to zero indicates no differentiation. On the other hand, based on the proportion of the total genetic variance contained in a subpopulation, the *Fst* test provides insights into the evolutionary processes that influence the structure of genetic variation within and among populations, (Hudson et al., 1992). *Nm*, the number of migrants successfully entering a population per generation, was used to measure gene flow (migration) between populations [$Fst \neq 1/(4Nm+1)$]. Finally, the effect of the geographical location and the age of the isolates on the genetic diversity of CiLV-C were evaluated using an analysis of molecular variance (AMOVA) performed with Arlequin v. 3.5.2.2.

3.3 RESULTS

The presence of CiLV-C was confirmed in all the 424 symptomatic samples collected in 298 plants of sweet orange, six of mandarin, and in other five citrus plants whose species could not be determined (Supplementary Table 1, Annex I). RT-PCR tests for the specific detection of citrus-infecting *Brevipalpus*-transmitted viruses other than CiLV-C indicated the absence of the cilevirus CiLV-C2 and the dichorhaviruses CiLV-N, CiCSV, and OFV. The set of new samples compiled in this work comprises CiLV-C isolates collected in Argentina, Brazil, Bolivia, Colombia, and Paraguay from 1932 to 2019. According to its economic importance and the size of the farming area, approximately 92% of the samples were gathered from the citrus belt *São Paulo – Minas Gerais*, Brazil. All the analyzed samples showed typical symptoms of citrus leprosis disease, *i.e*. chlorotic and/or necrotic lesions on leaves and fruits and necrotic lesions on branches (Figure 1).

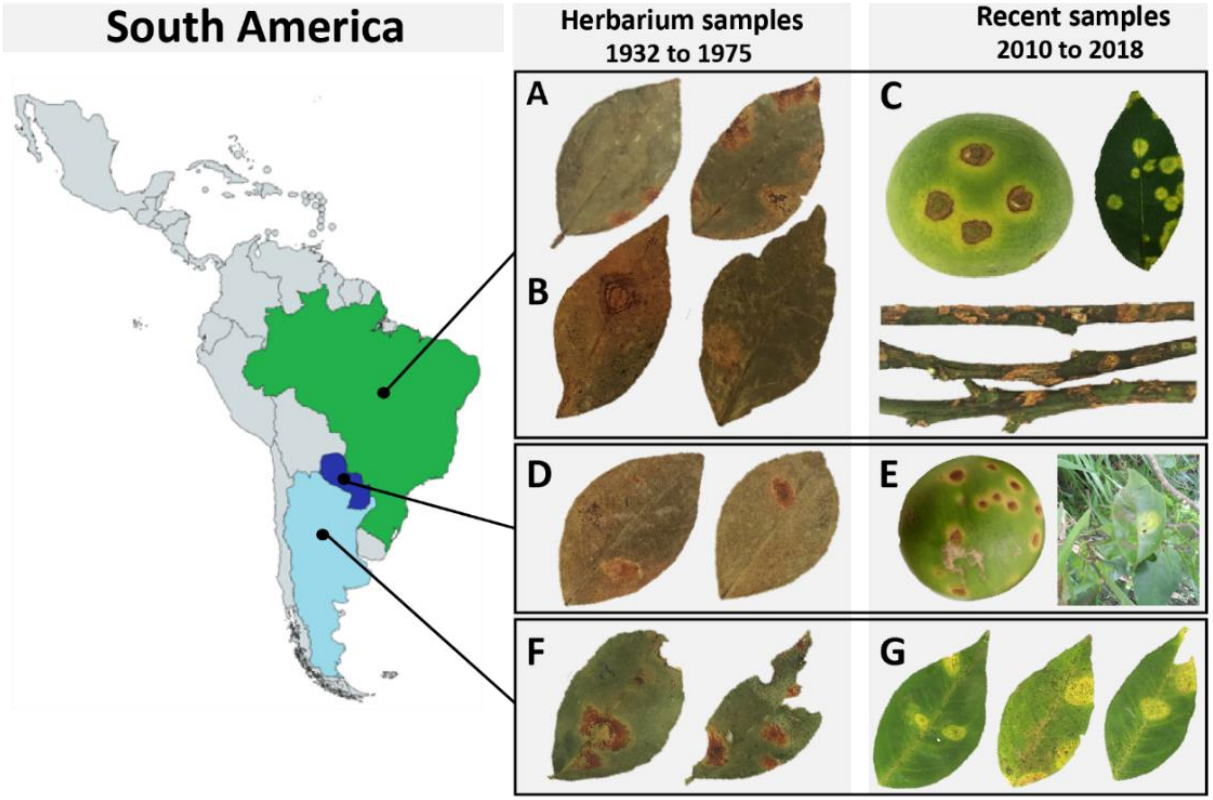

Figure 1. Symptoms associated with citrus leprosis (CL) disease in *Citrus sinensis* tissues. A, B, D, F: herborized leaf samples, maintained in the Herbarium of Instituto Biológico, São Paulo, SP; C, E, G: citrus samples recently collected from orchards. Sample information: CiLV-C strain identified, locality, and year of collection: **A**. CiLV-C CRD, from Jaboticabal, SP, Brazil, 1975; **B**. CiLV-C CRD, from Uruguaiana, RS, Brazil, 1937; **C**. CiLV-C SJP, from Barretos, Brazil, 2018; **D**. CiLV-C_ASU, from Asuncion, Paraguay, 1937; **E**. CiLV-C CRD, from Paraguay, 2010 (fruit) and 2015 (leaf); **F**. CiLV-C CRD, from Misiones, Argentina, 1937 and **G**. CiLV-C CRD, from Corrientes, Argentina, 2017.

3.3.1 Near-complete genome sequencing of new CiLV-C isolates reveals a novel divergent strain in America

Total RNA extracts of leaves from eight herbarium, five fresh, and one -80°C frozen-conserved samples were obtained (Table 3). RNA integrity number (RIN) of the extracts prepared from the herbarium samples was generally low, *e.g.* 1.6 – 2.1, but despite that, *de novo* assembling using the SPAdes algorithm enabled the recovery of more than 80 – 90% of the CiLV-C genomes from the HTS libraries. Particularly, from a sample of sweet orange collected in 1941, few and shorter contigs were obtained and only approximately 60% of the CiLV-C genome could be retrieved. In this particular case, gaps between contiguous contigs were filled after a new round of assembling using BBMap and the CiLV-C genome as a reference. Combined routines raised the genome coverages about 100% in several samples. Initial lower recoveries in some herbarium samples could be correlated with neither the year of collection nor the laboratory where the HTS libraries were processed. It rather seemed to be intrinsically associated with the conservation procedure of every single sample. Recovery rates of viral genomes higher than 98% were obtained from fresh or -80°C- conserved samples using the same pieces of software. Besides viruses in the citrus samples, we recovered the genome of another CiLV-C strain from a siRNA library of *A. thaliana* infected with viruliferous *B. yothersi*, collected in São Jose do Rio Preto, SP, Brazil, in 2015 (Ramos-González et al., 2016). Overall, the complete or near-complete genomes of 14 new isolates of CiLV-C were obtained.

The pairwise comparison of the genomes of the new CiLV-C isolates with those of the type viruses of the clades CRD (NC_008169.1 and NC_008170.1) and SJP (KP336746.1 and KP336747.1) showed values of nucleotide sequence identity that ranged from 84.0 to 99.8% and separates them into three groups (Figure 2) (Supplementary Table 3, Annex I). Twelve isolates showed the highest identity values with the reference sequence of the clade CRD, one with that of the clade SJP, while the isolate collected in Asunción, Paraguay, CiLV-C_PY_Asu02, was almost equally divergent from viruses in the former groups, sharing a global nucleotide sequence identity no higher than 86.0% with the reference sequences.

CiLV-C_PY_Asu02 shows the same genomic organization of the type member of the genus *Cilevirus*. The profile of nucleotide sequence identity between the isolates PY_Asu02 and the type CRD follows the same pattern observed in the comparison between the type viruses of clades SJP and CRD (Figure 2). Deduced amino acid sequences from cistrons of CiLV-C_PY_Asu02 and CiLV-C_CRD show identity values ranging from 81.0%, in the instance of P61, to 100%, for P15, which resembles what is observed in the comparison among proteins from viruses of the clades SJP and CRD (Table 4). Notably, the stretch of nucleotide sequences

at the 5'-end of the RNA2 in CiLV-C_PY_Asu02, which includes the ORF *p15* and part of the IR, is highly conserved between the three isolates, suggesting a common origin of this genomic region. Overall, CiLV-C_PY_Asu02 shows percentages of nucleotide sequence identity lower than 50% with the cileviruses CiLV-C2 and PfGSV (Table 4), confirming that the isolate PY_Asu02 represents a viral diversity previously unknown among members of the species *Citrus leprosis virus C*.

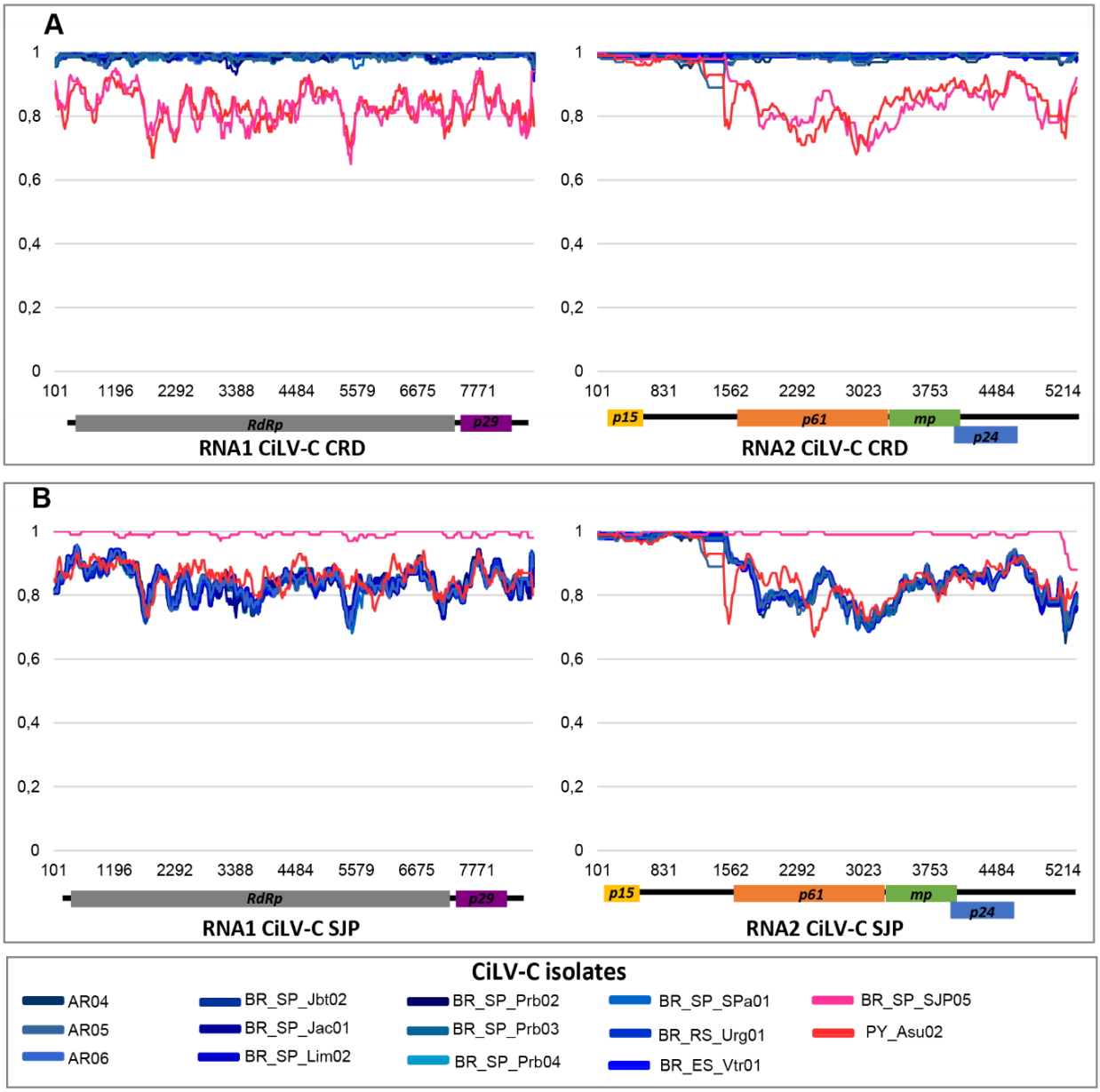

Figure 2. Similarity plots of the nucleotide sequences of RNA1 and RNA2 of CiLV-C calculated by SimPlot version 3.5.1. The full length of the genome nucleotide sequences of 14 CiLV-C isolates sequenced in this study were compared to those of the CiLV-C CRD (**A**) and CiLV-C SJP (**B**). The vertical axis indicates the nucleotide identities between each CiLV-C strain, expressed as percentages, and the horizontal axis indicates the nucleotide positions of RNA1 and RNA2.

Table 4. Identity and similarity between CiLV-C_PY_Asu02 and other members of the genus *Cilevirus.*

CiLV-C PY_Asu02	**CiLV-C CRD**		**CiLV-C SJP**		**CiLV-C2 Co**		**CiLV-C2 Hw**		**PfGSV Snp**	
	nt	aa	nt	aa	nt	aa	nt	aa	nt	aa
RNA1	86.2	-	85.1	-	57.2	-	58.0	-	57.1	-
RdRp	86.3	93.4	88.2	94.9	59.6	58.86	59.8	58.7	59.2	57.9
p29	86.0	94.0	85.6	89.8	43.7	34.54	45.5	33.9	44.4	32.6
RNA2	85.8	-	85.1	-	44.3	-	43.3	-	43.4	-
p15	**98.5**	**100**	**98.5**	**100**	28.5	19.61	34.9	20.4	27.7	19.2
IR	85.0	-	84.0	-	29.1	-	31.4	-	26.9	-
p61	82.1	81.1	82.9	83.8	44.7	31.72	43.4	33.9	45.3	32.6
mp	89.3	95.0	86.5	94.0	55.3	51.16	54.9	50.5	52.5	53.9
p24	88.6	94.0	89.2	94.4	60.9	60.63	60.3	59.7	60.9	60.4

[1]GenBank Accession numbers*:* CiLV-C_PY_Asu02: MT554532 (RNA1) and MT554546 (RNA2) CiLV-C CRD: DQ352194 (RNA1) and DQ352195 (RNA2); CiLV-C SJP: KP336746 (RNA1) and KP336747 (RNA2); CiLV-C2 Co: NC038848 (RNA1) and NC038849 (RNA2); CiLV-C2 Hw: MG253805 (RNA1) and MG253804 (RNA2); and PfGSV Snp: MK804171 (RNA1) and MK804172 (RNA2).

3.3.2 RNA2 of CiLV-C strains harbor signals of recombination

Using GARD and RDP software version 5.5 (Kosakovsky Pond et al., 2006; Martin et al., 2015), the putative signals of recombination events were detected in the RNA2 viral segments of CiLV-C. Pieces of evidence were detected using both the complete (n=18) and partial sequences of the RNA2 molecules (n=51). Partial RNA2 molecules contained the concatenate sequences of p15-IR-mp (Figure 3, Supplementary Table 4).

In the analyses of the complete RNA2 molecules, at least five out of seven programs implemented in the RDP version 5.5 identified recombinant events involving p15 and the intergenic region (IR) (Figure 3, Supplementary Table 4). For instance, in the isolate CiLV-C_BR_SP_SJP01, as well as in the isolate CiLV-C_PY_Asu02, all programs suggested two breakpoints, one inside the IR and the second one closer to the 3'-end of the molecule. In both cases, CiLV-C_BR_SP11 (clade CRD) was detected as the major parent while the minor parents remained unknown. Using the alignments of the concatenates, although the artificial organization of the sequences, two different events were detected. The first one was identified in the p15 gene and the IR of ten isolates belonging to the clade SJP, with CiLV-C_BR_PA_Bel01 as the minor parent and unknown major parents; and the second one in the IR and the beginning of the mp gene, in 29 isolates belonging to the clade CRD, with the isolate CiLV-C_ BR_SE_AJu01 as the major parent and unknown minor parents (Figure 3, Supplementary Table 4). However, no recombination event was detected when only the partial sequences of mp (n= 265) and sequences of the p29 (n= 185) genes were analyzed.

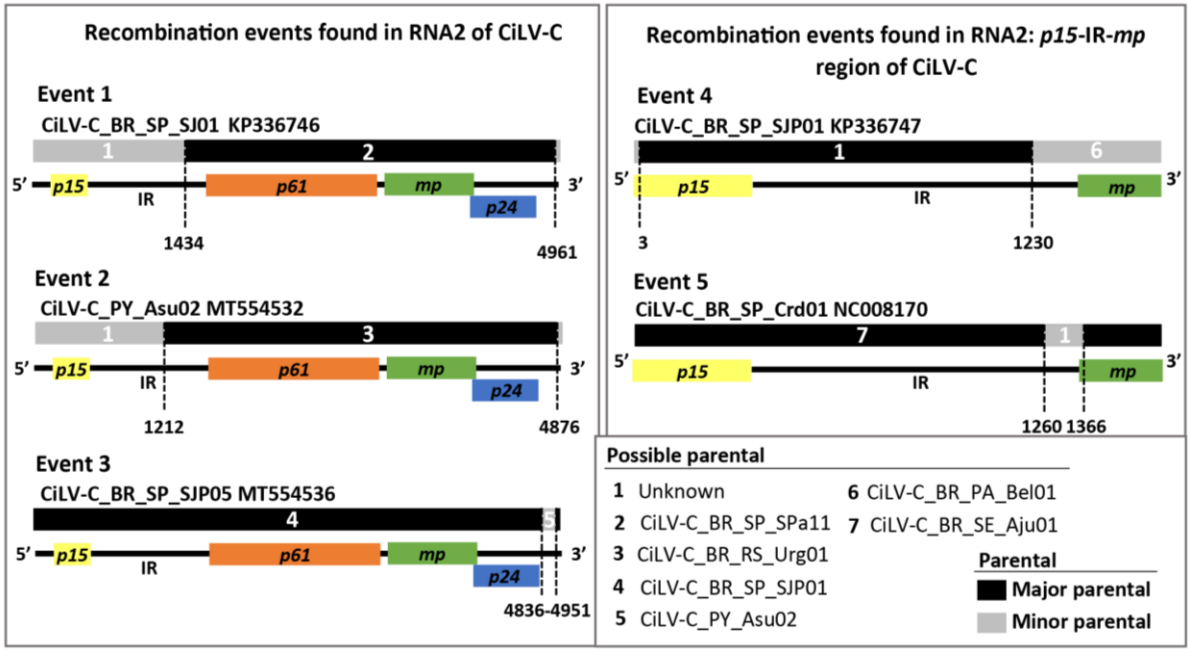

Figure 3. Recombination events found in RNA2 of CiLV-C sequences determined by RDP software version 5.5. Events 1, 2 and 3 were found using 18 complete RNA2 sequences from CiLV-C isolates and events 4 and 5 were found using 51 concatenate sequences of CiLV-C RNA2 fragments [*p15* (393 nt)- intergenic region (934 nt)- *mp* (288)]. Events detected by more than four programs implemented in the software were considered. Event 1 was found in: BR_SP_SJP01 and BR_SP_SJP05; event 2: PY_Asu02; event 3: BR_SP_SJP05; event 4: BR_SP_Csm01, BR_SP_SJP01, BR_SP_SJP03, BR_SP_SJP05, BR_SP_SdM01, BR_SP_SdM02, BR_SP_SdM03, BR_SP_SdM04, BR_SP_SdM05 and BR_SP_SdM06; event 5: BR_SP_Amp01, AR06, BR_SP_Ara01, BR_SP_Bel01, BR_SP_Brm02, BR_DF_Bsb01, BR_SP_Cch01, BR_SP_Crd01, BR_SP_Crd02, BR_GO_Gyn01, BR_SP_Jbt01, BR_SP_Jbt02, BR_SP_Jac01, BR_SP_Lim01, BR_AM_Mao01, BR_PR_ Mgf01, BR_SP_Mrn01, BR_TO_Pnw01, PA01, BR_SP_Prb01, BR_SP_Prb02, BR_SP_Prb04, BR_SP_Prt01, BR_SP_SPa01, BR_SP_Tng01, BR_SP_Tti01, BR_MS_Trn01 and BR_ES_Vtr01.

3.3.3. Phylogenetic and genetic analyses support the existence of three distinct clades of CiLV-C: CRD, SJP, and ASU

Data sets grouping CiLV-C sequences generated in this work and those retrieved from GenBank were used for phylogenetic analyses. They comprised, in sum, 18 complete or near-genomes, 167 *p29* genes, and 247 *mp* genes from strains collected in six countries across Latin America in the period 1932 and 2019.

Bayesian phylogenetic reconstructions using the data sets of *p29* and *mp* genes show three major branches (Figure 4 and Supplementary Figure 1, Annex II), the two largest comprising the isolates of the previously identified lineages CRD and SJP (Figure 4A). The third branch, supported with a high value of posterior probability (0.88) and hereafter calls as the lineage ASU, has only the isolate CiLV-C_PY_Asu02. Separation in three clades is also supported by the analysis of intra- e inter- clades genetic distances. Using both *p29* and *mp*

cistron sequences, interclade distances were, generally, eleven-fold higher than the intraclade distances ($d_{intraclade} \leq 0.01$; $0.116 \leq d_{interclade} \leq 0.173$) (Figure 4B). In the trees constructed using the complete genome sequences, despite the reduced number of sequences available, the organization in clades was the same observed in the analyses of the independent genes (Figure 4C). Remarkably, in the construction of the RNA2 tree, the first 1434 nucleotides of the 5'-end of each molecule were removed considering the putative origin by interclade recombination of this genomic region.

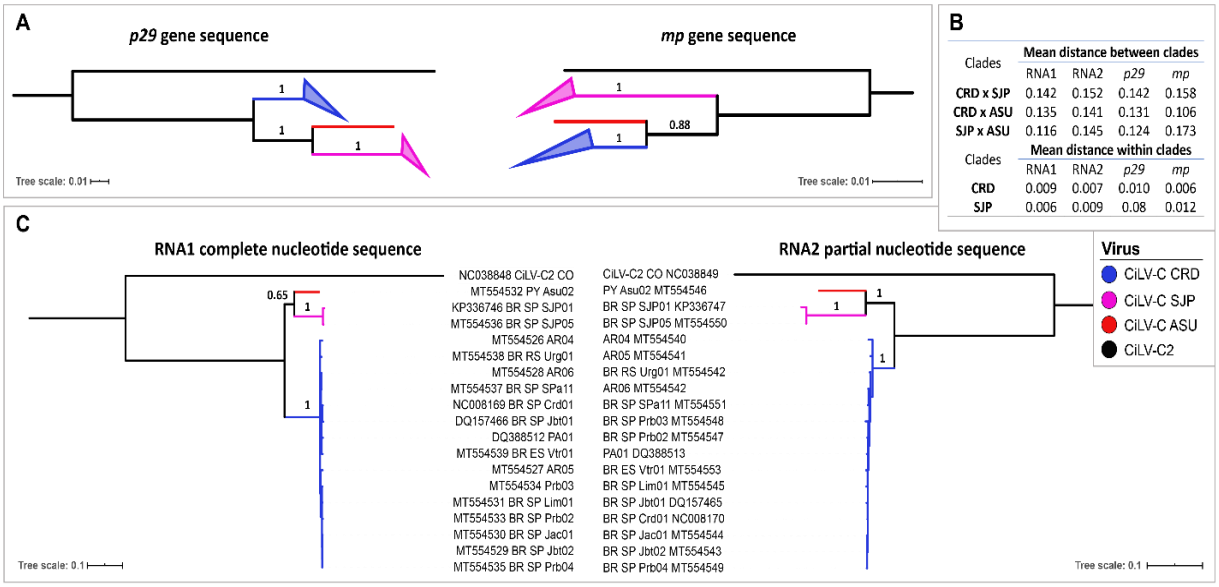

Figure 4. Phylogenetic trees generated by Bayesian inference using MrBayes based on the complete sequence of CiLV-C isolates. The trees were based on *p29* (185 isolates) and *mp* (265 isolates) genes sequences (A), the complete sequence of RNA1 and partial sequence of RNA2 (*p61*, *mp* and *p24* genes) of the 18 CiLV-C isolates (C). (B) The nucleotide distance inter and intra-clades was calculated using MEGA version 7.0.21. The trees were generated with 6,000,000 generations and CiLV-C2_Colombia (NC038848 and NC038849) was used as an outgroup. The names of CiLV-C isolates are based on the collection site and color-coded based according to the CiLV-C strain: CRD (blue), SJP (pink), ASU (red), in addition to CiLV-C2 (black).

Nucleotide (π) and haplotype diversity (Hd) values intrinsic to the CiLV-C population were calculated considering both all and clade-specific members (Table 5). Although the nucleotide diversity of the whole population (SJP+CRD+ASU) is relatively very low ($\pi \sim 0.07$), its values are roughly tenth-fold higher than those observed for the independent clades SJP and CRD ($\pi \sim 0.0006 – 0.001$), which show a haplotype diversity close to 1. The pattern is almost similar regardless of the analyzed gene, *p29* or *mp*.

Table 5. Population genetic parameters and selection estimates for CiLV-C *p29* and *mp* genes.

Dataset populations (isolates number)	H	Hd	π	ω (dN/dS)
***p29* gene**				
SJP+CRD+ASU (185)	154	0.9974	0.07520	0.276
SJP+CRD (184)	153	0.9973	0.07501	0.293
SJP (103)	84	0.994	0.00800	0.341
CRD (81)	69	0.995	0.00991	0.475
***mp* gene**				
SJP+CRD+ASU (265)	69	0.931	0.07267	0.138
SJP+CRD (264)	68	0.931	0.07206	0.166
SJP (187)	49	0.920	0.01017	0.362
CRD (77)	34	0.838	0.00680	0.148

3.3.4 Viruses of the clade CRD are spread across de continent whereas those of the clade SJP are circumscribed to the citrus belt of São Paulo and Minas Gerais

Spatial and temporal distribution of isolates of the clades CRD and SJP were assessed by RT-PCR using clade-specific primers for the detection of *p29* (RNA1) and *p24* (RNA2) genes. Sample distribution reflects preponderance of surveys carried out in commercial field of the citrus belt during last five years according with the prevalence of CL in this region and period. Results were convenient screened indicating the spatial and temporal distribution of members of each clade [Table 6, Figure 5 and Supplementary Table 1 (Annex I)]. Unfortunately, genomic information of the isolate CiLV-C_PY_Asu02 were obtained when a large number of samples had been already evaluated. *In silico* analyses indicated that primers detecting members of the clade CRD and SJP would not be able to detect viruses of the ASU clade under the thermocycling condition carried.

Table 6. Result summary of the differential detection of CiLV-C CRD and SJP strains by RT-PCR and HTS from individual or mixed lesions of *Citrus* spp. Samples

Collection site	Orchard type	Year	CiLV-C distribution				Total
Brazil			CRD	SJP	CDR+SJP same tree[2]	CDR+SJP same lesion[3]	
SP and MG[1]	non-commercial	1932-2019	17	2	0	0	19
SP and MG	commercial	2003-2019	61	237	5	74	377
Other states	non-commercial	1937-2018	10	0	0	0	10
Other countries							
Argentina	non-commercial	1937-2019	14	0	0	0	14
Colombia	non-commercial	2008	1	0	0	0	1
Bolivia	non-commercial	2003	1	0	0	0	1
Paraguay	non-commercial	2010-2019	2	0	0	0	2
							Total = 424

[1]Brazilian states abbreviations: São Paulo (SP) and Minas Gerais (MG); [2]Members of the clades SJP and CRD detected in samples from the same tree; [3]Members of the clades SJP and CRD detected in the same CL lesion.

A broad-based analysis of the data indicates the presence of members of the clade CRD distributed between commercial (57.5%) and non-commercial (42.4%) orchards all over the period 1932-2019. In contrast, members of the clade SJP were almost exclusively found in commercial orchards in the citrus belt São Paulo – Minas Gerais (Table 6, Figure 5). In commercial orchards, in samples collected in the period 2003 – 2019, 62.7% of lesions were infected with viruses of the clade SJP, 16.2% with of the CRD, and 19.6% exhibited mixed infections involved viruses of the two clades (Figure 5). Interestingly, out of commercial orchards, strains of the clade SJP were detected in only two samples collected in a backyard tree in São José do Rio Preto, SP, in the vicinity of the citrus belt São Paulo – Minas Gerais.

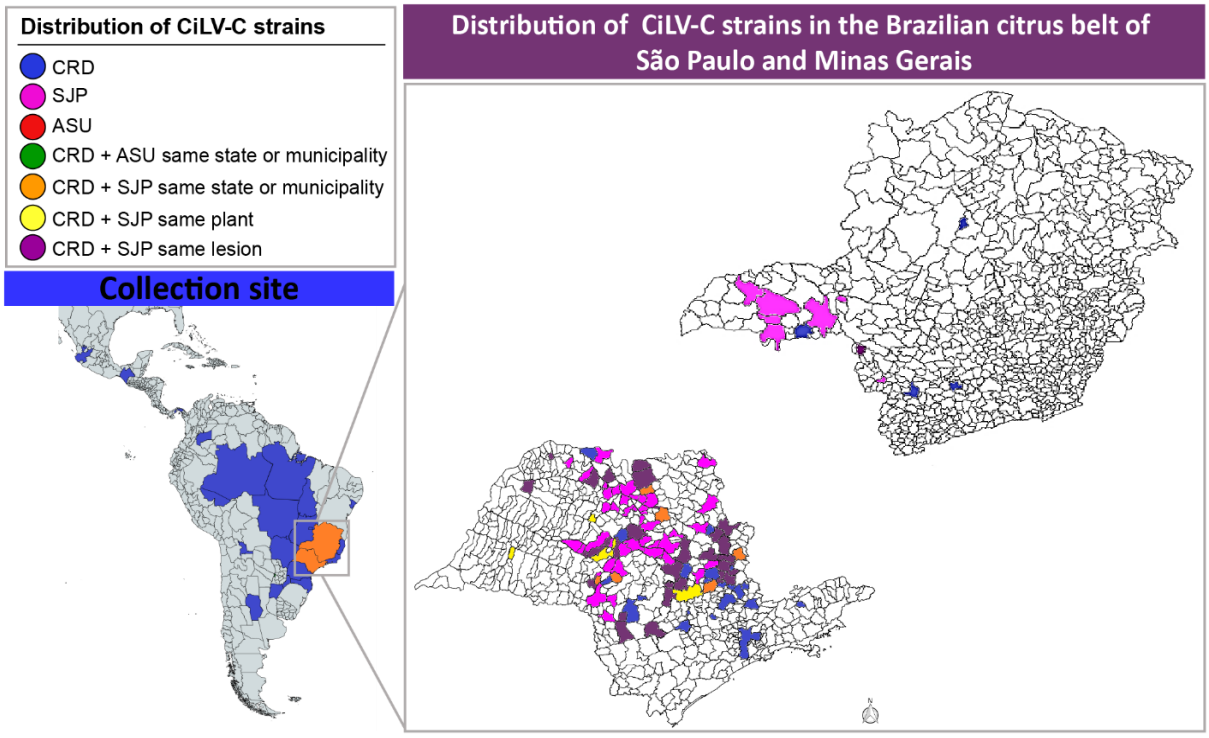

Figure 5. Geographic distribution of CiLV-C strains in Latin America during the period 1932 to 2019. Detection based on RT-PCR assays for the specific identification of *p29* and *p24* genes of CiLV strains CRD and SJP and on HTS for ASU strain. The distribution is color-coded in the American continent i.e. CRD strain (blue), CRD+ASU strains (green) and CRD+SJP strains (orange). Within the citrus belt of Brazil, the distribution is color-coded based on municipalities i.e. CRD strain (blue), SJP strain (pink), both strains in the same lesion (purple), in the same plant (yellow) or in the same municipality (orange). According to only individualized lesion the color-coded based on lesion i.e. CRD strain (blue), SJP strain (pink), both strains in the same lesion (purple).

3.3.5 CiLV-C SJP and CRD subpopulations are mainly under purifying selection

Nucleotide sequences of *p29* and *mp* cistrons suggest purifying selection on the CiLV-C subpopulations CRD and SJP (Table 5). The strength of negative selection is weaker on *p29* (ω = 0.276) than on *mp* (ω = 0.138), but the highest values were detected for the *mp* gen of the clade SJP (ω_{mp} = 0.362).

According with the general ω values, a large number of amino acids were detected under negative selection as supported by the FUBAR, FEL, and MEME programs implemented in Datamonkey 2.0 (Weaver et al., 2018) (Supplementary Table 5, Annex I). Much of the positions detected under negative selection using the FEL method conform those described in a previous report (Ramos-González et al., 2016).

3.3.6 Genetic differentiation, neutrality and pairwise mismatch distribution tests reveal that CiLV-C SJP and CRD are two genetically distinct and expanding subpopulations

Hudson's estimates of the Nearest-neighbor statistic (*Snn*), Fixation index (*Fst*) and *Kst* and *Hst* tests were implemented to evaluate the genetic differentiation between the CiLV-C subpopulations Firstly, values ≥1 for *Snn* and *Fst* tests indicated a highly structured population with significant genetic differentiation between the clades CRD and SJP **(**Table 7). Second, *Kst* and *Hst* values indicated higher level of genetic differentiation considering the *p29* than *mp* genes sequences, and finally, the gene flow (*Nm*) values calculated for both genes were smaller than 0.1 indicating that gene flow among populations was infrequent or almost non-existent (Table 7).

Table 7. Summary of population genetic differentiation analysis of the *p29* and *mp* genes of CiLV-C populations.

Gene	Population	*Snn*	[1]K_{st}	[1]H_{st}	F_{st}[2]	Nm[2]
p29	CRD and SJP	1.00000	0.00260	0.00248	0.93691	0.02
mp	CRD and SJP	1.00000	0.48854	0.05257	0.94267	0.01

[1] P-value: 0.01<P<0.05; [2]Hudson, Slatkin and Maddison 1992: *Fst* and Nm

Additionally, a molecular variance (AMOVA) test was also used for the detection of genetic differentiation between the CiLV-C subpopulations (Table 8). This analysis revealed that the variance between the subpopulations CDR and SJP is about 94%, whereas it was only 6% within the populations (Table 8). With AMOVA statistics close to 1, the Fst results were corroborated the hypothesis of differentiation between CiLV-C subpopulations cannot be rejected.

Table 8. Summary of the analysis of molecular variance (AMOVA) for populations of CiLV-C strains CRD and SJP based on *p29* and *mp* genes.

Source of variance	d.f.	Sum of squares	Variance components	Percentage	AMOVA statistics	*p* value
***p29* gene**						
Among populations	1	5049.741	55.64594 Va	94.08	0.94081	0.00000
Within populations	182	637.193	3.50106 Vb	5.92		
Total	183	5686.935	59.14701			
***mp* gene**						
Among populations	1	2191.733	20.07944 Va	93.48	0.93480	0.00000
Within populations	262	366.904	1.40040 Vb	6.52		
Total	263	2558.636	21.47984			

Analyses of neutrality tests in CiLV-C subpopulations were estimated using three statistic tests (Fu and Li's D and F, Fu's Fs and Tajima's D) (Table 9). All values for *p29* and the *mp* genes were negative or non-significant. These observations led us to hypothesize that CiLV-C subpopulations are not neutral, possibly in expansion. To address this question, we determined whether the data fit the sudden expansion model using the sum of square deviations (SSD) and Harpending's Raggedness index (HRI). Both, SSD and HR values were non-significant (Table 9), supporting the hypothesis of demographic expansion.

Table 9. Summary of genetic diversity indices, pairwise mismatch distributions and neutrality tests (Fu and Li's, Fu's Fs and Tajima's D) on *p29* and *mp* genes of CiLV-C subpopulations.

Sub-population	*s*	*k*	*ϴ*	Mismatch		Neutrality tests			
				SSD[a]	HRI[a]	Fu and Li's D[b]	Fu and Li's F[b]	Fu's Fs[c]	Tajima's D
***p29* gene**									
SJP	133	6.36	138	0.0064	0.0073	-5.3709	-4.97152	-34,434	-2.52017[d]
CRD	149	7.82	153	0.0045	0.0033	-5.9314	-5.43207	-82,418	-2.54014[d]
***mp* gene**									
SJP	51	2.93	51	0.0712	0.2123	-5.8343	-4.99830	-33,405	-1.99617[e]
CRD	36	1,96	27	0.0021	0.0383	-4.8247	-4.61901	-27,746	-2.26896[f]

P-value: [a] not significant; [b] $P < 0.02$, [c]none of the statistics gave significant p-values; [d]$P < 0.001$, [e]$P < 0.05$ and [f]$P < 0.01$. Nomenclature: Number segregating sites (*s*), mean number nucleotide differences (*k*), population mean mutation rate per site (*ϴ*), sum of squared deviation (SSD) and Harpending's Raggedness index (HRI).

3.3.7 Most recent common ancestor of CiLV-C lineages arose ~1,500 years ago

To investigate the evolutionary dynamic and the time to the most recent common ancestor (tMRCA) of CiLV-C strains, three MCC trees were constructed using the complete sequence of the *p29* gene, the partial sequence of the *mp* gene, and their concatenate. The tree generated with the concatenate of the *p29* and *mp* genes was selected according with its

temporal signal and trace files evaluated by TempEst version 1.5.3 (Rambaut et al., 2016) and Tracer version 1.7 software (Rambaut et al., 2018). It should be noted, however, that the topology of this tree was similar to the those generated using either the *p29* or *mp* sequences (data not shown).

The MCC phylogenetic tree was generated with 127 CiLV-C sequences isolated from *C. sinensis* (n= 125) and *Arabidopsis thaliana* (from experimental transmission n=2). In summary, it includes isolates collected in Argentina (n=4), Panama (n=1), Paraguay (n=1) and Brazil (n= 111) from the last 87 years. The linear regression exploration of root-to-tip distances as a function of sampling time revealed a moderate temporal signal in the dataset (correlation coefficient = 0.35 and R^2 = 0.13) (Supplementary Figure 2, Annex II). The characteristic of low genetic diversity within the CiLV-C subpopulations ($\pi < 0.02$) directly influences the non-relationship of diversity over time. However, the MCC was based on effective sample sizes >300 for the parameters.

The most recent common ancestor (MRCA) for CiLV-C was dated back to 500 A.D. [supported by a posterior probability (PP) of 1 and 95% highest probability density (HPD) of 94-856 years A.D.] (node A, Figure 6). From this putative ancestral virus diverged two lineages. One of them diversified into the clade SJP, while the another subsequently diverged into two new lineages that arose from an ancestor represented in the node B. Virus in the node B, likely gave rise to the lineages ASU and CRD in 740 A.D. (PP = 0.87 and HPD 95% = 380-1041 years A.D.). Considering the data comprised by the posterior probability distributions of the tMRCA, the diversification events depicted by the nodes A and B might overlap each other (Figure 6). However, these events took place before the intensive dispersion and diversification of viruses inside the clade CRD, dated in 1870 A.D. (node C, PP = 1 and HPD 95% = 1810-1895 years A.D.), and clade SJP, dated in 1950, less than 100 years ago (node D, PP = 1 and HPD 95%= 1904-1956 years A.D.) (Figure 6).

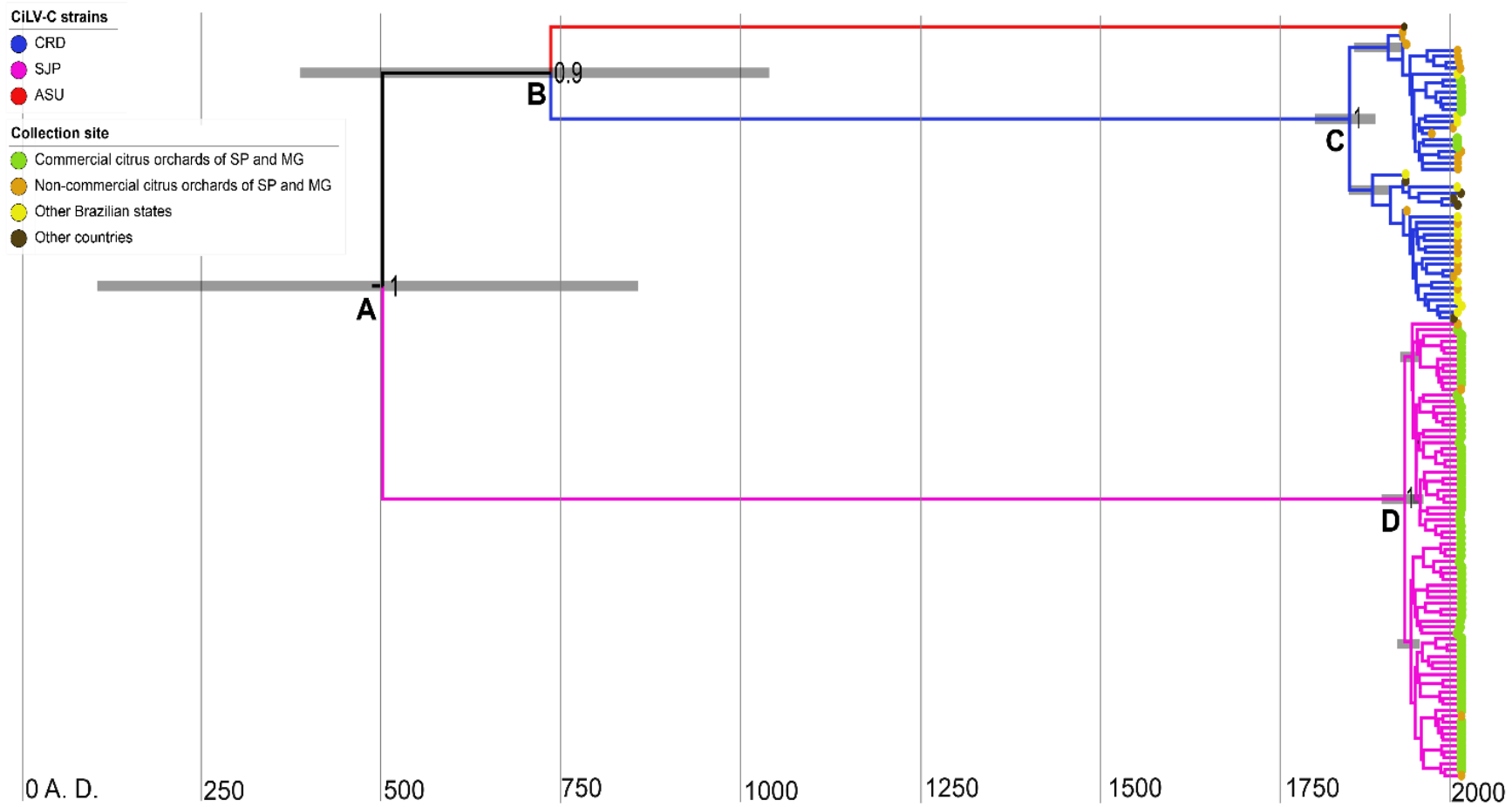

Figure 6. Bayesian phylogenetic analysis and divergence time estimation in BEAST version 1.10.4 based on the concatenate of the complete nucleotide sequence of the *p29* (795 nt) and partial sequence of the *mp* genes (288 nt) from 127 CiLV-C isolates of the last 87 years in South America. The X-axis shows the years (thousands of years, 0 A.D. to 2018), the color of the clades represent the three strains: CRD (blue), SJP (pink) and ASU (red) and the color of the labels represent the collection sites: commercial citrus orchards of São Paulo (SP) and Minas Gerais (MG) (green), non-commercial backyards of SP and MG (ocher), other Brazilian states (yellow), and other countries (brown). Node bars correspond to the 95% HPD interval of the node height, node labels represent the posterior probability and scale bar of the BEAST trees correspond to the time in years. The phylogenetic tree was viewed and edited using IcyTree.

3.4 DISCUSSION

Citrus leprosis disease (CL) is a serious multi-etiological viral pathology affecting citrus in Latin America. In Brazil, the type of CL caused by the cilevirus CiLV-C is the prevalent form and economically, the most detrimental viral disorder infecting the citrus orchards (Ramos-González et al., 2018a). A former study reported the existence of two viral clades inside the population of CiLV-C (Ramos-González et al., 2016), but the ecology of their subpopulations could not be deeply assessed due to the limited number of viral isolates available. In the present approach, which includes both fresh and herbarium citrus samples infected by CiLV-C, we obtained the complete and partial nucleotide sequences of the viral *p29* and *mp* cistrons, respectively, from 267 viral isolates. In particular, we revealed the near-complete genomes of 14 new isolates of CiLV-C mostly collected during the first half of the last century. Overall, this study comprises the largest collection of CiLV-C sequences ever considered.

Global analysis of the generated dataset by phylogenetic and populational statistics tools confirmed the existence of the two previously identified clades CRD and SJP (Ramos-González et al., 2016), whereas negative results of the Fu and Li's D and Tajima's D neutrality tests and the non-significative pairwise mismatch distribution indicate a viral population in expansion (Table 9). CRD and SJP subpopulations are genetically well-differentiated ($Fst \geq 0.94$), show a very low genetic diversity ($\pi = \sim 0.01$) where almost each haplotype is unique ($0.8 < Hd < 0.99$), and, as a whole, are under purifying selection ($\omega < 0.5$). Such values are the quantitative expression ensuing the sum of biological factors underlying the CL pathosystem, which, in general, lead the CiLV-C subpopulations to continuous bottlenecks (Ramos-González et al., 2016). CiLV-C has a very limited host range, infects a reduced number of cells around the inoculation sites, and is exclusively transmitted by *Brevipalpus* mites, the only way the virus can reach new infection foci even within a single leaf due to its reduced cell to cell movement capacity (Freitas-Astúa et al., 2018). Similarly, low variability and purification have been also observed in the population of coffee ringspot virus, a dichorhavirus that, as CiLV-C, is transmitted by *Brevipalpus* mites and also cause non-systemic infections (Ramalho et al., 2015).

While the majority of the evaluated samples comprised CiLV-C isolates belonging to the clades CRD and SJP, the herbarium sample collected in Paraguay, in 1932, revealed unique (Figures 4 and 6). In the phylogenetic analyses using either partial or complete genomic sequences, the isolate CiLV-C_PY_Asu02 found in that sample diverged from the others forming a third clade, identified as ASU (Figure 4). The genome of CiLV-C_PY_Asu02 has the typical organization of cileviruses, with roughly 86.0% nucleotide sequence identity with

the reference genomes of type members in the clades CRD and SJP. Notably, the stretch encompassing the 5'-end of its RNA2 shows high conservation with members of the other two clades. According to *in silico* analyses, this fragment has a putative origin by recombination, not only in the isolate CiLV-C_PY_Asu02 but also in members of the clade CRD, as previously indicated (Ramos-González et al., 2016) (Figure 3). Recombination can result in viruses with improved virulence, adaptability to a changing environment, or expansion in the host and vector ranges (García-Arenal et al., 2001). Despite the role of the 5'-end of the CiLV-C RNA2 is not well understood yet, its extremely conserved nucleotide sequence across viruses of the three CiLV-C clades (Figure 2) highlights the participation of this region on the viral biology and, particularly, points out the involvement of recombination events shaping the genome of cileviruses.

The collection of CiLV-C infected samples compiled in this work is the largest ever obtained. Its composition is heterogeneous, showing temporal and geographical biases following the trend of the relative importance of citrus crop and the incidence of CL across the continent. Despite this, the holistic analysis of the dataset discloses ecological relationships between members of the clades CRD and SJP, and identifies some corollaries whose authenticity still need to be proven in future works: (*i*) inside the citrus belt SP-MG, viruses of both lineages are unevenly distributed, (*ii*) members of the clade SJP are more frequently found in single infection (63,0%) than those of the CRD (16%), (*iii*) mixed infections in the same lesion were detected in 20% of samples, whereas (*iv*) simultaneous infection of viruses of the clades CRD-SJP in the same orchard or tree accounts for 1% of samples (Figure 5), (*v*) viruses of the clade SJP were detected neither in areas out the citrus belt SP-MG nor in samples collected before 2015, and (*vi*) except for the isolate Asu02, belongs to tentative clade ASU, all other samples collected out of the citrus belt were infected by viruses of the clade CRD. The high prevalence of viruses of the clade SJP in commercial orchards of the citrus belt suggests this population could have some adaptive advantages over those in the CRD population. However, although preliminary studies on the diversity of *Brevipalpus* mites in Brazil revealed a large genetic variability of the *B. yothersi* population, the association between the mite haplotypes and either host plants or geographical origin remains to be studied (Sánchez-Velázquez et al., 2015; Salinas-Vargas et al., 2016). Similarly, vector interaction with clade-specific viruses and its significance on virus ecology are also lacking. On the other hand, the detection of mixed infections in a large number of CL lesions, besides gives physical support to the recombination processes detected *in silico*, supposes the simultaneous presence of viruses from different clades transmitted by a single mite, or the sequential arrival of individuals

bearing a single viral strain to the same lesion. Perhaps all possibilities may happen in nature, and whatever the case, the increased attractiveness of *Brevipalpus* mites by CiLV-C infected leaves of *Arabidopsis thaliana* (Arena et al., 2016) might certainly contribute to the occurrence of mixed infections.

Natives of Southwest Asia, plants of the genus *Citrus* have spread worldwide and their introduction into America is intrinsically linked to the advent of the European colonization in the early 16th century. Commercial exploration of the citrus crop in Brazil began in the 17th century (Carvalho et al., 2019; Passos et al., 2019), but expanded and became one of the most important Brazilian commodities in the middle of the 20th century (Mattos Jr. et al., 2005; Neves et al., 2011; Carvalho et al., 2019). According to the phylodynamic analysis carried out in this work, the time of the most recent common ancestor (tMRCA) of CiLV-C lineages was dated in 500 A.D., whereas intensive but less deep diversification processes inside the clades CRD and SJP have been occurring from the 19th century. Bringing together the temporal lines of these two events, some straightforward interpretations reveal that, besides the brief coevolution of CiLV-C with its citrus hosts, ancestral of the three viral clades originated in contact with wild ecosystems of South America, and that, upon their interaction with citrus plants, the expansion of the citriculture in Brazil and other American countries likely contributed with the intraclade diversification of CiLV-C.

CL is considered an emerging disease affecting a crop with a relatively low genetic diversity and high-density plantings. Increasing pieces of evidence indicate that wild ecosystems are a major source of diversity of plant viruses, which have co-evolved with their wild hosts long before they were domesticated (Pagan and Holmes, 2010; Rodríguez-Nevado et al., 2017). Besides some *Citrus* spp., only plants of the species *Commelina benghalensis*, and *Swinglea glutinosa* are reported as natural hosts of CiLV-C (León et al., 2008; Nunes et al., 2012; Garita et al., 2014; Freitas-Astúa et al., 2018), all of them are exotic to the Americas (Weniger et al., 2001; Webster et al., 2005). Therefore, the natural host range of CiLV-C is likely not yet fully known or the interaction with its wild hosts no longer exists in nature. The distribution and dispersion of cileviruses are mediated by the polyphagous *Brevipalpus* mites, capable of feeding on more than 150 genera of plants, including several crops, ornamentals, and forest plants (Childers et al., 2003a). Consequently, the CiLV-C vector can be the main path between native plants in the Americas and exotic plants (Freitas-Astúa et al., 2018). Similarly to CiLV-C, the cilevirus CiLV-C2, which also infects citrus plants, shows a narrow range of known natural hosts, *e.g. Citrus* sp., *S. glutinosa*, *Hibiscus* sp., and *Dieffenbachia* sp. (Melzer et al., 2013b; Roy et al., 2015a, 2019). In contrast, PfGSV is the only known cilevirus

infecting native plants of the Americas, e.g. *Passiflora* spp., it can be found naturally infecting more than other twenty plant species and, notably, symptoms are not as restricted as those observed in citrus plants infected by CiLV-C (Kitajima et al., 1997; Ramos-González et al., 2020). Obviosly, since the interaction of CiLV-C with citrus plants is dominated by an hipersensitive-like response, the expansion of the host range to *Citrus* spp. has resulted in CiLV-C fittnes reduction.

3.5 CONCLUSIONS

Altogether this study provides the most complete snapshot of the CiLV-C population. Throughout molecular epidemiology analyses, we have revealed the structure, sources of the genetic variability, and forces involved in the evolution of this viral population. The evolutionary history of CiLV-C might be intensively marked by the interaction with its main host, *Citrus* spp. from the last 500 years. Maximum values of variability inside the population are typified by its subdivision into the clades ASU, first identified in this study, CRD, and SJP, which are the consequence of diversification processes that occurred before the viral contact with citrus host. Moreover, besides the highly frequent bottlenecks as a result of mite transmission, the incompatible host-virus interaction with an intensive crop with a relatively low genetic variability, likely prevents the expansion and diversification of the CiLV-C subpopulations. In practical terms, our results confirm the prevalence and wide distribution of CiLV-C in the largest citrus commercial area of Brazil and reveal the urgency for updated detection systems able to identify the presence of CiLV-C variants whose epidemiological profiles are currently unknown.

REFERENCES

Arena, G. D., Bergamini, M. P., Tassi, A. D., Kitajima, E. W., Kubo, K. S., and Freitas-Astúa, J. (2013). Citrus leprosis virus C infects *Arabidopsis thaliana*, the model for plant-pathogen interactions. *J. Plant Pathol.* 95, 448. doi:10.4454/JPP.V95I2.003.

Arena, G. D., Ramos-González, P. L., Falk, B. W., Clare, L., Ramos-González, P. L., Freitas-astúa, J., et al. (2020). Plant immune system activation upon citrus leprosis virus C infection is mimicked by the ectopic expression of the P61 viral protein. *Front. Microbiol.* 11, 0–24. doi:10.3389/fpls.2020.01188.

Arena, G. D., Ramos-González, P. L., Nunes, M. A., Alves, M. R., Camargo, L. E. A., Kitajima, E. W., et al. (2016). Citrus leprosis virus C infection results in hypersensitive-like response, suppression of the JA/ET plant defense pathway and promotion of the colonization of its mite vector. *Front. Plant Sci.* 7, 1757. doi:10.3389/FPLS.2016.01757.

Bankevich, A., Nurk, S., Antipov, D., Gurevich, A. A., Dvorkin, M., Kulikov, A. S., et al. (2012). SPAdes: A new genome assembly algorithm and its applications to single-cell

sequencing. *J. Comput. Biol.* 19, 455–477. doi:10.1089/cmb.2012.0021.

Bassanezi, R. B., Czermainski, A. B. C., Laranjeira, F. F., Moreira, A. S., Ribeiro, P. J., Krainski, E. T., et al. (2019). Spatial patterns of the Citrus leprosis virus and its associated mite vector in systems without intervention. *Plant Pathol.* doi:10.1111/ppa.12930.

Bastianel, M., Pereira-Martin, J. A., Novelli, V. M., Freitas-Astúa, J., and Nunes, M. A. (2018). Citrus leprosis resistance within the citrus group. *VirusDisease*, 1–8. doi:10.1007/s13337-018-0489-6.

Bolger, A. M., Lohse, M., and Usadel, B. (2014). Genome analysis Trimmomatic: a flexible trimmer for Illumina sequence data. 30, 2114–2120. doi:10.1093/bioinformatics/btu170.

Bushnell, B. (2014). BBMap : A Fast , Accurate , Splice-Aware Aligner. *Splice-Aware Aligner*, 3–5. Available at: https://escholarship.org/uc/item/1h3515gn [Accessed September 22, 2020].

Carvalho, S. A., Girardi, E. A., Filho, F. de A. A. M., Ferrarezi, R. S., and Filho, H. D. C. (2019). *Advances in citrus propagation in Brazil*. doi:10.1590/0100-29452019422.

Chabi-Jesus, C., Ramos-González, P. L., Guerra-Peraza, O., Kitajima, E. W., Harakava, R., Beserra Jr., J. E. A., et al. (2018). Identification and characterization of citrus chlorotic spot virus, a new dichorhavirus associated with citrus leprosis-like symptoms. *Plant Dis.* 102, 1588–1598. doi:10.1094/PDIS-09-17-1425-RE.

Childers, C. C., French, J. V., and Rodrigues, J. C. V. (2003). *Brevipalpus californicus*, *B. obovatus*, *B. phoenicis*, and *B. lewisi* (Acari: Tenuipalpidae): a review of their biology, feeding injury and economic importance. *Exp. Appl. Acarol.* 30, 5–28. doi:10.1023/B:APPA.0000006543.34042.b4.

Excoffier, L., and Lischer, H. E. L. (2010). Arlequin suite ver 3 . 5 : a new series of programs to perform population genetics analyses under Linux and Windows. 564–567. doi:10.1111/j.1755-0998.2010.02847.x.

Freitas-Astúa, J., Ramos-González, P. L., Arena, G. D., Tassi, A. D., and Kitajima, E. W. (2018). *Brevipalpus*-transmitted viruses: parallelism beyond a common vector or convergent evolution of distantly related pathogens? *Curr. Opin. Virol.* 33, 66–73. doi:10.1016/j.coviro.2018.07.010.

Fu, Y.-X., and Li, W.-H. (1993). Statistical tests of neutrality of mutations. Available at: http://www.genetics.org/content/genetics/133/3/693.full.pdf [Accessed March 25, 2019].

Fu, Y. X. (1997). Statistical tests of neutrality of mutations against population growth, hitchhiking and background selection. *Genetics* 147, 915–925.

García-Arenal, F., Fraile, A., and Malpica, J. M. (2001). Variability and genetic structure of plant virus populations. *Annu. Rev. Phytopathol.* 39, 157–186. doi:10.1146/annurev.phyto.39.1.157.

Garita, L. C., Tassi, A. D., Calegario, R. F., Freitas-Astúa, J., Salaroli, R. B., Romão, G. O., et al. (2014). Experimental host range of citrus leprosis virus C (CiLV-C). *Trop. Plant Pathol.* 39, 43–55. doi:10.1590/S1982-56762014005000004.

Harpending, H. C., and Harpend, H. C. (1994). Signature of ancient population growth in a low-resolution mitochondrial dna mismatch distribution. *Hum. Biol.* 66, 591–600.

Hudson, R. R. (2000). A new statistic for detecting genetic differentiation. *Genetics* 155, 2011–2014.

Hudson, R. R., Slatkin, M., and Maddison, W. P. (1992). Estimation of levels of gene flow from DNA sequence data. *Genetics* 132, 583–589.

Huelsenbeck, J. P., and Ronquist, F. (2001). MRBAYES: Bayesian inference of phylogenetic trees. Yang and Rannala doi:10.1093/bioinformatics/17.8.754.

Kearse, M., Moir, R., Wilson, A., Stones-havas, S., Cheung, M., Sturrock, S., et al. (2012). Geneious Basic : An integrated and extendable desktop software platform for the organization and analysis of sequence data. *Bioinformatics* 28, 1647–1649. doi:10.1093/bioinformatics/bts199.

Kitajima, E. W., Chagas, C. M., and Rodrigues, J. C. V (2003). *Brevipalpus*-transmitted plant virus and virus-like diseases: cytopathology and some recent cases. *Exp. Appl. Acarol.* 30, 135–60.

Kitajima, E. W., Kubo, K. S., Ferreira, P. de T. O., Alcântara, B. K. de, Boari, A. J., Gomes, R. T., et al. (2008). Chlorotic spots on *Clerodendrum*, a disease caused by a nuclear type of Brevipalpus (Acari:Tenuipalpidae) transmitted virus. *Sci. Agric.* 65, 36–49. doi:10.1590/S0103-90162008000100006.

Kitajima, E. W., Rezende, J. A. M., Rodrigues, J. C. V., Chiavegato, L. G., Piza Júnior, C. T., and Morozini, W. (1997). Green spot of passion fruit, a possible viral disease associated with infestation by the mite *Brevipalpus phoenicis*. *Fitopatol. Bras.* 22, 555–559.

Kondo, H., Fujita, M., Hisano, H., Hyodo, K., Andika, I. B., and Suzuki, N. (2020). Virome analysis of aphid populations that infest the barley field: the discovery of two novel groups of nege/kita-like viruses and other novel rna viruses. *Front. Microbiol.* 11, 509. doi:10.3389/fmicb.2020.00509.

Kosakovsky Pond, S. L., Posada, D., Gravenor, M. B., Woelk, C. H., and Frost, S. D. W. (2006). GARD: a genetic algorithm for recombination detection. *Bioinformatics* 22, 3096–8. doi:10.1093/bioinformatics/btl474.

Kubo, K. S., Stuart, R. M., Freitas-Astúa, J., Antonioli-Luizon, R., Locali-Fabris, E. C., Coletta-Filho, H. D., et al. (2009). Evaluation of the genetic variability of orchid fleck virus by single-strand conformational polymorphism analysis and nucleotide sequencing of a fragment from the nucleocapsid gene. *Arch. Virol.* 154, 1009–14. doi:10.1007/s00705-009-0395-8.

Kumar, S., Stecher, G., and Tamura, K. (2016). MEGA7: Molecular evolutionary genetics analysis version 7.0 for bigger datasets. *Mol. Biol. Evol.* 33, 1870–1874. doi:10.1093/molbev/msw054.

Langmead, B., and Salzberg, S. L. (2012). Fast gapped-read alignment with Bowtie 2. *Nat. Methods* 9, 357–359. doi:10.1038/nmeth.1923.

Leastro, M. O., Yorlenis, D., Castro, O., and Freitas-astúa, J. (2020). Citrus Leprosis Virus C encodes three proteins with gene silencing suppression activity. 11, 1–16. doi:10.3389/fmicb.2020.01231.

León, M. G., Becerra, C. H., Freitas-Astúa, J., Salaroli, R. B., and Kitajima, E. W. (2008). Natural infection of *Swinglea glutinosa* by the citrus leprosis virus cytoplasmic type (CiLV-C) in Colombia. *Plant Dis.* 92, 1364–1364. doi:10.1094/PDIS-92-9-1364C.

Letunic, I., and Bork, P. (2019). Interactive Tree of Life (iTOL) v4: Recent updates and new developments. *Nucleic Acids Res.* 47, 256–259. doi:10.1093/nar/gkz239.

Locali-Fabris, E. C., Freitas-Astúa, J., and Machado, M. A. (2012). “Genus *Cilevirus*.

International Committee on Taxonomy of Viruses," in *Virus Taxonomy*, eds. A. King, M. Adams, E. Carstens, and E. Lefkowitz (London, United Kingdom: Elsevier/Academic Press), 1139–1142.

Locali-Fabris, E. C., Freitas-Astúa, J., Souza, A. A., Takita, M. A., Astúa-Monge, G., Antonioli-Luizon, R., et al. (2006). Complete nucleotide sequence, genomic organization and phylogenetic analysis of Citrus leprosis virus cytoplasmic type. *J. Gen. Virol.* 87, 2721–9. doi:10.1099/vir.0.82038-0.

Locali, E. C., Freitas-Astua, J., de Souza, A. A., Takita, M. A., Astua-Monge, G., Antonioli, R., et al. (2003). Development of a molecular tool for the diagnosis of leprosis, a major threat to citrus production in the Americas. *Plant Dis.* 87, 1317–1321. doi:10.1094/PDIS.2003.87.11.1317.

Martin, D. P., Murrell, B., Golden, M., Khoosal, A., and Muhire, B. (2015). RDP4: Detection and analysis of recombination patterns in virus genomes. *Virus Evol.* 1, vev003–vev003. doi:10.1093/ve/vev003.

Mattos Jr., D. de, Negri, ose D. De, Pio, R. M., and Junior Pompeu, J. (2005). *Citros*. doi:10.1146/annurev-phyto-080417-050052.

Melzer, M. J., Sether, D. M., Borth, W. B., and Hu, J. S. (2013a). Characterization of a virus infecting *Citrus volkameriana* with citrus leprosis-like symptoms. *Phytopathology* 102, 122–7. doi:10.1094/PHYTO-01-11-0013.

Melzer, M. J., Simbajon, N., Carillo, J., Borth, W. B., Freitas-Astúa, J., Kitajima, E. W., et al. (2013b). A cilevirus infects ornamental hibiscus in Hawaii. *Arch. Virol.* doi:10.1007/s00705-013-1745-0.

Mushegian, A. R., and Elena, S. F. (2015). Evolution of plant virus movement proteins from the 30K superfamily and of their homologs integrated in plant genomes. *Virology* 476, 304–315. doi:10.1016/j.virol.2014.12.012.

Neves, M. F., Trombin, V. G., Lopes, F. F., Kalaki, R., and Milan, P. (2011). "The citrus sector in Brazil," in *The orange juice business* (Wageningen: Wageningen Academic Publishers), 18–20. doi:10.3920/978-90-8686-739-4_1.

Nguyen, L. T., Schmidt, H. A., Von Haeseler, A., and Minh, B. Q. (2015). IQ-TREE: A fast and effective stochastic algorithm for estimating maximum-likelihood phylogenies. *Mol. Biol. Evol.* 32, 268–274. doi:10.1093/molbev/msu300.

Nunes, M. A., Bergamini, M. P., Coerini, L. F., Bastianel, M., Novelli, V. M., Kitajima, E. W., et al. (2012). Citrus leprosis virus C naturally infecting *Commelina benghalensis* , a prevalent monocot weed of citrus orchards in Brazil. *Plant Dis.* 96, 770–770. doi:10.1094/PDIS-11-11-0925-PDN.

Nunes, M. A., de Carvalho Mineiro, J. L., Rogero, L. A., Ferreira, L. M., Tassi, A. D., Novelli, V. M., et al. (2018). First report of *Brevipalpus papayensis* Baker (Acari: Tenuipalpidae) as vector of Coffee ringspot virus and Citrus leprosis virus C. *Plant Dis.* doi:10.1094/PDIS-07-17-1000-PDN.

Pagan, I., and Holmes, E. C. (2010). Long-Term Evolution of the *Luteoviridae*: Time Scale and Mode of Virus Speciation. *J. Virol.* 84, 6177–6187. doi:10.1128/jvi.02160-09.

Passos, O. S., Souza, J. S., Bastos, D. C., Girardi, E. A., Gurgel, F. de L., Garcia, M. V. B., et al. (2019). "Citrus Industry in Brazil with Emphasis on Tropical Areas," in *Citrus - Health Benefits and Production Technology* (IntechOpen). doi:10.5772/intechopen.80213.

Quito-Avila, D. F., Brannen, P. M., Cline, W. O., Harmon, P. F., and Martin, R. R. (2013). Genetic characterization of Blueberry necrotic ring blotch virus, a novel RNA virus with unique genetic features. *J. Gen. Virol.* 94, 1426–1434. doi:10.1099/vir.0.050393-0.

Quito-Avila, D. F., Freitas-Astúa, J., and Melzer, M. J. (2020). "Bluner-, Cile-, and Higreviruses (*Kitaviridae*).," in *Reference Module in Life Sciences* (Elsevier). doi:10.1016/B978-0-12-809633-8.21248-X.

Ramalho, T. O., Figueira, A. R., Wang, R., Jones, O., Harris, L. E., Goodin, M. M., et al. (2015). Detection and survey of coffee ringspot virus in Brazil. *Arch. Virol.* 161, 335–343. doi:10.1007/s00705-015-2663-0.

Rambaut, A., Drummond, A. J., Xie, D., Guy, B., and Marc, A. S. (2018). Posterior summarization in bayesian phylogenetics using Tracer 1 . 7. 67, 901–904. doi:10.1093/sysbio/syy032.

Rambaut, A., Lam, T. T., Carvalho, L. M., and Pybus, O. G. (2016). Exploring the temporal structure of heterochronous sequences using TempEst (formerly Path-O-Gen). *Virus Evol.* 2, 1–7. doi:10.1093/ve/vew007.

Ramos-González, P. L., Chabi-Jesus, C., Arena, G. D., Tassi, A. D., Kitajima, E. W., Freitas-Astúa, J., et al. (2018). Citrus leprosis: a unique multietiologic disease. *Cítricos en las Américas* 1, 1–9.

Ramos-González, P. L., Chabi-Jesus, C., Guerra-Peraza, O., Breton, M. C., Arena, G. D. G. D. G. D., Nunes, M. A. M. A., et al. (2016). Phylogenetic and molecular variability studies reveal a new genetic clade of Citrus leprosis virus C. *Viruses* 8, 153. doi:10.3390/v8060153.

Ramos-González, P. L. P. L., Chabi-Jesus, C., Guerra-Peraza, O., Tassi, A. D. A. D., Kitajima, E. W. E. W., Harakava, R., et al. (2017). Citrus leprosis virus N: A new dichorhavirus causing Citrus leprosis disease. *Phytopathology* 107, 963–976. doi:10.1094/PHYTO-02-17-0042-R.

Ramos-González, P. L., Santos, G. F. dos, Chabi-Jesus, C., Harakava, R., Kitajima, E. W., and Freitas-Astúa, J. (2020). Passion fruit green spot virus genome harbors a new orphan ORF and highlights the flexibility of the 5′-end of the rna2 segment across cileviruses. *Front. Microbiol.* 11, 206. doi:10.3389/fmicb.2020.00206.

Rodríguez-Nevado, C., Montes, N., and Pagán, I. (2017). Ecological factors affecting infection risk and population genetic diversity of a novel potyvirus in its native wild ecosystem. *Front. Plant Sci.* 8, 1–16. doi:10.3389/fpls.2017.01958.

Rogers, A. R., and Harpending, H. (1992). Population growth makes waves in the distribution of pairwise genetic differences. *Mol. Biol. Evol.* 9, 552–569. doi:10.1093/oxfordjournals.molbev.a040727.

Roy, A., Choudhary, N., Guillermo, L. M., Shao, J., Govindarajulu, A., Achor, D., et al. (2013a). A novel virus of the genus *Cilevirus* causing symptoms similar to citrus leprosis. *Phytopathology* 103, 488–500. doi:10.1094/PHYTO-07-12-0177-R.

Roy, A., Hartung, J. S., Schneider, W. L., Shao, J., Leon M, G., Melzer, M. J., et al. (2015). Role bending: Complex relationships between viruses, hosts, and vectors related to citrus leprosis, an emerging disease. *Phytopathology* 105, 872–884. doi:10.1094/PHYTO-12-14-0375-FI.

Roy, A., Leon, M. G., Stone, A. L., Schneider, W. L., Hartung, J., and Brlansky, R. H. (2014). First report of citrus leprosis virus nuclear type in sweet orange in Colombia. *Plant Dis.*

98, 1162. doi:10.1094/PDIS-02-14-0117-PDN.

Roy, A., Shao, J., Hartung, J. S., Schneider, W., and Brlansky, R. (2013b). A case study on discovery of novel citrus leprosis virus cytoplasmic type 2 utilizing small rna libraries by next generation sequencing and bioinformatic analyses. *J. Datamining Genomics Proteomics* 4.

Roy, A., Stone, A. L., Melzer, M. J., Shao, J., Hartung, J. S., Mavrodieva, V., et al. (2019). Complete nucleotide sequence of a novel hibiscus-infecting cilevirus from Florida and its relationship with closely associated cileviruses. *Genome Announc.* 6, 1–2. doi:10.1128/genomeA.01521-17.

Rozas, J., Ferrer-Mata, A., Sanchez-DelBarrio, J. C., Guirao-Rico, S., Librado, P., Ramos-Onsins, S. E., et al. (2017). DnaSP 6: DNA sequence polymorphism analysis of large data sets. *Mol. Biol. Evol.* 34, 3299–3302. doi:10.1093/molbev/msx248.

Salinas-Vargas, D., Santillán-Galicia, M. T., Guzmán-Franco, A. W., Hernández-López, A., Ortega-Arenas, L. D., and Mora-Aguilera, G. (2016). Analysis of genetic variation in *Brevipalpus yothersi* (Acari: Tenuipalpidae) populations from four species of citrus host plants. *PLoS One* 11, 1–11. doi:10.1371/journal.pone.0164552.

Sánchez-Velázquez, E. J., Santillán-Galicia, M. T., Novelli, V. M., Nunes, M. A., Mora-Aguilera, G., Valdez-Carrasco, J. M., et al. (2015). Diversity and genetic variation among *Brevipalpus* populations from Brazil and Mexico. *PLoS One* 10, e0133861. doi:10.1371/journal.pone.0133861.

Suchard, M. A., Lemey, P., Baele, G., Ayres, D. L., Drummond, A. J., and Rambaut, A. (2018). Bayesian phylogenetic and phylodynamic data integration using BEAST 1.10. *Virus Evol.* 4, 1–5. doi:10.1093/ve/vey016.

Tajima, F. (1989). Statistical Method for Testing the Neutral Mutation Hypothesis by DNA Polymorphism. Available at: http://www.genetics.org/content/genetics/123/3/585.full.pdf [Accessed March 25, 2019].

Tassi, A. D., Garita-Salazar, L. C., Amorim, L., Novelli, V. M., Freitas-Astúa, J., Childers, C. C., et al. (2017). Virus-vector relationship in the Citrus leprosis pathosystem. *Exp. Appl. Acarol.* 71, 227–241. doi:10.1007/s10493-017-0123-0.

Vaughan, T. G. (2017). IcyTree: Rapid browser-based visualization for phylogenetic trees and networks. *Bioinformatics* 33, 2392–2394. doi:10.1093/bioinformatics/btx155.

Weaver, S., Shank, S. D., Spielman, S. J., Li, M., Muse, S. V., and Kosakovsky Pond, S. L. (2018). Datamonkey 2.0: A modern web application for characterizing selective and other evolutionary processes. *Mol. Biol. Evol.* 35, 773–777. doi:10.1093/molbev/msx335.

Webster, T. M., Burton, M. G., Culpepper, A. S., York, A. C., and Prostko, E. P. (2005). Tropical Spiderwort (*Commelina benghalensis*): A tropical invader threatens agroecosystems of the Southern United States . *Weed Technol.* 19, 501–508. doi:10.1614/wt-04-234r.1.

Weniger, B., Um, B. H., Valentin, A., Estrada, A., Lobstein, A., Anton, R., et al. (2001). Bioactive acridone alkaloids from *Swinglea glutinosa*. *J. Nat. Prod.* 64, 1221–1223. doi:10.1021/np0005762.

ANNEX I

Supplementary Table 1. List of plant samples collected from 1932-2019 analyzed and citrus leprosis virus C (CiLV-C) sequences obtained in this study.

Nº sample	Nº host	Host name (species/variety)	Lesions type[1]	Tissue type	Collection site City, state, country[2]	Orchard type	Year	CiLV-C strain detected[3]	CiLV-C isolate identification[4]	Genomic region analyzed[5]	GenBank accession number
Stored in the Herbarium of Instituto Biológico											
1	1	*C. sinensis*	pool	Leaf	Jacareí, SP, BR	non-commercial	1932	CRD	BR_SP_Jac01	RNA1	MT554530
										RNA2	MT554544
2	2	*C. sinensis*	pool	Leaf	Piracicaba, SP, BR	non-commercial	1932	CRD	BR_SP_Prb04	RNA1	MT554535
										RNA2	MT554549
3	3	*C. sinensis*	pool	Leaf	Uruguaiana, RS, BR	non-commercial	1937	CRD	BR_RS_Urg01	RNA1	MT554538
										RNA2	MT554552
4	4	*C. sinensis*	pool	Leaf	Santa'Ana, Misiones, AR	non-commercial	1937	CRD	AR06	RNA1	MT554528
										RNA2	MT554542
5	5	*C. sinensis*	pool	Leaf	Assuncion, PY	not available	1937	ASU	PY_Asu02	RNA1	MT554532
										RNA2	MT554546
6	6	*C. sinensis*	pool	Leaf	Limeira, SP, BR	non-commercial	1939	CRD	BR_SP_Lim01	RNA1	MT554531
										RNA2	MT554545
7	7	*C. sinensis*	pool	Leaf	São Paulo, SP, BR	non-commercial	1941	CRD	BR_SP_SPa11	RNA1	MT554551
										RNA2	MT554537
8	8	*C. sinensis*	pool	Leaf	Jaboticabal, SP, BR	non-commercial	1975	CRD	BR_SP_Jbt02	RNA1	MT554529
										RNA2	MT554543
Stored at - 80ºC											
9	9	*Citrus reticulata*	pool	Leaf	Amparo, SP, BR	commercial	2003	CRD	BR_SP_Amp03	*p29*	Not sequenced (NS)
										mp	NS
10	10	*Citrus* sp.	pool	Leaf	Yapacaní, BO	non-commercial	2003	CRD	BO_ Ypc01	*p29*	NS
										mp	NS
11	11	*Citrus* sp.	pool	Leaf	Maringá, PR	non-commercial	2004	CRD	BR_PR_Mgf02	*p29*	NS
										mp	NS
12	12	*C. sinensis*	pool	Leaf	Argentina	non-commercial	2006	CRD	AR04	RNA1	MT554526
										RNA2	MT554540
13	13	*C. sinensis*	pool	Leaf	Colombia	non-commercial	2008	CRD	CO02	*p29*	NS
										mp	NS
14	14	*Citrus* sp.	pool	Leaf	Paraguay	non-commercial	2010	CRD	PY03	*p29*	NS
										mp	NS
15	15	*C. sinensis*	pool	Leaf	Amparo, SP, BR	commercial	2012	CRD	BR_SP_Amp02	*p29*	MN954965

										mp	NS
16	16	*C. sinensis*	pool	Leaf	Araras, SP, BR	non-commercial	2012	CRD	BR_SP_Ara02	*p29*	MN954966
										mp	NS
17	17	*C. sinensis*	pool	Leaf	Borborema, SP, BR	commercial	2012	CRD	BR_SP_Brm03	*p29*	MN954987
										mp	NS
18	18	*C. sinensis*	pool	Leaf	Brasilia, DF, BR	non-commercial	2012	CRD	BR_DF_Bsb02	*p29*	MN954988
										mp	NS
19	19	*C. sinensis*	pool	Leaf	Colina, SP, BR	commercial	2012	CRD	BR_SP_Cln02	*p29*	MN955004
										mp	NS
20	20	*C. sinensis*	pool	Leaf	Comendador Gomes, MG, BR	commercial	2012	CRD	BR_MG_Cgz02	*p29*	MN955010
										mp	NS
21	21	*C. sinensis*	pool	Leaf	Conchal, SP, BR	commercial	2012	CRD	BR_SP_Cch02	*p29*	MN955011
										mp	NS
22	22	*C. sinensis*	pool	Leaf	Cordeirópolis, SP, BR	non-commercial	2012	CRD	BR_SP_Crd04	*p29*	MN955012
										mp	NS
23	23	*C. sinensis*	pool	Leaf	Cordeirópolis, SP, BR	non-commercial	2012	CRD	BR_SP_Crd05	*p29*	NS
										mp	NS
24	24	*C. sinensis*	pool	Leaf	Cordeirópolis, SP, BR	non-commercial	2012	CRD	BR_SP_Crd06	*p29*	NS
										mp	NS
25	25	*C. sinensis*	pool	Leaf	Cordeirópolis, SP, BR	commercial	2012	CRD	BR_SP_Crd07	*p29*	NS
										mp	NS
26	26	*C. sinensis*	pool	Leaf	Itú, SP, BR	commercial	2012	CRD	BR_SP_Itu01	*p29*	MN955038
										mp	NS
27	27	*C. sinensis*	pool	Leaf	Londrina, PR, BR	non-commercial	2012	CRD	BR_PR_Ldb02	*p29*	MN955018
										mp	NS
28	28	*C. sinensis*	pool	Leaf	Manaus, AM, BR	non-commercial	2012	CRD	BR_AM_Mao02	*p29*	MN955019
										mp	NS
29	29	*C. sinensis*	pool	Leaf	Mirandópolis, SP, BR	commercial	2012	CRD	BR_SP_Mrn02	*p29*	MN955020
										mp	NS
30	30	*C. sinensis*	pool	Leaf	Palmas, TO, BR	non-commercial	2012	CRD	BR_TO_Pnw02	*p29*	MN955066
										mp	NS
31	31	*C. sinensis*	pool	Leaf	Santo Antônio da Posse, SP, BR	commercial	2012	CRD	BR_SP_SAP02	*p29*	MN955046
										mp	NS
32	32	*C. sinensis*	pool	Leaf	Serra Negra, SP, BR	non-commercial	2012	CRD	BR_SP_Sng02	*p29*	MN955047
										mp	NS
33	33	*C. sinensis*	pool	Leaf	Tanguá, RJ, BR	non-commercial	2012	CRD	BR_RJ_Tng02	*p29*	MN955057
										mp	NS
34	34	*C. sinensis*	pool	Leaf	Tatuí, SP, BR	commercial	2012	CRD	BR_SP_Tti02	*p29*	MN955063
										mp	NS
35	35	*C. sinensis*	pool	Leaf	Terenos, MS, BR	non-commercial	2012	CRD	BR_MS_Trn02	*p29*	MN955064
									BR_MS_Trn03	*p29*	MN955065

36	36	*C. sinensis*	pool	Leaf	Argentina	non-commercial	2012	CRD	AR03	*p29*	MN954967
										mp	NS
37	37	*Citrus sp.*	pool	Leaf	Argentina	non-commercial	2012	CRD	AR07	*p29*	NS
										mp	NS
38	38	*C. sinensis* (Hamlin)	pool	Leaf	Argentina	non-commercial	2013	CRD	AR08	*p29*	NS
										mp	NS
39	39	*C. sinensis* (Hamlin)	pool	Leaf	Argentina	non-commercial	2013	CRD	AR09	*p29*	NS
										mp	NS
40	40	*C. reticulata* (Clementina)	pool	Leaf	Argentina	non-commercial	2013	CRD	AR10	*p29*	NS
										mp	NS
41	41	*C. sinensis*	pool	Leaf	Piracicaba, SP, BR	non-commercial	2014	CRD	BR_SP_Prb05	*p29*	NS
										mp	NS
42	42	*C. sinensis*	pool	Leaf	Araras, SP, BR	commercial	2014	CRD	BR_SP_Ara03	*p29*	NS
										mp	NS
43	43	*C. sinensis*	pool	Leaf	Cosmorama, MG, SP	commercial	2015	SJP	BR_SP_Csm02	*p29*	MN955013
									BR_SP_Csm03	*p29*	MN955014
44	44	*C. sinensis*	pool	Leaf	Sud Mennuci, SP, BR	commercial	2015	SJP	BR-SP_SdM02	*p29*	MN955077
										mp	NS
45	45	*C. sinensis*	pool	Leaf	Sud Mennuci, SP, BR	commercial	2015	SJP	BR-SP_SdM04	*p29*	MN955078
										mp	NS
46	46	*C. sinensis*	pool	Leaf	Sud Mennuci, SP, BR	commercial	2015	SJP	BR-SP_SdM06	*p29*	MN955079
										mp	NS
47	47	*C. sinensis*	pool	Leaf	Sud Mennuci, SP, BR	commercial	2015	SJP	BR-SP_SdM08	*p29*	MN955080
										mp	NS
48	48	*C. sinensis*	pool	Leaf	Sud Mennuci, SP, BR	commercial	2015	SJP	BR-SP_SdM10	*p29*	MN955081
										mp	NS
49	49	*C. sinensis*	pool	Leaf	Sud Mennuci, SP, BR	commercial	2015	SJP	BR-SP_SdM12	*p29*	MN955082
										mp	NS
Experimental transmission[6]											
50	50	*Arabidopsis thaliana*	pool	Leaf	Viruliferous mites	non-commercial	2015	SJP	BR_SP_SJP05	RNA1	MT554536
										RNA2	MT554550
Fresh tissue											
51	51	*Citrus* sp.	pool	Leaf	Argentina	non-commercial	2015	CRD	AR11	*p29*	NS
										mp	NS
52	52	*C. sinensis*	pool	Fruit	Barretos, SP, BR	commercial	2015	SJP	BR_SP_Bar19	*p29*	NS
										mp	NS
53	53	*C. sinensis*	pool	Fruit	Barretos, SP, BR	commercial	2015	SJP	BR_SP_Bar20	*p29*	NS
										mp	NS
54	54	*C. sinensis*	pool	Fruit	Barretos, SP, BR	commercial	2015	SJP	BR_SP_Bar21	*p29*	NS
										mp	NS
55	55	*C. sinensis*	pool	Fruit	Barretos, SP, BR	commercial	2015	SJP	BR_SP_Bar22	*p29*	NS

										mp	NS
56	56	*C. sinensis*	pool	Fruit	Barretos, SP, BR	commercial	2015	SJP	BR_SP_Bar23	*p29*	NS
										mp	NS
57	57	*C. sinensis*	pool	Fruit	Barretos, SP, BR	commercial	2015	SJP	BR_SP_Bar24	*p29*	NS
										mp	NS
58	58	*C. sinensis*	pool	Fruit	Itirapina, SP, BR	commercial	2015	CRD	BR_SP_Irp01	*p29*	NS
										mp	NS
59	59	*C. reticulata*	pool	Fruit	São Jose do Rio Preto, SP, BR	commercial	2015	SJP	BR_SP_SJP06	*p29*	NS
										mp	NS
60	60	*C. reticulata*	pool	Fruit	São Jose do Rio Preto, SP, BR	commercial	2015	SJP	BR_SP_SJP07	*p29*	NS
										mp	NS
61	61	*C. sinensis*	pool	Fruit	Adolfo, SP, BR	commercial	2016	CRD+SJP	BR_SP_Adf01	*p29*	NS
									BR_SP_Adf02	*mp*	NS
62	62	*C. sinensis*	pool	Fruit	Araraquara, SP, BR	commercial	2016	SJP	BR_SP_Arq01	*p29*	NS
										mp	NS
63	63	*C. sinensis* (Valência)	pool	Fruit	Avaré, SP, BR	commercial	2016	CRD	BR_SP_Avr01	*p29*	NS
										mp	NS
64	64	*C. sinensis*	pool	Fruit	Bebedouro, SP, BR	commercial	2016	SJP	BR_SP_Beb32	*p29*	NS
										mp	NS
65	65	*C. sinensis*	pool	Leaf	Brasília, DF, BR	non-commercial	2016	CRD	BR_DF_Bsb03	*p29*	NS
										mp	NS
66	66	*C. sinensis*	pool	Fruit	Caiabu, SP, BR	commercial	2016	CRD+SJP	BR_SP_Cab01	*p29*	NS
									BR_SP_Cab02	*mp*	NS
67	67	*C. sinensis*	pool	Fruit	Colômbia, SP, BR	commercial	2016	SJP	BR_SP_Clb10	*p29*	NS
										mp	NS
68	68	*C. sinensis*	pool	Fruit	Colômbia, SP, BR	commercial	2016	SJP	BR_SP_Clb11	*p29*	NS
										mp	NS
69	69	*C. sinensis*	pool	Fruit	Colômbia, SP, BR	commercial	2016	SJP	BR_SP_Clb12	*p29*	NS
										mp	NS
70	70	*C. sinensis*	pool	Fruit	Colômbia, SP, BR	commercial	2016	SJP	BR_SP_Clb13	*p29*	NS
										mp	NS
71	71	*C. sinensis*	pool	Fruit	Colômbia, SP, BR	commercial	2016	SJP	BR_SP_Clb14	*p29*	NS
										mp	NS
72	72	*C. sinensis*	pool	Fruit	Colômbia, SP, BR	commercial	2016	SJP	BR_SP_Clb15	*p29*	NS
										mp	NS
73	73	*C. sinensis*	pool	Fruit	Colômbia, SP, BR	commercial	2016	SJP	BR_SP_Clb16	*p29*	NS
										mp	NS
74	74	*C. sinensis*	pool	Fruit	Comendador Gomes, MG, BR	commercial	2016	CRD	BR_MG_Cgz03	*p29*	NS
										mp	NS
75	75	*C. sinensis*	pool	Fruit	Comendador Gomes, MG, BR	commercial	2016	CRD	BR_MG_Cgz04	*p29*	NS
										mp	NS

76	76	*C. sinensis*	pool	Fruit	Frutal, MG, BR	commercial	2016	SJP	BR_MG_Frt01	*p29*	NS
										mp	NS
77	77	*C. sinensis*	pool	Fruit	Guarantã, SP, BR	commercial	2016	SJP	BR_SP_Grt01	*p29*	NS
										mp	NS
78	78	*C. sinensis*	pool	Fruit	Guimbê, SP, BR	commercial	2016	SJP	BR_SP_Gua09	*p29*	NS
										mp	NS
79	79	*C. sinensis*	pool	Fruit	Jaboticabal, SP, BR	commercial	2016	SJP	BR_SP_Jbt03	*p29*	NS
										mp	NS
80	80	*C. sinensis*	pool	Fruit	Limeira, SP, BR	commercial	2016	SJP	BR_SP_Lim02	*p29*	NS
										mp	NS
81	81	*C. sinensis*	pool	Fruit	Olímpia, SP, BR	commercial	2016	SJP	BR_SP_Olm01	*p29*	NS
										mp	NS
82	82	*C. sinensis*	pool	Leaf	Piracicaba, SP, BR	non-commercial	2016	CRD	BR_SP_Prb02	RNA1	MT554533
										RNA2	MT554547
83	83	*C. sinensis*	pool	Leaf	Piracicaba, SP, BR	non-commercial	2016	CRD	BR_SP_Prb06	*p29*	NS
										mp	NS
84	84	*C. sinensis*	pool	Fruit	Pirajuí, SP, BR	commercial	2016	CRD+SJP	BR_SP_Prj01	*p29*	NS
									BR_SP_Prj02	*mp*	NS
85	85	*C. sinensis*	pool	Fruit	Pirapora, MG, BR	commercial	2016	CRD	BR_MG_Prp01	*p29*	NS
										mp	NS
86	86	*C. sinensis*	pool	Fruit	Pirassununga, SP, BR	commercial	2016	SJP	BR_SP_Prg06	*p29*	NS
										mp	NS
87	87	*C. sinensis* (Pera)	pool	Fruit	Santa Cruz do Rio Pardo, SP, BR	commercial	2016	SJP	BR_SP_SCP01	*p29*	NS
										mp	NS
88	88	*C. sinensis*	pool	Fruit	Tabatinga, SP, BR	commercial	2016	SJP	BR_SP_Tbt01	*p29*	NS
										mp	NS
89	89	*C. sinensis*	pool	Fruit	Tremenbé, SP, BR	commercial	2016	SJP	BR_SP_Tmb01	*p29*	NS
										mp	NS
90	90	*C. sinensis*	pool	Fruit	Uru, SP, BR	commercial	2016	CRD	BR_SP_Uru01	*p29*	NS
										mp	NS
91	91	*C. sinensis*	pool	Leaf	Corrientes, Argentina	non-commercial	2017	CRD	AR04	*p29*	NS
										mp	NS
92	92	*C. sinensis* (Folha murcha)	single	Fruit	Aguaí, SP, BR	commercial	2017	CRD+SJP	BR_SP_Agi01	*p29*	MN954955
										mp	MN955083
										p24	NS
									BR_SP_Agi02	*p29*	MN954956
										mp	MN955084
										p24	NS
									BR_SP_Agi03	*p29*	MN954957
										mp	MN955085
										p24	NS

									BR_SP_Agi04	*p29*	NS
										mp	MN955086
										p24	NS
									BR_SP_Agi05	*p29*	NS
										mp	MN955087
										p24	NS
									BR_SP_Agi06	*p29*	NS
										mp	MN955088
										p24	NS
									BR_SP_Agi07	*p29*	NS
										mp	MN955089
										p24	NS
93-107								CRD+SJP	BR_SP_Agi13 to Agi27	*p29*	NS
										mp	NS
										p24	NS
108	93	*C. sinensis* (Valência)	single	Fruit	Aguaí, SP, BR	commercial	2017	CRD+SJP	BR_SP_Agi08	*p29*	MN954958
										mp	MN955090
										p24	NS
									BR_SP_Agi09	*p29*	MN954959
										mp	MN955091
										p24	NS
									BR_SP_Agi10	*p29*	MN954960
										mp	NS
										p24	NS
									BR_SP_Agi11	*p29*	MN954961
										mp	NS
										p24	NS
									BR_SP_Agi12	*p29*	NS
										mp	NS
										p24	NS
109	94	*C. sinensis* (Hamlin)	single	Fruit	Altinópolis, SP, BR	commercial	2017	SJP	BR_SP_Alt01	*p29*	MN954962
										mp	MN955092
										p24	NS
									BR_SP_Alt02	*p29*	MN954963
										mp	MN955093
										p24	NS
									BR_SP_Alt03	*p29*	MN954964
										mp	MN955094
										p24	NS
									BR_SP_Alt04	*p29*	NS
										mp	MN955095

										p24	NS
									BR_SP_Alt05	*p29*	NS
										mp	MN955096
										p24	NS
									BR_SP_Alt06	*p29*	NS
										mp	NS
										p24	MN955097
									BR_SP_Alt07	*p29*	NS
										mp	NS
										p24	NS
110-124			single					SJP	BR_SP_Alt08 to Alt22	*p29*	NS
										mp	NS
										p24	NS
125	95	*C. sinensis* (New hall)	pool	Leaf	Argentina	non-commercial	2017	CRD	AR12	*p29*	NS
										mp	NS
										p24	NS
126	96	*C. sinensis* (Hamlin)	single	Fruit	Barretos, SP, BR	commercial	2017	SJP	BR_SP_Bar01	*p29*	MN954970
										mp	MN955100
										p24	NS
									BR_SP_Bar02	*p29*	MN954971
										mp	MN955101
										p24	NS
									BR_SP_Bar03	*p29*	MN954972
										mp	MN955102
										p24	NS
									BR_SP_Bar04	*p29*	MN954973
										mp	MN955103
										p24	NS
									BR_SP_Bar05	*p29*	MN954974
										mp	MN955104
										p24	NS
									BR_SP_Bar06	*p29*	NS
										mp	MN955105
										p24	NS
									BR_SP_Bar07	*p29*	NS
										mp	MN955106
										p24	NS
127			single					SJP	BR_SP_Bar08	*p29*	MN954975
										mp	MN955107
										p24	NS
									BR_SP_Bar09	*p29*	MN954976

										mp	MN955108
										p24	NS
									BR_SP_Bar10	*p29*	MN954977
										mp	MN955109
										p24	NS
									BR_SP_Bar11	*p29*	MN954978
										mp	MN955110
										p24	NS
									BR_SP_Bar12	*p29*	MN954979
										mp	MN955111
										p24	NS
									BR_SP_Bar13	*p29*	NS
										mp	MN955112
										p24	NS
									BR_SP_Bar14	*p29*	NS
										mp	MN955113
										p24	NS
									BR_SP_Bar15	*p29*	NS
										mp	MN955114
										p24	NS
									BR_SP_Bar16	*p29*	NS
										mp	MN955115
										p24	NS
128-129			single					SJP	BR_SP_Bar17 and Bar18	*p29*	NS
										mp	NS
										p24	NS
130	97	*C. sinensis* (Hamlin)	single single	Fruit	Bebedouro, SP, BR	commercial	2017	SJP	BR_SP_Beb01	*p29*	MN954980
										mp	MN955116
										p24	NS
									BR_SP_Beb02	*p29*	MN954981
										mp	MN955117
										p24	NS
									BR_SP_Beb03	*p29*	MN954982
										mp	MN955118
										p24	NS
									BR_SP_Beb04	*p29*	MN954983
										mp	MN955119
										p24	NS
									BR_SP_Beb05	*p29*	MN954984
										mp	MN955120
										p24	NS

									BR_SP_Beb06	*p29*	NS
										mp	MN955121
										p24	NS
									BR_SP_Beb07	*p29*	NS
										mp	MN955122
										p24	NS
									BR_SP_Beb08	*p29*	NS
										mp	MN955123
										p24	NS
									BR_SP_Beb09	*p29*	NS
										mp	MN955124
										p24	NS
									BR_SP_Beb10	*p29*	NS
										mp	MN955125
										p24	NS
									BR_SP_Beb11	*p29*	NS
										mp	MN955126
										p24	NS
131			single					SJP	BR_SP_Beb12	*p29*	MN954985
										mp	MN955127
										p24	NS
									BR_SP_Beb13	*p29*	MN954986
										mp	MN955128
										p24	NS
									BR_SP_Beb14	*p29*	NS
										mp	MN955129
										p24	NS
									BR_SP_Beb15	*p29*	NS
										mp	MN955130
										p24	NS
									BR_SP_Beb16	*p29*	NS
										mp	MN955131
										p24	NS
									BR_SP_Beb17	*p29*	NS
										mp	MN955132
										p24	NS
									BR_SP_Beb18	*p29*	NS
										mp	MN955133
										p24	NS
									BR_SP_Beb19	*p29*	NS
										mp	MN955134

										p24	NS
									BR_SP_Beb20	*p29*	NS
										mp	MN955135
										p24	NS
									BR_SP_Beb21	*p29*	NS
										mp	MN955136
										p24	NS
									BR_SP_Beb22	*p29*	NS
										mp	MN955137
										p24	NS
									BR_SP_Beb23	*p29*	NS
										mp	MN955138
										p24	NS
									BR_SP_Beb24	*p29*	NS
										mp	MN955139
										p24	NS
									BR_SP_Beb25	*p29*	NS
										mp	MN955140
										p24	NS
132			single					SJP	BR_SP_Beb26	*p29*	NS
										mp	MN955141
										p24	NS
									BR_SP_Beb27	*p29*	NS
										mp	MN955142
										p24	NS
									BR_SP_Beb28	*p29*	NS
										mp	MN955143
										p24	NS
									BR_SP_Beb29	*p29*	NS
										mp	MN955144
										p24	NS
									BR_SP_Beb30	*p29*	NS
										mp	MN955145
										p24	NS
									BR_SP_Beb31	*p29*	NS
										mp	MN955146
										p24	NS
133	98	*C. sinensis* (Valencia)	pool	Leaf	Bella Vista, Corrientes, AR	non-commercial	2017	CRD	AR05	RNA1	MT554528
										RNA2	MT554542
134	99	*C. sinensis* (Pera)	single	Fruit	Brotas, SP, BR	commercial	2017	SJP	BR_SP_Bro01	*p29*	MN954989
										mp	MN955147

										p24	NS
									BR_SP_Bro02	*p29*	MN954990
										mp	MN955148
										p24	NS
									BR_SP_Bro03	*p29*	MN954991
										mp	MN955149
										p24	NS
									BR_SP_Bro04	*p29*	MN954992
										mp	NS
										p24	NS
135			single					SJP	BR_SP_Bro12	*p29*	NS
										mp	NS
										p24	NS
136	100	*C. sinensis* (Natal)	single	Fruit	Brotas, SP, BR	commercial	2017	SJP	BR_SP_Bro05	*p29*	MN954993
										mp	MN955150
										p24	NS
									BR_SP_Bro06	*p29*	MN954994
										mp	MN955151
										p24	NS
									BR_SP_Bro07	*p29*	MN954995
										mp	MN955152
										p24	NS
									BR_SP_Bro08	*p29*	NS
										mp	MN955153
										p24	NS
									BR_SP_Bro09	*p29*	NS
										mp	MN955154
										p24	NS
									BR_SP_Bro10	*p29*	NS
										mp	MN955155
										p24	NS
									BR_SP_Bro11	*p29*	NS
										mp	MN955154
										p24	NS
									BR_SP_Bro11	*p29*	NS
										mp	MN955157
										p24	NS
137-138			single					SJP	BR_SP_Bro13 and Bro14	*p29*	NS
										mp	NS
										p24	NS
139	101	*C. sinensis* (Natal)	single	Fruit	Cafelândia, SP, BR	commercial		SJP	BR_SP_Cfl01	*p29*	NS

										mp	NS
										p24	NS
140	102	*C. sinensis* (Natal)	single	Fruit	Cerqueira Cesar, SP, BR	commercial	2017	SJP	BR_SP_CrC01	*p29*	MN954996
										mp	MN955158
										p24	NS
									BR_SP_CrC02	*p29*	MN954997
										mp	MN955159
										p24	NS
									BR_SP_CrC03	*p29*	MN954998
										mp	MN955160
										p24	NS
									BR_SP_CrC04	*p29*	MN954999
										mp	MN955161
										p24	NS
									BR_SP_CrC05	*p29*	NS
										mp	NS
										p24	NS
									BR_SP_CrC06	*p29*	MN955000
										mp	MN955162
										p24	NS
									BR_SP_CrC07	*p29*	NS
										mp	MN955163
										p24	NS
									BR_SP_CrC08	*p29*	NS
										mp	MN955164
										p24	NS
141			single					SJP	BR_SP_CrC09	*p29*	MN955001
										mp	MN955165
										p24	NS
									BR_SP_CrC10	*p29*	MN955002
										mp	MN955166
										p24	NS
									BR_SP_CrC11	*p29*	MN955003
										mp	MN955167
										p24	NS
									BR_SP_CrC12	*p29*	NS
										mp	MN955168
										p24	NS
142-155			single					SJP	BR_SP_CrC13 to CrC28	*p29*	NS
										mp	NS
										p24	NS

156	103	*C. sinensis* (Hamlin)	single	Fruit	Colômbia, SP, BR	commercial	2017	SJP	BR_SP_Clb01	*p29*	MN955005
										mp	NS
										p24	NS
									BR_SP_Clb02	*p29*	MN955006
										mp	NS
										p24	NS
									BR_SP_Clb03	*p29*	MN955007
										mp	NS
										p24	NS
									BR_SP_Clb04	*p29*	MN955008
										mp	NS
										p24	NS
									BR_SP_Clb05	*p29*	MN955009
										mp	NS
										p24	NS
157-160			single				RT-PCR	RT-PCR	BR_SP_Clb06 to Clb09	*p29*	NS
										mp	NS
										p24	NS
161	104	*C. sinensis* (Pera)	single	Fruit	Guaimbê, SP, BR	commercial	2017	SJP	BR_SP_Gua01	*p29*	MN955015
										mp	MN955169
										p24	NS
									BR_SP_Gua02	*p29*	MN955016
										mp	MN955170
										p24	NS
									BR_SP_Gua03	*p29*	NS
										mp	MN955171
										p24	NS
									BR_SP_Gua04	*p29*	NS
										mp	MN955172
										p24	NS
									BR_SP_Gua05	*p29*	NS
										mp	MN955173
										p24	NS
									BR_SP_Gua06	*p29*	NS
										mp	MN955174
										p24	NS
									BR_SP_Gua07	*p29*	NS
										mp	MN955175
										p24	NS
									BR_SP_Gua08	*p29*	NS
										mp	MN955176

										p24	NS
162-183			single					SJP	BR_SP_Gua09 to Gua30	*p29*	NS
										mp	NS
										p24	NS
184	105	*C. sinensis* (Pera)	single	Fruit	Guapiaçu, SP, BR	commercial	2017	SJP SJP	BR_SP_Gup01	*p29*	NS
										mp	MN955177
										p24	NS
									BR_SP_Gup02	*p29*	NS
										mp	MN955178
										p24	NS
									BR_SP_Gup03	*p29*	NS
										mp	MN955179
										p24	NS
									BR_SP_Gup04	*p29*	NS
										mp	MN955180
										p24	NS
									BR_SP_Gup05	*p29*	NS
										mp	MN955181
										p24	NS
									BR_SP_Gup06	*p29*	NS
										mp	MN955182
										p24	NS
									BR_SP_Gup07	*p29*	NS
										mp	MN955183
										p24	NS
									BR_SP_Gup08	*p29*	NS
										mp	MN955184
										p24	NS
									BR_SP_Gup09	*p29*	NS
										mp	MN955185
										p24	NS
									BR_SP_Gup10	*p29*	NS
										mp	MN955186
										p24	NS
									BR_SP_Gup11	*p29*	NS
										mp	MN955187
										p24	NS
									BR_SP_Gup12	*p29*	NS
										mp	MN955188
										p24	NS
185			single					SJP	BR_SP_Gup13	*p29*	NS

										mp	MN955189
										p24	NS
									BR_SP_Gup14	*p29*	NS
										mp	MN955190
										p24	NS
									BR_SP_Gup15	*p29*	NS
										mp	MN955191
										p24	NS
									BR_SP_Gup16	*p29*	NS
										mp	MN955192
										p24	NS
									BR_SP_Gup17	*p29*	NS
										mp	MN955193
										p24	NS
									BR_SP_Gup18	*p29*	NS
										mp	MN955194
										p24	NS
186	106	*C. sinensis* (Valencia)	single	Fruit	Leme, SP, BR	commercial	2017	SJP	BR_SP_Lem01	*p29*	NS
										mp	NS
										p24	NS
187	107	*C. sinensis* (Hamlin)	single	Fruit	Mogi Mirim, SP, BR	commercial	2017	CRD+SJP	BR_SP_MgM01	*p29*	MN955021
										mp	MN955197
										p24	NS
									BR_SP_MgM02	*p29*	MN955022
										mp	MN955198
										p24	NS
									BR_SP_MgM03	*p29*	MN955023
										mp	MN955199
										p24	NS
									BR_SP_MgM04	*p29*	MN955024
										mp	MN955200
										p24	NS
									BR_SP_MgM05	*p29*	MN955025
										mp	MN955201
										p24	NS
									BR_SP_MgM06	*p29*	MN955026
										mp	MN955202
										p24	NS
									BR_SP_MgM07	*p29*	MN955027
										mp	MN955203
										p24	NS

									BR_SP_MgM08	*p29*	NS
										mp	MN955204
										p24	NS
									BR_SP_MgM09	*p29*	NS
										mp	MN955205
										p24	NS
									BR_SP_MgM10	*p29*	NS
										mp	MN955206
										p24	NS
188			single					SJP	BR_SP_MgM11	*p29*	MN955028
										mp	MN955207
										p24	NS
									BR_SP_MgM12	*p29*	MN955029
										mp	MN955208
										p24	NS
									BR_SP_MgM13	*p29*	MN955030
										mp	MN955209
										p24	NS
									BR_SP_MgM14	*p29*	MN955031
										mp	MN955210
										p24	NS
									BR_SP_MgM15	*p29*	MN955032
										mp	MN955211
										p24	NS
									BR_SP_MgM16	*p29*	NS
										mp	MN955212
										p24	NS
									BR_SP_MgM17	*p29*	NS
										mp	MN955213
										p24	NS
									BR_SP_MgM18	*p29*	NS
										mp	MN955214
										p24	NS
									BR_SP_MgM19	*p29*	NS
										mp	MN955215
										p24	NS
									BR_SP_MgM20	*p29*	NS
										mp	MN955216
										p24	NS
189-195			single					SJP or CRD+SJP	BR_SP_MgM31 to MgM37	*p29*	NS
										mp	NS

										p24	NS
196	108	*C. sinensis* (Pera)	single	Fruit	Mogi Mirim, SP, BR	commercial	2017	CRD	BR_SP_MgM21	*p29*	NS
										mp	MN955217
										p24	NS
									BR_SP_MgM22	*p29*	NS
										mp	MN955218
										p24	NS
									BR_SP_MgM23	*p29*	NS
										mp	MN955219
										p24	NS
									BR_SP_MgM24	*p29*	NS
										mp	MN955220
										p24	NS
									BR_SP_MgM25	*p29*	NS
										mp	MN955221
										p24	NS
									BR_SP_MgM26	*p29*	NS
										mp	MN955222
										p24	NS
									BR_SP_MgM27	*p29*	NS
										mp	MN955223
										p24	NS
									BR_SP_MgM28	*p29*	NS
										mp	MN955224
										p24	NS
									BR_SP_MgM29	*p29*	NS
										mp	MN955225
										p24	NS
									BR_SP_MgM30	*p29*	NS
										mp	MN955226
										p24	NS
197-199			single					CRD or SJP	BR_SP_MgM38 to MgM40	*p29*	NS
										mp	NS
										p24	NS
200	109	*C. sinensis*	pool	Leaf	Piracicaba, SP, BR	non-commercial	2017	CRD	BR_SP_Prb07	*p29*	NS
										mp	NS
										p24	NS
201	110	*C. sinensis* (Westin)	single	Fruit	Pirassununga, SP, BR	commercial	2017	SJP	BR_SP_Prg01	*p29*	MN955035
										mp	MN955229
										p24	
									BR_SP_Prg02	*p29*	MN955036

										mp	MN955230
										p24	NS
									BR_SP_Prg03	*p29*	MN955037
										mp	NS
										p24	NS
202			single						BR_SP_Prg04	*p29*	NS
										mp	MN955231
										p24	NS
									BR_SP_Prg05	*p29*	NS
										mp	MN955232
										p24	NS
203			single					SJP	BR_SP_Prg05	*p29*	NS
										mp	NS
										p24	NS
204	111	*C. sinensis* (Valencia)	single	Fruit	Pongaí, SP, BR	commercial	2017	CRD+SJP	BR_SP_Png01	*p29*	NS
										mp	MN955233
										p24	NS
									BR_SP_Png02	*p29*	NS
										mp	MN955234
										p24	NS
									BR_SP_Png03	*p29*	NS
										mp	MN955235
										p24	NS
									BR_SP_Png04	*p29*	NS
										mp	MN955236
										p24	NS
									BR_SP_Png05	*p29*	NS
										mp	MN955237
										p24	NS
									BR_SP_Png06	*p29*	NS
										mp	MN955238
										p24	NS
									BR_SP_Png07	*p29*	NS
										mp	MN955239
										p24	NS
									BR_SP_Png08	*p29*	NS
										mp	MN955240
										p24	NS
205			single					CRD+SJP	BR_SP_Png09	*p29*	NS
										mp	MN955241
										p24	NS

									BR_SP_Png10	*p29*	NS
										mp	MN955242
										p24	NS
									BR_SP_Png11	*p29*	NS
										mp	MN955243
										p24	NS
206	112	*C. sinensis* (Valencia)	single	Fruit	Santa Maria da Serra, SP, BR	commercial	2017	SJP	BR_SP_SSr01	*p29*	MN955039
										mp	MN955244
										p24	NS
									BR_SP_ SSr 02	*p29*	MN955040
										mp	MN955245
										p24	NS
									BR_SP_ SSr 03	*p29*	MN955041
										mp	NS
										p24	NS
									BR_SP_ SSr04	*p29*	MN955042
										mp	NS
										p24	NS
									BR_SP_ SSr05	*p29*	MN955043
										mp	NS
										p24	NS
									BR_SP_ SSr06	*p29*	MN955044
										mp	NS
										p24	NS
									BR_SP_ SSr 07	*p29*	MN955045
										mp	NS
										p24	NS
207	113	*C. sinensis*	single	Fruit	São Paulo, BR	commercial	2017	SJP	BR_SP01	*p29*	NS
										mp	MN955246
										p24	NS
									BR_SP02	*p29*	NS
										mp	MN955247
										p24	NS
									BR_SP03	*p29*	NS
										mp	MN955248
										p24	NS
									BR_SP04	*p29*	NS
										mp	MN955249
										p24	NS
									BR_SP05	*p29*	NS
										mp	MN955250

										p24	NS
208	114	*C. sinensis*	single	Fruit	São Paulo, BR	commercial	2017	CRD	BR_SP06	*p29*	NS
										mp	MN955251
										p24	NS
									BR_SP07	*p29*	NS
										mp	MN955252
										p24	NS
									BR_SP08	*p29*	NS
										mp	MN955253
										p24	NS
									BR_SP09	*p29*	NS
										mp	MN955254
										p24	NS
									BR_SP10	*p29*	NS
										mp	MN955255
										p24	NS
209	115	*C. sinensis* (Pera)	single	Fruit	Tambaú, SP, BR	commercial	2017	CRD	BR_SP_Tmb01	*p29*	MN955048
										mp	MN955256
										p24	NS
									BR_SP_Tmb02	*p29*	MN955049
										mp	MN955257
										p24	NS
									BR_SP_Tmb03	*p29*	MN955050
										mp	MN955258
										p24	NS
									BR_SP_Tmb04	*p29*	NS
										mp	MN955259
										p24	NS
									BR_SP_Tmb05	*p29*	NS
										mp	MN955260
										p24	NS
									BR_SP_Tmb06	*p29*	NS
										mp	MN955261
										p24	NS
									BR_SP_Tmb07	*p29*	NS
										mp	MN955262
										p24	NS
210-213			single					CRD	BR_SP_Tmb14 to Tmb17	*p29*	NS
										mp	NS
										p24	NS
214	116		single	Fruit	Tambaú, SP, BR	commercial	2017	CRD+SJP	BR_SP_Tmb08	*p29*	MN955051

		C. sinensis (Valencia)								*mp*	MN955263
										p24	NS
									BR_SP_Tmb09	*p29*	MN955052
										mp	NS
										p24	NS
									BR_SP_Tmb10	*p29*	MN955053
										mp	NS
										p24	NS
									BR_SP_Tmb11	*p29*	MN955054
										mp	NS
										p24	NS
									BR_SP_Tmb12	*p29*	MN955055
										mp	NS
										p24	NS
									BR_SP_Tmb13	*p29*	MN955056
										mp	NS
										p24	NS
215-232			single					CRD or CRD+SJP	BR_SP_Tmb18 to Tmb33	*p29*	NS
										mp	NS
										p24	NS
233	117	*C. sinensis* (Hamlin)	single	Fruit	Taquaral, SP, BR	commercial	2017	SJP	BR_SP_Tql01	*p29*	MN955058
										mp	MN955264
										p24	NS
									BR_SP_Tql02	*p29*	MN955059
										mp	MN955265
										p24	NS
									BR_SP_Tql03	*p29*	MN955060
										mp	MN955266
										p24	NS
									BR_SP_Tql04	*p29*	NS
										mp	MN955267
										p24	NS
									BR_SP_Tql05	*p29*	NS
										mp	MN955268
										p24	NS
									BR_SP_Tql06	*p29*	NS
										mp	MN955269
										p24	NS
									BR_SP_Tql07	*p29*	NS
										mp	MN955270
										p24	NS

234-238			single					CRD+SJP	BR_SP_Tql08-Tql12	*p29*	NS
										mp	NS
										p24	NS
239	118	*C. sinensis* (Pera)	single	Fruit	Taquaritinga, SP, BR	commercial	2017	SJP	BR_SP_Tqt01	*p29*	MN955061
										mp	MN955271
										p24	NS
									BR_SP_Tqt02	*p29*	MN955062
										mp	MN955272
										p24	NS
									BR_SP_Tqt03	*p29*	NS
										mp	MN955273
										p24	NS
									BR_SP_Tqt04	*p29*	NS
										mp	MN955274
										p24	NS
240	119	*C. sinensis* (Pera)	single	Fruit	Uberaba, MG, BR	commercial	2017	SJP	BR_MG_Uba02	*p29*	MN955067
										mp	MN955275
										p24	NS
									BR_MG_Uba03	*p29*	MN955068
										mp	MN955276
										p24	NS
									BR_MG_Uba04	*p29*	MN955069
										mp	MN955277
										p24	NS
									BR_MG_Uba05	*p29*	NS
										mp	MN955278
										p24	NS
									BR_MG_Uba06	*p29*	NS
										mp	MN955279
										p24	NS
									BR_MG_Uba07	*p29*	NS
										mp	MN955280
										p24	
241			single					SJP	BR_MG_Uba08	*p29*	MN955070
										mp	MN955281
										p24	NS
									BR_MG_Uba09	*p29*	MN955071
										mp	MN955282
										p24	NS
									BR_MG_Uba10	*p29*	NS
										mp	MN955283

										p24	NS
									BR_MG_Uba11	*p29*	NS
										mp	MN955284
										p24	NS
									BR_MG_Uba12	*p29*	NS
										mp	MN955285
										p24	NS
									BR_MG_Uba13	*p29*	NS
										mp	MN955286
										p24	NS
									BR_MG_Uba14	*p29*	NS
										mp	MN955287
										p24	NS
									BR_MG_Uba15	*p29*	NS
										mp	MN955288
										p24	NS
									BR_MG_Uba16	*p29*	NS
										mp	MN955289
										p24	NS
242			single					SJP	BR_MG_Uba17	*p29*	MN955072
										mp	NS
										p24	NS
									BR_MG_Uba18	*p29*	MN955073
										mp	NS
										p24	NS
									BR_MG_Uba19	*p29*	MN955074
										mp	NS
										p24	NS
									BR_MG_Uba20	*p29*	MN955075
										mp	NS
										p24	NS
243-246			single					SJP	BR_MG_Uba21 to Uba24	*p29*	NS
										mp	NS
										p24	NS
2447	120	*C. sinensis*	single	Fruit	Aguaí, SP, BR	commercial	2018	SJP	BR_SP_Agi_27	*p29*	NS
										p24	NS
248	121	*C. sinensis* (Natal)	single	Fruit	Aguaí, SP, BR	commercial	2018	CRD+SJP	BR_SP_Agi_28	*p29*	NS
										p24	NS
249	122	*C. sinensis*	single	Fruit	Aguaí, SP, BR	commercial	2018	SJP	BR_SP_Agi_29	*p29*	NS
										p24	NS
250	123	*C. sinensis* (Pera)	single	Fruit	Aguaí, SP, BR	commercial	2018	SJP	BR_SP_Agi_30	*p29*	NS

										p24	NS
251	124	*C. sinensis* (Pera)	single	Fruit	Aguaí, SP, BR	commercial	2018	CRD+SJP	BR_SP_Agi_31	*p29*	NS
										p24	NS
									BR_SP_Agi_32	*p29*	NS
										p24	NS
252	125	*C. sinensis* (Pera)	single	Fruit	Aguaí, SP, BR	commercial	2018	CRD	BR_SP_Agi_33	*p29*	NS
										p24	NS
253	126	*C. sinensis* (Pera)	single	Fruit	Águas de Santa Barbara, SP, BR	commercial	2018	SJP	BR_SP_ASB01	*p29*	NS
										p24	NS
254	127	*C. sinensis*	single	Fruit	Altinópolis, SP, BR	commercial	2018	SJP	BR_SP_Alt23	*p29*	NS
										p24	NS
255	128	*C. sinensis* (Pera)	single	Fruit	Angatuba, SP, BR	commercial	2018	CRD+SJP	BR_SP_Ang01	*p29*	NS
										p24	NS
256	129	*C. sinensis* (Pera)	single	Fruit	Anhembi, SP, BR	commercial	2018	CRD+SJP	BR_SP_Amb01	*p29*	NS
										p24	NS
257	130	*C. sinensis* (Pera)	single	Fruit	Arandu, SP, BR	commercial	2018	CRD+SJP	BR_SP_Ard01	*p29*	NS
										p24	NS
258	131	*C. sinensis* (Pera)	single	Fruit	Artur Nogueira, SP, BR	commercial	2018	CRD	BR_SP_ArN01	*p29*	NS
										p24	NS
259	132	*C. sinensis* (Pera)	single	Fruit	Avaí, SP, BR	commercial	2018	SJP	BR_SP_Ava01	*p29*	NS
										p24	NS
260	133	*C. sinensis* (Pera)	single	Fruit	Avaré, SP, BR	commercial	2018	CRD+SJP	BR_SP_Avr02	*p29*	NS
										p24	NS
									BR_SP_Avr03	*p29*	NS
										p24	NS
261	134	*C. sinensis* (Pera)	single	Fruit	Avaré, SP, BR	commercial	2018	SJP	BR_SP_Avr04	*p29*	NS
										p24	NS
262	135	*C. sinensis* (Pera)	single	Fruit	Avaré, SP, BR	commercial	2018	CRD	BR_SP_Avr05	*p29*	NS
										p24	NS
263	136	*C. sinensis* (Pera)	single	Fruit	Barretos, SP, BR	commercial	2018	CRD+SJP	BR_SP_Bar25	*p29*	NS
										p24	NS
264	137	*C. sinensis* (Pera)	single	Fruit	Bauru, SP, BR	commercial	2018	SJP	BR_SP_Bur01	*p29*	NS
										p24	NS
265	138	*C. sinensis* (Pera)	single	Fruit	Bebedouro, SP, BR	commercial	2018	SJP	BR_SP_Beb33	*p29*	NS
										p24	NS
266	139	*C. sinensis*	single	Fruit	Boa Esperança do Sul, SP, BR	commercial	2018	SJP	BR_SP_BES01	*p29*	NS
										p24	NS
267	140	*C. sinensis*	single	Fruit	Boa Esperança do Sul, SP, BR	commercial	2018	SJP	BR_SP_BES02	*p29*	NS
										p24	NS
268	141	*C. sinensis* (Pera)	single	Fruit	Brotas, SP, BR	commercial	2018	CRD+SJP	BR_SP_Bro15	*p29*	NS
										p24	NS

269	142	*C. sinensis*	single	Fruit	Brotas, SP, BR	commercial	2018	SJP	BR_SP_Bro16	*p29*	NS
										p24	NS
270	143	*C. sinensis* (Pera)	single	Fruit	Brotas, SP, BR	commercial	2018	SJP	BR_SP_Bro17	*p29*	NS
										p24	NS
271	244	*C. sinensis*	single	Fruit	Cabrália Paulista, SP, BR	commercial	2018	CRD	BR_SP_CbP01	*p29*	NS
										p24	NS
272	145	*C. sinensis*	single	Fruit	Cajobi, SP, BR	commercial	2018	SJP	BR_SP_Cjb01	*p29*	NS
										p24	NS
273	146	*C. sinensis*	single	Fruit	Casa Branca, SP, BR	commercial	2018	CRD+SJP	BR_SP_CsB02	*p29*	NS
										p24	NS
									BR_SP_CsB03	*p29*	NS
										p24	NS
274	147	*C. sinensis*	single	Fruit	Casa Branca, SP, BR	commercial	2018	CRD+SJP	BR_SP_CsB04	*p29*	NS
										p24	NS
									BR_SP_CsB05	*p29*	NS
										p24	NS
275	148	*C. sinensis* (Pera)	single	Fruit	Casa Branca, SP, BR	commercial	2018	CRD+SJP	BR_SP_CsB06	*p29*	NS
									BR_SP_CsB07	*p24*	NS
276	149	*C. sinensis* (Pera)	single	Fruit	Casa Branca, SP, BR	commercial	2018	CRD	BR_SP_CsB08	*p29*	NS
										p24	NS
277	150	*C. sinensis*	single	Fruit	Casa Branca, SP, BR	commercial	2018	CRD	BR_SP_CsB09	*p29*	NS
										p24	NS
278	151	*C. sinensis*	single	Fruit	Casa Branca, SP, BR	commercial	2018	CRD+SJP	BR_SP_CsB10	*p29*	NS
										p24	NS
									BR_SP_CsB11	*p29*	NS
										p24	NS
279	152	*C. sinensis* (Pera)	single	Fruit	Cedral, SP, BR	commercial	2018	SJP	BR_SP_Cdl01	*p29*	NS
										p24	NS
280	153	*C. sinensis* (Pera)	single	Fruit	Cerqueira Cesar, SP, BR	commercial	2018	SJP	BR_SP_CrC29	*p29*	NS
										p24	NS
281	154	*C. sinensis*	single	Fruit	Colina, SP, BR	commercial	2018	CRD	BR_SP_Cln03	*p29*	NS
										p24	NS
282	155	*C. sinensis* (Pera)	single	Fruit	Colina, SP, BR	commercial	2018	SJP	BR_SP_Cln04	*p29*	NS
										p24	NS
283	156	*C. sinensis*	single	Fruit	Colômbia, SP, BR	commercial	2018	CRD+SJP	BR_SP_Clb17	*p29*	NS
									BR_SP_Clb18	*p24*	NS
284	157	*C. sinensis*	single	Fruit	Comendador Gomes, MG, BR	commercial	2018	SJP	BR_MG_Cgz05	*p29*	NS
										p24	NS
285	158	*C. sinensis*	single	Fruit	Conchal, SP, BR	commercial	2018	CRD+SJP	BR_SP_Cch03	*p29*	NS
									BR_SP_Cch04	*p24*	NS
286	159	*C. sinensis*	single	Fruit	Conchal, SP, BR	commercial	2018	CRD+SJP	BR_SP_Cch05	*p29*	NS

									BR_SP_Cch06	*p24*	NS
287	160	*C. sinensis*	single	Fruit	Conchal, SP, BR	commercial	2018	CRD	BR_SP_Cch07	*p29*	NS
										p24	NS
288	161	*C. sinensis* (Natal)	single	Fruit	Conchal, SP, BR	commercial	2018	SJP	BR_SP_Cch08	*p29*	NS
										p24	NS
289	162	*C. sinensis* (Natal)	single	Fruit	Conchal, SP, BR	commercial	2018	SJP	BR_SP_Cch09	*p29*	NS
										p24	NS
290	163	*C. sinensis*	single	Fruit	Conchal, SP, BR	commercial	2018	CRD+SJP	BR_SP_Cch10	*p29*	NS
									BR_SP_Cch11	*p24*	NS
291	164	*C. sinensis*	single	Fruit	Engenheiro Coelho, SP, BR	commercial	2018	SJP	BR_SP_EgC01	*p29*	NS
										p24	NS
292	165	*C. sinensis*	single	Fruit	Engenheiro Coelho, SP, BR	commercial	2018	CRD+SJP	BR_SP_EgC02	*p29*	NS
										p24	NS
293	166	*C. sinensis* (Natal)	single	Fruit	Estiva Gerbi, SP, BR	commercial	2018	CRD	BR_SP_EtG01	*p29*	NS
										p24	NS
294	167	*C. sinensis*	single	Fruit	Fernando Prestes, SP, BR	commercial	2018	SJP	BR_SP_FrP01	*p29*	NS
										p24	NS
295	168	*C. sinensis* (Pera)	single	Fruit	Fernão, SP, BR	commercial	2018	SJP	BR_SP_Frn01	*p29*	NS
										p24	NS
296	169	*C. sinensis* (Pera)	single	Fruit	Frutal, MG, BR	commercial	2018	SJP	BR_MG_Frt02	*p29*	NS
										p24	NS
297	170	*C. sinensis*	single	Fruit	Frutal, MG, BR	commercial	2018	SJP	BR_MG_Frt03	*p29*	NS
										p24	NS
298	171	*C. sinensis*	single	Fruit	Gavião Peixoto, SP, BR	commercial	2018	SJP	BR_SP_GvP01	*p29*	NS
										p24	NS
299	172	*C. sinensis*	single	Fruit	Gavião Peixoto, SP, BR	commercial	2018	SJP	BR_SP_GvP02	*p29*	NS
										p24	NS
300	173	*C. sinensis* (Pera)	single	Fruit	Getulina, SP, BR	commercial	2018	SJP	BR_SP_Gtl01	*p29*	NS
										p24	NS
301	174	*C. sinensis*	single	Fruit	Guarantã, SP, BR	commercial	2018	SJP	BR_SP_Grt02	*p29*	NS
										p24	NS
302	175	*C. sinensis*	single	Fruit	Guarantã, SP, BR	commercial	2018	CRD+SJP	BR_SP_Grt03	*p29*	NS
									BR_SP_Grt04	*p24*	NS
303	176	*C. sinensis* (Pera)	single	Fruit	Iacanga, SP, BR	commercial	2018	SJP	BR_SP_Icg01	*p29*	NS
										p24	NS
304	177	*C. sinensis*	single	Fruit	Ibirá, SP, BR	commercial	2018	SJP	BR_SP_Ibr01	*p29*	NS
										p24	NS
305	178	*C. sinensis* (Natal)	single	Fruit	Ibiraci, MG, BR	commercial	2018	CRD+SJP	BR_SP_Ibc01	*p29*	NS
									BR_SP_Ibc02	*p24*	NS
306	179	*C. sinensis* (Pera)	single	Fruit	Ibitinga, SP, BR	commercial	2018	SJP	BR_SP_Ibt01	*p29*	NS
										p24	NS

307	180	*C. sinensis* (Natal)	single	Fruit	Ibitinga, SP, BR	commercial	2018	SJP	BR_SP_Ibt02	*p29*	NS
										p24	NS
308	181	*C. sinensis*	single	Fruit	Ipiguá, SP, BR	commercial	2018	SJP	BR_SP_Ipg01	*p29*	NS
										p24	NS
309	182	*C. sinensis*	single	Fruit	Itápolis, SP, BR	commercial	2018	SJP	BR_SP_Itp01	*p29*	NS
										p24	NS
310	183	*C. sinensis* (Natal)	single	Fruit	Itápolis, SP, BR	commercial	2018	SJP	BR_SP_Itp02	*p29*	NS
										p24	NS
311	184	*C. sinensis* (Pera)	single	Fruit	Itápolis, SP, BR	commercial	2018	SJP	BR_SP_Itp03	*p29*	NS
										p24	NS
312	185	*C. sinensis* (Pera)	single	Fruit	Itápolis, SP, BR	commercial	2018	SJP	BR_SP_Itp04	*p29*	NS
										p24	NS
313	186	*C. sinensis*	single	Fruit	Itápolis, SP, BR	commercial	2018	CRD	BR_SP_Itp05	*p29*	NS
										p24	NS
314	187	*C. sinensis* (Natal)	single	Fruit	Itápolis, SP, BR	commercial	2018	SJP	BR_SP_Itp06	*p29*	NS
										p24	NS
315	188	*C. sinensis*	single	Fruit	Itápolis, SP, BR	commercial	2018	CRD+SJP	BR_SP_Itp07	*p29*	NS
									BR_SP_Itp08	*p24*	NS
316	189	*C. sinensis*	single	Fruit	Itápolis, SP, BR	commercial	2018	SJP	BR_SP_Itp08	*p29*	NS
										p24	NS
317	190	*C. sinensis*	single	Fruit	Itápolis, SP, BR	commercial	2018	CRD+SJP	BR_SP_Itp09	*p29*	NS
										p24	NS
									BR_SP_Itp10	*p29*	NS
										p24	NS
318	191	*C. sinensis* (Pera)	single	Fruit	Ituiutaba, MG, BR	commercial	2018	SJP	BR_MG_Itb01	*p29*	MN955017
										p15	MT304683
										mp	MN955195
										p24	NS
									BR_MG_Itb02	*p29*	NS
										p15	NS
										mp	MN955196
										p24	NS
319	192	*C. sinensis* (Pera)	single	Fruit	Júlio Mesquita, SP, BR	commercial	2018	SJP	BR_SP_JlM01	*p29*	NS
										p24	NS
320	193	*C. reticulata*	single	Fruit	Júlio Mesquita, SP, BR	commercial	2018	CRD+SJP	BR_SP_JlM02	*p29*	NS
										p24	NS
									BR_SP_JlM03	*p29*	NS
										p24	NS
321	194	*C. sinensis*	single	Leaf	Jumirin, SP, BR	commercial	2019	CRD	BR_SP_Jmr01	*p29*	NS
										p24	NS
322	195	*C. sinensis* (Pera)	single	Fruit	Limeira, SP, BR	commercial	2018	SJP	BR_SP_Lim03	*p29*	NS

										p24	NS
323	196	*C. sinensis*	single	Fruit	Limeira, SP, BR	commercial	2018	SJP	BR_SP_Lim04	*p29*	NS
										p24	NS
324	197	*C. sinensis*	single	Fruit	Limeira, SP, BR	commercial	2018	CRD+SJP	BR_SP_Lim05	*p29*	NS
										p24	NS
									BR_SP_Lim06	*p29*	NS
										p24	NS
325	198	*C. sinensis*	single	Fruit	Limeira, SP, BR	commercial	2018	SJP	BR_SP_Lim07	*p29*	NS
										p24	NS
326	199	*C. sinensis*	single	Fruit	Limeira, SP, BR	commercial	2018	CRD	BR_SP_Lim08	*p29*	NS
										p24	NS
327	200	*C. sinensis*	single	Fruit	Lucianópolis, SP, BR	commercial	2018	CRD	BR_SP_Lcp01	*p29*	NS
										p24	NS
328	201	*C. sinensis*	single	Fruit	Lucianópolis, SP, BR	commercial	2018	SJP	BR_SP_Lcp02	*p29*	NS
										p24	NS
329	202	*C. sinensis* (Natal)	single	Fruit	Lucianópolis, SP, BR	commercial	2018	SJP	BR_SP_Lcp03	*p29*	NS
										p24	NS
330	203	*C. sinensis* (Pera)	single	Fruit	Mococa, SP, BR	commercial	2018	SJP	BR_SP_Mcc01	*p29*	NS
										p24	NS
331	204	*C. sinensis*	single	Fruit	Mococa, SP, BR	commercial	2018	CRD+SJP	BR_SP_Mcc02	*p29*	NS
										p24	NS
									BR_SP_Mcc03	*p29*	NS
										p24	NS
332	205	*C. sinensis*	single	Fruit	Mococa, SP, BR	commercial	2018	CRD	BR_SP_Mcc04	*p29*	NS
										p24	NS
334	206	*C. sinensis*	single	Fruit	Mococa, SP, BR	commercial	2018	SJP	BR_SP_Mcc05	*p29*	NS
										p24	NS
334	207	*C. sinensis* (Natal)	single	Fruit	Mogi Guaçu, SP, BR	commercial	2018	SJP	BR_SP_MgG01	*p29*	NS
										p24	NS
335	208	*C. sinensis* (Natal)	single	Fruit	Mogi Guaçu, SP, BR	commercial	2018	CRD+SJP	BR_SP_MgG02	*p29*	NS
										p24	NS
									BR_SP_MgG03	*p29*	NS
										p24	NS
336	209	*C. sinensis* (Pera)	single	Fruit	Mogi Guaçu, SP, BR	commercial	2018	SJP	BR_SP_MgG04	*p29*	NS
										p24	NS
337	210	*C. sinensis*	single	Fruit	Mogi Guaçu, SP, BR	commercial	2018	CRD	BR_SP_MgG05	*p29*	NS
										p24	NS
338	211	*C. sinensis*	single	Fruit	Mogi Mirim, SP, BR	commercial	2018	CRD+SJP	BR_SP_MgM41	*p29*	NS
										p24	NS
									BR_SP_MgM42	*p29*	NS
										p24	NS

339	212	*C. sinensis*	single	Fruit	Monte Azul Paulista, SP, BR	commercial	2018	SJP	BR_SP_MAP01	*p29*	NS
										p24	NS
340	213	*C. sinensis* (Pera)	single	Fruit	Monte Azul Paulista, SP, BR	commercial	2018	SJP	BR_SP_MAP02	*p29*	NS
										p24	NS
341	214	*C. sinensis*	single	Fruit	Monte Azul Paulista, SP, BR	commercial	2018	SJP	BR_SP_MAP03	*p29*	NS
										p24	NS
342	215	*C. sinensis* (Pera)	single	Fruit	Monte Azul Paulista, SP, BR	commercial	2018	SJP	BR_SP_MAP04	*p29*	NS
										p24	NS
343	216	*C. sinensis*	single	Fruit	Nova Granada, SP, BR	commercial	2018	CRD+SJP	BR_SP_NvG01	*p29*	NS
										p24	NS
									BR_SP_NvG02	*p29*	NS
										p24	NS
344	217	*C. sinensis* (Natal)	single	Fruit	Olímpia, SP, BR	commercial	2018	SJP	BR_SP_Olm02	*p29*	NS
										p24	NS
345	218	*C. sinensis* (Pera)	single	Fruit	Olímpia, SP, BR	commercial	2018	SJP	BR_SP_Olm03	*p29*	NS
										p24	NS
346	219	*C. sinensis* (Pera)	single	Fruit	Olímpia, SP, BR	commercial	2018	SJP	BR_SP_Olm04	*p29*	NS
										p24	NS
347	220	*C. sinensis* (Natal)	single	Fruit	Paulo de Faria, SP, BR	commercial	2018	SJP	BR_SP_PlF01	*p29*	NS
										p24	NS
348	221	*C. sinensis*	single	Fruit	Pedranópolis, SP, BR	commercial	2018	SJP	BR_SP_Pdp01	*p29*	NS
										p24	NS
349	222	*C. sinensis* (Natal)	single	Fruit	Pedregulho, SP, BR	commercial	2018	SJP	BR_SP_Pdg01	*p29*	NS
										p24	NS
350	223	*C. sinensis* (Natal)	single	Fruit	Pedregulho, SP, BR	commercial	2018	SJP	BR_SP_Pdg02	*p29*	NS
										p24	NS
351	224	*C. sinensis*	single	Fruit	Pedregulho, SP, BR	commercial	2018	SJP	BR_SP_Pdg03	*p29*	NS
										p24	NS
352	225	*C. sinensis* (Natal)	single	Fruit	Pedrinópolis, MG, BR	commercial	2018	SJP	BR_MG_Pdp01	*p29*	NS
										p24	NS
353	226	*C. reticulata*	pool	Leaf	Piracicaba, SP, BR	non-commercial	2018	CRD	BR_SP_Prb03	RNA1	MT554534
										RNA2	MT554548
354	227	*C. sinensis*	single	Fruit	Piracicaba, SP, BR	commercial	2018	SJP	BR_SP_Prb08	*p29*	NS
										p24	NS
355	228	*C. sinensis*	single	Fruit	Piracicaba, SP, BR	commercial	2018	CRD+SJP	BR_SP_Prb09	*p29*	NS
										p24	NS
									BR_SP_Prb10	*p29*	NS
										p24	NS
356	229	*C. sinensis*	single	Fruit	Piracicaba, SP, BR	commercial	2018	SJP	BR_SP_Prb11	*p29*	NS
										p24	NS
357	230	*C. sinensis*	single	Fruit	Pirajuí, SP, BR	commercial	2018	SJP	BR_SP_ Prj03	*p29*	NS

										p24	NS
358	231	*C. sinensis*	single	Fruit	Pirangi, SP, BR	commercial	2018	SJP	BR_SP_Png01	*p29*	NS
										p24	NS
359	232	*C. sinensis*	single	Fruit	Pirassununga, SP, BR	commercial	2018	CRD	BR_SP_Prg07	*p29*	NS
										p24	NS
360	233	*C. sinensis* (Pera)	single	Fruit	Pirassununga, SP, BR	commercial	2018	CRD+SJP	BR_SP_Prg08	*p29*	NS
										p24	NS
									BR_SP_Prg09	*p29*	NS
										p24	NS
361	234	*C. sinensis* (Pera)	single	Fruit	Piratininga, SP, BR	commercial	2018	SJP	BR_SP_Ptn01	*p29*	NS
										p24	NS
362	235	*C. sinensis* (Pera)	single	Fruit	Piratininga, SP, BR	commercial	2018	CRD	BR_SP_Ptn02	*p29*	NS
										p24	NS
363	236	*C. sinensis*	single	Fruit	Piratininga, SP, BR	commercial	2018	SJP	BR_SP_Ptn03	*p29*	NS
										p24	NS
364	237	*C. sinensis*	single	Fruit	Potirendaba, SP, BR	commercial	2018	SJP	BR_SP_Pob01	*p29*	NS
										p24	NS
365	238	*C. sinensis* (Pera)	single	Fruit	Potirendaba, SP, BR	commercial	2018	SJP	BR_SP_Pob02	*p29*	NS
										p24	NS
366	239	*C. sinensis* (Pera)	single	Fruit	Prata, MG, BR	commercial	2018	SJP	BR_MG_Prt01	*p29*	NS
										p24	NS
367	240	*C. sinensis* (Pera)	single	Fruit	Reginópolis, SP, BR	commercial	2018	CRD+SJP	BR_SP_Rgp01	*p29*	NS
										p24	NS
									BR_SP_Rgp02	*p29*	NS
										p24	NS
368	241	*C. sinensis*	single	Fruit	Ribeirão Bonito, SP, BR	commercial	2018	SJP	BR_SP_RbB01	*p29*	NS
										p24	NS
369	242	*C. sinensis*	single	Fruit	Ribeirão Bonito, SP, BR	commercial	2018	SJP	BR_SP_RbB02	*p29*	NS
										p24	NS
370	243	*C. sinensis*	single	Fruit	Rincão, SP, BR	commercial	2018	SJP	BR_SP_Rnc01	*p29*	NS
										p24	NS
371	244	*C. sinensis*	single	Fruit	Rio Claro, SP, BR	commercial	2018	SJP	BR_SP_RiC01	*p29*	NS
										p24	NS
372	245	*C. sinensis*	single	Fruit	Riolândia, SP, BR	commercial	2018	CRD	BR_SP_Rld01	*p29*	NS
										p24	NS
373	246	*C. sinensis*	single	Fruit	Santa Cruz do Rio Pardo, SP, BR	commercial	2018	SJP	BR_SP_SCP02	*p29*	NS
										p24	NS
374	247	*C. sinensis*	single	Fruit	Santa Cruz do Rio Pardo, SP, BR	commercial	2018	SJP	BR_SP_SCP03	*p29*	NS
										p24	NS
375	248	*C. sinensis* (Pera)	single	Fruit	Santa Rosa de Viterbo, SP, BR	commercial	2018	CRD	BR_SP_SRV01	*p29*	NS
										p24	NS

376	249	*C. sinensis* (Pera)	single	Fruit	Santa Salete, SP, BR	commercial	2018	SJP	BR_SP_SnS01	*p29*	NS
										p24	NS
377	250	*C. sinensis*	single	Fruit	Santa Salete, SP, BR	commercial	2018	SJP	BR_SP_SnS02	*p29*	NS
										p24	NS
378	251	*C. sinensis*	single	Fruit	Santa Salete, SP, BR	commercial	2018	SJP	BR_SP_SnS03	*p29*	NS
										p24	NS
379	253	*C. sinensis*	single	Fruit	São Carlos, SP, BR	commercial	2018	CRD+SJP	BR_SP_SaC01	*p29*	NS
										p24	NS
									BR_SP_SaC02	*p29*	NS
										p24	NS
380	254	*C. sinensis*	single	Fruit	São Carlos, SP, BR	commercial	2018	SJP	BR_SP_SaC02	*p29*	NS
										p24	NS
381	255	*C. sinensis* (Pera)	single	Fruit	São João da Boa Vista, SP, BR	commercial	2018	SJP	BR_SP_SJV01	*p29*	NS
										p24	NS
382	256	*C. sinensis* (Pera)	single	Fruit	São João da Boa Vista, SP, BR	commercial	2018	CRD	BR_SP_SJV02	*p29*	NS
										p24	NS
383	257	*C. sinensis*	single	Fruit	São João da Boa Vista, SP, BR	commercial	2018	CRD	BR_SP_SJV03	*p29*	NS
										p24	NS
384	258	*C. sinensis*	single	Fruit	São João da Boa Vista, SP, BR	commercial	2018	SJP	BR_SP_SJV04	*p29*	NS
										p24	NS
385	259	*C. sinensis*	single	Fruit	São Pedro da União, MG, BR	commercial	2018	SJP	BR_MG_SPU01	*p29*	NS
										p24	NS
386	260	*C. sinensis* (Natal)	single	Fruit	São Pedro da União, MG, BR	commercial	2018	SJP	BR_MG_SPU02	*p29*	NS
										p24	NS
387	261	*C. sinensis* (Natal)	single	Fruit	São Pedro, SP, BR	commercial	2018	CRD+SJP	BR_SP_SPe01	*p29*	NS
										p24	NS
									BR_SP_SPe02	*p29*	NS
										p24	NS
388	262	*C. sinensis* (Natal)	single	Fruit	São Pedro, SP, BR	commercial	2018	SJP	BR_SP_SPe03	*p29*	NS
										p24	NS
389	263	*C. sinensis*	single	Fruit	São Pedro, SP, BR	commercial	2018	SJP	BR_SP_SPe04	*p29*	NS
										p24	NS
390	264	*C. sinensis*	single	Fruit	São Pedro, SP, BR	commercial	2018	SJP	BR_SP_SPe05	*p29*	NS
										p24	NS
391	265	*C. sinensis* (Pera)	single	Fruit	São Pedro, SP, BR	commercial	2018	CRD+SJP	BR_SP_SPe06	*p29*	NS
										p24	NS
									BR_SP_SPe07	*p29*	NS
										p24	NS
392	266	*C. sinensis* (Natal)	single	Fruit	São Sebastião do Paraíso, MG, BR	commercial	2018	SJP	BR_MG_SSP01	*p29*	NS
										p24	NS
393	267	*C. sinensis*	single	Fruit	São Simão, SP, BR	commercial	2018	SJP	BR_SP_SaS01	*p29*	NS

										p24	NS
394	268	*C. sinensis*	single	Leaf	Sinop, MT, BR	commercial	2019	CRD	BR_MT_Snp01	*p29*	NS
										p24	NS
395	269	*C. sinensis*	single	Fruit	Sud Mennucci, SP, BR	commercial	2018	CRD+SJP	BR_SP_SdM13	*p29*	NS
										p24	NS
									BR_SP_SdM14	*p29*	NS
										p24	NS
396	270	*C. sinensis*	single	Fruit	Tabapuã, SP, BR	commercial	2018	SJP	BR_SP_Tbp01	*p29*	NS
										p24	NS
397	271	*C. sinensis*	single	Fruit	Tabatinga, SP, BR	commercial	2018	SJP	BR_SP_Tbt02	*p29*	NS
										p24	NS
398	272	*C. sinensis*	single	Fruit	Tabatinga, SP, BR	commercial	2018	SJP	BR_SP_Tbt03	*p29*	NS
										p24	NS
399	273	*C. sinensis*	single	Fruit	Tabatinga, SP, BR	commercial	2018	SJP	BR_SP_Tbt04	*p29*	NS
										p24	NS
400	274	*C. sinensis*	single	Fruit	Tambaú, SP, BR	commercial	2018	SJP	BR_SP_Tmb34	*p29*	NS
										p24	NS
401	275	*C. sinensis* (Pera)	single	Fruit	Tanabi, SP, BR	commercial	2018	SJP	BR_SP_Tnb01	*p29*	NS
										p24	NS
402	276	*C. sinensis* (Pera)	single	Fruit	Tanabi, SP, BR	commercial	2018	CRD+SJP	BR_SP_Tnb02	*p29*	NS
										p24	NS
									BR_SP_Tnb03	*p29*	NS
										p24	NS
403	277	*C. sinensis* (Natal)	single	Fruit	Taquaritinga, SP, BR	commercial	2018	SJP	BR_SP_Tqt05	*p29*	NS
										p24	NS
404	278	*C. sinensis* (Pera)	single	Fruit	Tatuí, SP, BR	commercial	2018	CRD	BR_SP_Tti03	*p29*	NS
										p24	NS
405	279	*C. sinensis* (Pera)	single	Fruit	Trabiju, SP, BR	commercial	2018	SJP	BR_SP_Trb01	*p29*	NS
										p24	NS
406	280	*C. sinensis* (Pera)	single	Fruit	Turmalina, SP, BR	commercial	2018	CRD+SJP	BR_SP_Trm01	*p29*	NS
										p24	NS
									BR_SP_Trm02	*p29*	NS
										p24	NS
407	281	*C. sinensis* (Pera)	single	Fruit	Ubirajara, SP, BR	commercial	2018	CRD+SJP	BR_SP_Ubj01	*p29*	NS
										p24	NS
									BR_SP_Ubj02	*p29*	NS
										p24	NS
408	282	*C. sinensis* (Natal)	single	Fruit	Ubirajara, SP, BR	commercial	2018	SJP	BR_SP_Ubj02	*p29*	NS
										p24	NS
409	283	*C. sinensis* (Natal)	single	Fruit	Uru, SP, BR	commercial	2018	SJP	BR_SP_Uru02	*p29*	NS
										p24	NS

410	284	*C. sinensis* (Natal)	single	Fruit	Uru, SP, BR	commercial	2018	SJP	BR_SP_Uru03	*p29*	NS
										p24	NS
411	285	*C. sinensis* (Pera)	single	Fruit	Uru, SP, BR	commercial	2018	SJP	BR_SP_Uru04	*p29*	NS
										p24	NS
412	286	*C. sinensis* (Pera)	single	Fruit	Uru, SP, BR	commercial	2018	SJP	BR_SP_Uru05	*p29*	NS
										p24	NS
413	287	*C. sinensis*	pool	Fruit	Vista Alegre do Alto, SP, BR	commercial	2018	SJP	BR_SP_VAA01	*p29*	NS
										p24	NS
414	288	*C. sinensis*	single	Leaf	Vitoria, ES, BR	non-commercial	2018	CRD	BR_ES_Vtr01	RNA1	MT554539
										RNA2	MT554553
415	289	*C. sinensis*	single	Leaf	Bebedouro, SP, BR	commercial	2019	SJP	BR_SP_Beb34	*p29*	NS
										p24	NS
416	290	*C. sinensis*	single	Leaf	Bebedouro, SP, BR	commercial	2019	SJP	BR_SP_Beb35	*p29*	NS
										p24	NS
417	291	*C. sinensis*	single	Leaf	Bebedouro, SP, BR	commercial	2019	SJP	BR_SP_Beb36	*p29*	NS
										p24	NS
418	292	*C. sinensis*	single	Fruit	Bebedouro, SP, BR	commercial	2019	SJP	BR_SP_Beb37	*p29*	NS
										p24	NS
419	293	*C. sinensis* (Valencia)	pool	Fruit, leaf and branc	Jaboticabal, SP, BR	commercial	2019	SJP	BR_SP_Jbt04	*p29*	NS
										p24	NS
420	294	*C. sinensis*	single	Leaf	Caazapa, PY	non-commercial	2019	CRD	PY_Czp01	*p29*	NS
										p24	NS
421	295	*C. sinensis*	single	Fruit	Braganca Paulista, SP, BR	non-commercial	2019	CRD	BR_SP_BgP01	*p29*	NS
										p24	NS
422	296	*C. sinensis*	single	Leaf	Braganca Paulista, SP, BR	non-commercial	2019	CRD	BR_SP_BgP02	*p29*	NS
										p24	NS
423	297	*C. sinensis*	single	Branch	Braganca Paulista, SP, BR	non-commercial	2019	CRD	BR_SP_BgP03	*p29*	NS
										p24	NS
424	298	*C. sinensis*	pool	Leaf	Bella Vista, Coorientes, AR	non-commercial	2019	CRD	AR13	*p29*	NS
										p24	NS
425	299	*C. sinensis* (Valencia)	pool	Leaf	Bella Vista, Coorientes, AR	non-commercial	2019	CRD	AR14	*p29*	NS
										p24	NS
426	300	*C. sinensis* (Hamlim)	pool	Leaf	Bella Vista, Coorientes, AR	non-commercial	2019	CRD	AR15	*p29*	NS
										p24	NS

[1]The viruses were detected from the pool of lesions = pool or a unique lesion = single; [2] Country abbreviations= BR: Brazil, AR: Argentina, CO: Colombia, and PY: Paraguay; Brazilian states abbreviations= AM: Amazonas, DF: Distrito Federal; MG: Minas Gerais, MS: Mato Grosso do Sul, PR: Paraná, RJ: Rio de Janeiro; RS: Rio Grande do Sul; SE: Sergipe, SP: São Paulo, and TO: Tocantins; [3]The presence of CiLV-C strains was assessed by detection by RT-PCR from different regions of the genome (*p29*, *p15*, *mp* or *p24*) and/or high throughput sequencing (HTS). The results were according to the presence of only CRD strain, SJP strain, ASU strain, or of the presence of CRD and SJP strains in a sample or a single lesion (CRD + SJP). [4]The detected CiLV-C isolates were classified

according to the collection site (Country / State / City) followed by numerical order. [5]For samples subjected to HTS has recovered total genome of CiLV -C (RNA1 and RNA2) for some samples were obtained the partial sequences by the Sanger method, and the other sequences detected were not sequenced (NS). [6] The sample obtained from the experimental transmission of CiLV-C SJP from viruliferous *Brevipalpus yothersi* mites to *Arabidopsis thaliana* (Ramos-González et al., 2016). The mites were collected from *Citrus sinensis* infected with CiLV-C_BR_SP_SJP01. In addition to the sequences obtained in this work, the sequences of CiLV-C isolates available at GenBank were incorporated: AR01 and PY01 (Caceres et al., 2013); CO01 (Leon et al., 2006); MX01 (Castillo et al., 2011); PA01 (Unpublished); BR_SP_Brm01 (Nunes et al., 2012); BR_SP_Crd01 (Localli et al., 2006); BR_SP_Jbt01 (Pascon et al., 2006) and AR02, BR_MGAfe_01, BR_SP_Amp01, BR_SE_Aju01, BR_SP_Ara01, BR_PA_Bel01, BR_SP_Brm02, BR_DF_Bsb01, BR_SP_Cmp01, BR_SP_CsB01, BR_SP_Cln01, BR_MG_CGz01, BR_SP_Cch01, BR_SP_Crd02, BR_SP_Crd03, BR_SP_Csm01, BR_GO_Gyn01, BR_MG_Lav01, BR_SC_Lsp01, BR_PR_Ldb01, BR_AM_Mao01, BR_PR_Mgf01, BR_SP_Mrn01, BR_SC_NCh01, BR_SC_NTb01, BR_TO_Pmw01, BR_SP_Prb01, BR_GO_Pnt01, BR_SP_Prt01, BR_AC_RBr01, BR_SP_Itu01, BR_MG_Stc01, BR_SP_SAP01, BR_SP_SNg01, BR_SP_SJP01, BR_SP_SJP02, BR_SP_SJP03, BR_SP_SJP04, BR_SP_SdM01, BR_SP_SdM02, BR_SP_SdM_03, BR_SP_SdM_04, BR_SP_SdM_05, BR_SP_SdM_06, BR_RJ_Tng01, BR_SP_Tti01, BR_MT_Trn01, BR_MG_Uba01 (Ramos-González et al., 2016).

Supplementary Table 2. Nucleotide and haplotypic diversity of different clones of the *p29* and *mp* genes of CiLV-C sequenced from samples of *Citrus sinensis* collected in commercial orchards in the citrus belt of Brazil.

Sample collection location	***p29* gene sequences**			***mp* gene sequences**			**Isolates selected for the concatenate analysis**
	Number of		**Nucleotide diversity (π)**	**Number of**		**Nucleotide diversity (π)**	
	Isolates	**Haplotypes**		**Isolates**	**Haplotypes**		
Aguaí, SP	4	4	0..00440	9	4	0..00752	**4**
Altinópolis, SP	3	3	0..00252	6	3	0..00231	**3**
Barretos, SP	10	7	0..00579	16	4	0..00749	**7**
Bebedouro, SP	7	6	0..00252	31	6	0..00175	**7**
Brotas, SP	7	7	0..00276	11	5	0..00795	**7**
Cerqueira Cesar, SP	8	7	0..00557	11	6	0..00568	**7**
Guaimbê, SP	2	2	0..00503	8	3	0..00260	**2**
Mogi Mirim, SP	12	11	0..00496	27	7	0..00785	**11**
Pirassununga, SP	3	3	0..00252	4	2	0..00174	**3**
Santa Maria da Serra, SP	7	7	0..00288	2	2	0..00347	**2**
Sud Mennucci, SP	12	6	0..00739	6	3	0..00301	**6**
Tambaú, SP	8	6	0..00299	8	3	0..00260	**6**
Taquaral, SP	3	3	0..00168	7	4	0..00364	**3**
Taquaritinga, SP	2	1	0	4	1	0	**1**
Uberaba, MG	9	9	0..00538	15	7	0..00370	**9**

Supplementary Table 3. Nucleotide and deduced amino acids identities among the CiLV-C isolates sequenced in this study and the reference members of the CiLV-C CRD (DQ352194 and DQ352195) and SJP strain (KP336746 and KP336747).

CiLV-C isolate	CiLV-C_BR_SP_Crd01														
	RNA1	*RdRp*		*p29*		RNA2	*p15*		IR	*p61*		*mp*		*p24*	
	nt	nt	aa	nt	aa	nt	nt	aa	nt	nt	aa	nt	aa	nt	aa
AR04	99	99	99	99	100	98	99	98	98	98	98	99	99	99	99
AR05	99	99	99	99	100	98	98	97	97	99	99	99	99	100	100
AR06	99	99	100	100	100	100	99	100	99	100	99	100	100	100	100
BR_ES_Vtr01	99	99	100	100	100	100	99	100	99	100	99	100	100	100	100
BR_RS_Urg01	99	99	99	99	100	99	99	99	98	100	100	99	100	100	100
BR_SP_Jac01	98	98	99	100	100	99	99	99	100	100	100	100	99	100	100
BR_SP_Jbt02	99	99	100	99	100	100	100	100	99	100	100	100	99	100	100
BR_SP_Lim01	99	99	100	99	100	100	100	99	99	100	100	100	100	100	100
BR_SP_Prb02	99	99	100	99	100	100	99	99	99	100	100	100	100	100	100
BR_SP_Prb03	99	99	99	100	100	99	100	100	99	99	99	99	100	100	100
BR_SP_Prb04	99	99	100	100	100	100	100	100	99	100	100	100	95	100	100
BR_SP_SJP05	86	86	93	85	94	89	99	100	97	82	84	87	92	88	94
BR_SP_SPa11	99	99	100	100	100	100	99	100	99	99	99	100	100	100	100
PY_Asu02	86	86	93	86	94	86	98	100	85	82	81	89	95	89	94
	CiLV-C_BR_SP_SJP01														
	RNA1	*RdRp*		*p29*		RNA2	*p15*		*IR*	*p61*		*mp*		*p24*	
	nt	nt	aa	nt	aa	nt	nt	aa	nt	nt	aa	nt	aa	nt	aa
AR04	88	85	93	85	90	88	99	98	96	82	85	87	92	87	93
AR05	88	85	93	85	90	88	98	97	95	82	84	87	92	88	93
AR06	88	85	93	85	90	88	99	100	97	82	84	87	92	88	93
BR_ES_Vtr01	88	85	93	85	90	88	99	100	97	82	84	87	92	87	93
BR_RS_Urg01	88	85	93	84	90	88	99	99	97	82	84	86	92	88	93
BR_SP_Jac01	88	85	92	85	90	88	99	99	97	82	84	87	92	87	93
BR_SP_Jbt02	88	86	93	85	90	88	99	100	97	82	84	87	92	87	93
BR_SP_Lim01	88	86	93	85	90	88	99	99	97	82	84	87	92	87	93
BR_SP_Prb02	88	85	93	85	90	88	99	99	97	82	84	87	92	88	93
BR_SP_Prb03	88	85	93	85	90	88	99	100	97	81	83	87	92	88	93
BR_SP_Prb04	88	86	93	85	90	88	99	100	97	82	84	87	92	87	93
BR_SP_SJP05	99	99	100	99	99	99	99	100	100	99	100	99	99	99	100
BR_SP_SPa11	88	85	93	85	90	88	99	100	97	82	84	87	92	87	93
PY_Asu02	85	88	95	86	90	85	98	100	85	83	84	87	94	89	94

Supplementary Table 4. Recombination events detected in CiLV-C sequences determined by RDP software version 5.5.

Event	Found	Recombination	Major parent	Minor parent	Detection method[1]						
					R	G	B	M	C	S	T
RNA2 (n=18)											
1	1	BR_SP_SJP01	Unknown	BR_SP_Spa11	+	+	+	+	+	+	+
	2	BR_SP_SJP05			+	+	+	+	+	+	+
2	1	PY_Asu02	Unknown	BR_RS_Urg01	+	+	-	+	+	-	+
3	1	BR_SP_SJP05	BR_SP_SJP01	PY_Asu02	-	+	+	+	+	-	+
RNA2: *p15*-IR-*mp* (n=51)											
4	1	BR_SP_Csm01	Unknown	BR_PA_Bel01	+	-	+	+	+	+	+
	2	BR_SP_SJP01			+	-	+	+	+	+	+
	3	BR_SP_SJP03			+	-	+	+	+	+	+
	4	BR_SP_SJP05			+	-	+	+	+	+	+
	5	BR_SP_SdM01			+	-	+	+	+	+	+
	6	BR_SP_SdM02			+	-	+	+	+	+	+
	7	BR_SP_SdM03			+	-	+	+	+	+	+
	8	BR_SP_SdM04			+	-	+	+	+	+	+
	9	BR_SP_SdM05			+	-	+	+	+	+	+
	10	BR_SP_SdM06			+	-	+	+	+	+	+
5	1	BR_SP_Amp01	BR_SE_Aju01	Unknown	-	-	-	+	+	+	+
	2	AR05			-	-	-	+	+	+	+
	3	BR_SP_Ara01			-	-	-	+	+	+	+
	4	BR_PA_Bel01			-	-	-	+	+	+	+
	5	BR_SP_Brm01			-	-	-	+	+	+	+
	6	Brasília_DF_I			-	-	-	+	+	+	+
	7	BR_SP_Cch01			-	-	-	+	+	+	+
	8	BR_SP_Crd01			-	-	-	+	+	+	+
	9	BR_SP_Crd02			-	-	-	+	+	+	+
	10	BR_GO_Gyn01			-	-	-	+	+	+	+
	11	BR_SP_Jbt01			-	-	-	+	+	+	+
	12	BR_SP_Jbt02			-	-	-	+	+	+	+
	13	BR_SP_Jac01			-	-	-	+	+	+	+
	14	BR_SP_Lim01			-	-	-	+	+	+	+
	15	BR_PR_Ldb01			-	-	-	+	+	+	+
	16	BR_AM_Mao01			-	-	-	+	+	+	+
	17	BR_PR_Mgf01			-	-	-	+	+	+	+
	18	BR_SP_Mrn01			-	-	-	+	+	+	+
	19	BR_TO_Pnw01			-	-	-	+	+	+	+
	20	PA01			-	-	-	+	+	+	+
	21	BR_SP_Prb01			-	-	-	+	+	+	+
	22	BR_SP_Prb02			-	-	-	+	+	+	+
	23	BR_SP_Prb04			-	-	-	+	+	+	+
	24	BR_SP_Prt01			-	-	-	+	+	+	+
	25	BR_SP_Spa11			-	-	-	+	+	+	+
	26	BR-RJ_Tng01			-	-	-	+	+	+	+
	27	BR_SP_Tti01			-	-	-	+	+	+	+
	28	BR_MS_Trn01			-	-	-	+	+	+	+
	29	BR_ES_Vtr			-	-	-	+	+	+	+

[1] Methods abbreviation = R: RDP; G: GENECONV; B: Bootscan; M: Maxchi; C: Chimaera; S: SiScan; and T: Topal.

Supplementary Table 5. Summary of selection analysis of the *p29* and *mp* genes in CiLV-C population sequences.

Method	Dataset	Selection	p-value	Number	Amino acid numbers
***p29* gene**					
FUBAR	SJP+CRD+ASU (185)	purification	0.9	45	7, 29, 30, 32, 33, 47, 58, 61, 69,76, 99, 100, 101, 106, 112, 113, 116, 136, 137, 138, 139, 154, 157, 161, 165, 171, 173, 175, 181, 195, 196, 198, 201, 207, 208, 209, 213, 217, 219, 220, 227, 240, 245, 254 and 259
	SJP+CRD (184)	purification	0.9	42	7, 12, 29, 30, 32, 33, 48, 58, 61, 76, 100, 101, 106, 112, 113, 116, 136, 137, 139, 151, 154, 157, 161, 165, 173, 181, 195, 196, 198, 201, 202, 207, 209, 213, 217, 219, 227, 234, 240, 245, 254 and 259
	SJP (103)	purification	0.9	14	7, 29, 48, 61, 68, 69, 76, 137, 139, 157, 173, 198, 219 and 240
		diversification	0.9	1	16
	CRD (81)	purification	0.9	13	7, 32, 58, 99, 105, 111, 134, 159, 169, 179, 209, 215 and 225
FEL	SJP+CRD+ASU (185)	purification	0.1	53	7, 15, 23, 29, 30, 32, 33, 47, 58, 61, 69, 76, 83, 99, 100, 101, 106, 113, 116, 117, 136, 137, 138, 139, 147, 154, 157, 159, 161, 165, 173, 175, 181, 186, 194, 195, 196, 198, 201, 207, 208, 209, 211, 213,217, 219, 220, 227, 240, 245, 251, 254 and 259
	SJP+CRD (184)	purification	0.1	48	5, 7, 12, 13, 15, 29, 30, 32, 33, 58, 61, 76, 100, 101, 106, 113, 116, 136, 137, 138, 139, 151, 154, 157, 159, 161, 165, 173, 181, 195, 196, 198, 201, 202, 205, 207, 209, 211, 213, 217, 219, 220, 227, 234, 240, 245, 254 and 259
		diversification	0.1	1	93
	SJP (103)	purification	0.1	19	5, 7, 12, 29, 30, 33, 38, 61, 68, 69, 92, 139, 157, 198, 209, 213, 234, 240 and 255
	CRD (81)	diversification	0.1	1	147
		purification	0.1	17	7, 32, 47, 58, 72, 85, 97, 99, 104, 105, 111, 134, 165, 179, 209, 215 and 225
MEME	SJP+CRD+ASU (185)	diversification	0.1	5	16, 26, 104, 140 and 163

	SJP+CRD (184)	diversification	0.1	6	16, 26, 93, 104, 140 and 163
	SJP (103)	diversification	0.1	1	16
	CRD (81)	diversification	0.1	3	26, 102 and 138
FUBAR+FEL	SJP+CRD+ASU (185)	purification	0.1	43	7, 29, 30, 32, 33, 47, 58, 61, 69, 76, 99, 100, 101, 106, 113, 116, 136, 137, 138, 139, 154, 157, 161, 165, 173, 175, 181, 195, 196, 198, 201, 207, 208, 209, 213, 217, 219, 220, 227, 240, 245, 254 and 259
	SJP+CRD (184)	purification	0.1	40	7, 12, 29, 30, 32, 33, 58, 61, 76, 100, 101, 106, 113, 116, 136, 137, 139, 151, 154, 157, 161, 165, 173, 181, 195, 196, 198, 201, 202, 207, 209, 213, 217, 219, 227, 234, 240, 245, 254 and 259
	SJP (103)	purification	0.1	9	7, 29, 61, 68, 69, 139, 157, 198 and 240
	CRD (81)	purification	0.1	11	7, 32, 58, 99, 105, 111, 134, 179, 209, 215 and 225
***mp* gene**[1]					
FUBAR	SJP+CRD+ASU (265)	purification	0.9	23	68, 71, 72, 73, 74, 75, 76, 77, 80, 84, 93, 95, 96, 97, 98, 99, 100, 112, 115, 118, 146, 147 and 148
	SJP+CRD (264)	purification	0.9	19	68, 71, 72, 75, 76, 80, 84, 93, 96, 97, 98, 99, 100, 101, 103, 115, 146, 147, and 148
	SJP (187)	purification	0.9	1	75
	CRD (77)	purification	0.9	5	75, 97, 103, 112 and 136
FEL	SJP+CRD+ASU (265)	purification	0.1	34	57, 68, 70, 71, 72, 73, 74, 75, 76, 77, 79, 80, 84, 93, 95, 96, 97, 98, 99, 102, 103, 111, 112, 115, 119, 121, 126, 129, 138, 142, 145, 146, 147 and 148
	SJP+CRD (264)	purification	0.1	27	57, 68, 71, 72, 74, 75, 76, 77, 80, 84, 85, 93, 96, 97, 98, 99, 102, 103, 111, 112, 115, 119, 121, 145, 146, 147 and 148
	SJP (187)	purification	0.1	10	57, 64, 68, 72, 75, 84, 119, 125, 145 and 146
	CRD (77)	purification	0.1	14	68, 69, 73, 75, 77, 85, 93, 96, 97, 98, 103, 136, 146 and 148
MEME	SJP+CRD+ASU (265)	diversification	0.1	2	56 and 64
	SJP+CRD (264)	diversification	0.1	1	64
	SJP (187)	diversification	0.1	0	-
	CRD (77)	diversification	0.1	0	-

FUBAR+FEL	SJP+CRD+ASU (265)	purification	0.1	23	68, 71, 72, 73, 74, 75, 76, 77, 80, 84, 93, 95, 96, 97, 98, 99, 103, 112, 115, 138, 146, 147 and 148
	SJP+CRD (264)	purification	0.1	19	68, 71, 72, 75, 76, 80, 84, 93, 96, 97, 98, 99, 102, 103, 112, 115, 146, 147 and 148
	SJP (187)	purification	0.1	1	75
	CRD (77)	purification	0.1	4	75, 97, 103 and 136

[1]The sequence of the *mp* gene analyzed corresponding to the amino acid stretch between positions 55 and 150 of the protein

ANNEX II

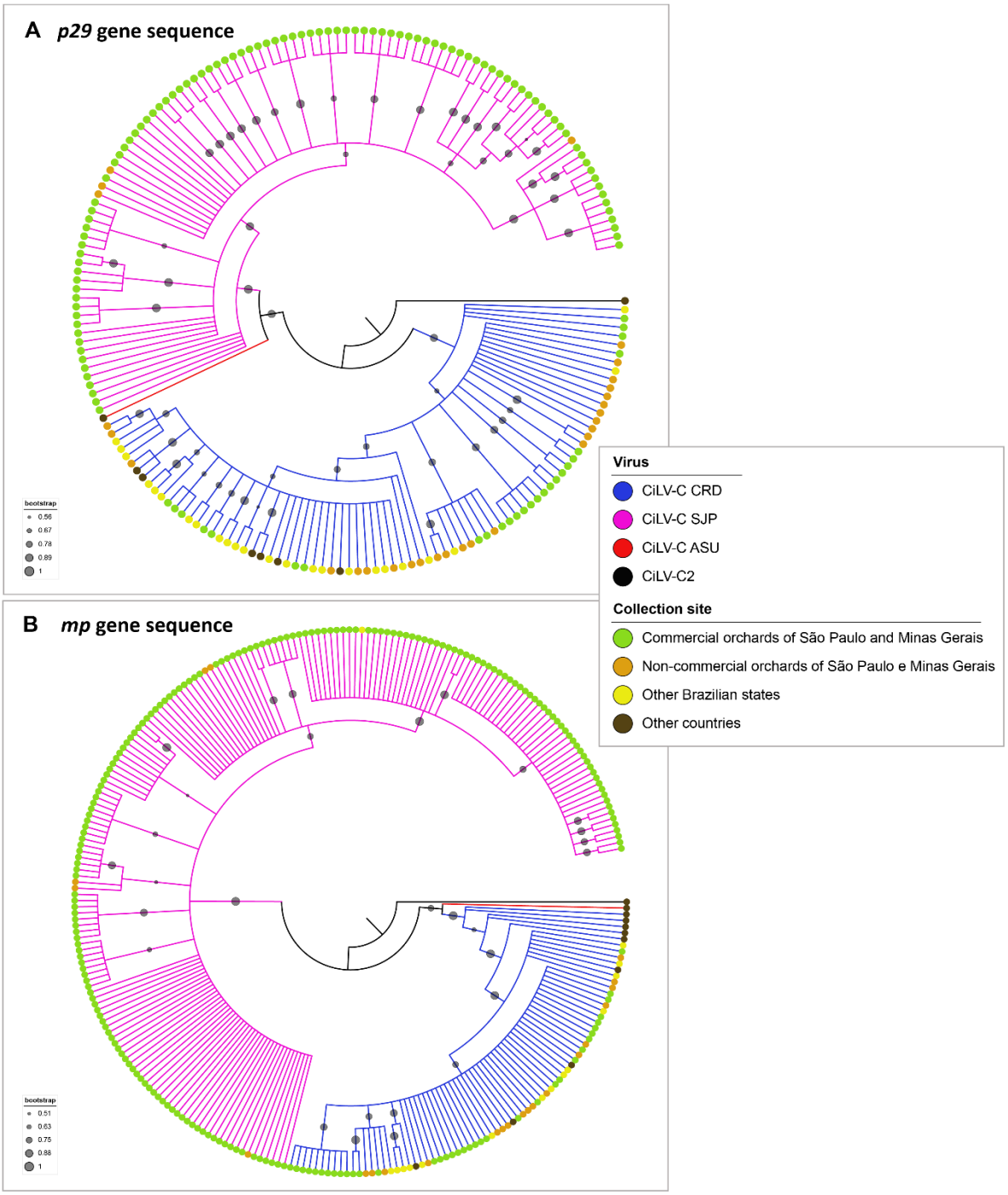

Supplementary Figure 1. Bayesian inference of CiLV-C strain CRD (blue branches), SJP (pink branches) and ASU (red branches) lineages based on P29 (**A**) and MP proteins (**B**). CiLV-C2 sequences (black branches) were used as an outgroup and trees were generated with 6,000,000 generations. The color-coded based collection sites show whether the sample was obtained from commercial orchards in the citrus belt of São Paulo (SP) and Minas Gerais (MG) states (in green), from non-commercial citrus trees of SP and MG (in ocher), from other Brazilian states (in yellow) or from other countries i.e. Argentina, Colombia, Mexico, Panama and Paraguay (in brown).

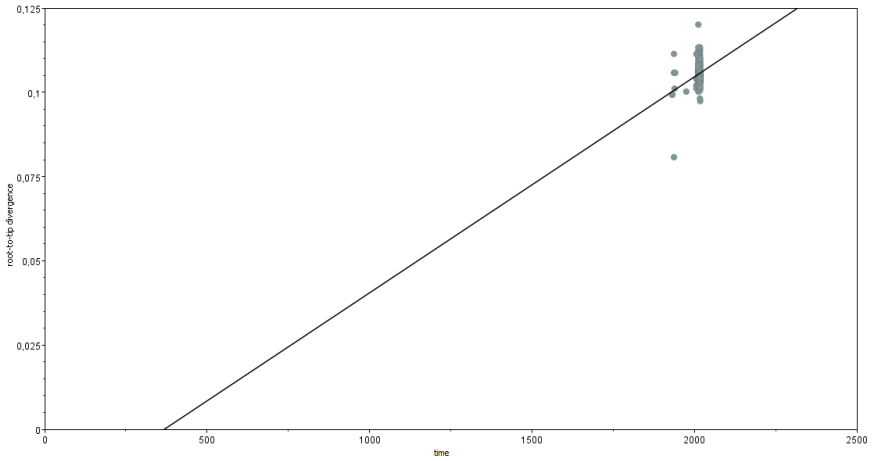

Supplementary Figure 2. Analyses of the temporal signal by linear regression approach from the concatenate of the complete sequence of the *p29* gene (795 nt) and partial sequence of the *mp* gene (288 nt) of 125 isolates of CiLV-C using TempEst v. 1.5.3 software. Root-to-tip divergence as a function of sampling time for Maximum likelihood non-clock tree generated by IQtree v. 1.5.5 software.

4. CHAPTER 2

CITRUS LEPROSIS VIRUS N: IDENTIFICATION AND CHARACTERIZATION OF A NEW CAUSAL AGENT OF CITRUS LEPROSIS DISEASE IN SOUTH AMERICA

Published

Ramos-González, Pedro; Chabi-Jesus, Camila; Guerra-Peraza, Orlene; Tassi, Aline D.; Kitajima, Elliot; Harakava, Ricardo; Salaroli, Renato B.; Freitas-Astúa, Juliana. Citrus leprosis virus N: a new dichorhavirus causing citrus leprosis disease. **Phytopathology,** v.107, p.963 - 976, 2017. https://doi.org/10.1094/PHYTO-02-17-0042-R. P. L. Ramos-González and C. Chabi-Jesus have contributed equally to this work.

ABSTRACT

Citrus leprosis (CL) is a viral disease endemic to the Western Hemisphere that produces local necrotic and chlorotic lesions on leaves, branches, and fruit and causes serious yield reduction in citrus orchards. Samples of sweet orange (*Citrus sinensis*) trees showing CL symptoms were collected during a survey in noncommercial citrus areas in the southeast region of Brazil in 2013 to 2016. Transmission electron microscopy analyses of foliar lesions confirmed the presence of rod-like viral particles commonly associated with CL in the nucleus and cytoplasm of infected cells. However, every attempt to identify these particles by reverse-transcription polymerase chain reaction tests failed, even though all described primers for the detection of known CL-causing cileviruses and dichorhaviruses were used. Next-generation sequencing of total RNA extracts from three symptomatic samples revealed the genome of distinct, although highly related (>92% nucleotide sequence identity), viruses whose genetic organization is similar to that of dichorhaviruses. The genome sequence of these viruses showed <62% nucleotide sequence identity with those of orchid fleck virus and coffee ringspot virus. Globally, the deduced amino acid sequences of the open reading frames they encode share 32.7 to 63.8% identity with the proteins of the dichorhavirids. Mites collected from both the naturally infected citrus trees and those used for the transmission of one of the characterized isolates to Arabidopsis plants were anatomically recognized as *Brevipalpus phoenicis* sensu stricto. Molecular and biological features indicate that the identified viruses belong to a new species of CL-associated dichorhavirus, which we propose to call Citrus leprosis N dichorhavirus. Our results, while emphasizing the increasing diversity of viruses causing CL disease, lead to a reevaluation of the nomenclature of those viruses as- signed to the genus Dichorhavirus. In this regard, a comprehensive discussion was presented, which later on the dissemination of these results enabled the reorganization of the taxonomy of dichorhaviruses and recognition of the species citrus leprosis virus N.

Keywords: *Brevipalpus* mites; *Rhabdoviridae*; Nuclear leprosis; BTV.

4.1 INTRODUCTION

Citrus leprosis (CL) is a nonsystemic disease caused by a heterogenic group of RNA viruses endemic to the Western Hemisphere (Bastianel et al., 2010; Roy et al., 2015a). The disease is characterized by necrotic or chlorotic spots in leaves, branches, and fruit, which progressively leads to the early drop of leaves and fruit, branch dieback, and, occasionally, to the death, predominantly, of the youngest citrus trees. Yield reduction of the infected orchards and costs to prevent or manage the CL infection foci make the disease a determinant economic burden to the citrus industry wherever it occurs.

CL-causing viruses belong to three distinguishing genera: *Cilevirus* (bipartite positive-sense [+] single-stranded RNA [ssRNA]), *Higrevirus* (tripartite [+]ssRNA), and *Dichorhavirus* (bipartite negative-sense [–]ssRNA, family *Rhabdoviridae*, order *Mononegavirales*) (Locali-Fabris et al., 2012; Melzer et al., 2013; Dietzgen et al., 2014; Afonso et al., 2016). Viroplasms of such viruses occur in either the cytoplasm (for cileviruses and higreviruses) or the nucleus (for dichorhaviruses) of the infected plant cells, resulting in the wonted subclassification of CL in the types CL-cytoplasmic (CL-C) and CL-nuclear (CL-N).

Most of the CL reports confirmed by sequencing or reverse transcription polymerase chain reaction (RT-PCR) are of the type CL-C, particularly of cileviruses (Bastianel et al., 2010; León et al., 2014; Ramos-González et al., 2016), and, less frequently, type CL-N, which has been only detected in restricted areas in Mexico and Colombia (Roy et al., 2014, 2015b). Incidence of CL-N was also reported a few decades ago in some cool-weather localities in Brazil and in higher elevations in Panama, although the diagnosis was only based on the morphology of the observed virions and the apparent cytopathic effects in transmission electron microscopy (TEM) analyses (Kitajima et al., 1972, 2004; Dominguez et al., 2001; Freitas-Astúa et al., 2004; Chagas et al., 2006). It is likely that CL-N was also the cause of successive leprosis epidemics that severely affected citrus orchards in Florida in the United States, mostly during the 1920s and 1930s until the mid-20th century (Kitajima et al., 2011; Hartung et al., 2015). However, due to several freezes and intense sulfur applications to control the mite vector, CL disappeared from that state in the 1960s and, despite careful surveys, it has not been reported in the United States since (Childers et al., 2003b).

Dichorhaviruses such as orchid fleck virus (OFV, type member of the genus), have short, rod-like nonenveloped particles (40 to 50 by 100 to 110 nm) and encapsidate two (-)ssRNA molecules that are template for transcription of monocistronic polyadenylated messenger RNA (mRNA) for the expression of six viral proteins (Kondo et al., 2006). As for rhabdoviruses, contiguous transcriptional units in OFV are separated by non-transcribed stretches of a few

nucleotides known as intergenic (IG) sequences. These IG sequences are delimited by the gene start sequences and the polyadenylation signals of the flanking open reading frames (ORF) (Jackson et al., 2005; Kondo et al., 2014). RNA1 (approximately 6.4 kb) of OFV isolate orchid (OFV-orchid) harbors the information for the nucleocapsid protein (gene *N*, ORF1) and four other putative proteins identified as phosphoprotein (gene *P*, ORF2), movement protein (gene *MP*, ORF3), matrix protein (gene *M*, ORF4), and glycoprotein (gene *G*, ORF5). Its RNA2 (approximately 6.0 kb) encodes the RNA-dependent RNA polymerase (gene *L*, ORF6) (Kondo et al,. 2006). Each genomic RNA of OFV-orchid ends in untranslated extragenic regions (UTR) in the 39 and 59 termini called leader and trailer, respectively. During the infection, leader regions from both genomic RNA are transcribed into polyadenylated short transcripts (Kondo et al., 2014).

The genomes of two OFV isolates that cause CL-N were fully characterized. First named as Citrus leprosis virus nuclear type (Roy et al., 2015b) and Citrus necrotic spot virus (Cruz-Jaramillo et al., 2014), these viruses were further reclassified as strains of OFV, as indicated in the newest taxonomic report of the order Mononegavirales (Afonso et al., 2016). Globally, the genome of the OFV-orchid and those from the citrus-infecting isolates (OFV-citrus) show 90 to 91% nucleotide sequence identity, whereas the citrus isolates share nucleotide sequence identity values higher than 96% (Cruz-Jaramillo et al., 2014; Roy et al., 2015b). Nevertheless, historically, CL-N has not been restricted to infections by OFV strains. Sequences recovered from herbarium specimens of CL-symptomatic tissues collected in Florida in 1948 showed the existence of a presumably extinguished virus that would represent a novel dichorhavirus related to but different from the currently circulating strains of OFV (Hartung et al., 2015).

The host range of OFV-orchid comprises at least 50 orchid species and several other non-orchid plants following mechanical transmission, which include the rutaceae *Citrus hassaku* Hort. ex Tanaka (Kondo et al., 2003). OFV recovered from orchid is persistently transmitted by nymphs and adults of the false-spider mite species *Brevipalpus californicus* (Acari: Tenuipalpidae) (Kondo et al., 2003). Isolates of OFV-citrus found in Mexico and Colombia naturally infect several citrus species, among them grapefruit (*Citrus* × *paradise* Macfadyen), lemon (*Citrus* × limon (L.) Burm. F.), lime (*C. aurantiifolia* (Christm.) Swingle), mandarin (*C. reticulata* Blanco), sour orange (*C. aurantium* L.), sweet or navel lime (*C. limetta*), sweet orange (*Citrus* × *sinensis* (L.) Osbeck), and Persian lime (*Citrus* × *latifolia* Tanaka); however, there is no evidence that these isolates can infect any orchid species (Cruz-Jaramillo et al., 2014; Roy et al., 2015b, 2015a). Although confirmatory tests remain to be conducted, current

evidence indicates that isolates of OFV-citrus are transmitted by *B. californicus* (Roy et al., 2015a). Transmission experiments also indicated that *B. californicus* and *B. obovatus* acted as vectors of the putative dichorhavirus responsible for CL-N that affected the citrus orchards in Florida decades ago (Knorr, 1968), although only the presence of *B. californicus* could be confirmed in the voucher specimens collected by Knorr when they were later reexamined (Childers et al., 2003b).

In this work, we characterized viral isolates that were collected from sweet orange trees exhibiting CL symptoms in the State of São Paulo (SP), Brazil. These specimens became of particular interest because dichorhavirus-like particles detected in the infected tissues by TEM were negative in RT-PCR tests using a set of specific primers for the detection of OFV isolates citrus and orchid, and because no *B. californicus* was found on the infected plants. Next-generation sequencing (NGS) of the poly (A)-enriched fraction from three infected citrus plants and bioinformatics analyses revealed that the sequenced genomes represent isolates of a new dichorhavirus, whose RNA1 and RNA2 show 53.2 and 60.4% nucleotide sequence identity, respectively, with the cognates from OFV-orchid. Viral transmission to sweet orange and *Arabidopsis thaliana* (L.) Heynh. plants allowed identification of *B. phoenicis* sensu stricto as a vector of the new CL-causing virus.

Finally, we provide several reasons to claim the use of the name citrus leprosis virus N and the corresponding acronym CiLV-N to call the CL-associated dichorhaviruses that are currently circulating in the field using citrus as primary plant host. Consequently, we propose the creation of the species Citrus leprosis N dichorhavirus to assign the molecular variants of CiLV-N.

4.2 MATERIALS AND METHODS

4.2.1 Biological materials

Leaf samples from sweet orange (*Citrus sinensis* (L.) Osbeck) trees showing typical CL symptoms (small bright-yellow lesions with a necrotic spot in the center) (Figure 1) were collected in backyard orchards of São Bento do Sapucaí (SBS) (S 22°409590, W 45°449460, approximately 900 m in altitude), São Roque (SRq) (S 23°539500, W 47°119920, approximately 800 m in altitude), Ibiúna (Ibi) (S 23°379270, W 47°199550, approximately 1,000 m in altitude), and Monte Alegre do Sul (MAS) (S 22°419480, W 46°389100, approximately 800 m in altitude) counties in SP, Brazil, during 2013 to 2016. SBS and MAS are located north of São Paulo city, while Ibi and SRq are located west of the city, at 20 km from one another and approximately 130 to 170 km away from

SBS and MAS. Sweet orange samples from Amparo, SP, Brazil (S 22°429110,W 46°459540, approximately 674 m in altitude) and Serra Negra, SP, Brazil (S 22°369440, W 46°429020, approximately 925 m in altitude) with similar CL-N symptoms were used in the validation of the RT-PCR- based diagnostic method. Small pieces of symptomatic tissue were prefixed for at least 2 h in a modified Karnovsky solution (2.5% glutaraldehyde and 2% paraformaldehyde in 0.05 M cacodylate buffer, pH 7.2) for further TEM analyses (Kitajima and Nome 1999). The rest were kept at -80ºC for RNA extraction. For taxonomic analysis, field collected *Brevipalpus* mite samples were fixed in a 70% ethanol solution. Some mites were kept alive for viral transmission experiments.

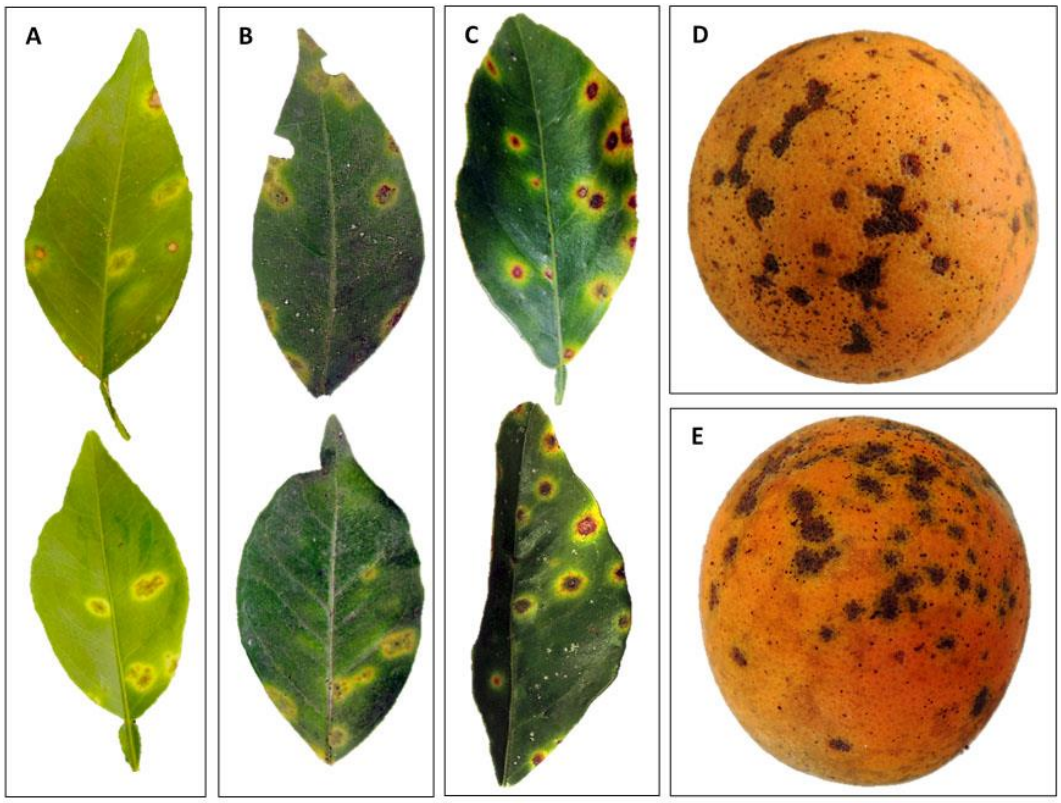

Figure 1. Sweet orange (*Citrus sinensis*) leaves and fruits showing chlorotic and necrotic symptoms typically recognized as outcome of citrus leprosis infection. Samples were collected in São Bento de Sapucaí (A), Ibiúna (B and D) and São Roque (C and E) counties, State of São Paulo, Brazil in 2015.

4.2.2 Transmission electron microscopy (TEM) analyses

Symptomatic leaf samples were post fixed in a solution of OsO_4 (1%) for 1 h, dehydrated in acetone, infiltrated, and embedded in the low-viscosity Spurr's epoxy resin. Blocks were sectioned in a Leica Ultracut C ultramicrotome (Vienna) equipped with a Diatome Diamond knife (Biel, Switzerland). Sections were mounted on 300-mesh copper grids, stained with 3% uranyl acetate and Reynold's lead citrate, and examined in a Zeiss EM 900 (Carl Zeiss AG, Oberkochen,

Germany) or a JEOL JEM 1011 (JEOL, Akishima, Japan) transmission electron microscope and images were digitally recorded. Longitudinally or cross-sectioned rod-like particles from each sample were measured to evaluate their dimensions.

4.2.3 RNA extraction and RT-PCR detection of CL-associated viruses

Small leaf tissue fragments with CL lesions were ground to powder with mortar and pestle using liquid nitrogen. Total RNA was extracted using Trizol® Reagent (Life Technologies, Foster City, CA, USA) and cDNA solutions were generated from 500 ng of RNA extracts using random primers following the manufacturer´s recommendations for RevertAid H Minus First Strand cDNA Synthesis Kit (Thermo Scientific, Madison, WI, USA). Three µL of cDNA solutions were assayed in independent PCR assays for the specific detection of citrus leprosis virus C (CiLV-C), Citrus leprosis virus cytoplasmic type 2 (CiLV-C2), and OFV (Kubo et al. 2009; Locali et al. 2003; Roy et al. 2014, 2013a) (Supplementary Table 1, Annex I). Moreover, degenerate primers for the detection of the *L* gene (RNA2) from OFV-citrus were also used (Ramos-González et al., 2015) (Supplementary Table 1, Annex I).

4.2.4 Viral genome sequencing

Tissue fragments (500 mg) showing CL lesions were removed from sweet orange leaves collected in SBS, Ibi, and SRq localities. Each source was independently processed and their RNA extracts were obtained as described above. RNA extracts were further purified using the RNeasy Mini Kit (Qiagen, Venlo, The Netherlands). RNA quantification and ratios of absorbance at 260/280 nm were estimated using a NanoDrop ND-8000 microspectrophotometer (Thermo Scientific, Waltham, MA). RNA samples were sent to the Animal Biotech Laboratory, Esalq/USP (Piracicaba, SP, Brazil) for sequencing using HiSeq 2500 Technology. Library preparation and paired sequencing (2 × 125 bp) were carried out using the Illumina TruSeq Stranded mRNA Library Prep Kit and HiSeq SBS v4 High-Output Kit, respectively (Illumina, San Diego, CA). Reads were assembled de novo, using the RNA-Seq assembler Shannon (Kannan et al. 2016). Genomic scaffolds were the base to prepare a set of 19 primer pairs using Primer3 software (Untergasser et al. 2012) (Supplementary Table 2, Annex I). Overlapping fragments were amplified using Taq DNA polymerase and subsequently sequenced by the Sanger method to confirm the NGS data. 5’ and 3’ termini of genomic RNA from the three isolates were determined by rapid amplification of cDNA ends (RACE) using the corresponding primers and following the manufacturer´s recommendations for the

SMARTer RACE 59/39 Kit (Clontech Laboratories, Mountain View, CA). All generated amplicons were cloned and at least five independent clones were sequenced. Once fully sequenced, the genomes of three CL-N-associated viruses were annotated and the acronym CiLV-N was used to provisionally name them. The genomic information of a fourth isolate collected in MAS was only obtained via RT-PCR using the specific primers for the Sanger-based sequencing of CiLV-N isolates Ibi, SBS, and SRq.

4.2.5 Sequence analysis

Viral ORF were identified *in silico* using Vector NTI software (Invitrogen, Carlsbad, CA, USA). Nucleotide and deduced amino acid sequences were aligned using MUSCLE or T-Coffee algorithms (Edgar, 2004) implemented in the Molecular Evolutionary Genetic Analysis (MEGA) software version 6.0 for Windows (Tamura et al., 2013) and in Unipro UGene v1.24.1 (Okonechnikov et al., 2012). Presence of genomic repeated nucleotide sequences were identified using REPFIND program (Betley et al., 2002), whereas signal peptide, nuclear localization signals (NLS) and nuclear export signals (NES) in putative viral proteins were recognized using SignalP 4.1 (Petersen et al., 2011), cNLS Mapper (Kosugi et al., 2009), and NetNES 1.1 Server (la Cour et al., 2004), respectively.

4.2.6 RT-PCR tests for the detection of CL-associated viruses

Sequences of *N* and *L* genes of CiLV-N isolates were aligned with their cognates from OFV-orchid (GenBank accession numbers AB244417 and AB244418) and OFV-citrus isolates Ja1 (KF198064 and KF198065) and Qto (KF209275 and KF209276), whose sequences were retrieved from the GenBank database. Based on the alignment of the *N* gene, the primer pair *N*-DC_Br-Fwd (5'-CCGTACCCATTGTGAAAATA-3') and *N*-DC_Br-Rev (5'-GAACCCCTTTGAGGAATG-3') was designed with the ultimate goal of detecting exclusively CiLV-N (Figure 2A). In addition, in an attempt to develop an RT-PCR-based universal detection method for the known CL-causing dichorhaviruses, information obtained from the alignment of the L gene was used to design the pair of degenerate primers *L*-DC-Fwd (5'-CAASTGTCATGCCTGCATGG-3') and *L*-DC-Rev (5'-TTGATRCATGATGCRAGRCTGTATG-3') that target conserved nucleotide sequences (Figure 2B). Primer performance in PCR was validated using a set of field samples collected in Brazil, Paraguay, and Mexico that showed CL-N symptoms or had tested positive for dichorhavirus infection in TEM analyses.

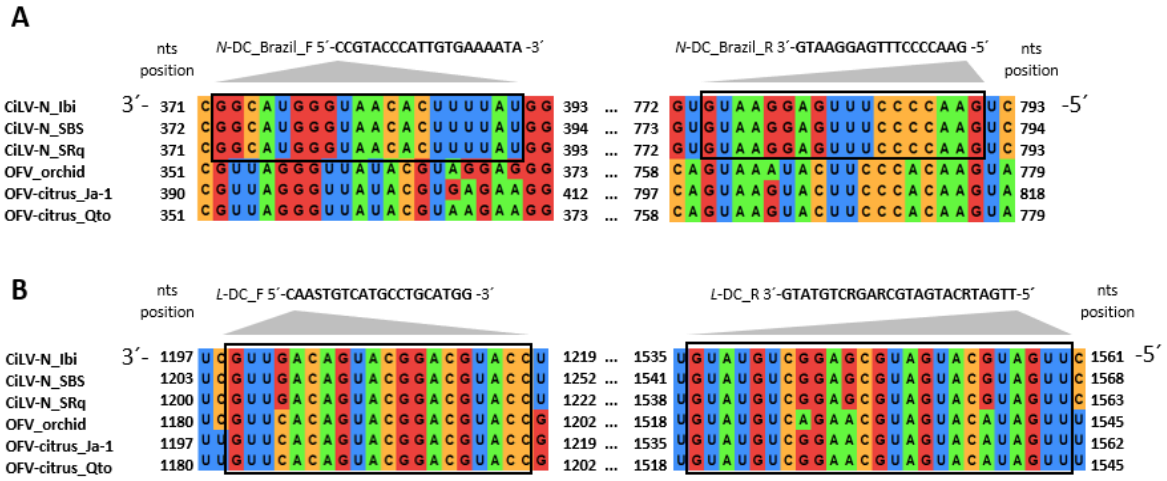

Figure 2. Alignments of partial sequences of the A, RNA1 and B, RNA2 genomic molecules from orchid fleck virus (OFV) and citrus leprosis virus N (CiLV-N). Bottom line of each panel indicates forward and reverse primer sequences used in virus detection. Target sequences for each primer are highlighted inside open boxes. Primer pair N-DC_Brazil is specific for detection of CiLV-N (A) whereas the degenerate primer L-DC detects all known citrus leprosis-causing dichorhaviruses (B). N= *N* gene, L= *L* gene, and DC = Dichorhavirus-citrus. Nucleotide code: S = C or G and R = G or A. Sequences of RNA1 and RNA2 of each virus were retrieved from GenBank. Accession numbers are as follows: CiLV-N_Ibi (KX982176 and KX982179), CiLV-N_SBS (KX982178 and KX982181), CiLVN_SRq (KX982177 and KX982180), CiLV-N_MAS (KY751404 and KY751405), OFV-orchid (AB244417 and AB244418), OFV-citrus_Ja-1 (KF198064 and KF198065), and OFV-citrus_Qto (KF209275 and KF209276).

4.2.7 Mite-mediated virus transmission

In all, 45 adults or nymphs of *Brevipalpus* spp. mites collected from citrus plants in Ibi showing CL symptoms were transferred to three pots (15 mites per pot) containing 2-week-old *A. thaliana* Col 0 plants. Plants were kept at 23 ± 1°C and with a 14-h photoperiod inside a controlled growth chamber (Adaptis AR A1000; Conviron, Winnipeg, MB, Canada) throughout the experiment. At 10 to 20 days after infestation, 12 *Brevipalpus* mites were recovered from the plants and kept in a 70% ethanol solution until further characterization. Additionally, six pots with healthy sweet orange plants were placed under the leprosis-infected trees to allow a seminatural infection (i.e., leaves and fruit exhibiting CL-N symptoms from the source trees were detached and put in contact with the leaves of the potted trees). After symptoms appeared, leaves from both sweet orange and *Arabidopsis* were collected and carefully rinsed with sterile distilled water to remove mites, eggs, and other contaminants, and their RNA extracts were obtained as indicated above. Viral presence in the collected leaves was detected by RT-PCR using the primer pairs *L*-DC and *N*-DC_Br previously described in this work (Figure 2), and also using the specific primer pair *G*-DC_Br for amplification of a fragment of the *G* gene of CiLV-N (*G*-DC_Br-Fwd 5'-CATGGATTTCACAAGGGAAC-3' and *G*-DC_Br-Rev 5'-CACAGATGTTGGCAAAGTAT-3').

4.2.8 Mite identification

Adult *Brevipalpus* mites collected in Ibi, MAS, and SBS were fixed in 70% ethanol, mounted for light microscopy in Hoyle's medium, and examined by differential interference contrast in a Zeiss Axioimager microscope (Carl Zeiss AG, Jena, Germany). The images were registered digitally. Additional details were observed under a JEM IT 300 scanning electron micro- scope (JEOL). For this, mites were dehydrated in ethanol, critical point dried (Leica CPD 300), mounted in double-coated carbon tape on stubs, and sputter coated (Baltec SPD 050; Balzers, Liechtenstein) with gold. Identification of mites was made using morpho- logical criteria recently established for the taxa assignation within the genus *Brevipalpus* (Beard et al., 2015). A similar protocol was carried out to confirm the identity of mites used in the viral transmission experiments.

4.3 RESULTS

4.3.1 Symptoms, cytopathic effects, and molecular detection tests suggest infections by uncharacterized CL-causing dichorhaviruses

Samples of sweet orange trees suspected to be infected with CL-causing viruses were collected in SBS, Ibi, SRq, and MAS counties in SP, Brazil. Leaves, stems, and fruit showed small, local, necrotic spots. In leaves, they were mostly surrounded by a yellow-bright chlorotic halo (Figure 1). Remarkably, in some collection sites in the four localities, lime, lemon, and mandarin trees planted next to the symptomatic sweet orange trees remained free of CL symptoms.

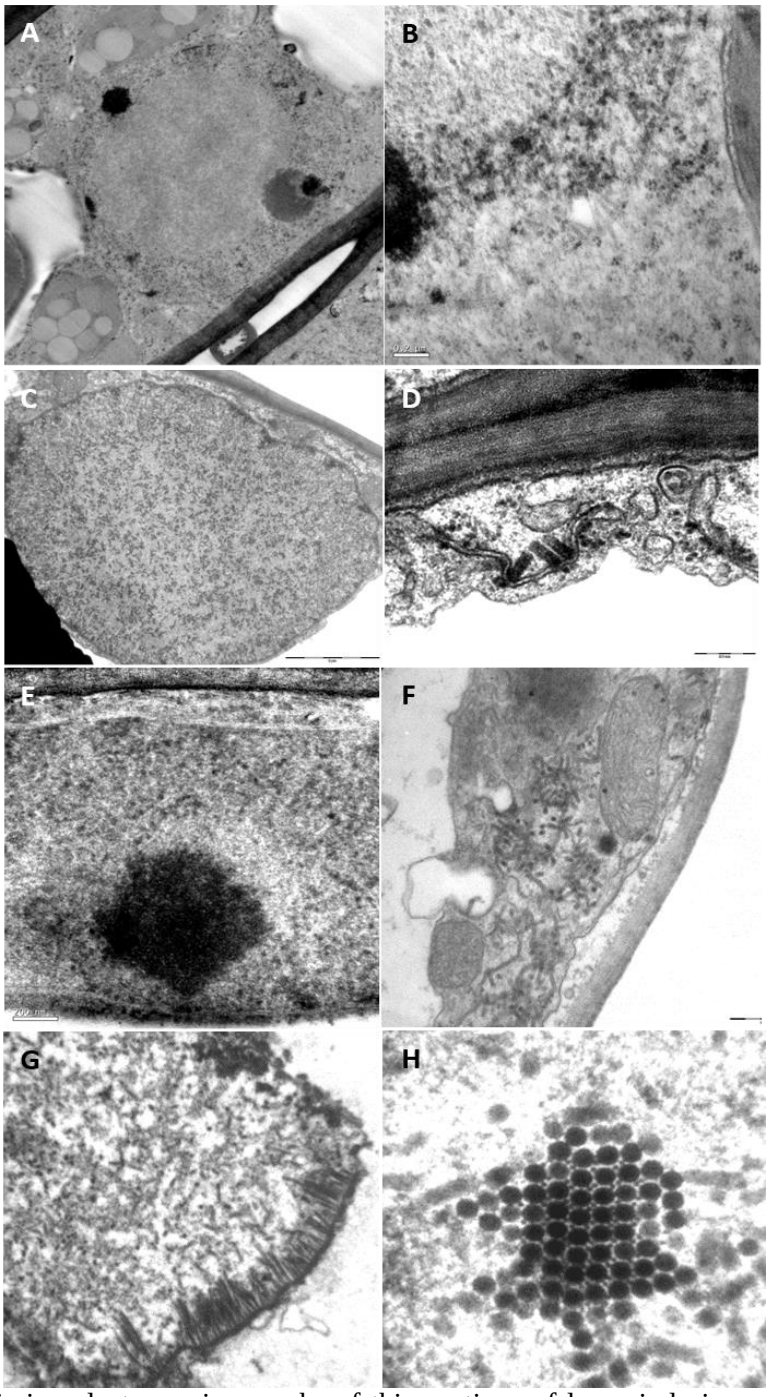

Figure 3. Transmission electron micrographs of thin sections of leprosis lesions on leaves of sweet orange trees from A and B, São Bento do Sapucaí; C and D São Roque; E, Ibiúna; and F, G, and H, Monte Alegre do Sul. A, Low-magnification image showing a large electron lucent viroplasm (*, area inside dashed line) in the nucleus (N) of a palisade parenchyma cell. B, Detail showing some rod-like particles (arrows) in the periphery of the nucleus. C, Nucleus in a spongy parenchyma cell with the viroplasm (*) filled with short rod-like, putative viral particles. D, Cell periphery of a palisade parenchyma cell showing rod-like particles (arrow) attached perpendicularly onto elements of the endoplasmic reticulum. E, Electron lucent viroplasm (*) close to a nucleolus (Nu) in the nucleus of a palisade parenchyma cell. F, Image of a spongy parenchyma cell. Groups of rod-like particles (arrows), presumed virions, are arranged perpendicularly onto membranes of endoplasmic reticulum. G, Nucleus with viroplasm filled with rod-like particles (arrows), which are arranged perpendicularly onto the nuclear membrane of a spongy parenchyma infected cell. H, High-magnification image of a group of rod-like particles in a paracrystalline array, sectioned transversally. A thin fiber-like material is present between adjacent particles.

TEM analysis of leaf lesions from these symptomatic sweet orange plants revealed the presence of rod-like particles interspersed in the nucleoplasm of the infected cells, suggesting the presence of dichorhaviruses (Figure 3). In some of these cells, the particles appeared arranged perpendicularly onto the inner nuclear envelope or they formed large parallel and paracrystalline arrays. Rod-like particles were also found in the cytoplasm, and associated perpendicularly onto membranes of the endoplasmic reticulum. Occasionally, this association resulted in a configuration in which particles appear radially arranged and surrounded by endoplasmic reticulum membrane, forming typical "spoke wheel" structures (Kitajima et al., 1972, 2003). Measurements of 50 of these particles revealed that the virions are approximately 40 nm wide and l00 to 110 nm long.

RNA extracts from all collected symptomatic trees were tested by RT-PCR using a set of specific primers for the detection of all known CL-causing dichorhaviruses and cileviruses (i.e., CiLV-C, CiLV-C2, and OFV-citrus strains) (Locali et al., 2003; Kubo et al., 2009; Roy et al., 2013b; Ramos-González et al., 2016). No amplicons were obtained with any of the assayed primer combinations, suggesting that virions detected by TEM differ molecularly from those previously studied.

4.3.2 Genome characterization reveals new CL-associated dichorhaviruses

Total RNA extracts from one infected tree of the localities SBS, SRq, and Ibi were independently sequenced using NGS technology. Reads from each sample were individually assembled to produce a pool of contigs from which those corresponding to the citrus plant genome were separated. In each of the three remaining pools and after BLASTX analyses using a plant virus database as reference, two contigs were identified with relatively low BLASTe-values ($<e^{-80}$ to e^{-30}) with the two genomic fragments of the dichorhaviruses OFV (GenBank accession numbers AB244417 and AB244418) and coffee ringspot virus (CoRSV) (KF812525 and KF812526). Citrus tristeza virus and other virus- derived contigs were not detected. Size of overlapping amplicons generated during the Sanger-based secondary sequencing agreed with the expected values according to the organization of the input scaffolds, proving the correct array of reads and contigs during the assembling processes (data not shown). The full genomes of three different although related viruses were finally obtained after the sequencing of the 3' and 5' ends of the two genomic fragments amplified by RACE. It is noteworthy that most of the virus-derived NGS reads corresponded to positive-sense RNA, a fact probably reflecting the enrichment of poly(A) RNA carried out during the RNA library preparation. However, considering that dichorhaviruses, like other members of the order *Mononegavirales*, have negative- sense genomes (Dietzgen et al., 2014, 2017; Mann and Dietzgen, 2014; Afonso et al.,

2016),nucleotide sequences in the 3' to 5' orientation were defined as the genome of the identified viruses.

RNA1 of the viruses found in SBS, SRq, and Ibi were 6,708, 6,722, and 6,724 nucleotides (nt) long, respectively, whereas their RNA2 were 6,051, 6,048, and 6045 nt, respectively. All these sequences were deposited into GenBank and their accession numbers are as follow: isolate Ibi RNA1: KX982176 and RNA2: KX982179, isolate SRq RNA1: KX982177 and RNA2: KX982180, and isolate SBS RNA1: KX982178 and RNA2: KX982181. Between the three RNA1 molecules, those from the isolates SRq and Ibi showed the highest nucleotide identity (97%), whereas the comparison of each of these molecules with that from the isolate SBS revealed lower values (approximately 92%). RNA2 of the three isolates were less divergent and, regardless the pair compared, they displayed similar values of sequence identity (97%) (Supplementary Table 3, Annex I). By contrast, the genome sequence of the three isolates were notably different from those of OFV and CoRSV. RNA1 and RNA2 showed 52.2 to 53.9 and 59.8 to 62.0% sequence identity, respectively (Table 1), where the highest values in each range always corresponded to comparisons with CoRSV.

Table 1. Nucleotide and deduced amino acids identities between citrus leprosis virus N (CiLV-N) and known dichorhaviruses.

CiLV-N[b]	**Nucleotide identity/amino acid identity[a]**			
	OFV-orchid	OFV-citrus Qto[c]	OFV-citrus Ja1[d]	CoRSV
RNA1	53.2/nd[e]	52.2/nd	52.9/nd	53.9/nd
ORF *N*	56.8/50.7	57.3/50.0	57.4/50.2	60.2/57.9
ORF *P*	52.2/36.2	51.6/35.8	52.7/36.6	55.3/46.9
ORF *MP*	64.0/61.0	57.8/54.7	58.3/55.0	63.4/58.6
ORF *M*	49.2/36.8	51.6/36.3	51.9/36.8	57.0/49.7
ORF *G*	48.6/33.9	49.7/32.7	49.4/33.4	50.5/39.0
RNA2	60.4/nd	59.8/nd	60.5/nd	62.0/nd
ORF *L*	61.2/57.5	61.6/57.6	61.7/57.2	62.8/63.8

[a]OFV = orchid fleck virus and CoRSV = coffee ringspot virus; [b]Sequences from isolate Ibi were selected for the comparisons (GenBank accession numbers RNA1 = KX982176 and RNA2 = KX982179). ORF = open reading frame; [c]Isolate from Queretaro, Mexico; [d]Isolate from Jalisco, Mexico; [e]nd = data not determined.

Sanger-based sequencing of amplicons obtained from the isolate collected in MAS allowed the recovery of 93.0 and 94.7% of its RNA1 (GenBank accession number KY751404) and RNA2 (GenBank accession number KY751405), respectively. The missing sequences were confined to the 3' and 5' UTR of both genomic molecules. Nucleotide sequence identities of the sequenced genome and those from the individual ORF with the cognates from the isolates Ibi, SRq, and SBS

were always higher than 91%. Highest values in these comparisons were observed with the isolate SBS (data not shown).

In view of the fact that the nucleotide sequence identity between the genomes of the isolates SRq, Ibi, SBS, and MAS are higher than 90%, they were considered to be molecular variants from the same virus. The isolate identified in Ibi was recognized as its prototype, considering that it was found in the region with largest number of CL-N-infected trees. Moreover, given that this virus seems to be uncharacterized, we named it citrus leprosis virus N, and used the acronym CiLV-N to identify it throughout the article.

By analogy with the OFV genome, the five coding regions in the RNA1 of CiLV-N were annotated as genes *N*, *P*, *MP*, *M*, and *G* (Figure 4A). Its RNA2 comprised only one ORF, the largest of the genome, identified as the *L* gene. Basically, ORF sizes and their relative positions are consistent with those observed in known dichorhaviruses (Cruz-Jaramillo et al. 2014; Dietzgen et al. 2014; Kondo et al. 2006; Ramalho et al. 2014; Roy et al. 2015b) (Supplementary Table 4, Annex I). In both viral RNA molecules, modular structures encompassed in the gene junctions (Gj) that include the putative gene transcription start site, the IG region, and the polyadenylation signal (3'-UAA AUUU-5') were identified (Figure 4B). Throughout the genome of CiLV-N isolates, the IG regions were regularly formed by the tetra- nucleotide GXXX and, next to this, there was always a dinucleotide UU which, by analogy with OFV-orchid (Kondo et al. 2014), might represent the transcriptional start site for the upcoming gene. The classic modular organization of the IG region could not be recognized in either Gj_1 (leader/ORF1) or Gj_6 (ORF5/trailer) of the RNA1, as well as in Gj_7 (leader/ORF6) or Gj_8 (ORF6/trailer) of the RNA2. In Gj_1 and Gj_7, although U-rich regions were detected, they differed from the canonical polyadenylation signal sequence. Thus, if any short transcripts are expressed from the leader regions of the genomic RNA of CiLV-N, or whether or not they are polyadenylated, cannot be inferred in silico.

Genome analysis of CiLV-N isolates also revealed that the inter-ORF regions harboring the Gj_3, Gj_4, and Gj_5 are two or three times larger than those observed in OFV, being closer in length to the cognates from CoRSV (less than 20% size difference). Lengths of 39 UTR (approximately 247 nt) and 59 UTR (approximately 200 nt) flanking the RNA1 and their A + U contents (55.5 to 59.5%) were similar to those exhibited by OFV. In the RNA2, these sequence stretches also had lengths similar to those in OFV (less than 12% size difference) but the A + U content of its 59 UTR was slightly higher (64.6 to 65.5% in CiLV-N versus 56.2% in OFV). In this regard, the presence of leader RNA in both genome molecules of CiLV-N makes

a marked contrast with OFV-citrus isolate Qto, in which these sequences are lacking (Roy et al., 2015b).

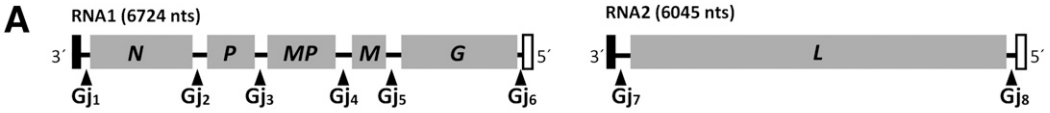

B

Gene junction structure

3´- Polyadenylation signal | IG | Transcription start site -5´

		nt position				nt position
Gj1	SBS	163	-	-	UUACU	172
	SRq	162				171
	Ibi	162				171
Gj2	SBS	1662	UAAAUUUAUUUU	G**U**AG	UUA**U**U	1682
	SRq	1659		G**G**AG	UUA**C**U	1678
	Ibi	1659		G**U**AG		1678
Gj3	SBS	2683	UAAAUUUAUUUU	GUAG	UUACG	2702
	SRq	2682				2701
	Ibi	2682				2701
Gj4	SBS	3941	UAAAUUUAUUUU	GU**G**G	UUGUU	3961
	SRq	3942		GU**A**G		3962
	Ibi	3942				3964
Gj5	SBS	4843	UAAAUUUAUUUU	GUUG	UUGU**G**	4863
	SRq	4841			UUGU**A**	4861
	Ibi	4843				4863
Gj6	SBS	6551	UAAAUUUGUUUU	G**UC**C	-	6566
	SRq	6564		G**GU**C		6579
	Ibi	6566				6581
Gj7	SBS	179	-	-	UUGAG	187
	SRq	176				184
	Ibi	173			UUUUG	181
Gj8	SBS	5863	UAAAUUUGUUUU	GAUU	-	5878
	SRq	5860				5875
	Ibi	5857				5872

Figure 4. A- Genomic organization of Brazilian citrus leprosis virus N (BrCiLV-N) isolate Ibiúna. Gray boxes indicate the six viral ORFs encoded by the bipartite genome. *N*- nucleocapsid protein, *P*- phosphoprotein, *MP*- movement protein, *M*- matrix protein, *G*- glycoprotein and *L*- RNA-dependent RNA polymerase. Solid and open boxes designate the leader and trailer sequences on the 3´ and 5´ ends, respectively, of each RNA molecule. Arrowheads show gene junction (Gj) distribution in the genome. **B**- Structure and sequence of Gjs of the isolates São Bento de Sapucaí (SBS), São Roque (SRq) and Ibiúna (Ibi) are depicted. Non-conserved sequences are highlighted in bold. IG- intergenic region.

Deduced amino acid sequences of protein encoded by each ORF detected in the genomes of each isolate of CiLV-N showed high values of identity between them (≥96%). However, in the evaluations including proteins from OFV and CoRSV, the values were notably reduced (Table 1). Overall, the percentage of identity in these analyses ranged from the lowest values (32.7 to 39%), corresponding to the G protein, to the highest in comparisons involving the N (50.0 to 57.9%), MP (54.7 to 61.0%), and L (57.2 to 63.8%) proteins. De- tailed analyses of these proteins using several bioinformatics tools predicted the presence of NLS, NES, signal peptides, and

trans- membrane regions, which might be relevant for their functions during the infection cycle according to studies with OFV and CoRSV (Kondo et al., 2013; Ramalho et al., 2014). NES were identified in the nucleocapsid protein (peptides AAITYICLSLLRLCV, amino acid positions 151 to 171; and IPYGMYIDLKMGLPL, amino acid positions 261 to 275), phosphoprotein (SWLLIDYLS, amino acid positions 169 to 177), and matrix protein (SLSLIN, amino acid positions 43 to 48). The phosphoprotein also has two NLS predicted between amino acid positions 125 to 134 and 226 to 236 (peptides QSSKRKHEDT and RLSKSKKPCLN, respectively). The G protein has a predicted signal peptide whose cleavage site is between the residues Gly21 and Met22 and a putative transmembrane helix domain near its C terminus (amino acid positions 483 to 502). The L protein from CiLV-N shows large stretches of conserved amino acid sequences, including the characteristic four motifs identified inside the domain III of RNA-dependent RNA polymerase of dichorhaviruses (Ramalho et al., 2014; Roy et al., 2015b) and mononegaviruses (Poch et al., 1990). The sequence of the motif D of the L protein was the less conserved (data not shown), as also was described for other dichorhaviruses (Ramalho et al., 2014; Roy et al., 2015b).

Phylogenetic analyses using the deduced amino acid sequences of the N, G, and L proteins from several plant-infecting rhabdoviruses revealed trees with similar topology (Figure 5). Clusters corresponding to genera *Cytorhabdovirus*, *Nucleorhabdovirus*, *Varicosavirus*, and *Dichorhavirus* were well defined although, in the L protein-based tree, the branch including dichorhaviruses arose from the same node where the nucleorhabdoviruses maize fine streak virus, datura yellow vein virus, and sonchus yellow net virus probably descended, denoting their putative closer ancestrally. Inside the branch corresponding to the genus *Dichorhavirus*, the members were always subclustered in such a way that the OFV isolates from both orchid and citrus were clearly separated from CoRSV and from the isolates of CiLV-N.

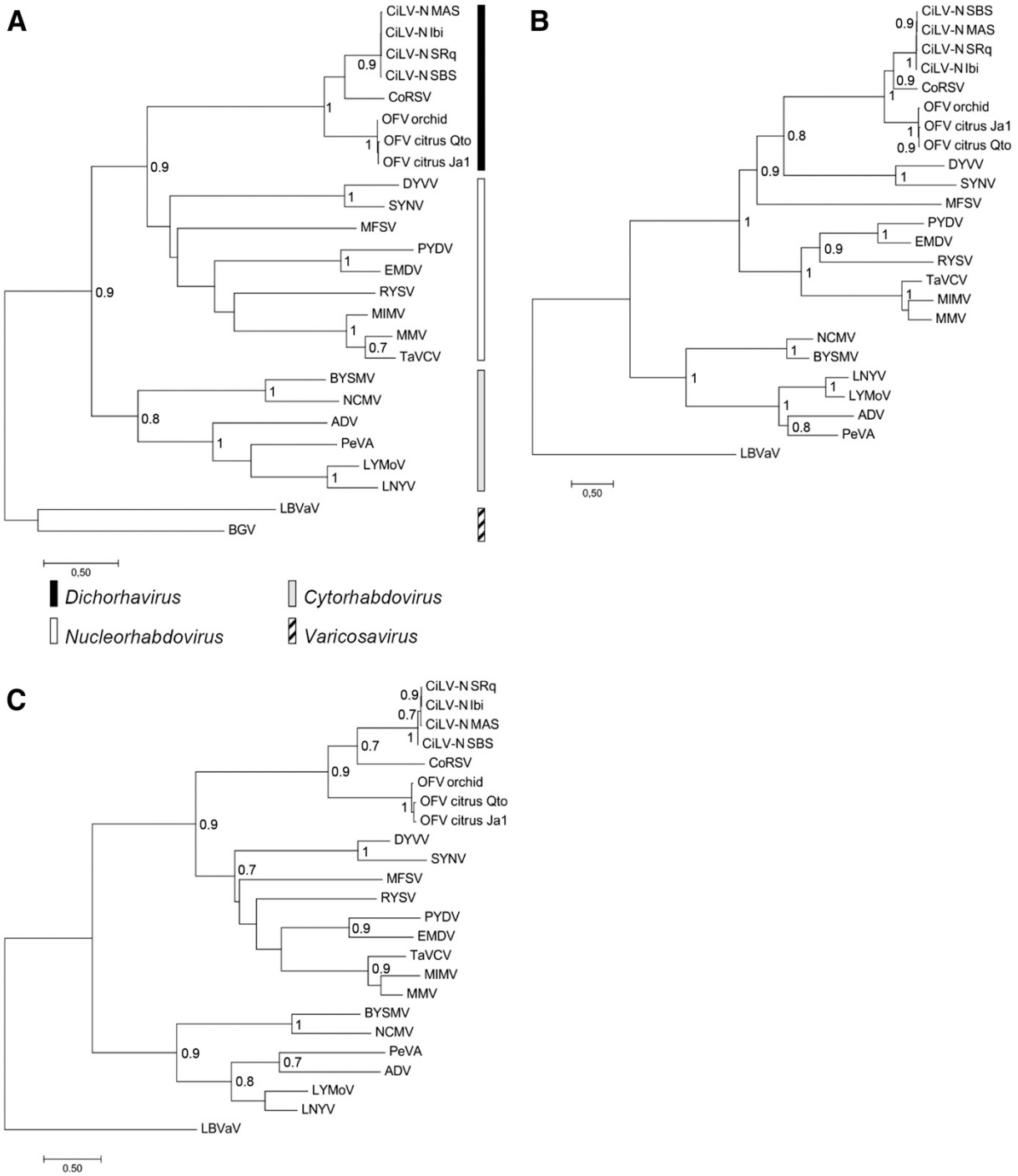

Figure 5. Phylogenetic reconstruction for plant-infecting viruses of the family *Rhabdoviridae*. Maximum-likelihood-inferred trees include members of the genera *Dichorhavirus*, *Cytorhabdovirus*, *Nucleorhabdovirus*, and *Varicosavirus*, and they are based on the amino acid sequences of A, N proteins; B, L proteins; and C, G proteins. Bootstrap support values (1,000 iterations) of branches are indicated near to the nodes if greater than 70%. Lettuce big vein associated virus (LBVaV)- derived sequences were used as outgroup. CiLV-N = citrus leprosis virus N, CoRSV = coffee ringspot virus, OFV = orchid fleck virus, DYVV = datura yellow vein virus, SYNV = sonchus yellow net virus, MFSV = maize fine streak virus, PYDV = potato yellow dwarf virus, EMDV = eggplant mottled dwarf virus, RYSV = rice yellow stunt virus, MIMV = maize Iranian mosaic virus, MMV = maize mosaic virus, TaVCV = taro vein chlorosis virus, BYSMV = barley yellow striate mosaic virus, NCMV = northern cereal mosaic virus, ADV = alfalfa dwarf virus, PeVA = persimmon virus A, LNYV = lettuce necrotic yellows virus, BGV = black grass varicosavirus-like virus (GenBank accession number NC026801), and LYMoV = lettuce yellow mottle virus.

4.3.3 Specific and generic detection of dichorhaviruses infecting citrus

The performance of the primer pairs *N*-DC_Br and *L*-DC designed in this work (Figure 2) were tested using cDNA extracts obtained from 12 CL-N-infected citrus plants collected in Brazil and Mexico, and from orchid plants infected with OFV collected in Brazil and Paraguay. As would be expected according to the in silico analyses, using the specific *N*-DC_Br primers, amplicons of approximately 420 bp were observed only in samples of CiLV-N, which were collected in Ibi, SRq, SBS, MAS, Amparo, and Serra Negra (Figure 6A). PCR with primers *L*-DC, designed to amplify the *L* gene of all CL- associated dichorhaviruses, resulted in amplification from a wider range of samples (Figure 6B). In addition of those corresponding to isolates of CiLV-N, bands of approximately 360 bp were obtained from the cDNA extracts of orchid collected in Piracicaba, SP, Brazil and Asuncion, Paraguay and in citrus plants collected in Atotonilco and Ameca, State of Jalisco, Mexico, where the presence of OFV was previously detected (Ramos-González et al. 2016b). Amplicon- derived sequences of samples from Ibi, SRq, SBS, and MAS showed >99% identity with the cognate reference genome which allowed the validation of the effectiveness of the designed primers. In the case of samples from Amparo (GenBank accession numbers KY711427 and KY711429) and Serra Negra (GenBank accession numbers KY711428 and KY711430), the sequences exhibited >93% identity with the genome of CiLV-N isolate Ibi.

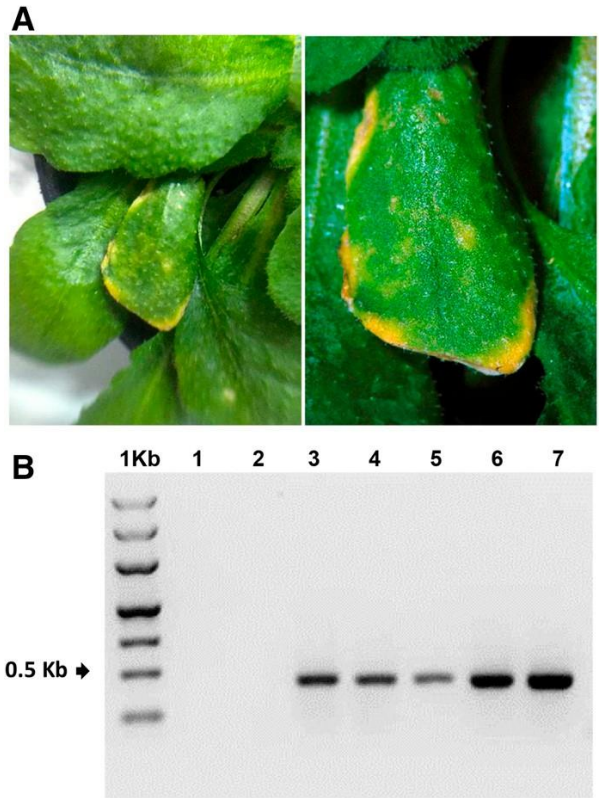

Figure 6. Transmission of citrus leprosis virus N (CiLV-N) to *Arabidopsis* thaliana using viruliferous *Brevipalpus phoenicis* sensu stricto mites collected in Ibiúna, SP, Brazil. A, Chlorotic symptoms in Arabidopsis leaves after 8 to 10 days of infestation with viruliferous mites. B, Agarose gel (1%) electrophoresis of reverse-transcription polymerase chain reaction (RT-PCR) products for the detection of CiLV-N using a specific primer pair for the N gene (*N*-DC_Br). Expected amplicon size = 420 bp. 1Kb: Molecular weight marker M1121 (Sinapse Biotecnologia, SP, Brazil), lane 1: no-template RT-PCR control, lane 2: healthy Arabidopsis plant, lanes 3 to 5: symptomatic leaves from three different *Arabidopsis*-infested plants, and lane 6: sweet orange (*Citrus sinensis*) tree infected with CiLV-N isolate Ibi.

4.3.4 Mite-mediated transmission of CiLV-N to *Arabidopsis* and sweet orange plants

At 8 to 10 days after infestation with *Brevipalpus* mites collected in Ibi, symptoms of local chlorotic lesions were evident in some leaves of the inoculated *Arabidopsis* plants (Figure 7A). Symptoms of CL-N in the sweet orange plants left under the canopy of the CL-N source plants were observed after 3 months. However, in the case of sweet orange plants, this time should not be judged as the minimal period required for symptom appearance; it only represents the interval between the first (beginning of the experiment) and second visits to the experimental area.

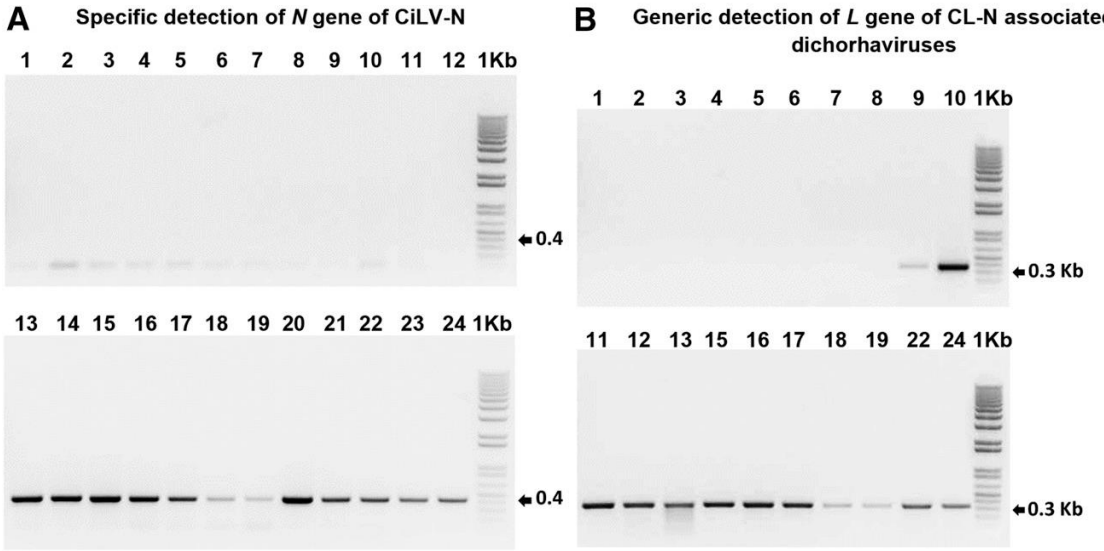

Figure 6. Gel electrophoresis of reverse-transcription polymerase chain reaction (RT-PCR) products for A, specific detection of citrus leprosis virus N (CiLV-N) using the primer pair *N*-DC_Br (expected amplicon size: 420 bp) and B, generic detection of citrus leprosis-nuclear (CL-N)-associated dichorhaviruses using the primer pair L-DC (expected amplicon size: 360 bp). Lane 1: no- template PCR control, lane 2: no-template RT control, lane 3: healthy citrus plant, lane 4: healthy orchid plant, lane 5: healthy *Arabidopsis* plant, lane 6: CiLV-C- infected citrus plant (Cordeirópolis, Brazil), lane 7: CiLV-C2-infected citrus plant (Meta, Colombia), lane 8: coffee ringspot virus-infected coffee plant (Limeira, Brazil), lanes 9 and 10: orchid fleck virus (OFV)-infected orchid plants (Piracicaba, Brazil and Asuncion, Paraguay, respectively), lanes 11 and 12: OFV-citrus infected plants (Atotonilco and Ameca, Mexico, respectively), lanes 13 to 17 and 20 to 24: CiLV-N-infected sweet orange plants (Ibiúna, São Roque, Monte Alegre do Sul, Amparo, and Serra Negra, Brazil), lanes 18 to 19: CiLV-N-infected Arabidopsis plants (inoculated with *Brevipalpus phoenicis* sensu stricto collected in Ibiúna), and 1Kb: molecular weight marker 1-kb Plus DNA Ladder (Thermo Fisher Scientific, Waltham, MA).

Presence of CiLV-N in the RNA extracts from symptomatic leaves from the infested plants of the two species was confirmed by using *N*-DC_Br, *L*-DC, and *G*-DC_Br primer pairs (Figures 6, lanes 17 to 19, and 7B). Nucleotide sequences of the amplicons (GenBank accession numbers KY711421-22 and KY711425-26) showed >95% identity with the sequence of CiLV-N isolate Ibi.

4.3.5 Mite characterization

In total, 65 mites collected in citrus trees showing CL-N symptoms (that also proved positive for CiLV-N) from Ibi (50 specimens), MAS (12 specimens), and SBS (3 specimens) were evaluated according to the current taxonomical criteria for members of the genus *Brevipalpus* (Beard et al. 2015) (Figure 8). All the specimens were identified as *B. phoenicis* sensu stricto. The following traits were observed: (i) central cuticle with strong broad areolae in the prodorsum; (ii) in the dorsal opisthosoma, *d1-d1* to *e1-e1,* cuticle with a few transverse folds and sublateral cuticle exhibiting rounded cells in bands; (iii) cuticle of the ventral plate forming transverse bands; (iv) genital plate with large cells; (v) spermathecal apparatus ending in a bulb; and (vi) palp femorogenu dorsal seta flat, barbed, and broad. Moreover, cuticular microplates over the dorsal surface of these mites showed irregular multidirectional ridges (Figure 8C).

Mites that transitorily fed on *Arabidopsis* plants during the transmission experiments of CiLV-N were anatomized as well. All structural details observed in the field-collected specimens were also discerned across the specimens of the subpopulation.

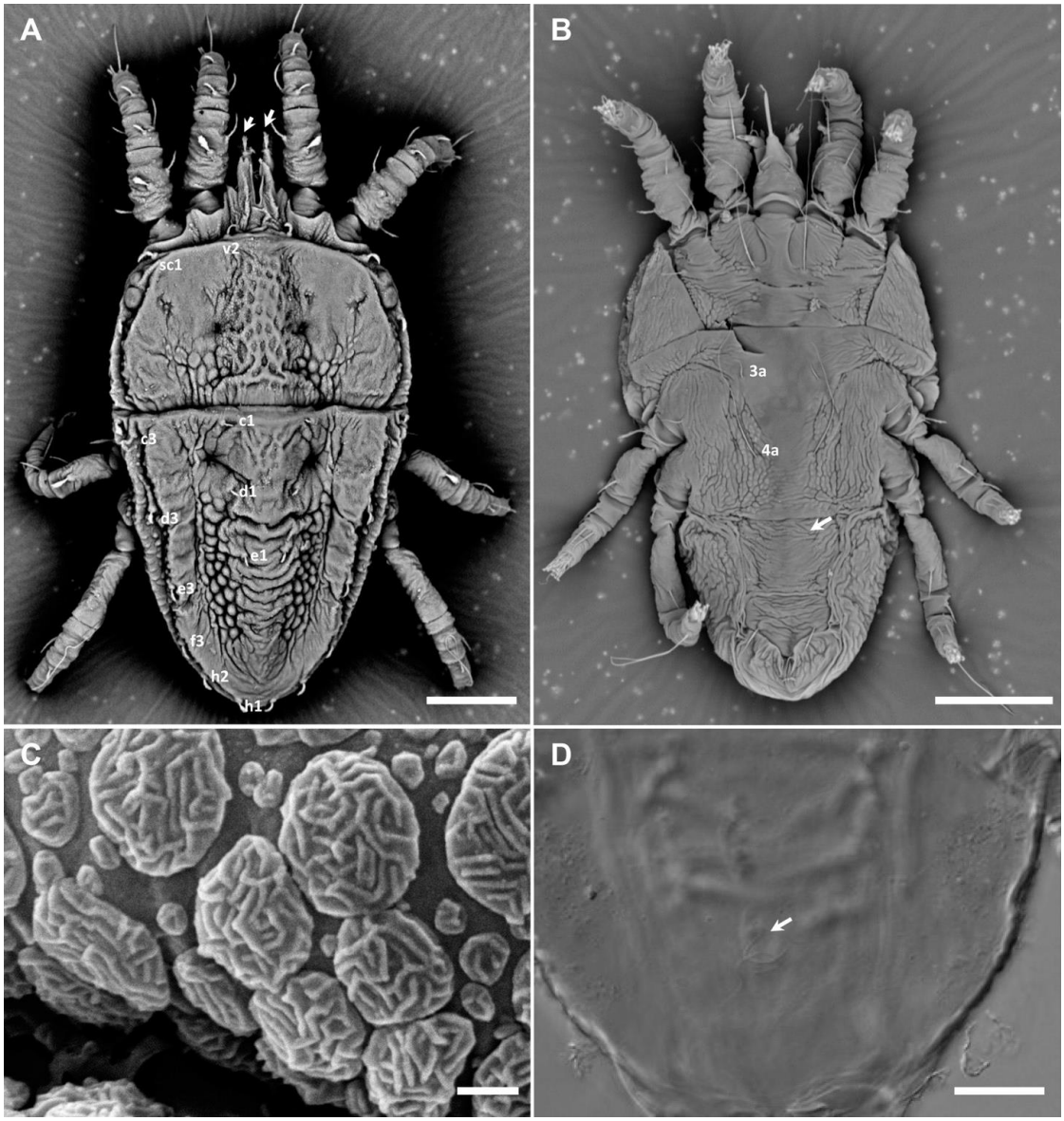

Figure 6. Microphotographs of *Brevipalpus phoenicis* sensu stricto mites collected in sweet orange (*Citrus sinensis*) trees showing citrus leprosis-nuclear (CL-N) symptoms (individuals from Ibiuúna, SP, Brazil). Morphological characteristics are depicted in four panels. A, Dorsal view. Cuticle of the propodosoma, sc1 = scapular seta and v2 = vertical seta, presence of strong, broad areolae on the median area of prodorsum. White arrows show palp femorogenu with dorsal seta broad, flat, and barbed; dorsal cuticle of the opisthosoma strongly reticulate, setae = c1, c3, d1, d3, e1, e3, f3, h1, h2; e1-e1 to h1-h1 cuticle with transverse folds, sublateral cuticle with a band of large distinctly round cells. B, Ventral view of the cuticle between aggential setae 3a and 4a. White arrow shows the ventral and genital shield with fused transverse bands. C, Microplates. D, White arrow shows spermatheca, a thick duct terminating in a bulb. Calibration bars: A and B = 50 µm, C = 0.5 µm, and D = 20 µm.

4.3 DISCUSSION

In this work, we provide biological and molecular evidence to support the conclusion that the causal agent of CL-N in Brazil, which we propose to call citrus leprosis virus N (CiLV-N), is different from those characterized elsewhere. CL symptoms were described in the

Americas in the early 1900s but only in the 1970s did Kitajima and collaborators associate the conspicuous symptoms with the presence of either one of the two types of short-bacilliform or rod-like particles observed in TEM (Kitajima et al., 1972, 1974b) and later considered "cytoplasmic and nuclear types" of citrus leprosis virus (Rodrigues et al., 2003).

In 2012, the species *Citrus leprosis virus C* was accepted by the International Committee on Taxonomy of Viruses (ICTV) to classify the prevalent virus that cause CL-C, and it was defined as the type member of genus *Cilevirus* (Locali-Fabris et al., 2012). CL-N is of rare occurrence and, in contrast to CL-C, it has not received much attention over the years and its possible economic losses were not yet assessed (Bastianel et al., 2010). Its causal agent has been generally called citrus leprosis virus nuclear type (Rodrigues et al., 2003), which seemed appropriate until recently, when the diversity of CL-N- associated viruses began to be unraveled. Two research groups reported the complete genome sequences of viruses causing CL-N in Mexico and named them Citrus leprosis virus nuclear type and Citrus necrotic spot virus (Roy et al., 2013b; Cruz-Jaramillo et al., 2014). Shortly after that, it was decided by the ICTV Mononegavirales Study Group and collaborators that, in fact, both viruses are citrus strains of OFV, because they share more than 90% nucleotide sequence identity (Afonso et al., 2016). Hence, for the sake of clarity and unambiguity, the designations citrus leprosis virus nuclear type and citrus necrotic spot virus should not be used any longer to designate those viruses, which should instead be referred to as citrus strains of OFV.

Yet another CL-N virus was recently characterized. Hartung et al. (2015) obtained a herbarium sample collected in Volusia County, FL, in 1948 and were able to partially sequence and assemble the viral genome. The authors not only confirmed the hypothesis formulated by Kitajima et al. (2011), who suggested that the Floridian causal agent of leprosis might have been of the nuclear type, but also showed that it was probably a different dichorhavirus, sharing approximately 80% nucleotide sequence identity with the OFV- citrus strain from Mexico (Hartung et al., 2015). However, the genome sequence obtained corresponds to only approximately 61% of the two RNA and the virus does not occur in nature any longer, which makes it impossible to determine unequivocally whether it indeed belongs to a different virus species.

The first confirmed report of a CL-N-associated virus in citrus was from SP, Brazil, when Kitajima et al. (1972) detected the presence of short rod-like particles in sweet orange and grapefruit plants through TEM analyses. Later, similar analyses revealed the occurrence of CL-N in at least six municipalities in SP, as well as in two other Brazilian states (Rio Grande do Sul and Minas Gerais) (Bastianel et al., 2010). A pattern could be observed in all of these cases:

CL-N occurred in sweet orange plants grown in residential backyards at higher altitudes and under cooler weather conditions (Bastianel et al., 2010).

Based on recent data on citrus-infecting dichorhaviruses, and considering that the CL-N causal agent in Brazil could not be detected by primers that specifically detect strains of OFV (from either orchid or citrus) by RT-PCR, a thorough biological and molecular characterization of the Brazilian CL-N pathogen was per- formed. Taken together, the following features placed it within the dichorhavirids: (i) induction of typical localized chlorotic or necrotic leprosis-like symptoms in sweet orange plants; (ii) presence of short rod-like virions of approximately 40 to 100 nm in length, spoke-wheel structure, or electron-lucent viroplasms in infected cells analyzed by TEM; (iii) *Brevipalpus* mite transmission to both sweet orange and *A. thaliana* plants yielding localized lesions in the latter, which was recently shown to be a good experimental host for at least two other dichorhaviruses (CoRSV and the tentative dichorhavirids *Clerodendrum* chlorotic spot virus [ClCSV]) (Arena et al., 2017); and (iv) genome size and organization similar to that of dichorhaviruses. This newly sequenced virus has a bipartite (-)ssRNA genome of approximately 6.7 and 6.0 kb for each molecule, of which the RNA1 encodes five ORF, equivalent to genes *N*, *P*, *MP*, *M*, and *G* of rhabdovirids, whereas the RNA2 accommodates a single ORF, corresponding to the *L* gene. Moreover, all genes are separated by Gj, which include the putative gene transcription start site, the conserved IG region, and the polyadenylation signal (Dietzgen et al., 2017)

Of particular interest was the observation that, for RNA1, the lengths of some the Gj of CiLV-N were much more similar to those of CoRSV than those of OFV. Variability of inter-ORF regions and, in general, of the genomes throughout viruses of the family *Rhabdoviridae* was previously reported (Walker et al., 2015). This extensive study on the evolution of 99 animal rhabdoviruses showed that lengths of Gj are extremely variable within the family, being responsible for up to 48.5% of the variation in genome size from the smallest to the largest evaluated genomes(Walker et al., 2015). It is believed that the plasticity of the genome length of these viruses is a reflection of the discontinuous transcription strategy used for the expression of their genes and might be used to reveal phylogenetic relation- ships among rhabdoviruses (Walker et al., 2015). However, and sim- ilar to other RNA viruses, their monopartite genome sizes should be restricted due to high error rates leading to deleterious mutations (Holmes, 2003; Walker et al., 2015). The question of whether or not rhabdoviruses with a bipartite genome such as those from the genus *Dichorhavirus* arose from the need, at least partially, to overcome such size limitations needs to be addressed.

Altogether, our data do not leave doubts regarding the assignment of CiLV-N within the dichorhavirids. Moreover, they support the idea that the four sequenced isolates might be assigned to a new species of *Dichorhavirus*. According to the proposal of Dietzgen et al. (2014), accepted by the ICTV (Walker et al., 2014),species demarcation within the genus *Dichorhavirus* includes differences of >25% in the *L* gene nucleotide sequence and >10% in the complete genome sequence identity. CiLV-N RNA1 and RNA2 share less than 62% identity with the two definitive members of the genus, OFVand CoRSV (Table 1). Moreover, identities between the *L* gene of CiLV-N and those of OFV and CoRSV reach 61.2 and 62.8%, respectively (Table 1), falling below the 75% threshold of species demarcation.

As expected for such low identity values between CiLV-N and known dichorhaviruses, the primers used for the amplification of OFV, including the citrus strain of the virus, cannot detect CiLV-N. Hence, we designed a primer pair that specifically amplifies CiLV-N and can be used to differentiate it from other CL-N-causing viruses (Figure 6A). In addition, we also designed primers for the *L* gene that are able to detect both circulating CL-N viruses (i.e., OFV and CiLV-N). These primers were validated and can be useful for surveys and further characterization of these and perhaps other CL-associated dichorhaviruses (Figure 6B).

Phylogenetic analyses reveal that the CiLV-N isolates are more closely related to CoRSV than to OFV (Figure 5). Coincidently or not, reports of both CL and coffee ringspot diseases in Brazil date from 1930s (Bitancourt, 1938, 1940), whereas orchid fleck was first re- ported decades later in Japan (Doi et al., 1969) and Brazil (Kitajima et al., 1974a). Obviously, which of the CL-C- and CL-N-associated viruses were present in Brazil more than 80 years ago may never be known. However, it is reasonable to speculate that CiLV-N has been associated with the recurrently reported cases of CL-N in Brazil and, accordingly, this virus may be the first described among the citrus- associated dichorhaviruses that are currently circulating in the field. Although the biological characterization may not be always es sential for species demarcation within a particular genus (Dietzgen et al., 2014; Simmonds et al., 2017), we consider that, for CiLV-N, it clearly strengthens the proposal for creating a new species within genus *Dichorhavirus* due to several distinct features it presents when compared with other members of the genus. Moreover, some of the biological features observed may have an impact on the epidemiology of the disease and help explain the distribution of such pathogens in citrus orchards.

Brevipalpus specimens collected in symptomatic orange trees from Ibi, SBS, and MAS were all identified as *B. phoenicis* sensu stricto based on the taxonomic features proposed by Beard et al. (2015). Experimental transmission of CiLV-N using viruliferous *B. phoenicis* sensu stricto to *A. thaliana* was achieved. Our results also indicated that *B. phoenicis* sensu

stricto mediated the trans- mission of this virus to healthy sweet orange plants in seminatural conditions. Viral detection in the infested plants using specific primers and the high identity of the amplicon sequences with those from the virus genome confirmed the capacity of *B. phoenicis* sensu stricto as a dichorhavirus vector. In agreement with these findings, rod-like particles similar to those observed in CiLV-N-infected plants were found in previous TEM analyses of *Brevipalpus* mites collected from the same infected sweet orange trees in MAS (Kitajima and Alberti, 2014). As described for other nuclear-type *Brevipalpus*- transmitted viruses (Dietzgen et al. 2014), in those samples, the authors observed not only virions but also the presence of viroplasm in the nucleus of infected mite cells, suggesting the replication of the virus in its vector. Hence, the relationship between CiLV-N and *B. phoenicis* sensu stricto, as well as other dichorhaviruses and their *Brevipalpus* vectors, appears to be of the persistent-replicative type (Kitajima and Alberti 2014).

CL-N diseases from Florida, Mexico, and Colombia have been associated with *B. californicus*, the known vector of OFV (Kondo et al. 2003; Roy et al. 2015a). *B. californicus* colonizes citrus in several countries of the Americas (Knorr, 1968; Childers et al., 2003a; Salinas-Vargas et al., 2013, 2016; Roy et al., 2015a) but, in Brazil, this mite species is rarely found in citrus orchards. The only existing report found in our search indicates an incidence of *B. californicus* at less than 0.1% (Bobot et al., 2011). Apparently, there are no reports of *B. californicus* colonizing citrus in SP, and our attempts to rear such species on citrus fruit (at 25 ± 1°C) were not successful (data not shown).

To our knowledge, this work is the first formal report of *B. phoenicis* sensu stricto in citrus in Brazil. Sánchez-Velázquez et al. (2015), in a recent survey in citrus orchards in this country, identified the prevalent *B. yothersi* and the less common *B. papayensis* species but not *B. phoenicis* sensu stricto in the production areas. The study was conducted in tropical regions, where most of the citrus is grown in Brazil and high temperatures are reached during several months of the year, favoring those mite species. Conversely, according to Beard et al. (2015), *B. phoenicis* sensu stricto was first identified in 1930s in the arecaceae plant *Phoenix canariensis* in a greenhouse in The Netherlands. Because the authors confirmed only a limited number of specimens as *B. phoenicis* sensu stricto from a few places (The Netherlands, the United States, and Costa Rica), it cannot be ruled out that the development of this mite species might be favored by cooler weather conditions. Interestingly enough, CL-N symptoms were identified only in marginal citrus production regions of Brazil, in a cooler climate zone associated with higher altitudes. This could partially explain the restricted dissemination of the *B. phoenicis*-transmitted viruses because, for plant rhabdoviruses, geographical distribution may be directly

linked to that of their vectors due to a close interaction between them (Kormelink et al., 2011; Barandoc-Alviar et al., 2016).

Another difference between the newly characterized CiLV-N and the OFV-citrus from Mexico is their host ranges. The citrus strain of OFV is able to naturally infect at least seven citrus species, including sweet orange, grapefruit, mandarin, lemon, lime, sweet lime, and sour orange plants (Roy et al., 2015b). On the other hand, CiLV-N seems to have a narrow host range. Even though we have not made an extensive survey on citrus species, CiLV-N has been identified only in sweet orange plants, even when mandarin and lime are grown nearby, suggesting that it does not infect those hosts (data not shown). Kitajima et al. (1972) reported the presence of a CL-N-associated virus in grapefruit trees in SP but no further diseased grapefruit plants have been detected since. It should be noted, however, that Brazil is not a relevant producer of grapefruit and it is difficult to find such citrus species both in orchards and in backyards.

In addition to the natural sweet orange host, we were able to transmit CiLV-N using *B. phoenicis* sensu stricto mites from sweet orange to sweet orange plants as well as to the experimental host *A. thaliana*, as reported for CoRSV and ClCSV (Arena et al., 2017). Similar to what was observed for these viruses, the time of symptom appearance ranged from 8 to 10 days, and the symptoms appeared as localized lesions. However, CiLV-N induced the appearance of typical pinpoint lesions, smaller than those observed for the other two viruses (Arena et al. 2017). The infection of *Arabidopsis* by this virus opens new doors for understanding the interactions between this host, a CL-N-associated virus, and the *Brevipalpus* mite, as established for the CL-C pathosystem (Arena et al., 2016). In addition, it will allow the comparison between the responses of *Arabidopsis* to CL-associated viruses from the nuclear and cytoplasmic types belonging to viral genera that display contrasting molecular biology. Comprehensively, our molecular and biological data show that CiLV-N should be assigned to a new species within the genus *Dichorhavirus*.

4.5 CONCLUSIONS

We propose this species should be definitively named Citrus leprosis N dichorhavirus both because this is the first characterized dichorhavirus with citrus as its primary host and also due to historical priority, because this is the oldest circulating virus associated with citrus leprosis that can be currently detected in fields. Dietzgen et al. (2014) mentions that, because the Mexican CL-N virus is a strain of OFV, sequencing of other viruses causing CL-N should help to determine whether or not the acronym CiLV-N, previously used for the Mexican CL-N virus, should be abandoned. Here, we demonstrate that it should not.

REFERENCES

Afonso, C. L., Amarasinghe, G. K., Bányai, K., Bào, Y., Basler, C. F., Bavari, S., et al. (2016). Taxonomy of the order Mononegavirales: update 2016. *Arch. Virol.* 161, 2351–60. doi:10.1007/s00705-016-2880-1.

Arena, G. D., Ramos-González, P. L., Nunes, M. A., Alves, M. R., Camargo, L. E. A., Kitajima, E. W., et al. (2016). Citrus leprosis virus C infection results in hypersensitive-like response, suppression of the JA/ET plant defense pathway and promotion of the colonization of its mite vector. *Front. Plant Sci.* 7, 1757. doi:10.3389/FPLS.2016.01757.

Arena, G. D., Ramos-González, P. L., Nunes, M. A., Jesus, C. C., Calegario, R. F., Kitajima, E. W., et al. (2017). *Arabidopsis thaliana* as a model host for *Brevipalpus* mite-transmitted viruses. *Sci. Agric.* 74, 85–89. doi:10.1590/1678-992x-2015-0380.

Barandoc-Alviar, K., Badillo-Vargas, I. E., and Eld, A. E. W. (2016). *Interactions Between Insect Vectors and Propagative Plant Viruses*. Cham doi:10.1007/978-3-319-24049-7.

Bastianel, M., Novelli, V. M., Kitajima, E. W., Kubo, K. S., Bassanezi, R. B., Machado, M. A., et al. (2010). Citrus Leprosis: Centennial of an unusual mite–virus pathosystem. *Plant Dis.* 94, 284–292. doi:10.1094/PDIS-94-3-0284.

Beard, J. J., Ochoa, R., Braswell, W. E., and Bauchan, G. R. (2015). *Brevipalpus phoenicis* (Geijskes) species complex (Acari: Tenuipalpidae)-a closer look. *Zootaxa* 3944, 1–67. Available at: http://www.ncbi.nlm.nih.gov/pubmed/25947538 [Accessed June 30, 2015].

Betley, J. N., Frith, M. C., Graber, J. H., Choo, S., and Deshler, J. O. (2002). A ubiquitous and conserved signal for RNA localization in chordates. *Curr. Biol.* 12, 1756–61. Available at: http://www.ncbi.nlm.nih.gov/pubmed/12401170 [Accessed April 13, 2016].

Bitancourt, A. (1938). A mancha anular, uma nova doença do cafeeiro. *Biol.* 4, 404–405.

Bitancourt, A. (1940). A leprose dos citrus. *Biol.* 6, 39–45.

Bobot, T. da E., Franklin, E., Navia, D., Gasnier, T. R. J., Lofego, A. C., and Oliveira, B. M. de (2011). Mites (Arachnida, Acari) on *Citrus sinensis* L. Osbeck orange trees in the state of Amazonas, Northern Brazil. *Acta Amaz.* 41, 557–566. doi:10.1590/S0044-59672011000400013.

Chagas, C., Colariccio, A., and Harakava, R. (2006). Novos registros da leprose tipo nuclear (CiLV-N): Andradas (MG) e São Roque (SP). *Fitopatol Bras* 39, 139.

Childers, C. C., French, J. V., and Rodrigues, J. C. V. (2003a). *Brevipalpus californicus, B. obovatus*, *B. phoenicis*, and *B. lewisi* (Acari: Tenuipalpidae): a review of their biology, feeding injury and economic importance. *Exp. Appl. Acarol.* 30, 5–28. doi:10.1023/B:APPA.0000006543.34042.b4.

Childers, C. C., Rodrigues, J. C. V, Derrick, K. S., Achor, D. S., French, J. V, Welbourn, W. C., et al. (2003b). Citrus leprosis and its status in Florida and Texas: past and present. *Exp. Appl. Acarol.* 30, 181–202.

Cruz-Jaramillo, J. L., Ruiz-Medrano, R., Rojas-Morales, L., López-Buenfil, J. A., Morales-Galván, O., Chavarín-Palacio, C., et al. (2014). Characterization of a proposed dichorhavirus associated with the citrus leprosis disease and analysis of the host response. *Viruses* 6, 2602–22. doi:10.3390/v6072602.

Dietzgen, R. G., Kondo, H., Goodin, M. M., Kurath, G., and Vasilakis, N. (2017). The family *Rhabdoviridae*: mono- and bipartite negative-sense RNA viruses with diverse genome organization and common evolutionary origins. *Virus Res.* 227, 158–170.

doi:10.1016/j.virusres.2016.10.010.

Dietzgen, R. G., Kuhn, J. H., Clawson, A. N., Freitas-Astúa, J., Goodin, M. M., Kitajima, E. W., et al. (2014). Dichorhavirus: a proposed new genus for *Brevipalpus* mite-transmitted, nuclear, bacilliform, bipartite, negative-strand RNA plant viruses. *Arch. Virol.* 159, 607–19. doi:10.1007/s00705-013-1834-0.

Doi, Y., Arai, K., and Yora, K. (1969). Ultrastructure of bacilliform virus found in *Euonymus japonicum* with mosaic and *Cymbidium* with ringspot. *Ann Phytopathol Soc Jpn* 35, 388.

Dominguez, F., Bernal, A., Childers, C. C., Kitajima, E. W., de Dominguez, F. S., Bernal, A., et al. (2001). First report of citrus leprosis virus in Panama. *Plant Dis.* 85, 228–228. doi:10.1094/PDIS.2001.85.2.228A.

Edgar, R. C. (2004). MUSCLE: multiple sequence alignment with high accuracy and high throughput. *Nucleic Acids Res.* 32, 1792–7. doi:10.1093/nar/gkh340.

Freitas-Astúa, J., Kitajima, E., and Bastianel, M. (2004). Identification of Citrus leprosis virus-nuclear type (CiLV-N) in sweet orange in the State of Rio Grande do Sul. *Virus Rev Res* 9, 247.

Hartung, J. S., Roy, A., Fu, S., Shao, J., Schneider, W. L., and Brlansky, R. H. (2015). History and diversity of citrus leprosis virus recorded in herbarium specimens. *Phytopathology* 105, 1277–84. doi:10.1094/PHYTO-03-15-0064-R.

Holmes, E. C. (2003). Error thresholds and the constraints to RNA virus evolution. *Trends Microbiol.* 11, 543–546. doi:10.1016/j.tim.2003.10.006.

Jackson, A. O., Dietzgen, R. G., Goodin, M. M., Bragg, J. N., and Deng, M. (2005). Biology of plant rhabdoviruses. *Annu. Rev. Phytopathol.* 43, 623–60. doi:10.1146/annurev.phyto.43.011205.141136.

Kitajima, E., Ferreira, P., Freitas-Astúa, J., and Ma (2004). Ocorrência da leprose dos citros, tipo nuclear (CiLV-N) nos municípios paulistas de Monte Alegre do Sul e Amparo. *Summa Phytopathol* 30, 68.

Kitajima, E. W., and Alberti, G. (2014). Anatomy and fine structure of *Bevipalpus* mites (Tenuipalpidae) – Economically important plant virus vectors. Part 7. Ultrastructural detection of cytoplasmic and nuclear types of *Brevipalpus* transmitted viruses. *Zoologica* 160, 174–192.

Kitajima, E. W., Blumenschein, A., and Costa, A. S. (1974a). Rodlike particles associated with ringspot symptoms in several orchid species in Brazil. *J. Phytopathol.* 81, 280–286. doi:10.1111/j.1439-0434.1974.tb02801.x.

Kitajima, E. W., Chagas, C. M., Harakava, R., Calegario, R. F., Freitas-Astúa, J., Rodrigues, J. C. V., et al. (2011). Citrus leprosis in Florida, USA, appears to have been caused by the Nuclear type of citrus leprosis virus (CiLV-N). *VIRUS Rev. Res.* 16, 4. doi:10.17525/vrr.v16i1-2.51.

Kitajima, E. W., Chagas, C. M., and Rodrigues, J. C. V (2003). *Brevipalpus*-transmitted plant virus and virus-like diseases: cytopathology and some recent cases. *Exp. Appl. Acarol.* 30, 135–60.

Kitajima, E. W., Müller, G. W., Costa, A. S., and Yuki, W. (1972). Short, rod-like particles associated with Citrus leprosis. *Virology* 50, 254–8.

Kitajima, E. W., Rosillo, M. A., Portillo, M. M., Muller, G. W., and Costa, A. S. (1974b). Microscopia eletrônica de tecidos foliares de laranjeiras infectadas pela lepra explosiva da

Argentina. *Fitopatologia* 9, 55–56.

Knorr, L. C. (1968). Studies on the Etiology of Leprosis in Citrus. in *Proc. 4th Conf. Int. Organ. Citrus. Virol.* (Gainesville Fla: University of Florida Press), 332–341.

Kondo, H., Chiba, S., Andika, I. B., Maruyama, K., Tamada, T., and Suzuki, N. (2013). Orchid fleck virus structural proteins N and P form intranuclear viroplasm-like structures in the absence of viral infection. *J. Virol.* 87, 7423–34. doi:10.1128/JVI.00270-13.

Kondo, H., Maeda, T., Shirako, Y., and Tamada, T. (2006). Orchid fleck virus is a rhabdovirus with an unusual bipartite genome. *J. Gen. Virol.* 87, 2413–2421. doi:10.1099/vir.0.81811-0.

Kondo, H., Maeda, T., and Tamada, T. (2003). Orchid fleck virus: *Brevipalpus californicus* mite transmission, biological properties and genome structure. *Exp. Appl. Acarol.* 30, 215–223. Available at: http://www.ncbi.nlm.nih.gov/pubmed/14756418 [Accessed July 25, 2016].

Kondo, H., Maruyama, K., Chiba, S., Andika, I. B., and Suzuki, N. (2014). Transcriptional mapping of the messenger and leader RNAs of orchid fleck virus, a bisegmented negative-strand RNA virus. *Virology* 452–453, 166–74. doi:10.1016/j.virol.2014.01.007.

Kormelink, R., Garcia, M. L., Goodin, M., Sasaya, T., and Haenni, A.-L. (2011). Negative-strand RNA viruses: The plant-infecting counterparts. *Virus Res.* 162, 184–202. doi:10.1016/j.virusres.2011.09.028.

Kosugi, S., Hasebe, M., Tomita, M., and Yanagawa, H. (2009). Systematic identification of cell cycle-dependent yeast nucleocytoplasmic shuttling proteins by prediction of composite motifs. *Proc. Natl. Acad. Sci. U. S. A.* 106, 10171–6. doi:10.1073/pnas.0900604106.

Kubo, K. S., Freitas-Astúa, J., Machado, M. A., and Kitajima, E. W. (2009). Orchid fleck symptoms may be caused naturally by two different viruses transmitted by *Brevipalpus*. *J. Gen. Plant Pathol.* 75, 250–255. doi:10.1007/s10327-009-0167-z.

la Cour, T., Kiemer, L., Mølgaard, A., Gupta, R., Skriver, K., and Brunak, S. (2004). Analysis and prediction of leucine-rich nuclear export signals. *Protein Eng. Des. Sel.* 17, 527–36. doi:10.1093/protein/gzh062.

León, G., Roy, A., Choudhary, N., and Brlansky, R. (2014). Citrus leprosis virus cytoplasmic type 2 (CiLV-C2) detection in Meta and Casanare States. *Corpoica Cienc. y Tecnol. Agropecu.* 15, 207–217.

Locali-Fabris, E. C., Freitas-Astúa, J., and Machado, M. A. (2012). "Genus *Cilevirus*. International Committee on Taxonomy of Viruses," in *Virus Taxonomy*, eds. A. King, M. Adams, E. Carstens, and E. Lefkowitz (London, United Kingdom: Elsevier/Avademic Press), 1139–1142.

Locali, E. C., Freitas-Astua, J., de Souza, A. A., Takita, M. A., Astua-Monge, G., Antonioli, R., et al. (2003). Development of a molecular tool for the diagnosis of leprosis, a major threat to citrus production in the Americas. *Plant Dis.* 87, 1317–1321. doi:10.1094/PDIS.2003.87.11.1317.

Mann, K. S., and Dietzgen, R. G. (2014). Plant rhabdoviruses: new insights and research needs in the interplay of negative-strand RNA viruses with plant and insect hosts. *Arch. Virol.* 159, 1889–900. doi:10.1007/s00705-014-2029-z.

Melzer, M. J., Sether, D. M., Borth, W. B., and Hu, J. S. (2013). Characterization of a virus infecting *Citrus volkameriana* with citrus leprosis-like symptoms. *Phytopathology* 102,

122–7. doi:10.1094/PHYTO-01-11-0013.

Okonechnikov, K., Golosova, O., Fursov, M., and Team, the U. (2012). Unipro UGENE: a unified bioinformatics toolkit. *Bioinformatics* 28, 1166–1167. doi:10.1093/bioinformatics/bts091.

Petersen, T. N., Brunak, S., von Heijne, G., and Nielsen, H. (2011). SignalP 4.0: discriminating signal peptides from transmembrane regions. *Nat. Methods* 8, 785–6. doi:10.1038/nmeth.1701.

Poch, O., Blumberg, B. M., Bougueleret, L., and Tordo, N. (1990). Sequence comparison of five polymerases (L proteins) of unsegmented negative-strand RNA viruses: theoretical assignment of functional domains. *J. Gen. Virol.* 71 (Pt 5), 1153–62. doi:10.1099/0022-1317-71-5-1153.

Ramalho, T. O., Figueira, A. R., Sotero, A. J., Wang, R., Geraldino Duarte, P. S., Farman, M., et al. (2014). Characterization of *Coffee* ringspot virus-Lavras: a model for an emerging threat to coffee production and quality. *Virology* 464–465, 385–96. doi:10.1016/j.virol.2014.07.031.

Ramos-González, P. L., Chabi-Jesus, C., Guerra-Peraza, O., Breton, M. C., Arena, G. D. G. D. G. D., Nunes, M. A. M. A., et al. (2016). Phylogenetic and molecular variability studies reveal a new genetic clade of Citrus leprosis virus C. *Viruses* 8, 153. doi:10.3390/v8060153.

Ramos-González, P. L. P. L., Sarubbi-Orue, H., Gonzales-Segnana, L., Chabi-Jesus, C., Freitas-Astúa, J., and Kitajima, E. W. E. W. (2015). Orchid fleck virus infecting orchids in Paraguay: first report and use of degenerate primers for its detection. *J. Phytopathol.* 164, 342–347. doi:10.1111/jph.12420.

Rodrigues, J. C. V, Kitajima, E. W., Childers, C. C., and Chagas, C. M. (2003). Citrus leprosis virus vectored by *Brevipalpus phoenicis* (Acari: Tenuipalpidae) on citrus in Brazil. *Exp. Appl. Acarol.* 30, 161–79. Available at: http://www.ncbi.nlm.nih.gov/pubmed/14756415 [Accessed January 13, 2017].

Roy, A., Choudhary, N., Guillermo, L. M., Shao, J., Govindarajulu, A., Achor, D., et al. (2013a). A novel virus of the genus *Cilevirus* causing symptoms similar to citrus leprosis. *Phytopathology* 103, 488–500. doi:10.1094/PHYTO-07-12-0177-R.

Roy, A., Hartung, J. S., Schneider, W. L., Shao, J., Leon M, G., Melzer, M. J., et al. (2015a). Role bending: Complex relationships between viruses, hosts, and vectors related to citrus leprosis, an emerging disease. *Phytopathology* 105, 872–884. doi:10.1094/PHYTO-12-14-0375-FI.

Roy, A., Leon, M. G., Stone, A. L., Schneider, W. L., Hartung, J., and Brlansky, R. H. (2014). First report of citrus leprosis virus nuclear type in sweet orange in Colombia. *Plant Dis.* 98, 1162. doi:10.1094/PDIS-02-14-0117-PDN.

Roy, A., Stone, A. L., Shao, J., Otero-Colina, G., Wei, G., Choudhary, N., et al. (2015b). Identification and molecular characterization of nuclear citrus leprosis virus, a member of the proposed *Dichorhavirus* genus infecting multiple citrus species in Mexico. *Phytopathology* 105, 564–75. doi:10.1094/PHYTO-09-14-0245-R.

Roy, A., Stone, A., Otero-Colina, G., Wei, G., Choudhary, N., Achor, D., et al. (2013b). Genome assembly of citrus leprosis virus Nuclear type reveals a close association with orchid fleck virus. *Genome Announc.* 1, e00519-13-e00519-13. doi:10.1128/genomeA.00519-13.

Salinas-Vargas, D., Santillán-Galicia, M. T., Guzmán-Franco, A. W., Hernández-López, A., Ortega-Arenas, L. D., and Mora-Aguilera, G. (2016). Analysis of genetic variation in *Brevipalpus yothersi* (Acari: Tenuipalpidae) populations from four species of citrus host plants. *PLoS One* 11, 1–11. doi:10.1371/journal.pone.0164552.

Salinas-Vargas, D., Santillán-Galicia, M. T., Valdez-Carrasco, J., Mora-Aguilera, G., Atanacio-Serrano, Y., and Romero-Pescador, P. (2013). Species composition and abundance of *Brevipalpus* spp. on different citrus species in Mexican orchards. *Neotrop. Entomol.* 42, 419–25. doi:10.1007/s13744-013-0140-6.

Simmonds, P., Adams, M. J., Benkő, M., Breitbart, M., Brister, J. R., Carstens, E. B., et al. (2017). Consensus statement: Virus taxonomy in the age of metagenomics. *Nat. Rev. Microbiol. 10.1038/nrmicro.2016.177*. doi:10.1038/nrmicro.2016.177.

Tamura, K., Stecher, G., Peterson, D., Filipski, A., and Kumar, S. (2013). MEGA6: molecular evolutionary genetics analysis version 6.0. *Mol. Biol. Evol.* 30, 2725–9. doi:10.1093/molbev/mst197.

Walker, P., Blasdell, K. R., Calisher, C. H., Dietzgen, R. G., Kondo, H., Kurath, G., et al. (2014). Create 2 new species, Orchid fleck dichorhavirus and Coffee ringspot dichorhavirus, in a new genus, *Dichorhavirus*, in the family *Rhabdoviridae*. *ICTV [International Comm. Taxon. Viruses] Propos. No. 2014.003a-dV.* doi:DOI: 10.13140/RG.2.1.1832.4324.

Walker, P. J. P., Firth, C., Widen, S. S. G., Blasdell, K. R. K., Guzman, H., Wood, T. T. G., et al. (2015). Evolution of genome size and complexity in the *Rhabdoviridae*. *PLOS Pathog.* 11, e1004664. doi:10.1371/journal.ppat.1004664.

ANNEX I

Supplementary Table 1. Primers for detection of known dichorhavirus and cilevirus.

Virus	Primer sequence (5'-3')	Reference
CiLV-C	*mp*-F: GCGTATTGGCGTTGGATTTCTGAC *mp*-R: TGTATACCAAGCCGCCTGTGAACT	(Locali et al., 2003)
CiLV-C2	*p29*-F: ATGAGTAACATTGTGTCGTTTTCGTTGT *p29*-R: TCACTCTTCCTGTTCATCAACCTGTT	(Roy et al., 2013a)
OFV	*N*-F: TGTCATAGCCGACATAAACACC *N*-R: TGTAGAGCTTGCGAGATACAGG	(Kubo et al., 2009)
OFV and OFV-citrus	*L*dF: CCYGTGAGAGAATTCYTGGATG *L*dR: CCAGATTGGTGTARCCRAACAG	(Ramos-González et al., 2015)
OFV-citrus	*N*-F: ATGGCTAACCCAAGTGAGATCGATTA *N*-R: AGTTGCCTTGAGATCATCACATTGGT *M*-F: ATGTCTAAACAGATTAATATGTGCACTGTG *M*-R: CTAACCACTGGGTCCCGC	(Roy et al., 2014)

Supplementary Table 2. Primers for secondary sequencing and RACE (Rapid Amplification of cDNA Ends) of the genomes of Brazilian citrus leprosis virus N (BrCiLV-N).

Primer sequence (5′—3′)	Direction[1]	Target region	Amplicon size (bp)
RNA1			
TGATGATAGACTACACCACG	F	269-288[2]	1280
AGGCATATTGACAACTGGT	R	1530-1548	
GACTTCCCTTACTATCCCC	F	1070-1088	1505
AGGTTGTATCATCGTTCTCA	R	2555-2574	
AAGACTGACACCTGCTAGTA	F	1701-1720	1513
TCGTTGGGTCATGGTCAT	R	3197-3213	
AATCTTCATAGTTGTATTCCTCT	F	2734-2756	1471
CTTTGCCTTGGAGTTCAC	R	4187-4204	
TCTGAAGGATATCATGCGAA	F	3486-3505	1484
TGTCCATACCAGTGATTCTC	R	4950-4969	
ATGCTAGCCTGGAGATCA	F	4473-4490	1281
CACAGATGTTGGCAAAGTAT	R	5734-5753	
CATGGATTTCACAAGGGAAC	F	5277-5296	1275
TAACCTTAAATCGCATTGCC	R	6532-6551	
Specific primers for amplification of BrCiLV-N isolate Ibi			
CCATGATGATGGTTGCAGTT	F	537-556[3]	1507
GTTTATCAGGTGATGGTGCT	R	2024-2043	
AAATATTCTCCTGGCTCCTC	F	2261-2280	633
CTCTACATCGGATGACCTTC	R	2874-2893	
AAGGAATATCGGGGAAAGTA	F	3615-3634	1494
GGACGACATCATAACAAGGT	R	5089-5108	
RNA2			
TTATCATCTCAAGTCAGCATTG	F	200-221[2]	851
TCTCATAGTTCTTCCCCAAG	R	1131-1150	
TGACTTTGTGTCCTTCTGTG	Ra	569-588	289
TCTTTCGGTTATCTTATCGAG	Rb	865-885	586
AATGAAGCCTATAGGGGACT	F	1006-1025	987
CCACTTCCTGAAGTCAATGT	R	1973-1992	
TTCTGGAGTATTTTCCGATG	F	1853-1872	981
TCTTCACAGTCTTGACTCCA	R	2814-2833	

GGTCAACAACCATCCACTAT	F	2706-2725	984
AAGTCCTCTTCTCCGTAAGC	R	3670-3689	
ACTTCTGCATCAGAAAGCAT	F	3568-3587	980
GAGACCTCCAGACCCAAC	R	4530-4547	
CATATGATGAGGAGACACGA	F	4417-4436	974
CCTCCCCATCTTTCATCT	R	5373-5390	
CTCCTATATGAGAGATGCAAAAC	F	5269-5291	760
ACAAGTTCTTAAAATAGCACCAT	R	6006-6028	
RNA1 3' RACE. Gene *N* specific primer and nested gene *N* specific primer. Isolates SBS, SRq and Ibi			
GATTACGCCAAGCTTGCTGCTGAACCCCT TTGAGGAATGTGTC	F	-	805
GCTGCTGAACCCCTTTGAGGAATGTGTC	F		
RNA1 5' RACE. Gene *G* specific primer and nested gene *G* specific primer. Isolate SBS			
GATTACGCCAAGCTTACACCGATCGGCAA CTGGCTATCAG	R	-	915
ACACCGATCGGCAACTGGCTATCAG	R		
RNA1 5´RACE. Gene G specific primers and nested gene *G* specific primer. Isolates Ibi and SRq			
GATTACGCCAAGCTTGGGGAACAAGCCGG TTTGGTGGAATG	R		884
CACAGCTCATCAATGGGATC	R		460
RNA2 3' RACE. Gene *L* specific primer and nested gene *L* specific primer. Isolates SBS, SRq and Ibi			
GATTACGCCAAGCTTGGCTGACAGTCCCC TATAGGCTTCATTGCCTTC	R	-	1032
GGCTGACAGTCCCCTATAGGCTTCATTGC CTTC	R		
RNA2 5' RACE. Gene *L* specific primer and nested gene *L* specific primer. Isolates SBS, SRq and Ibi			
GATTACGCCAAGCTTGCCACTCAACAGGG CAATATGTGCTGTG	F	-	723
GCCACTCAACAGGGCAATATGTGCTGTG	F		

[1]F: forward and R: reverse; [2]Position according to the genome of BrCiLV-N isolate SBS (GenBank accession numbers RNA1: KX982178, RNA2: KX982181). [3] Position according to the genome of BrCiLV N isolate Ibi (GenBank accession numbers RNA1: KX982176, RNA2: KX982179).

Supplementary Table 3. Nucleotide and deduced amino acids identities between the isolate Ibi, prototype member of the putative species BrCiLV-N, and the isolates SBS, SRq and MAS.

Isolate of BrCiLV-N[1]	SRq		SBS		MAS	
Ibi	nt	aa	nt	aa	nt	aa
RNA1	97,0	-	92,0	-	92,3	-
N	98,0	99,0	93,0	98,0	94,0	98,0
P	98,0	100	95,0	97,0	96,0	98,0
MP	99,0	99,0	95,0	99,0	95,0	99,0
M	98,0	98,0	93,0	96,0	95,0	96,0
G	98,0	99,0	93,0	99,0	91,0	99,0
RNA2	97,0	-	97,0	-	98,0	-
L	97,0	98,0	97,0	98,0	98,0	99,0

[1]Genbank accession numbers of isolate Ibi: KX982176 and KX982179; isolate SRq: KX982177 and KX982180; and isolate SBS: KX982178 and KX982181.

Supplementary Table 4. Detailed description of the genomic organization of BrCiLV-N and known dichorhaviruses.

Virus	RNA1																
	3′UTR	ORF1		UTR ORF1–2	ORF2		UTR ORF2–3	ORF3		UTR ORF3–4	ORF4		UTR ORF4–5	ORF5		5′UTR
	Size	Position	Size	Size	Position	Size	Size	Position	Size	Size	Position	Size	Size	Position	Size	Size
BrCiLV-N_Ibi	247	248-1597	1350	168	1765-2472	708	**320**	2792-3781	990	**264**	4045-4602	558	**306**	4908-6521	1614	203
BrCiLV-N _SRq	247	248-1597	1350	168	1765-2472	708	**320**	2792-3781	990	**262**	4043-4600	558	**306**	4906-6519	1614	203
BrCiLV-N _SBS	248	249-1601	1353	163	1764-2474	711	**316**	2790-3779	990	**263**	4042-4602	561	**291**	4893-6506	1614	202
OFV	227	228-1580	1353	148	1728-2441	714	**136**	2577-3689	1113	**141**	3830-4381	552	**169**	4550-6208	1659	205
OFV-citrus_Qto	227	228-1580	1353	153	1733-2446	714	**136**	2582-3694	1113	**141**	3835-4386	552	**169**	4555-6213	1659	56
OFV-citrus_Ja1	266	267-1619	1353	157	1776-2489	714	**136**	2625-3737	1113	**141**	3878-4429	552	**169**	4598-6256	1659	239
CoRSV	104	105-1445	1341	232	1677-2393	717	**253**	2646-3632	987	**225**	3857-4408	552	**331**	4739-6343	1605	209

Virus	RNA2			
	3′UTR	ORF6		5′UTR
	Size	Position	Size	Size
BrCiLV-N_Ibi	199	200-5836	5637	209
BrCiLV-N _SRq	202	203-5839	5637	209
BrCiLV-N _SBS	205	206-5842	5637	209
OFV	182	183-5816	5634	185
OFV-citrus_Qto	182	183-5816	5634	31
OFV-citrus_Ja1	196	197-5830	5634	188
CoRSV	164	165-5759	5595	186

5. CHAPTER 3

IDENTIFICATION, FULL GENOMIC CHARACTERIZATION, AND PARTIAL HOST RANGE OF CITRUS CHLOROTIC SPOT VIRUS

Published

Chabi-Jesus, Camila; Ramos-González, Pedro; Tassi, Aline D.; Guerra-Peraza, Orlene; Kitajima, Elliot W.; Harakava, Ricardo; Beserra Jr., Jose Evando Aguiar; Salalori, Renato B.; Freitas-Astúa, Juliana. Identification and characterization of citrus chlorotic spot virus, a new dichorhavirus associated with citrus leprosis-like symptoms. **Plant Disease**, v.102, n.08, p-1–37. https://doi.org/10.1094/PDIS-09-17-1425-RE.

ABSTRACT

Local chlorotic spots resembling early lesions characteristic of citrus leprosis (CL) were observed in leaves of two sweet orange (*Citrus sinensis* L.) trees in Teresina, State of Piauí, Brazil, in early 2017. However, despite the similarities, these spots were generally larger than those of a typical CL and showed rare or no necrosis symptoms. In symptomatic tissues, transmission electron microscopy revealed the presence of viroplasms in the nuclei of the infected parenchymal cells and rod-shaped particles with an average size of approximately 40×100 nm, resembling those typically observed during in- fection by dichorhaviruses. A bipartite genome of the putative novel virus, tentatively named citrus chlorotic spot virus (CiCSV) (RNA1 = 6,518 nucleotides [nt] and RNA2 = 5,987 nt), revealed the highest nucleotide sequence identity values with the dichorhaviruses coffee ringspot virus strain Lavras (73.8%), citrus leprosis virus N strain Ibi1 (58.6%), and orchid fleck virus strain So (56.9%). In addition to citrus, CiCSV was also found in local chlorotic lesions on leaves of the ornamental plant beach hibiscus (*Taliparitiparitiliaceum* (L.) Fryxell). Morphological characterization of mites recovered from the infected plants revealed at least two different types of *Brevipalpus*. One of them corresponds to *Brevipalpus yothersi*. The other is slightly different from *B. yothersi* mites but comprises traits that possibly place it as another species. A mix of the two mite types collected on beach hibiscus successfully transmitted CiCSV to arabidopsis plants but addi- tional work is required to verify whether both types of flat mite may act as viral vectors. The current study reveals a newly described dichorhavirus as- sociated with a citrus disease in the northeastern region of Brazil.

Kewwords: *Rhabdoviridae*; *Brevipalpus* mites; BTV.

5.1 INTRODUCTION

Citrus leprosis (CL) is a viral disease endemic in the Americas that reduces yields and threatens the sustainability of citrus orchards (Bastianel et al., 2010; Roy et al., 2015a). CL does not systemically spread within the infected plants, only producing chlorotic lesions that are regularly accompanied by a central region, and sometimes concentric rings, displaying necrotic tissues. Commonly, the disease induces premature leaf and fruit drop. Severe infections of twigs and stems may also lead to the death of branches and, occasionally, the whole tree.

CL is caused by members of a heterogeneous group of rod-shaped or bacilliform single-stranded (ss)RNA viruses assigned to the genera *Cilevirus*, *Higrevirus*, and *Dichorhavirus* (Locali-Fabris et al., 2012; Melzer et al., 2013; Dietzgen et al., 2014). In the infected cells, viruses of the two first genera replicate in the cytoplasm, whereas dichorhaviruses replicate and accumulate in the nucleus, which is a trait that identifies two kinds of CL: cytoplasmic type (CL-C) and nuclear type (CL-N) (Rodrigues et al., 2003). CL-C is widely distributed throughout the main commercial citrus areas in Latin America. Citrus leprosis virus C (CiLV-C, genus *Cilevirus*) is prevalent in sweet orange orchards in the region, and its population is genetically subdivided into two clades which have a different and contrasted geographic distribution (Locali-Fabris et al., 2006; Ramos-González et al., 2016). CiLV-C strains from the clade SJP (São Jose do Rio Preto) have been only detected thus far in commercial areas in the State of São Paulo, Brazil, whereas those from the clade CRD (Cordeirópolis) circulate all over the continent. In addition to CiLV-C, in Colombia, CL-C is also caused by the cilevirus citrus leprosis virus C2 (CiLV-C2), whose genome shares only 55% nucleotide identity with CiLV-C (Roy et al., 2013a). Hibiscus green spot virus 2 is the only higrevirus identified to date and infects mainly hibiscus plants. However, it has been reported to be associated with CL-like symptoms in a few Volkamerian lemon (*Citrus volkameriana* Tan. & Pasq.) and navel sweet orange (*C. sinensis*) plants in Hawaii without causing any damage to the local citrus industry (Melzer et al., 2013; Roy et al., 2015a). Meanwhile, CL-N is much less frequent but it may affect a broader array of citrus commercial species; for example, sweet orange, lemon (*Citrus* × *limon*) (L.) Burm. F., sour orange (*C. aurantium* L.), grapefruit (*C.* × *paradise*) Macfadyen, lime (*C. aurantiifolia*) (Christm.) Swingle, mandarin (*C. reticulata*) Blanco, Persian lime (*C.*× *latifolia*) Tanaka, and so on (Cruz-Jaramillo et al., 2014; Roy et al., 2015b). Currently, two dichorhaviruses cause CL-N. Citrus-infecting strains of orchid fleck virus (OFV-citrus) have been found affecting small orchards in Mexico and Colombia (Cruz-Jaramillo et al., 2014; Roy et al., 2014, 2015b). Isolated foci of infection by citrus leprosis virus N (CiLV-N) have been detected in noncommercial areas of the State of São Paulo, Brazil (Ramos-González et al.,

2017). An archaic isolate of a CL-N- causing dichorhavirus was identified in a herbarium sample collected in Florida in 1948 but it seems that this virus may not exist in nature any longer (Hartung et al., 2015).

Genus *Brevipalpus* (Arachnida: Acari: Tenuipalpidae) comprises more than 280 valid species of known flat or false spider mites from which, thus far, 5 have been implicated in the transmission of CL-causing viruses (Childers et al., 2003; Kitajima and Alberti, 2014; Beard et al., 2015). Citrus-infecting strains of OFV are transmitted by *Brevipalpus californicus* (Banks) (García-Escamilla et al., 2017), and transmission of CiLV-N has been confirmed using viruliferous mites of the species *B. phoenicis* sensu stricto (Geijskes) (Ramos-González et al., 2017). Much earlier, *B. obovatus* mites were considered the vector of CL pathogens, probably those associated with the CL-C type of the disease, in Argentina (Frezzi 1940; Knorr 1968; Vergani 1945). Transmission of viruses causing CL-C also involves the mite species *B. yothersi* and *B. papayensis* (Ramos-González et al., 2016; Nunes et al., 2018).

In Brazil and Mexico, *B. yothersi* mites are frequently found in citrus orchards and in CiLV-C-infected trees (Roy et al., 2015a; Sánchez-Velázquez et al., 2015). In Colombia, in addition to the transmission of CiLV-C, *B. yothersi* seems to be the vector of CiLV-C2 (Guillermo et al., 2017). Apparent differences during transmission to sweet orange plants of members of the clades SJP and CRD of CiLV-C by *B. yothersi* mites have not been observed (Arena et al., 2016). Both cileviruses and dichorhaviruses are persistently transmitted by their corresponding vectors but, although dichorhaviruses appear to replicate in the mite cells (Kitajima and Alberti, 2014; Roy et al., 2015a), there is still some controversy regarding the cileviruses. Negative strand specific cDNA corresponding to cileviruses have been detected in *Brevipalpus* mites (Roy et al., 2015a) but extensive biological and anatomical evidence suggests no multiplication of these viruses in their vectors (Kitajima and Alberti, 2014; Tassi et al., 2017).

Virions of the genus *Dichorhavirus* (family *Rhabdoviridae*) encapsidate two (-)ssRNA molecules that globally encode six open reading frames (ORF) (Dietzgen et al., 2017). ORF 1 to 5 span over the RNA1, are nonoverlapped, and encode monocistronic messenger RNA for the translation of the nucleocapsid (*N*), phosphoprotein (*P*), putative movement protein (*MP*), matrix protein (*M*), and glycoprotein (*G*), respectively. RNA2 harbors only one ORF that encodes the RNA- dependent RNA polymerase (*RdRP* or *L*). Sequences comprising regulatory elements involved in the transcription initiation and the polyadenylation signaling processes flank all of these ORF. Nucleotide sequence stretches between contiguous ORF may show different lengths and composition, a trait linked to the evolutionary history of invertebrate and

vertebrate-infecting rhabdoviruses (Walker et al., 2015).

In this current work, we describe the ensemble of morphological and molecular evidence that allowed us to identify a new dichorhavirus associated with CL-like symptoms in sweet orange trees in Teresina, State of Piauí (PI), in northeastern Brazil. In addition to citrus, a similar virus was also found in beach hibiscus plants (*Talipariti tiliaceum* (L.) Fryxell), an ornamental tree used in public gardens of that city. We also describe the Brevipalpus mite transmission of CiCSV from infected beach hibiscus to *Arabidopsis* plants using two different types of mites found in beach hibiscus. In that natural host, in addition to *B. yothersi* mites, another type of mite, morphologically closer to *B. yothersi*, was found. The new type is slightly distinct and might represent a novel *Brevipalpus* sp. associated with viral transmission. Mites belonging to the new *Brevipalpus* type were only detected in the sweet orange trees infected by CiCSV thus far. In addition to citrus and beach hibiscus, CiCSV was found infecting agave plants in Teresina, PI, 2018. The detection and characterization of this isolate is described in Appendix I.

5.2 MATERIALS AND METHODS

5.2.1 Biological samples

Branches from two sweet orange (*C. sinensis* L., family Rutaceae) trees (i.e., samples 1 and 2) displaying large chlorotic spots were collected in urban areas of the city of Teresina, PI, Brazil, in February 2017. In addition, leaves of the ornamental beach hibiscus (*T. tiliaceum* (L.) Fryxell; syn. *Hibiscus tiliaceus* L., family Malvaceae) were collected 4 km away from the sampled citrus trees in November 2017. Beach hibiscus leaves showed localized chlorotic lesions, although smaller than those found in citrus. Rare necrotic lesions were observed. Each sample was subdivided and separately sent to two laboratories in the State of São Paulo, Brazil. Pieces from both symptomatic and asymptomatic leaf tissues were cut and conserved at −80°C until RNA extraction at the Instituto Biológico (Plant Biochemistry and Phytopathology Laboratory), in São Paulo. Transmission electron microscopy (TEM) analysis of plant tissues and the identification of mites found on samples were arried out at the Escola Superior de Agricultura Luiz de Queiroz, University of São Paulo, in Piracicaba. All mites from citrus samples were fixed in a 90% ethanol solution until their morphoanatomical inspection. Of the total number of mites found in the beach hibiscus sample, a fraction was used for virus transmission experiments and the rest were fixed to proceed with their taxonomical identification.

5.2.2 Transmission electron microscopy

Small fragments of leaf lesions from both citrus and beach hibiscus were prefixed for at least 2 h in a modified Karnovsky solution (2.5% glutaraldehyde and 2% paraformaldehyde in 0.05 M cacodylate buffer, pH 7.2) (Kitajima and Nome, 1999). Tissue samples were postfixed in 1% OsO4, dehydrated, embedded in low viscosity Spurr epoxy resin, and sectioned with a Leica EM UC6 ultramicrotome (Vienne, Austria) equipped with a Diatome diamond knife (Biel, Switzerland). Sections were mounted on 300-mesh copper grids and stained with uranyl acetate and Reynold's lead citrate and examined in a JEM 1011 (JEOL, Akishima, Japan) transmission electron microscope, and the images recorded digitally.

5.2.3 Detection of known CL viruses by reverse-transcription polymerase chain reaction

Total RNA was extracted from approximately 100 mg of plant samples using Trizol and following the manufacturer's recommendations (Life Technologies, Foster City, CA). Approximately 500 ng of the RNA template was used to obtain the cDNA using random hexamer primers and the GoScript reverse-transcription (RT) kit, as described by the manufacturer (Promega Corp., Madison, WI). The cDNA solution (3 ml) was tested by polymerase chain reaction (PCR) using an array of specific primers for the detection of all known citrus cileviruses and dichorhaviruses (Supplementary Table 1, Annex I). Amplicons were separated on 1.0% agarose gels in 1× Trisacetate-EDTA and visualized with ethidium bromide (0.1 mg/ml). RNA extracts from plants infected with the following viruses were used as control: coffee ringspot virus CoRSV (isolate collected in Limeira, SP, Brazil), CiLV-N (isolate collected in Ibiúna, SP, Brazil), OFV-citrus (isolate collected in Guadalajara, Mexico, kindly provided by Dr. Otero-Colina, Colegio de Postgraduados, Texcoco, Mexico), OFV-orchid (isolate collected in Piracicaba, SP, Brazil), clerodendrum chlorotic spot virus (ClCSV, putative dichorhavirus not yet molecularly characterized, isolate collected in Piracicaba, SP, Brazil), CiLV-C clade CRD (isolate collected in Cordeirópolis, SP, Brazil), and CiLV-C2 (kindly provided by Dr. Walther Turizo-Alvarez, Universidad Nacional de Colombia, Bogota, Colombia).

5.2.4 Viral genome discovery and sequence analysis

Approximately 500 mg of symptomatic tissues from citrus sample 1 were processed as described above. Preparation of both the RNA extract and the next-generation sequencing (NGS) library were carried out as previously defined (Ramos-Gonzalez et al., 2017). Reads were assembled de novo using both SPAdes, version 3.10.1 (Bankevich et al., 2012), available

in Geneious software package version 10.2.2 (Kearse et al., 2012), and Trinity (Grabherr et al., 2013), implemented on the Galaxy platform (https://usegalaxy.org) (Afgan et al., 2016). Recovered contigs were compared with viral genome sequences at the National Center for Biotechnology Information database (https://www.ncbi.nlm.nih.gov/genome/viruses/) using BLASTX, and those corresponding to putative viral sequences were selected (NCBI Resource Coordinators 2016; States and Gish 1994). Based on these sequences, a set of primers (Supplementary Table 2, Annex I) spanning all of the contigs were designed using Primer3 software (Untergasser et al., 2012). Fragments ensued from the amplification of the cDNA ends (SMARTer RACE 5'/3' Kit; Clontech Laboratories, Mountain View, CA) were cloned and both recombinant plasmids comprising the rapid amplification of cDNA ends (RACE) products (five independent clones per end) and each of the fragments covering the viral genome resulting from the overlapping reamplification by RT-PCR were sequenced by the Sanger method. After assembly, the virus recovered from the citrus tree 1 was named citrus chlorotic spot virus Trs1 isolate (CiCSV_Trs1). The genomic sequence of the CiCSV_Trs2 isolate (from citrus tree 2) and that of the CiCSV_Trs3 isolate (found in the beach hibiscus) were obtained via Sanger-based sequencing. Amplicons from Trs2 and Trs3 isolates were obtained by RT-PCR using the specific primers for the CiCSV_Trs1 isolate. Virus and isolate names were adopted considering the first identified host (citrus), characteristic symptom (chlorotic spot), city's name of the finding (Teresina = Trs), and order of collection (1 to 3).

Viral sequences were analyzed in silico for the identification of ORF, phylogenetic relationships, and presence of putative functional motives and domains such as signal peptide, nuclear localization signals (NLS), nuclear export signals (NES), glycosylation sites, and transmembrane helices using SignalP 4.1 (Petersen et al., 2011), cNLS Mapper (http://nls-mapper.iab.keio.ac.jp) (Kosugi et al., 2009), NetNES 1.1 Server (http://www.cbs.dtu.dk/services/NetNES/) (la Cour et al., 2004), and TMHMM Server v.2.0 (http://www.cbs.dtu.dk/services/TMHMM/). Viral nucleotide and deduced amino acid sequences were aligned using CLUSTAL algorithms (Chenna et al., 003) implemented in Geneious, version 10.2.2. Maximum clade credibility trees were inferred using a Markov Chain Monte Carlo (MCMC) Bayesian approach implemented on Mr. Bayes plugin at Geneious package under GTR+G+I substitution model. MCMC convergence was obtained for four independent runs with 10 million generations, which were sufficient to obtain a proper sample for the posterior at MCMC stationarity, assessed by effective sample sizes above 200.

5.2.5 Detection of CiCSV by RT-PCR

CiCSV was detected using a primer pair specific for the G gene (G_CiCSVF: 5'-CCTCCTCTTCTAGCGTCAT-3' and G_CiCSV-R: 5'-CTGTTTTGCCCATGCTAC-3'). PCR amplification was carried out using GoTaq reaction Mix (Promega Corp.), in which 3 µl of cDNA was used as a template for a 25µlreaction. The thermal cycling was as follows: an initial denaturation step at 95°C for 5 min, followed by 35 cycles of 95°C for 30 s, 58°C for 30 s, and 72°C for 40 s. An additional final extension for 5 min at 72°C was performed. Moreover, RNA extracts from CiCSV-infected plants were tested using a pair of primers previously described for the detection of CoRSV (CoRSV_F: 5'-GGACCATGAGACAGGAGGTG-3' and CoRSV_R: 5'-CTCTGCCAGTCCTCAATGTG-3') (Kitajima et al., 2011). All amplicons were electrophoretically separated on a 1% agarose gel. To confirm the identity of the generated fragments, they were purified using Wizard SV Gel and PCR Clean-Up System (Promega Corp.) and further sequenced by the Sanger method.

5.2.6 Mite-mediated virus transmission

In total, 20 mites collected from the beach hibiscus plant were transferred to three healthy *Arabidopsis thaliana* plants (8, 6, and 6 mites in each plant). Arabidopsis growth conditions and general guidelines for this experiment were as previously described (Ramos-González et al., 2017). After infestation, the arabidopsis growth chamber temperature was kept at 25°C. Arabidopsis leaves were collected 8 days after the infestationand the surviving mites were recovered and conserved in 90% ethanol for anatomical identification study. Leaves were carefully rinsed with distilled water to remove remaining mites, eggs, and any other contaminants, and processed for RNA purification. Viral presence in the leaves was detected by RT-PCR using a primer pair specific for the CiCSV *G* gene and CoRSV *L* gene (Kitajima et al., 2011). Amplicons were sequenced to confirm their identity.

5.2.7 Mite identification

Mites collected from the symptomatic leaves of citrus and beach hibiscus plants were examined by scanning electron microscopy or mounted for light microscopy. A number of specimens were preserved for further molecular analyses. Mites in different developmental stages, including larva, protonymph, deutonymph, and adults, previously fixed in 90% ethanol, were mounted on glass slides using Hoyer's medium and examined by differential interference contrast in a Zeiss Axioimager microscope (Carl Zeiss AG, Jena, Germany). The images were digitally registered and the measurements were obtained by means of the microscope software.

Moreover, palp setae, microplates, and other morphological details were observed under a JEM IT 300 scanning electron microscope (JEOL, Akishima, Japan). For this, mites were dehydrated in ethanol series, critical point dried using a Leica Critical Point Dryer 300 (Wechsler, Germany), mounted in double-coated carbon tape on stubs, and sputter coated (Baltec SPD 050; Balzers, Liechtenstein) with gold. The specimens were not tightly secured to the carbon tape; thus, it was possible to turn them over to their ventral position for additional imaging. Mite identification was carried out following morphological criteria established for the *B. phoenicis* sensu lato group (Beard et al., 2015). The holotype of the probably new specimen identified in Teresina, PI, Brazil, collected in sweet orange in February 2017 was deposited (MZLQ3449) at the reference collection of the Zoology Museum in Escola Superior de Agricultura "Luiz de Queiroz", Universidade de São Paulo, Piracicaba, SP, Brazil.

5.3 RESULTS

5.3.1 Chlorotic spot symptoms in affected sweet orange and beach hibiscus plants in northeastern Brazil are not associated with known cilevirus or dichorhavirus infections

Local chlorotic lesions resembling CL symptoms were detected in leaves of two sweet orange trees located in Teresina, PI, Brazil (Figure 1A). These spots were generally larger and less bright than those commonly observed in leaves of citrus plants affected by CL (Bastianel et al., 2010; Cruz-Jaramillo et al., 2014; Roy et al., 2015a; Ramos-González et al., 2017). Moreover, necrotic tissues that regularly accompany the CL lesions were seldom seen and, when detected, they were more evident at the boundaries of the lesions (Figure 1B). Regardless of the differences with the classical CL, total RNA extracts from the lesions were tested by RT-PCR using a set of primers for specific or generic detection of all known cileviruses and dichorhaviruses causing CL (e.g., CiLV-C, CiLV-C2, OFV-citrus, and CiLV-N) (Supplementary Figure 1, Annex II). All results were negative, suggesting a different etiological agent associated with CL-like symptoms. Similarly, the putative agent causing the chlorotic spots in beach hibiscus plants (Figure 1C) was undetectable using the same array of primers.

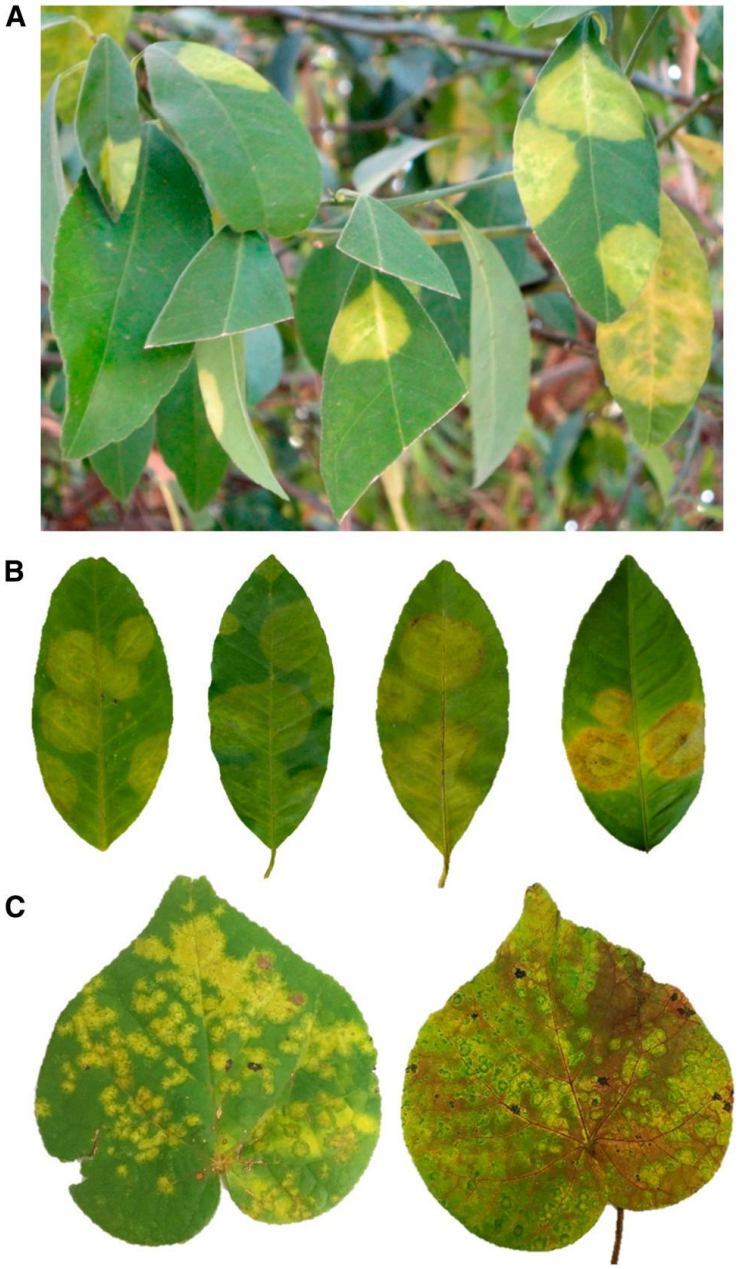

Figure 1. Localized chlorotic symptoms in sweet orange (*Citrus sinensis* L.) leaves infected with citrus chlorotic spot virus (CiCSV). B, Mature spots or older lesions may have necrotic areas (two leaves at the right). C, Localized chlorotic symptoms in beach hibiscus (*Hibiscus tiliaceus* L. syn. *Talipariti tiliaceum* (L.) Fryxell) leaves infected with CiCSV.

5.3.2 Morphology of viral particles and cytopathic effects suggest an infection by a dichorha-like virus in sweet orange and beach hibiscus plants

Examination of tissues from the lesions in citrus plants by TEM revealed the presence of large electron-lucent inclusions, referred to as viroplasm, in the nuclei of the infected palisade and spongy parenchyma cells (Figure 2A and B). Rod-like particles were found in the nucleus, though in a relatively scarce number across the screening of dozens of ultrathin sections (Figure 2C and D). According to the measurement of at least 20 of them, the rod-shaped particles were approximately 40 nm wide in cross sections and 100nm long in longitudinal sections, suggesting the presence of a typical dichorhavirus (Dietzgen et al., 2014). Neither viroplasm nor rod-like particles were observed in asymptomatic tissues. TEM of thin sections of chlorotic spots on leaves of beach hibiscus also revealed many nuclei containing electron-lucent inclusions (Figure 2E), similar to the viroplasm found in the infected citrus cells. Spoke-wheel structures, which are frequently observed in dichorhavirus-infected cells (Kitajima et al., 1972, 2003), could not be detected in any of the analyzed samples from the two plant species.

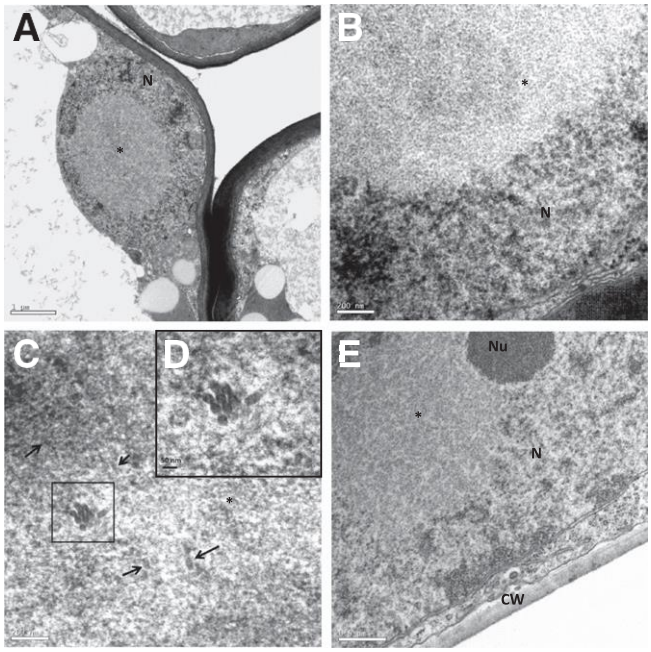

Figure 2. Transmission electron micrographs of thin sections of chlorotic lesions on citrus chlorotic spot virus-infected beach hibiscus leaves collected in Teresina, State of Piauí Brazil. A, Nucleus exhibiting electron-lucent viroplasm (*) in spongy parenchyma cells of the infected sweet orange plant. B, Details of the nuclear viroplasm shown in A. C, Rod-like particles approximately 40 nm wide and up to 100 nm long appear single (arrows) or grouped (boxed area) interspersed with the electron-lucent viroplasm detected in sweet orange. D, Longitudinal and cross-section details of the rod-like particles highlighted in C. E, Electron-lucent viroplasm in infected cells of beach hibiscus plant. Nucleoplasm area (N), nucleolus (Nu), and cell wall (CW).

5.3.3 Citrus chlorotic spot virus is a new dichorhavirus and most closely related to CoRSV

NGS and bioinformatic analysis of the RNA library from citrus tree 1 indicated the presence of an unknown virus. Further validation of the assembled sequence by the secondary sequencing of amplicons generated by RT-PCR and RACE definitively revealed the complete genome of a new virus related to known dichorhavirids. No citrus viroid and known-virus contigs were identified in the sequenced sample.

A negative-sense genome of CiCSV_Trs1 isolate was found to be 12,505 nucleotides (nt) in length, subdivided into two strands whose nucleotide sequences were deposited in the GenBank (GB) (RNA1:6,518 nt, accession number KY700685 and RNA2: 5,987 nt, KY700686). The CiCSV genome has all of the unique features of the bipartite genome of the dichorhaviruses (Figure 3). Following the convention for this genus, the five ORF detected in the orientation 3’ to 5’ of the RNA1 molecule were consecutively named as genes *N*, *P*, *MP*, *M*, and *G*, whereas a sixth ORF, the only one detected in the RNA2 over the entire genome, was identified as the putative RdRP (*L* gene). The CiCSV leader and trailer (the stretches of sequences at the two ends of both RNA1 and RNA2) span approximately 200 nt.

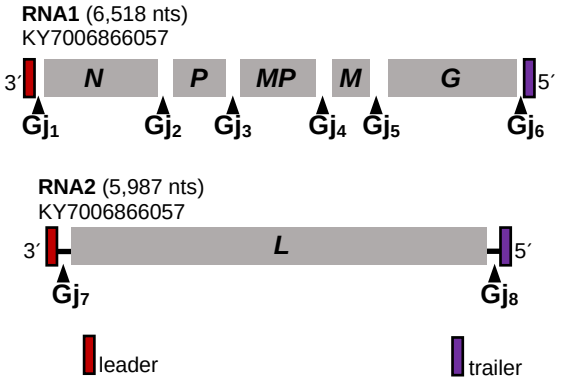

Figure 3. Genomic organization of citrus chlorotic spot virus. Gray solid boxes indicate viral open reading frame (ORF). Those in the RNA1 are designated as *N*= nucleocapsid, *P*= phosphoprotein, *MP*= movement protein, *M*= matrix protein, and *G*= glycoprotein. ORF in the RNA2 encodes the *L* (RNA-dependent RNA polymerase, *RdRP*) gene. Small boxes designate the leader and trailer sequences on the 3' and 5' ends, respectively, of each RNA molecule. Arrowheads show gene junction (Gj) distribution in the genome.

The complete genome of isolate CiCSV_Trs1 shares best identity values with the genome of CoRSV (GB accession numbers KF812525 and KF812526; RNA1: 70.5% and RNA2: 76.7%) and lower and approximately similar scores with OFV (AB244417 and AB244418) and CiLV-N (KX982176 and KX982179) (RNA1 approximately 55.0% and RNA2 approximately 62.0%) (Table 1). Consistently, gene-by-gene analyses revealed the highest values of nucleotide and amino acid identities with CoRSV (Table 1). Deduced sequences of the putative MP (91.8%) and N (89.5%) show the best identity values, followed by RdRP (87.2%). Analyses using the amino acid sequences of the P (81.2%), M (39.7%), and G (69.4%) unveiled lower levels of identity with their equivalents in the CoRSV genome. Identity values between proteins from CiCSV and their cognates in OFV and CiLV-N were always below 65%.

Table 1. Nucleotide and deduced amino acid identities between citrus chlorotic spot virus Trs1 isolate (CiCSV_Trs1) and the isolates Trs2 and Trs3 and known dichorhaviruses.

CiCSV_Trs1[b]	**Nucleotide/amino acid[a]**				
	CiCSV_Trs2	**CiCSV_Trs3**	**CiLV-N**	**OFV**	**CoRSV**
RNA2	96.6/-	95.6/-	55.2/-	53.0/-	70.5/-
N	97.5/99.6	95.0/99.6	61.0/58.3	57.1/50.4	78.6/89.5
P	98.3/100	96.5/100	54.3/44.5	51.0/33.6	77.3/81.2
MP	97.4/98.8	97.7/99.4	62.1/58.5	60.0/54.2	81.2/91.8
M	97.1/99.5	96.7/98.9	58.3/47.8	51.5/39.7	51.5/39.7
G	95.2/97.2	95.4/97.0	51.8/37.8	47.7/29.8	67.6/69.4
RNA2	98.5/-	98.6/-	62.1/-	60.8/-	76.7/-
L	98.5/99.2	98.6/98.9	63.4/64.1	61.8/58.4	77.1/87.2

[a]CiLV-N = Citrus leprosis virus N (GenBank accession numbers KX982176 and KX982179), OFV = orchid fleck virus (AB244417 and 244418), and CoRSV = coffee ringspot virus (KF812525 and KF812526); [b]N, P, MP, M, G, and L = nucleocapsid, phosphoprotein, putative movement protein, matrix protein, glycoprotein, and RNA-dependent RNA polymerase genes, respectively.

RNA1 and RNA2 sequences derived from the Trs2 isolate comprise 6,082 and 5,676 nt

(GB accession numbers MG717931 and MG717932), respectively. The 3' and 5' ends of each RNA molecule were not revealed because RACE analysis of this sample was not carried out. Regardless, these segments—RNA1 and RNA2 of Trs1 and Trs2 isolates—shared 96.6 and 98.5% nucleotide identity, respectively (Table 1). The deduced amino acid sequences derived from all Trs2 ORF showed more than 97% amino acid identity with the cognates in isolate CiCSV_Trs1, that we consider the CiCSV type. The genome sequence of the Trs3 isolate collected in the beach hibiscus plant was recovered by RT-PCR. RNA1 (6,078 nt, MG970598) and RNA2 (5,632 nt, MG970599) segments from this isolate displayed 95.6 and 98.6% nucleotide sequence identities, respectively, with their analogous from CiCSV_Trs1 (Table 1).

Deduced proteins from CiCSV_Trs1 display relevant structural and functional motifs. P contains two NLS located in its C-terminal half (amino acid stretches 127 to 136 [peptide PPMKRKVPIQ] and 228 to 238 [peptide RMNRKKKRCLD]). RdRP harbors the motifs Mononeg_RNA_pol (pfam00946), Mononeg_mRNAcap (pfam14318), and paramyx_RNAcap (TIGR04198) present in a large number of RdRP of mononegavirales, whereas the N terminus of the G contains a signal peptide whose cleavage site is located between the residues Ser27 and Gly28 (SignalP D score = 0.761). As observed in the G from other dichorhaviruses (Ramos-Gonzalez et al., 2017; Roy et al., 2015b), the G of CiCSV shows a transmembrane helix domain placed between the residues 458 and 480 of the putative mature protein (i.e., after the signal peptide removal). This membrane-spanning segment splits the protein into two subdomains: the largest and probably exposed on the virion surface harbors the N terminus and the smallest domain harbors the C terminus of the protein. The exposed domain contains two residues of Asn (positions 333 and 369 in the putative mature protein) predicted to be N-glycosylated. N, P, MP, and RdRP encoded by CiCSV also show one or more leucine-rich NES motifs like other dichorhaviruses (e.g., CiLV-N, OFV, and CoRSV) (Kondo et al., 2013; Ramalho et al., 2014; Ramos-González et al., 2017).

Phylogenetic analysis using the sequences of the N, G, and RdRP (L) proteins of a large number of plant-infecting rhabdoviruses supports the assignment of CiCSV to the genus *Dichorhavirus* (Figure 4). In the three trees, the sequences of CiCSV grouped together with its cognates from CoRSV, defining a topology in which definitive and putative members of this genus are redistributed in three lineages that we suggest calling subgroups OFV, CoRSV, and CiLV-N. In trees using N and G proteins, the dichorhavirus's branches were clearly separated from those containing other plant-infecting rhabdoviruses. This difference was less pronounced in the tree constructed based on L proteins. On the three generated trees, clade credibility values reached high posterior probabilities (>0.95).

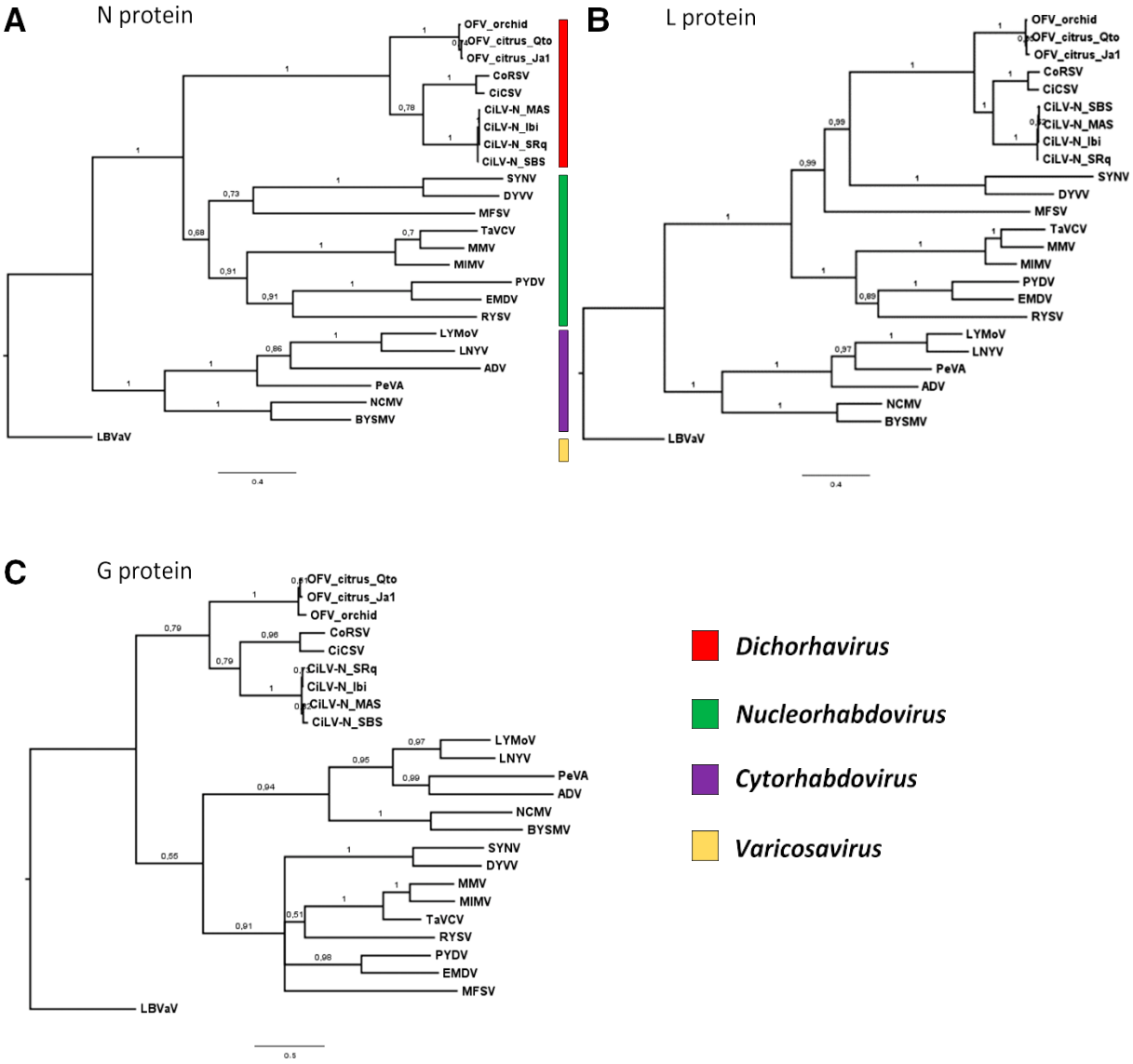

Figure 4. Phylogenetic reconstruction for plant-infecting viruses of the family *Rhabdoviridae*. Bayesian maximum clade credibility trees were inferred using the amino acid sequences of A, nucleocapsid protein (N); B, RNA-dependent RNA polymerase (L); and C, glycoprotein (G) of members of the genera *Dichorhavirus*, *Cytorhabdovirus*, *Nucleorhabdovirus*, and *Varicosavirus*. Trees were inferred using a Markov Chain Monte Carlo (MCMC) of 10 million generations. Lettuce big-vein associated virus (LBVaV)-derived sequences were used as outgroup. CiLV-N = Citrus leprosis virus N, CoRSV = coffee ringspot virus, CiCSV = citrus chlorotic spot virus, OFV = orchid fleck virus, DYVV = datura yellow vein virus, SYNV = sonchus yellow net virus, MFSV = maize fine streak virus, PYDV = potato yellow dwarf virus, EMDV = eggplant mottled dwarf virus, RYSV = rice yellow stunt virus, MIMV = maize Iranian mosaic virus, MMV = maize mosaic virus, TaVCV = taro vein chlorosis virus, BYSMV = barley yellow striate mosaic virus, NCMV = northern cereal mosaic virus, ADV = alfalfa dwarf virus, PeVA = persimmon virus A, LNYV = lettuce necrotic yellows virus, and LYMoV = lettuce yellow mottle virus. Bar size below each tree indicates the average number of amino acid substitutions per site.

5.3.4 CiCSV can be specifically identified by using primers based on its *G* gene and detected by primers designed for the detection of *L* gene from CoRSV

A pair of primers targeting 500 bp of the *G* gene was selected to establish a specific detection test for CiCSV and to guide further epidemiologic studies. Samples from six different leaves detached from the two naturally infected citrus trees (samples 1 and 2) yielded positive in the RT-PCR tests, whereas no results were obtained using samples from other plants infected with CiLV-C, CiLV-C2, CiLV-N, OFV-citrus, OFV-orchid, CoRSV, or ClCSV (Figure 5A). Two of six amplicons, one corresponding to each tree, were sequenced (GB accession numbers MG717933 and MG717934). They showed >98% nucleotide sequence identity with the cognate stretches in the RNA1 from CiCSV_Trs1 (KY700685) and CiCSV_Trs2 (MG717931) isolates, respectively. On the other hand, amplicons of 394 bp corresponding to CiCSV RNA2 were successfully amplified by primers designed for the detection of the *L* gene from CoRSV (Kitajima et al., 2011). These amplicons showed electrophoretic mobility similar to that from CoRSV-infected plants in 1% agarose gel (Figure 5B). Sequences of the generated amplicons (one from each citrus plant, GB accession numbers MG727716 and MG727717) showed >98.5% nucleotide sequence identity with the cognate sequences in the RNA2 of CiCSV_Trs1 (KY700686) and CiCSV_Trs2 (MG717932) isolates, respectively, but 77.0 to 78.0% nucleotide sequence identity with the equivalent genome region in the CoRSV genome.

CiCSV G gene-specific and CoRSV *L* gene primers were also used to analyze the chlorotic spot tissues in beach hibiscus (Figure 6, lanes 9 and 10). Amplicons of 500 and 394 bp were obtained with the primers corresponding to *G* and *L* genes, respectively, suggesting the presence of a CiCSV-like virus in this host. Recovered fragments showed >98% nucleotide sequence identity with sequences of the Trs1 isolate.

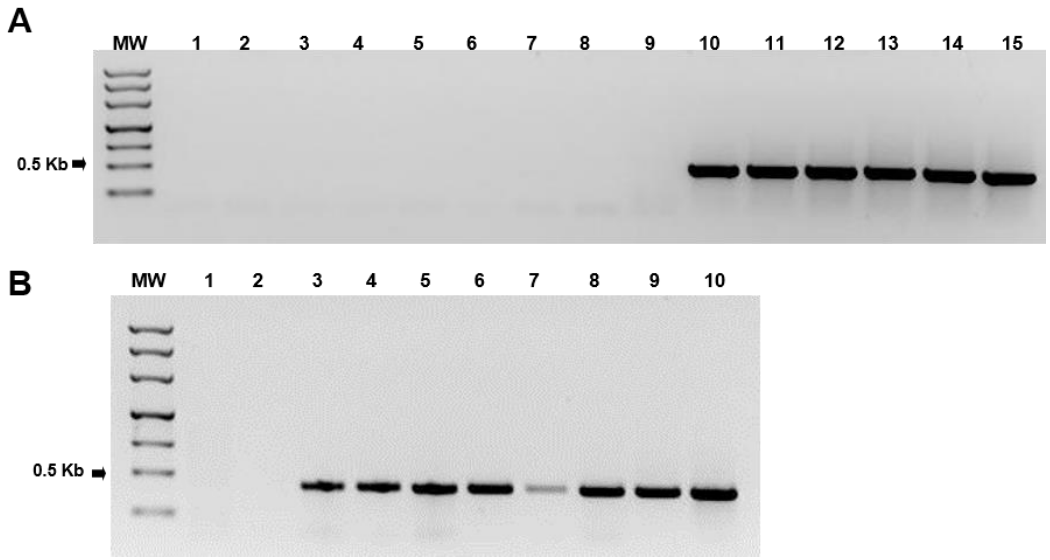

Figure 5. Analysis of reverse-transcription polymerase chain reaction (RT-PCR) amplicons for detection of citrus chlorotic spot virus (CiCSV) using 1% agarose gel electrophoresis. A, Primers are specific for the detection of glycoprotein (*G*) gene from CiCSV. MW = molecular weight marker, M1121 Ladder (Sinapse Biotechnology, Brazil). Lane 1 = Reversetranscription blank; lane 2 = asymptomatic leaf from CiCSV-infected sweet orange tree (plant 1), Teresina, PI; lane 3 = CiLV-C-infected citrus tree, Guaimbe, SP; lane 4 = CiLV-C2-infected citrus tree, Colombia; lane 5 = CiLV-N-infected citrus tree, São Roque, SP; lane 6 = orchid fleck virus (OFV)-citrus-infected citrus tree, Mexico; lane 7 = OFV-infected orchid plant, Piracicaba, SP; lane 8 = coffee ringspot virus (CoRSV)-infected coffee plant, Limeira, SP; lane 9 = ClCSV-infected Clerodendrum plant, Piracicaba, SP; lanes 10 to 12 = chlorotic lesions from three independent leaves collected in a CiCSV-infected sweet orange tree (plant 1), Teresina, PI; lanes 13 to 15 = chlorotic lesions from three independent leaves collected in a CiCSV-infected sweet orange tree (plant 2), Teresina, PI. B, RT-PCR products using primers for the detection of the RNA-dependent RNA polymerase (L) gene from CoRSV. MW= molecular weight marker, M1121 ladder. Lane 1 = RT blank; lane 2 = PCR blank; lanes 3 to 8 = chlorotic lesions from two sweet orange trees, Teresina, PI; lanes 9 and 10 = chlorotic lesions from two CoRSV-infected coffee plants collected in the cities of Piracicaba and Limeira, SP, Brazil, respectively.

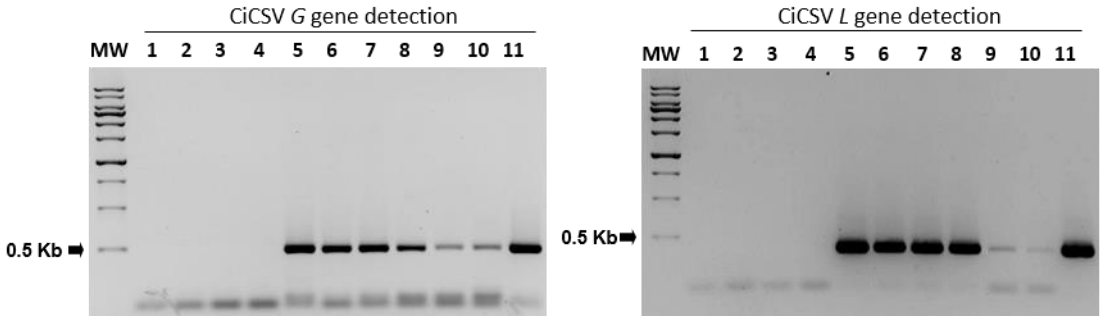

Figure 6. Analysis of reverse-transcription polymerase chain reaction (RT-PCR) products for detection of citrus chlorotic spot virus (CiCSV)-specific amplicons in naturally infected beach hibiscus and in experimental host arabidopsis using 1% agarose gel electrophoresis. Results obtained using primers for the detection of glycoprotein (*G*) and *L* genes are shown on top and bottom gels, respectively. MW= molecular weight marker, M1181 ladder (Sinapse Biotechnology, SP, Brazil). Lane 1 = RT blank, lane 2= PCR blank, lane 3 = tissue fragment of the leaf asymptomatic area from CiCSV-infected beach hibiscus, lane 4 = asymptomatic leaf from Arabidopsis plant, lanes 5 and 6 = symptomatic leaves from CiCSV-infected arabidopsis plant 1, lanes 7 and 8 = symptomatic leaves from CiCSV-infected Arabidopsis plant 2, lanes 9 and 10 = chlorotic leaf areas from two independent leaves collected in CiCSV-infected beach hibiscus, lane 11 = CiCSV-infected sweet orange tree, Teresina, PI.

5.3.5 *Arabidopsis* plant is an experimental host of CiCSV

Eight days after infestation with a mix of *Brevipalpus* mites recovered from the beach hibiscus plant, mild yellowish lesions were observed in some leaves of the three inoculated arabidopsis plants. Viral presence was detected in two leaves per each plant by using both CiCSV G genespecific and CoRSV L primers in the RT-PCR tests (Figure 6, lanes 5 to 8). Some amplicons were purified and their sequences (GB accession numbers MG970600 and MG970601) compared with the CiCSV_Trs1 and CiCSV_Trs3 genomes (KY700685, KY700686, MG970598, and MG970599). Both amplicons showed >93 and 98.0% nucleotide sequence identity with the analogous sequences of the Trs1 and Trs3 isolates, respectively.

5.3.6 At least two types of *Brevipalpus* mites are found in association with CiCSV symptoms

The number of *Brevipalpus* mites found infesting beach hibiscus was more than twice as many as that found in the infected citrus plants. Morphoanatomical examination of the adult mites collected from beach hibiscus trees allowed us to identify the presence of *B. yothersi* and another group of *Brevipalpus* mites that, though similar to *B. yothersi*, showed some morphological differences (Figure 7). Accordingly, they were temporarily designed as *B.* aff. *yothersi* regarding their best resemblance to specimens of that species and following the consensus about the use of qualifiers for provisional taxonomic status (aff. = abbreviation of affinis, from the Latin for “has affinity with”) (Sigovini et al., 2016). *B.* aff. *yothersi* mites were the only type that we could find in citrus plants.

B. aff. *yothersi* (Figure 7A) as well as *B. yothersi* (Figure 7F) mites show the dorsal opisthosomal setae c1, c3, d1, d3, e1, e3, f3, h1, and h2 but the seta f2 is absent. In *B.* aff. *yothersi*, the propodosoma shows crateriform pores in their center, forming irregular cells posteriorly and small cells anteriorly, a rostral shield, and a broad flat projection extending over coxae I-II (Figure 7A and B). The *B. yothersi* cuticle is smooth in the propodosoma anteriorly and posteriorly, and weakly reticulate (Figure 7F and G). Dorsal opisthosoma between c1-c1 and d1-d1 in *B.* aff. *yothersi* mites form regular cells whereas, in *B. yothersi*, it is weakly reticulate. In both type of specimens, a light V-shaped fold posterior to e1-e1 and a sublateral cuticle reticulate, with irregular polygons becoming wrinkled on the margins (Figure 7A, B, F, and G).

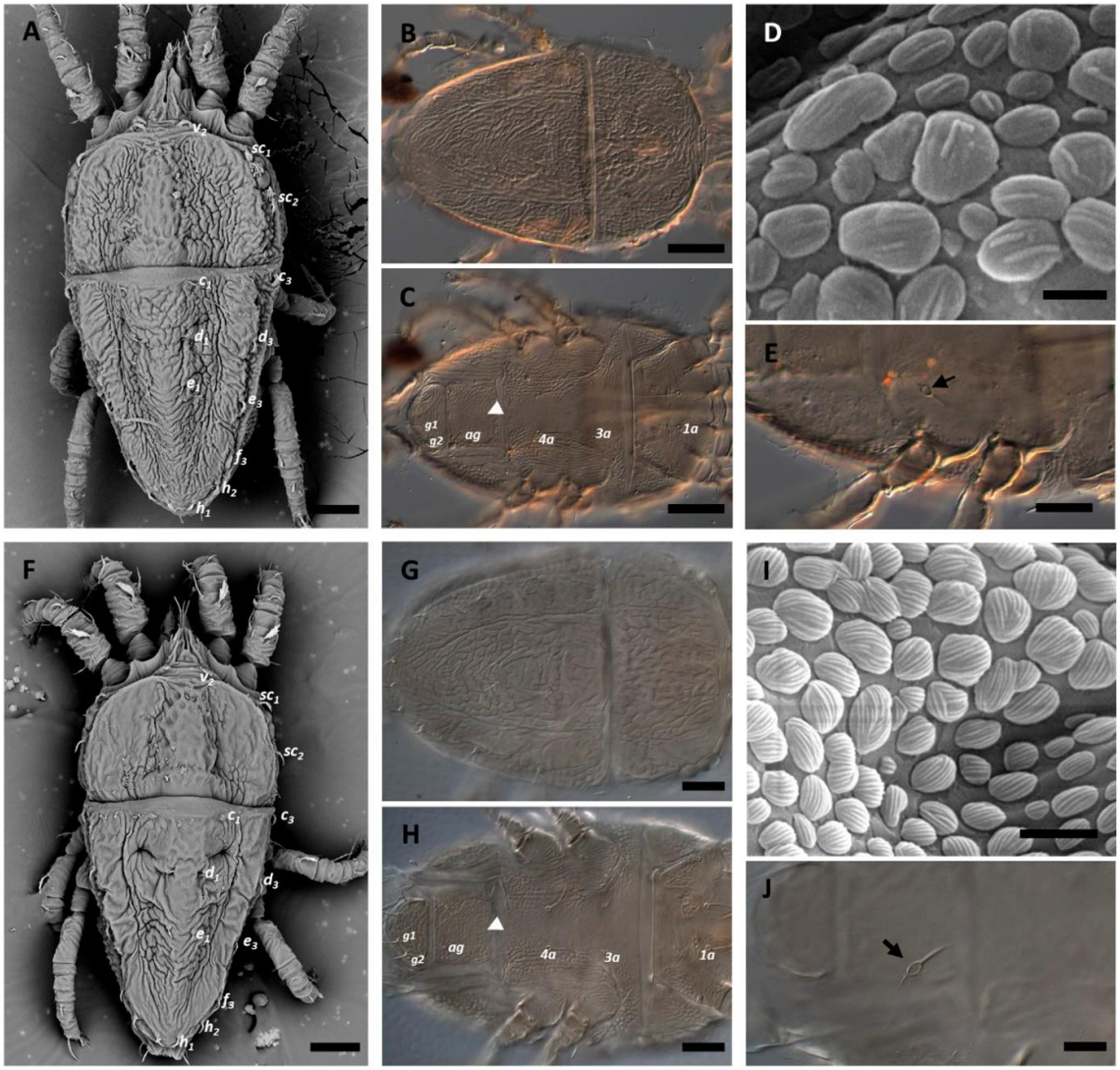

Figure 6. Microphotographs of A to E, *Brevipalpus* aff. *yothersi* and F to J, *B. yothersi*. A and F, Scanning electron microscopy (SEM) micrographs of the cuticle of dorsum showing the propodosoma setae sc1, sc2, and v2 and the opisthosoma setae c1, c3, d1, d3, e1, e3, f3, h1, and h2. B and G, Differential interference contrast (DIC) micrographs of dorsal view of the reticulation pattern. C and H, DIC micrographs of the ventral view of the cuticle, genital, and ventral plates with different ornamentations indicated by white arrowheads. Setae 1a, 3a, 4a, ag, g1, g2, ps1, and ps2 are designated. D and I, SEM micrographs of the microplates. E and J, DIC micrographs showing the oval vesicle with a distal stipe of spermatheca (black arrows). Calibration bars: A and F = 25 mm; B, C, G, and H = 40 mm; D = 1 mm; I = 0.5 mm; and E and J = 2.

Ventral plate cuticles of the *B.* aff. *yothersi* mites present elongated and transversal bands in the center and small cells in the lateral area; their genital plates have a cuticle with uniform bands (Figure 7C). In *B. yothersi*, the cuticle forms small, round cells in the ventral plate and large cells on the genital plate (Figure 7H). The palp femorogenu exhibits a dorsal seta setiform and is barbed in the two types of individuals, being longer in *B.* aff. *yothersi*. In both mites, the tarsus II bears two solenidia and the spermatheca shows a long, narrow duct ending in a sclerotized oval vesicle with thick distal stipe. In *B. yothersi*, the lumen of the vesicle

is larger (Figure 7E and J). Dorsal microplates of *B.* aff. *yothersi* mites are separate, individual, and irregularly shaped, with a series of small soft punctuations forming lines in different directions (Figure 7D). In *B. yothersi*, microplates show different ornamentation and are composed of a series of parallel ridges (Figure 7I). *B.* aff. *yothersi* body sizes are as follows: distance between setae v2 and h1 = 203 mm (range 198 to 210 mm), c3 to c3 =138 mm (range 130 to 145 mm), and palp femorogenu setae 14 mm (range 10 to 16 mm). For *B. yothersi*, the body sizes are as follows: v2 to h1 = 207 mm (range 200 to 215 mm), c3 to c3 = 146 mm (range 137 to 150 mm), and palp femorogenu setae = 10 mm (range 8 to 11 mm).

Mites from the hibiscus plant that were further used in the CiCSV transmission experiment were anatomically examined. Three of the five adults recovered from the infected arabidopsis plants after the end of the experiment were identified as *B. yothersi*, and the others as *B.* aff. *yothersi*.

5.4 DISCUSSION

In this work, the complete genome sequence of a new virus associated with CL-like symptoms is identified and characterized. The virus, tentatively called CiCSV, was first discovered infecting two sweet orange trees and subsequently detected in beach hibiscus plants, both occurring in the urban zone of Teresina, State of Piauí, in the northeastern region of Brazil. Viral sequences from three different sources showed more than 95% of nucleotide sequence identity among them. Both viral genomic structure and phylogenetic analysis indicated a close relationship of CiCSV with CoRSV and other members of the genus *Dichorhavirus*.

Genus *Dichorhavirus* was recently approved in the International Committee on Taxonomy of Viruses classification (Afonso et al., 2016) to accommodate bipartite rhabdoviruses transmitted by false spider mites of the genus *Brevipalpus* (Dietzgen et al., 2014, 2017). Pairwise comparisons of the nucleotide and deduced amino acid sequences from the three known dichorhaviruses reveal a relatively wide gap of genomic sequence identity between them, suggesting a presumed extensive speciation process from a putative common ancestor. Indeed, the identity values from the comparisons involving the pairs OFV and CoRSV, CiLV-N and OFV, and CiLV-N and CoRSV do not exceed 64.0% (Ramalho et al., 2014; Ramos-González et al., 2017; Roy et al., 2015a). Partially supported by these data, preliminary rules for species demarcation within the genus *Dichorhavirus* have contemplated a minimum nucleotide sequence divergence of 25% in the *L* gene and 10% in the whole genome (Dietzgen et al., 2014). Different from what it has been seen, CiCSV appears to be less divergent from CoRSV than to other dichorhaviruses, and its genome sequence only partially fulfills the rules

for its identification as a putative new species in the genus. Although the comparisons involving the RNA1 (best score 70.5% with CoRSV) and RNA2 (best score 76.7% with CoRSV) molecules show values lower than the adopted threshold (90%), the resulting value from the analysis of the L genes from CiCSV and CoRSV reaches 77.1% (i.e., slightly over the established cut-off value of 75%). The ambiguity ensuing from the analyses of the two criteria does not make obvious an accurate classification of CiCSV. However, although the intraspecific variability of dichorhaviruses has not been extensively studied, the divergence values between known isolates of OFV and CiLV-N are lower than 10 and 8%, respectively (Roy et al., 2013b; Cruz-Jaramillo et al., 2014; Kondo et al., 2017; Ramos-González et al., 2017). Taking into account these data, we chose to propose CiCSV as a new species, because the virus meets one of the criteria for the species demarcation in the genus, the second one is at the borderline, and in summary, the divergence of its nucleotide sequence with that from CoRSV is noticeably higher than the intraspecific diversity observed in other dichorhaviruses. However, we are aware that the addition of novel dichorhavirus sequences and the analysis of the trends of the identity profiles at both the nucleotide and amino acid levels between them will help to better address CiCSV classification.

In addition to the implications for viral classification, fluctuations in the nucleotide sequence identity throughout the CiCSV and CoRSV genomes effectively affect the results of molecular tools addressed to detect them. The pair of primers designed in this work to target the *G* gene of CiCSV specifically identifies this virus, without amplification from samples containing CoRSV or any other known dichorhavirus, while primers previously available for the detection of RNA2 of CoRSV (Kitajima et al., 2011) also detect CiCSV. This latter result, a consequence of the high conservation (≥90% identity) of the target sequences of these primers inside the CiCSV *L* gene, warns of the possibility of misidentification of these viruses in RT-PCR tests using them. However, from a practical point of view, the appropriate usage of these specific *G* gene and generic *L* gene primers might provide a suitable tool supporting epidemiological and phylogeographic studies of dichorhaviruses, particularly CiCSV and CoRSV.

Severity and morphology of distinguishing macroscopic symptoms caused by a viral infection may result from a combination of factors, including viral and host genotypes, abiotic influences, and concomitant infections with viruses and other pathogens (Prasch and Sonnewald, 2013; Kwak et al., 2016). CL is classically characterized by the presence of small chlorotic spots in which necrotic areas are regularly observed in leaves, twigs, and fruit. Leaves from the two sweet orange plants infected by CiCSV showed unusually large chlorotic spots.

The presence of necrotic tissues was rarely observed. In beach hibiscus, CiCSV infection also resulted in classic chlorotic spots, which become delimited by a green border in the senescent leaves. In broad terms, CiCSV symptoms in leaves from its two known hosts more closely resemble symptoms of CoRSV infection in coffee leaves and berries than classic CL. Perhaps molecular similarities between these two viruses may account for symptom resemblances in their respective hosts. CoRSV infection produces chlorotic irregular spots and ringspots with dark green or brownish borders and, occasionally, with a small central necrotic area (Chagas et al., 2003; Kitajima et al., 2011; Ramalho et al., 2014). Infected immature berries show whitish or yellowish areas that turn into greenish spots in mature fruit (Chagas et al., 2003). Unfortunately, at least for the time being, affected citrus plants did not bear fruit; therefore, symptoms in the putative CiCSV-infected plants, if any, could not be described yet. Regardless, this evidence unveils the existence of a spectrum of symptoms caused by dichorhaviruses and the lack of knowledge about the mechanisms underlying them.

Brevipalpus mites are the only identified vectors for viruses of the genus *Cilevirus* and *Dichorhavirus* (Kitajima and Alberti, 2014). *B. yothersi* and *B. papayensis* mites transmit CiLV-C, whereas *B. yothersi* mites are the only known vector of CiLV-C2 (Leon et al., 2017; Nunes et al., 2018; Tassi et al., 2017). *B. californicus* mites are the vectors of OFV, whereas mites of the species *B. phoenicis* sensu stricto vector CiLV-N in Brazil (Kondo et al., 2003; García-Escamilla et al., 2017; Ramos-González et al., 2017). Nevertheless, despite the efforts to revisit the *B. phoenicis* sensu lato group, *Brevipalpus* spp. have not yet been accurately identified (Beard et al., 2013; Navia et al., 2013) and, thus, the number of mite species actually involved in virus transmission and their role in viral epidemiology are largely unknown.

Based on their morphological characteristics, two different groups of mites were identified in association with CiCSV infection. Most of the collected mites in the beach hibiscus and those recovered from the arabidopsis plants used in the experimental transmission of CiCSV were identified as *B.* aff. *yothersi*. The description of these mites collected from beach hibiscus and citrus plants best matched with that of the *B. yothersi* holotype (Beard et al., 2015) but showed several inconsistencies. The main differences were observed in the size or the form of the following structures: microplates, reticulation in the dorsal (propodosoma, the area between c1-h1 and lateral areas) and ventral (ventral and genital plates) regions, and palp femorogenu setae.

Based on these data, these individuals were tentatively described as *B.* aff. *yothersi*. Further work will be carried out using genetic markers in order to define whether these mites represent a morphotype of *B. yothersi* or a new species within the genus *Brevipalpus*. Moreover,

because the two types of mites were unintentionally used during the experimental transmission of CiCSV, whether one or both kinds vector CiCSV is a point to be investigated. Recently, molecular characterization of *Brevipalpus* mites collected in sweet orange orchards in Mexico and Brazil revealed the existence of a greater genetic diversity within *Brevipalpus* populations than previously described (Sanchez-Velázquez et al., 2015). Similarly, the failed attempt to characterize all of the diversity of CiCSV-associated mite pecies launches a novel challenge whose answer will be a further step aimed at the comprehension of the diversity of *Brevipalpus* mites and their interaction with the transmitted viruses.

5.5 CONCLUSIONS

Identification and characterization of CiCSV have expanded our knowledge about the novel genus *Dichorhavirus* and have raised important questions regarding the taxonomy criteria to assign new species to it. Moreover, the existence of *Brevipalpus* mites whose morphology does not perfectly match with any of the anatomical descriptions from known species of its genus has been revealed. In our opinion, these two subjects and the growing diversity of viral species causing CL-like symptoms as well need to be highlighted and carefully debated in future work based on novel findings. In this sense, our laboratory is currently processing data involving new infections putatively caused by uncharacterized dichorhaviruses and *Brevipalpus* mites associated with them. Their analyses will shed light concerning this important issue.

REFERENCES

Afonso, C. L., Amarasinghe, G. K., Bányai, K., Bào, Y., Basler, C. F., Bavari, S., et al. (2016). Taxonomy of the order *Mononegavirales*: update 2016. *Arch. Virol.* 161, 2351–60. doi:10.1007/s00705-016-2880-1.

Arena, G. D., Ramos-González, P. L., Nunes, M. A., Alves, M. R., Camargo, L. E. A., Kitajima, E. W., et al. (2016). Citrus leprosis virus C infection results in hypersensitive-like response, suppression of the JA/ET plant defense pathway and promotion of the colonization of its mite vector. *Front. Plant Sci.* 7, 1757. doi:10.3389/FPLS.2016.01757.

Bankevich, A., Nurk, S., Antipov, D., Gurevich, A. A., Dvorkin, M., Kulikov, A. S., et al. (2012). SPAdes: A new genome assembly algorithm and its applications to single-cell sequencing. *J. Comput. Biol.* 19, 455–477. doi:10.1089/cmb.2012.0021.

Bastianel, M., Novelli, V. M., Kitajima, E. W., Kubo, K. S., Bassanezi, R. B., Machado, M. A., et al. (2010). Citrus Leprosis: Centennial of an unusual mite–virus pathosystem. *Plant Dis.* 94, 284–292. doi:10.1094/PDIS-94-3-0284.

Beard, J. J., Ochoa, R., Braswell, W. E., and Bauchan, G. R. (2015). *Brevipalpus phoenicis* (Geijskes) species complex (Acari: Tenuipalpidae)-a closer look. *Zootaxa* 3944, 1–67. Available at: http://www.ncbi.nlm.nih.gov/pubmed/25947538 [Accessed June 30, 2015].

Beard, J., Ochoa, R., Bauchan, G., Trice, T., Redford, A., Walters, T., et al. (2013). Flat mites

of the world. http://idtools.org/id/mites/flatmites/.

Chagas, C. M. M., Kitajima, E. W. W., and Rodrigues, J. C. V. C. V (2003). Coffee ringspot virus vectored by *Brevipalpus phoenicis* (Acari: Tenuipalpidae) in Coffee. *Exp. Appl. Acarol.* 30, 203–213. doi:10.1023/B:APPA.0000006549.87310.41.

Childers, C. C., Rodrigues, J. C. V., and Welbourn, W. C. (2003). Host plants of *Brevipalpus californicus*, *B. obovatus*, and *B. phoenicis* (Acari: Tenuipalpidae) and their potential involvement in the spread of viral diseases vectored by these mites. *Exp. Appl. Acarol.* 30, 29–105. doi:10.1023/B:APPA.0000006544.10072.01.

Cruz-Jaramillo, J. L., Ruiz-Medrano, R., Rojas-Morales, L., López-Buenfil, J. A., Morales-Galván, O., Chavarín-Palacio, C., et al. (2014). Characterization of a proposed dichorhavirus associated with the citrus leprosis disease and analysis of the host response. *Viruses* 6, 2602–22. doi:10.3390/v6072602.

Dietzgen, R. G., Kondo, H., Goodin, M. M., Kurath, G., and Vasilakis, N. (2017). The family *Rhabdoviridae*: mono- and bipartite negative-sense RNA viruses with diverse genome organization and common evolutionary origins. *Virus Res.* 227, 158–170. doi:10.1016/j.virusres.2016.10.010.

Dietzgen, R. G., Kuhn, J. H., Clawson, A. N., Freitas-Astúa, J., Goodin, M. M., Kitajima, E. W., et al. (2014). Dichorhavirus: a proposed new genus for *Brevipalpus* mite-transmitted, nuclear, bacilliform, bipartite, negative-strand RNA plant viruses. *Arch. Virol.* 159, 607–19. doi:10.1007/s00705-013-1834-0.

García-Escamilla, P., Duran-Trujillo, Y., Otero-Colina, G., Valdovinos-Ponce, G., Santillán-Galicia, M. T., Ortiz-García, C. F., et al. (2017). Transmission of viruses associated with cytoplasmic and nuclear leprosis symptoms by *Brevipalpus yothersi* and *B. californicus*. *Trop. Plant Pathol.* 43, 69–77. doi:10.1007/s40858-017-0195-8.

Grabherr, M. G. ., Brian J. Haas, Moran Yassour Joshua Z. Levin, Dawn A. Thompson, Ido Amit, Xian Adiconis, Lin Fan, Raktima Raychowdhury, Qiandong Zeng, Zehua Chen, Evan Mauceli, Nir Hacohen, Andreas Gnirke, Nicholas Rhind, Federica di Palma, Bruce W., N., Friedman, Regev, A., and Friedman, and A. R. (2013). Trinity: reconstructing a full-length transcriptome without a genome from RNA-Seq data. *Nat. Biotechnol.* 29, 644–652. doi:10.1038/nbt.1883.Trinity.

Guillermo, L. M., Roy, A., Choudhary, N., and Brlansky, R. (2017). Transmisión de leprosis de los cítricos por ácaros *Brevipalpus yothersi* a través de hospederos no cítricos. *Corpoica Cienc. y Tecnol. Agropecu.* 18, 307–319. doi:10.21930/rcta.vol18_num2_art:633.

Hartung, J. S., Roy, A., Fu, S., Shao, J., Schneider, W. L., and Brlansky, R. H. (2015). History and diversity of citrus leprosis virus recorded in herbarium specimens. *Phytopathology* 105, 1277–84. doi:10.1094/PHYTO-03-15-0064-R.

Kearse, M., Moir, R., Wilson, A., Stones-havas, S., Cheung, M., Sturrock, S., et al. (2012). Geneious Basic : An integrated and extendable desktop software platform for the organization and analysis of sequence data. *Bioinformatics* 28, 1647–1649. doi:10.1093/bioinformatics/bts199.

Kitajima, E. W., and Alberti, G. (2014). Anatomy and fine structure of *Bevipalpus* mites (Tenuipalpidae) – Economically important plant virus vectors. Part 7. Ultrastructural detection of cytoplasmic and nuclear types of *Brevipalpus* transmitted viruses. *Zoologica* 160, 174–192.

Kitajima, E. W., Chagas, C. M., Braghini, M. T., Fazuoli, L. C., Locali-Fabris, E. C., and

Salaroli, R. B. (2011). Natural infection of several *Coffea* species and hybrids and *Psilanthus ebracteolatus* by the coffee ringspot virus (CoRSV). *Sci. Agric.* 68, 503–507. doi:10.1590/S0103-90162011000400017.

Kitajima, E. W., Chagas, C. M., and Rodrigues, J. C. V (2003). *Brevipalpus*-transmitted plant virus and virus-like diseases: cytopathology and some recent cases. *Exp. Appl. Acarol.* 30, 135–60.

Kitajima, E. W., Müller, G. W., Costa, A. S., and Yuki, W. (1972). Short, rod-like particles associated with Citrus leprosis. *Virology* 50, 254–8.

Kitajima, E. W., and Nome, C. F. (1999). "Microscopia eletrônica em virologia vegetal," in *Métodos para detectar patógenos sistémicos*, eds. D. M. Docampo and S. L. Lenardón (Córdoba: IFFIVE/INTA-JICA), 59–87.

Kondo, H., Chiba, S., Andika, I. B., Maruyama, K., Tamada, T., and Suzuki, N. (2013). Orchid fleck virus structural proteins N and P form intranuclear viroplasm-like structures in the absence of viral infection. *J. Virol.* 87, 7423–34. doi:10.1128/JVI.00270-13.

Kondo, H., Hirota, K., Maruyama, K., Andika, I. B., and Suzuki, N. (2017). A possible occurrence of genome reassortment among bipartite rhabdoviruses. *Virology* 508, 18–25. doi:10.1016/j.virol.2017.04.027.

Kondo, H., Maeda, T., and Tamada, T. (2003). Orchid fleck virus: *Brevipalpus californicus* mite transmission, biological properties and genome structure. *Exp. Appl. Acarol.* 30, 215–223. Available at: http://www.ncbi.nlm.nih.gov/pubmed/14756418 [Accessed July 25, 2016].

Kosugi, S., Hasebe, M., Tomita, M., and Yanagawa, H. (2009). Systematic identification of cell cycle-dependent yeast nucleocytoplasmic shuttling proteins by prediction of composite motifs. *Proc. Natl. Acad. Sci. U. S. A.* 106, 10171–6. doi:10.1073/pnas.0900604106.

Kwak, H. R., Lee, Y. J., Kim, J. S. J., Kim, M. K., Kim, J. S. J., Choi, H. S., et al. (2016). A determinant of disease symptom severity is located in RNA2 of broad bean wilt virus 2. *Virus Res.* 211, 25–28. doi:10.1016/j.virusres.2015.09.018.

la Cour, T., Kiemer, L., Mølgaard, A., Gupta, R., Skriver, K., and Brunak, S. (2004). Analysis and prediction of leucine-rich nuclear export signals. *Protein Eng. Des. Sel.* 17, 527–36. doi:10.1093/protein/gzh062.

Locali-Fabris, E. C., Freitas-Astúa, J., and Machado, M. A. (2012). "Genus *Cilevirus*. International Committee on Taxonomy of Viruses," in *Virus Taxonomy*, eds. A. King, M. Adams, E. Carstens, and E. Lefkowitz (London, United Kingdom: Elsevier/Avademic Press), 1139–1142.

Locali-Fabris, E. C., Freitas-Astúa, J., Souza, A. A., Takita, M. A., Astúa-Monge, G., Antonioli-Luizon, R., et al. (2006). Complete nucleotide sequence, genomic organization and phylogenetic analysis of citrus leprosis virus cytoplasmic type. *J. Gen. Virol.* 87, 2721–9. doi:10.1099/vir.0.82038-0.

Melzer, M. J., Sether, D. M., Borth, W. B., and Hu, J. S. (2013). Characterization of a virus infecting *Citrus volkameriana* with citrus leprosis-like symptoms. *Phytopathology* 102, 122–7. doi:10.1094/PHYTO-01-11-0013.

Navia, D., Mendonça, R. S., Ferragut, F., Miranda, L. C., Trincado, R. C., Michaux, J., et al. (2013). Cryptic diversity in *Brevipalpus* mites (Tenuipalpidae). *Zool. Scr.* 42, 406–426. doi:10.1111/zsc.12013.

Nunes, M. A., de Carvalho Mineiro, J. L., Rogerio, L. A., Ferreira, L. M., Tassi, A., Novelli, V. M., et al. (2018). First Report of *Brevipalpus papayensis* as Vector of *Coffee ringspot virus* and *Citrus leprosis virus C*. *Plant Dis.* 102, 1046–1046. doi:10.1094/PDIS-07-17-1000-PDN.

Petersen, T. N., Brunak, S., von Heijne, G., and Nielsen, H. (2011). SignalP 4.0: discriminating signal peptides from transmembrane regions. *Nat. Methods* 8, 785–6. doi:10.1038/nmeth.1701.

Prasch, C. M., and Sonnewald, U. (2013). Simultaneous Application of heat, drought, and virus to arabidopsis plants reveals significant shifts in signaling networks. *Plant Physiol.* 162, 1849–1866. doi:10.1104/pp.113.221044.

Ramalho, T. O., Figueira, A. R., Sotero, A. J., Wang, R., Geraldino Duarte, P. S., Farman, M., et al. (2014). Characterization of Coffee ringspot virus-Lavras: a model for an emerging threat to coffee production and quality. *Virology* 464–465, 385–96. doi:10.1016/j.virol.2014.07.031.

Ramos-González, P. L., Chabi-Jesus, C., Guerra-Peraza, O., Breton, M. C., Arena, G. D. G. D. G. D., Nunes, M. A. M. A., et al. (2016). Phylogenetic and molecular variability studies reveal a new genetic clade of Citrus leprosis virus C. *Viruses* 8, 153. doi:10.3390/v8060153.

Ramos-González, P. L., Chabi-Jesus, C., Guerra-Peraza, O., Tassi, A. D., Kitajima, E. W., Harakava, R., et al. (2017). Citrus leprosis virus N: a new dichorhavirus causing citrus leprosis disease. *Phytopathology*, 1–48. doi:10.1094/PHYTO-02-17-0042-R.

Rodrigues, J. C. V, Kitajima, E. W., Childers, C. C., and Chagas, C. M. (2003). Citrus leprosis virus vectored by *Brevipalpus phoenicis* (Acari: Tenuipalpidae) on citrus in Brazil. *Exp. Appl. Acarol.* 30, 161–79. Available at: http://www.ncbi.nlm.nih.gov/pubmed/14756415 [Accessed January 13, 2017].

Roy, A., Hartung, J. S., Schneider, W. L., Shao, J., Leon M, G., Melzer, M. J., et al. (2015a). Role bending: Complex relationships between viruses, hosts, and vectors related to citrus leprosis, an emerging disease. *Phytopathology* 105, 872–884. doi:10.1094/PHYTO-12-14-0375-FI.

Roy, A., Leon, M. G., Stone, A. L., Schneider, W. L., Hartung, J., and Brlansky, R. H. (2014). First report of citrus leprosis virus nuclear type in sweet orange in Colombia. *Plant Dis.* 98, 1162. doi:10.1094/PDIS-02-14-0117-PDN.

Roy, A., Shao, J., Hartung, J. S., Schneider, W., and Brlansky, R. (2013a). A case study on discovery of novel citrus leprosis virus cytoplasmic type 2 utilizing small rna libraries by next generation sequencing and bioinformatic analyses. *J. Datamining Genomics Proteomics* 4.

Roy, A., Stone, A. L., Shao, J., Otero-Colina, G., Wei, G., Choudhary, N., et al. (2015b). Identification and molecular characterization of nuclear citrus leprosis virus, a member of the proposed *Dichorhavirus* genus infecting multiple citrus species in Mexico. *Phytopathology* 105, 564–75. doi:10.1094/PHYTO-09-14-0245-R.

Roy, A., Stone, A., Otero-Colina, G., Wei, G., Choudhary, N., Achor, D., et al. (2013b). Genome assembly of citrus leprosis virus Nuclear type reveals a close association with orchid fleck virus. *Genome Announc.* 1, e00519-13-e00519-13. doi:10.1128/genomeA.00519-13.

Sánchez-Velázquez, E. J., Santillán-Galicia, M. T., Novelli, V. M., Nunes, M. A., Mora-

Aguilera, G., Valdez-Carrasco, J. M., et al. (2015). Diversity and genetic variation among *Brevipalpus* populations from Brazil and Mexico. *PLoS One* 10, e0133861. doi:10.1371/journal.pone.0133861.

Tassi, A. D., Garita-Salazar, L. C., Amorim, L., Novelli, V. M., Freitas-Astúa, J., Childers, C. C., et al. (2017). Virus-vector relationship in the Citrus leprosis pathosystem. *Exp. Appl. Acarol.* 71, 227–241. doi:10.1007/s10493-017-0123-0.

Untergasser, A., Cutcutache, I., Koressaar, T., Ye, J., Faircloth, B. C., Remm, M., et al. (2012). Primer3-new capabilities and interfaces. *Nucleic Acids Res.* 40, e115. doi:10.1093/nar/gks596.

Walker, P. J. P., Firth, C., Widen, S. S. G., Blasdell, K. R. K., Guzman, H., Wood, T. T. G., et al. (2015). Evolution of Genome Size and Complexity in the *Rhabdoviridae*. *PLOS Pathog.* 11, e1004664. doi:10.1371/journal.ppat.1004664.

ANNEX I

Supplementary Table 1. List of primers for the detection of known cileviruses and dichorhaviruses.

Virus	Primer sequence (5'-3')	Reference
CiLV-C	*MP*-F: GCGTATTGGCGTTGGATTTCTGAC *MP*-R: TGTATACCAAGCCGCCTGTGAACT	(Locali et al., 2003)
CiLV-C2	*p29*-F: ATGAGTAACATTGTGTCGTTTTCGTTGT *p29*-R: TCACTCTTCCTGTTCATCAACCTGTT	(Roy et al., 2013a)
OFV	*N*-F: TGTCATAGCCGACATAAACACC *N*-R: TGTAGAGCTTGCGAGATACAGG	(Kubo et al., 2009)
OFV and OFV-citrus	*L*dF: CCYGTGAGAGAATTCYTGGATG *L*dR: CCAGATTGGTGTARCCRAACAG	(Ramos-González et al., 2015)
OFV-citrus	*N*-F: ATGGCTAACCCAAGTGAGATCGATTA *N*-R: AGTTGCCTTGAGATCATCACATTGGT *M*-F: ATGTCTAAACAGATTAATATGTGCACTGTG *M*-R: CTAACCACTGGGTCCCGC	(Roy et al., 2014)
CiLV-N	*N*-DC-F: CCGTACCCATTGTGAAAATA *N*-DC-R:GAACCCCTTTGAGGAATG	(Ramos-González et al., 2017)

Supplementary Table 2. List of primers for the secondary sequencing and RACE (Rapid Amplification of cDNA Ends) of the genome of citrus chlorotic spot virus (CiCSV).

Primer sequence (5′−3′)	Direction[1]	Target region[2]	Amplicon size (bp)
RNA1			
TACGCAGATGTCGACTACAC	F	244-263	941
CAGTACCTCCAGAACCTGTC	R	1165-1184	
GAGAGGTCTTCCTCTGCTG	F	1044-1062	933
CGGAGTATTTACGGGATATT	R	1957-1976	
GTCCCAGGTTCAACAAGA	F	1834-1851	950
GCCCTGAAACAACTGAAG	R	2766-2785	
CTCAGCAGGAATAAATGACA	F	2635-2654	944
GCACACCTGTGTAAAGGAT	R	3560-3578	
GACCAACCTGTCTGAGATTG	F	3430-3449	930
GTTGAAATTCCCACAGATG	R	4341-4359	
CCTTGAATGTCAAAGACAAC	F	4221-4240	933
GATTCCGCTCACATGATTA	R	5135-5153	
TATCGGAGTCCATATCACC	F	5005-5023	948
CGAACAGTTGCTTGACTG	R	5935-5952	
CCTCCTCTTCTAGCGTCAT	F	5809-5827	500
CTGTTTTGCCCATGCTAC	R	6291-6308	
RNA2			
CACATCATATACTGAAACAAACC	F	191-213	933
TCAAACTGAGCTCCCAAT	R	1106-1123	
AGTTTCGAGGCTCTATGTGT	F	1005-1024	920
CTCTTGGATGAGGTCTGC	R	1907-1924	
TCAAGATGAGGCTCTACTTTAC	F	1777-1798	941
ATGCGTTTGTCCAATGAC	R	2700-2716	
CACGATCTCATCTGCAGTC	F	2579-2597	940
ATAGTTGTGGTCGCAGTCAT	R	3499-3518	

GACTTGACTCCCTCAGCTT	F	3372-3390	949
ACCACATTGTGATGCTACTG	R	4301-4320	
GGCAGATGATAGAATTGTGA	F	4178-4197	942
GACATCTCCTCACTCATGG	R	5101-5119	
ACGAGGGGAACCATATTAG	F	4971-4989	891
TAGACCGCATGTTTTGATTA	R	5842-5861	
RNA1 3' RACE. *N* gene specific primer and nested *N* gene specific primer			
GATTACGCCAAGCTTGACAGTGGCTGGACCACAG CTCCT	F	-	546
GTGTGAGGCAGAATCCAA	F	486-502	
RNA1 5' RACE. *G* gene specific primer and nested *G* gene specific primer			
GATTACGCCAAGCTTCATTGGTGAGACCGCTGGTT GTATGCG	R	-	843
CCTCCTCTTCTAGCGTCAT	R	5809-5827	
RNA2 3' RACE. *L* gene specific primer and nested *L* gene specific primer			
GATTACGCCAAGCTTCATCACAAGCGGCAGCTCCT CCTC	R	-	524
CCAACATATCCTCATCCT	R	481-498	
RNA2 5' RACE. *L* gene specific primer and nested *L* gene specific primer			
GATTACGCCAAGCTTGAGGATGGGGCAACTTCCA ATCCCTG	F	-	647
CACATGTGAGTCAAGTCAAG	F	5395-5414	

ANNEX II

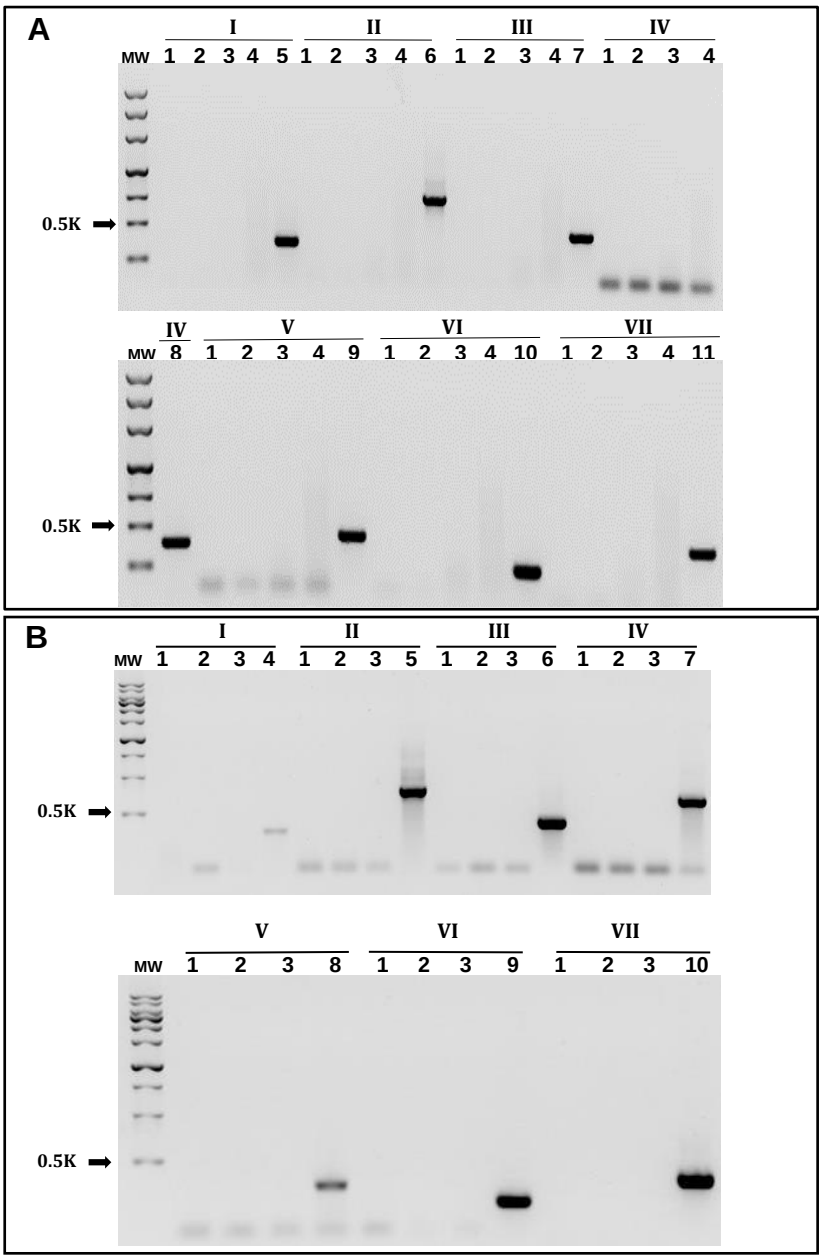

Supplementary Figure 1. 1% agarose gel electrophoresis of RT-PCR products for the detection of citrus leprosis associated viruses. Each RNA sample was analyzed with seven primer pairs, six of which are specific for the detection of the cileviruses: CiLV-C (I: *MP* gene) and CiLV-C2 (II: *p29* gene); and the dichorhaviruses: CiLV-N (III: *N* gene), OFV-citrus (IV: *N* gene), OFV (V: *N* gene), ClCSV (VI: *L* gene) and one pair is generic for detection of dichorhavirus-causing CL (VII: degenerate primer pair for the detection of *L* gene). **A**. MW: Molecular weight marker, M1121 Ladder (Sinapse Biotechnology, Brazil). Lane 1: Reverse-transcription blank; 2: PCR blank; 3 and 4: Chlorotic lesions from two sweet orange trees, respectively, Teresina, PI; 5: CiLV-C-infected citrus tree, Guaimbe, SP; 6: CiLV-C2-infected citrus tree, Colombia; 7 and 11: CiLV-N-infected citrus tree, São Roque, SP; 8: OFV-citrus-infected citrus tree, Mexico; 9: OFV-infected orchid plant, Piracicaba, SP; 10: ClCSV-infected clerodendrum plant, Piracicaba, SP. **B**. MW: Molecular weight marker, M1181 Ladder (Sinapse Biotechnology). Lane 1: Reverse-transcription blank; 2: PCR blank; 3: Leaf chlorotic area from beach hibiscus collected in Teresina, PI; 4: CiLV-C-infected citrus tree, Guaimbe, SP; 5: CiLV-C2-infected citrus tree, Colombia; 6 and 10: CiLV-N-infected citrus tree, Ibiuna, SP; 7: OFV-citrus-infected citrus tree, Mexico; 8: OFV infected orchid plant, Piracicaba, SP; 9: ClCSV-infected *Clerodendrum* plant, Piracicaba, SP.

APPENDIX I

First report of citrus chlorotic spot virus infecting the succulent plant *Agave desmettiana*

Published

Chabi-Jesus, Camila; Ramos-González, Pedro; Tassi, Aline D.; Barguil, Beatriz M. Beserra Jr., Jose Evando Aguiar; Harakava, Ricardo; Kitajima, Elliot W.; Freitas-Astúa, Juliana. First report of citrus chlorotic spot virus infecting the succulent plant *Agave desmettiana*. **Plant Disease Note**, v.103, p.1438-1438, 2019. https://doi.org/10.1094/PDIS-09-18-1617-PDN.

First Report of Citrus Chlorotic Spot Virus Infecting the Succulent Plant *Agave desmettiana*

Authors and Affiliations

C. Chabi-Jesus, Escola Superior de Agricultura "Luiz de Queiroz"/USP, Piracicaba, SP, Brazil and Instituto Biológico, SP, Brazil; **P. L. Ramos-González**, Instituto Biológico, SP, Brazil; **A. D. Tassi**,
Escola Superior de Agricultura "Luiz de Queiroz"/USP, Piracicaba, SP, Brazil; **B. M. Barguil**, Universidade Estadual do Piauí, Teresina, Piauí, Brazil; **J. E. A. Beserra Jr**, Universidade Federal do Piauí, Teresina, Piauí, Brazil; **R. Harakava**, Instituto Biológico, SP, Brazil; **E. W. Kitajima**, Escola Superior de Agricultura "Luiz de Queiroz"/USP, Piracicaba, SP, Brazil; **J. Freitas-Astúa**, Embrapa Mandioca e Fruticultura, Cruz das Almas, Bahia, Brazil and Instituto Biológico, SP, Brazil.

Published Online:2 Apr 2019 https://doi.org/10.1094/PDIS-09-18-1617-PDN

Endemic in the Americas, citrus leprosis (CL) is a viral disease that reduces yields and threatens the sustainability of citrus orchards. The disease is caused by a heterogeneous group of ssRNA viruses assigned to the genera *Dichorhavirus* (family *Rhabdoviridae,* order *Mononegavirales*) or *Cilevirus* (unassigned genus) (Freitas-Astúa et al. 2018). The typical dichorhavirus genome encompasses two (-)ssRNA molecules that encode six ORFs (Dietzgen et al. 2018). Isolates of the tentative dichorhavirus citrus chlorotic spot virus (CiCSV) were previously identified in Teresina, Piauí, Brazil (Chabi-Jesus et al. 2018). Besides affecting sweet orange (*Citrus sinensis*) trees producing symptoms resembling early lesions of a typical CL, CiCSV also infects beach hibiscus (*Taliparitі tiliaceum* syn. *Hibiscus tiliaceus* L.) plants. In 2018, a dozen of the ornamental *Agave desmettiana* Jacob plants (*Agavaceae*) showing chlorotic lesions were detected in the urban region of Teresina city within an area of approx. 30 km^2 including the region where the original CiCSV-infected plants have been described. Analyses of symptomatic agaves' tissues by transmission electron microscopy revealed the presence of viroplasms in the nucleus of the infected parenchymal cells, as a typical dichorhavirus infection (Dietzgen et al. 2018). Moreover, eight mites that were collected during the examination of the symptomatic leaves were morphologically identified as *Brevipalpus* aff. *yothersi,* the same species found in CiCSV-infected citrus (Chabi-Jesus et al. 2018). Total RNA from leaf lesions of three symptomatic agave plants (isolates Trs4, -5 and -6) were extracted using TRIzol Reagent (Life Technologies, Foster City, CA, USA), and the RT-PCR assays performed using all of the primer pairs available for the detection of known dichorhaviruses (Dietzgen et al. 2018) proved the presence of CiCSV. Additionally, the same RNA extracts reacted with a Digoxigenin-labeled probe derived from the *N* gene of CiCSV_Trs1 in a RNA dot-blot assay (Roche Diagnostics GmbH, Mannheim, Germany). Ninetyfive percent of the isolate Trs4´s genome was recovered after the Sanger sequencing of the overlapping amplicons generated by using 15 primers pairs (Chabi-Jesus et al. 2018). Globally, RNA1 (6082 nt, GB: MH595621) and RNA2 (5688 nt, MH595622) shows 96.4% nucleotide sequence identity with the type virus CiCSV_Trs1 (KY700685 and KY700686), and less than 75% nucleotide sequence identity with the dichorhaviruses orchid fleck virus (OFV; AB244417 and AB244418), coffee ringspot virus (CoRSV; KF812525 and KF812526), citrus leprosis virus N (CiLVN; KX982176 and KX982179) and Clerodendrum chlorotic spot virus (ClCSV; MG938506 and
MG938507). Comparisons of the deduced amino acid sequences of the putative proteins N, P,

MP, M, G, and L (encoded by ORFs 1-6, respectively) of CiCSV_Trs4 show 95–99% identity with CiCSV_Trs1 and 28-90% identity with OFV, CoRSV, CiLV-N, and ClCSV. Sequences of the generated amplicons corresponding to *G* and *L* genes from the isolates Trs5 and Trs6 (MH802037, MH802038, MH802039 and MH802040, respectively) showed >93% nucleotide sequence identity with CiCSV_Trs1 (KY700685 and KY700686) and with isolate Trs4. Comprehensively, results indicate that CiCSV_Trs4, -5 and -6 are isolates of the tentative species citrus chlorotic spot virus of the genus *Dichorhavirus,* whose transmission has been previously associated with the mite *B.* aff. *yothersi*. This is the first report of CiCSV naturally infecting the succulent plant *A. desmettiana* and, to our knowledge, it is also the first report of a (-)ssRNA virus infecting plants of this genus.

SUPPORT: FAPESP scholarship 2016/01960-6, FAPESP grants 2014/08458-9, 2017/50222-0 and 2017/50334-3, and CAPES scholarship PNPD20132154 - 33141010001P4.

REFERENCES

Chabi-Jesus et al. 2018. Plant Dis., 102, 8, 1588-1598, DOI : 10.1094/PDIS-09-17-1425-RE.
Dietzgen et al. 2018. Advances in Virus Research, DOI: 10.1016/bs.aivir.2018.06.001.
Freitas-Astúa et al. 2018. Current Opinion in Virology, 33, 66-73, DOI: 10.1016 5710.1016/j.coviro.2018.07.010.

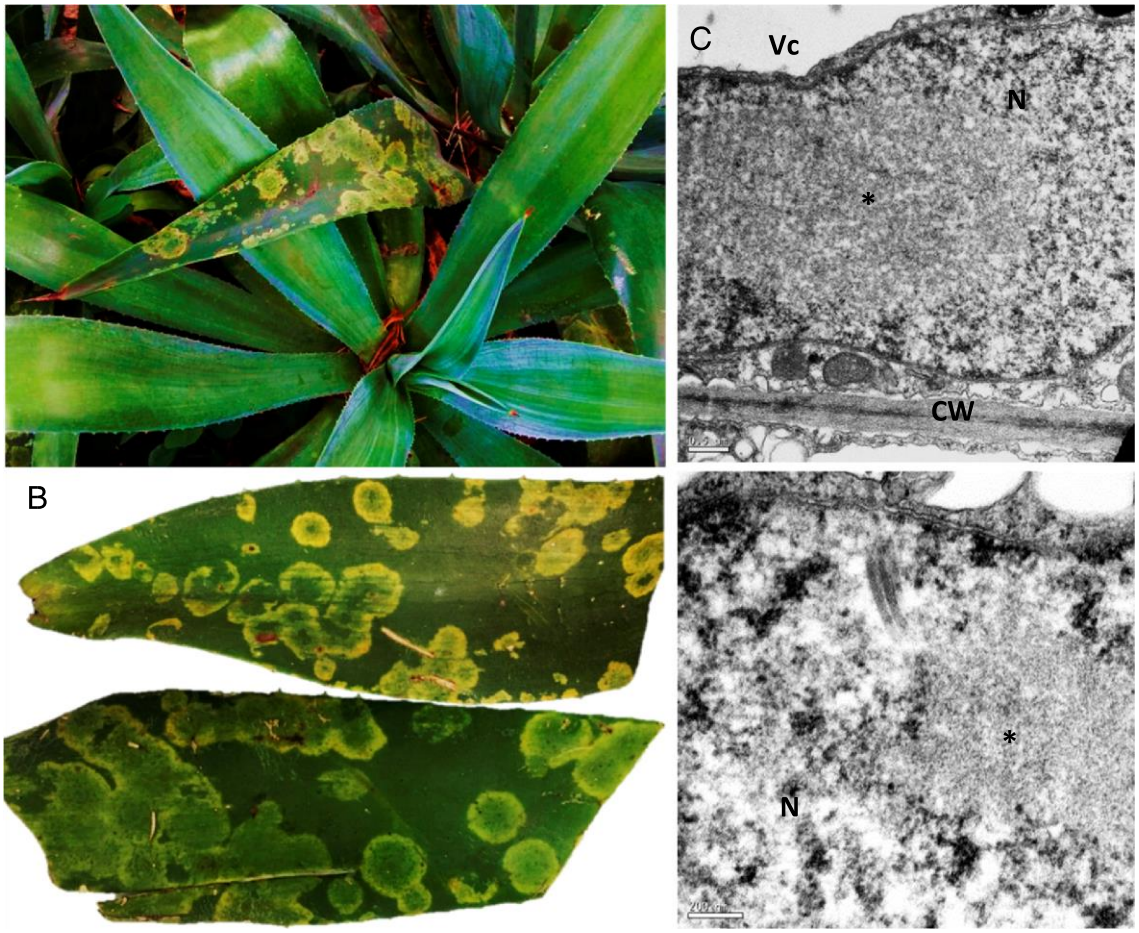

Supplementary Figure S1. **A** and **B**. Localized chlorotic symptoms in *Agave desmettiana* leaves infected with citrus chlorotic spot virus (CiCSV) collected in Teresina, State of Piau´ı, Brazil, 2018; C and D. Transmission electron micrographs of thin sections from lesions; C. Parenchymal cell showing a nucleus with electron lucent viroplasm (*); D. Similar to C, with the presence of viroplasm (*) in the nucleus (N). Nuclear envelope (NE), cell wall (CW), mitochondrion (M) and vacuole (Vc).

Supplementary Figure S2. Differential interference contrast (DIC) micrographs showing the diagnostic characters of a female *Brevipalpus* aff. *yothers*i mite found in symptomatic *Agave desmettiana* plants infected with the dichorhavirus citrus chlorotic spot virus. **A**. Oval spermatheca vesicle with a distal stipe; **B**. Ventral cuticle between coxae II-IV, genital and ventral plates with typical reticulation pattern; **C**. Dorsal overview showing the propodosomal and opisthosomal cuticle.

6. CHAPTER 4

GENOMIC ANALYSIS OF A NEW DICHORHAVIRUS ASSOCIATED WITH CITRUS LEPROSIS DISEASE SUPPORTS THE HYPOTHESIS LINKING THE DICHORAVIRUS PHYLOGENETIC GROUPS, THEIR MITE VECTORS, AND THEIR GEOGRAPHIC DISTRIBUTION

ABSTRACT

Citrus leprosis disease (CL) is the main viral disease affecting the Brazilian citriculture. Currently, three CL-associated dichorhaviruses have been described: orchid fleck virus (OFV), citrus leprosis virus N (CiLV-N) and citrus chlorotic spot virus (CiCSV). Recently, sweet orange trees (*Citrus sinensis*) showing leaves with characteristic necrotic and bright chlorotic symptoms of CL were identified in the states of Santa Catarina and Rio Grande do Sul, Southern region of Brazil. Transmission electron microscopy analyses of symptomatic tissues confirmed the presence of bacilliform particles with ~40x100 nm and viroplasm in the nucleus of infected cells. RNA extracts from two of the sampled plants that proved negative by RT-PCR for the detection of all known CL-causing viruses were analyzed by HTS. The complete genomes revealed viruses composed of ~13,000 nts each one, split into two molecules and with typical organizations of those found in known dichorhaviruses. Globally, the genomes of the two new isolates share 98-99% nucleotide sequence identity between them. In the comparison with the definitive and tentative members of the genus *Dichorhavirus* CiLV-N, OFV, CiCSV, coffee ring spot virus, and *Clerodendrum* chlorotic spot virus, the new viruses showed 72%, 57%, 60%, 59%, and 60% nucleotide sequence identity, respectively. These identity values are below the criteria for the demarcation of new species within the genus *Dichorhavirus* (< 80% RNA1 and <80% ORF *L*). Therefore, according to the symptoms observed in the infected plants, the morphology of the virions, the structure of the genome, and the nucleotide sequence identity with other dichorhaviruses, the two isolates were considered as members of a tentative new species of the genus *Dichorhavirus*, and the name citrus bright spot virus is suggested. Here, we report the first characterized dichorhavirus associated with citrus leprosis in Southern Brazil.

Keywords: *Mononegavirales*; *Rhabdoviridae*; Bright spot

6.1 INTRODUCTION

Dichorhaviruses are recently-described plant viruses belonging to the family *Rhabdoviridae* (Dietzgen et al., 2014, 2017, 2018). The genus *Dichorhavirus*, despite showing a bipartite genome [(-)ssRNA], belongs to the Order *Mononegavirales*, characterized by the monopartite genomes of their members (Dietzgen et al., 2014, 2018; Walker et al., 2015). The genome segmentation event of dichorhaviruses may be associated with the mite vectors of the genus *Brevipalpus* (Kondo et al., 2017; Dietzgen et al., 2018; Whitfield et al., 2018). Possibly, members of the genus *Dichorhavirus* have arthropod viruses as common ancestors, with the point of origin and diversification in South America (Dietzgen et al., 2018; Freitas-Astúa et al., 2018).

The predominant genome type in members of the family *Rhabdoviridae* is non-segmented, with five ORFs in a genetic arrangement "$^{3'}$-*N-P-M-G-L*-$^{5'}$" (Kuzmin et al., 2009; Walker et al., 2015; Amarasinghe et al., 2019). In dichorhaviruses, their genome comprise the same five ORFs and contain an additional gene for viral cell-to-cell movement, which was possibly acquired during the adaptation of rhabdoviruses to plant hosts (Dietzgen et al., 2018; Whitfield et al., 2018). The genome is subdivided into two (-)ssRNA molecules (Dietzgen et al., 2014, 2018). RNA1 (ca. 7 Kb) harbors five ORFs encoding the nucleocapsid protein (N), phosphoprotein (P), movement protein (MP), matrix protein (M), and glycoprotein (G). RNA2 (ca. 6 Kb) has a unique ORF that codes for the RNA-dependent RNA polymerase (*RdRp*), known as the L protein (Kondo et al., 2006; Dietzgen et al., 2018). All genes present in RNA 1 and RNA2, as well as the leader and trailer regions, are separated by conserved intergenic sequences containing predicted transcription start and stop signals (Dietzgen et al., 2018). Dichorhaviruses virions are non-enveloped and accumulate in the nucleus of host cells, forming structures known as spoke wheels (Kitajima et al., 1972, 2003; Dietzgen et al., 2018).

Orchid fleck virus (OFV) is the type member of genus *Dichorhavirus* (Kondo et al., 2006). Coffee ringspot virus (CoRSV), citrus leprosis virus N (CiLV-N), citrus chlorotic spot virus (CiCSV) and clerodendrum chlorotic spot virus (ClCSV) are the other dichorhaviruses characterized in the last five years (Ramalho et al., 2014; Ramos-González et al., 2017b, 2018; Chabi-Jesus et al., 2018). Cestrum nocturnum ringspot virus (CnRSV) is another tentative dichorhavirus that has not been completely characterized (Kitajima et al., 2010). In the past two years, three out of five species of the genus have been identified in Brazil, and the increasing knowledge of their diversity supported the creation of new species demarcation criteria for the genus *Dichorhavirus* (Freitas-Astúa et al., 2018; Amarasinghe et al., 2019). According to the

International Committee on Taxonomy of Viruses (ICTV), the cut-off values for new species are 80% or less nucleotide identity in the RNA1 and *L* gene (ICTV, 2018).

Dichorhaviruses are persistently transmitted by *Brevipalpus* mites (Acari: Tenuipalpidae) (Dietzgen et al., 2018; Freitas-Astúa et al., 2018). In natural conditions, they are unable to systematically infect their plant hosts, causing lesions around the feeding site of the mite vector. However, under high temperatures (> 28ºC), systemic infection has been reported for CoRSV, OFV, and ClCSV (kondo et al., 1995; Kitajima et al., 2008; Ramalho et al., 2015) . OFV is transmitted by *B. californicus* to orchids and citrus (kondo et al., 1995; Kondo et al., 2003; García-Escamilla et al., 2017; Cook et al., 2019). In citrus, OFV strains cause citrus leprosis disease (CL) in Mexico, Colombia and South Africa (Cruz-Jaramillo et al., 2014; Roy et al., 2014; Cook et al., 2019). In Brazil, although CL is predominantly caused by citrus leprosis virus C (CiLV-C; genus *Cilevirus*), there is an increasing number of dichorhavirus associated with the disease (Freitas-Astúa et al., 2018). Even though OFV-citrus strain has not been reported in our conditions, there are currently two dichorhaviruses, CiLV-N and CiCSV, associated with CL-symptoms in Brazil. *Brevipalpus phoenicis* sensu stricto (s.s.) is the vector of CiLV-N, and both *B. yothersi* and *B.* aff. *yothersi* are associated with CiCSV transmission (Ramos-González et al., 2017; Chabi-Jesus et al., 2018, 2019).

In this work, we analyzed *Citrus sinensis* (sweet orange) trees showing typical symptoms of citrus leprosis disease (CL) in the Southern region of Brazil (Figure 1). Transmission electron microscopy (TEM) analyses of symptomatic tissues confirmed the presence of bacilliform particles and viroplasm in the nucleus of infected cells, and cytopathic effects typical similar to those caused by dichorhaviruses. However, RT-PCR assays were negative for all known CL-associated viruses. High throughput sequencing (HTS) from two infected sweet orange trees revealed the existence of two highly related viral isolates (>98%), but distinct from the other known dichorhaviruses. Based on our results, we suggest that theses viruses belong to a tentative new species of the genus *Dichorhavirus*, named it citrus bright spot virus (CiBSV). Here, we report for the first time a dichorhavirus associated with CL in Southern Brazil.

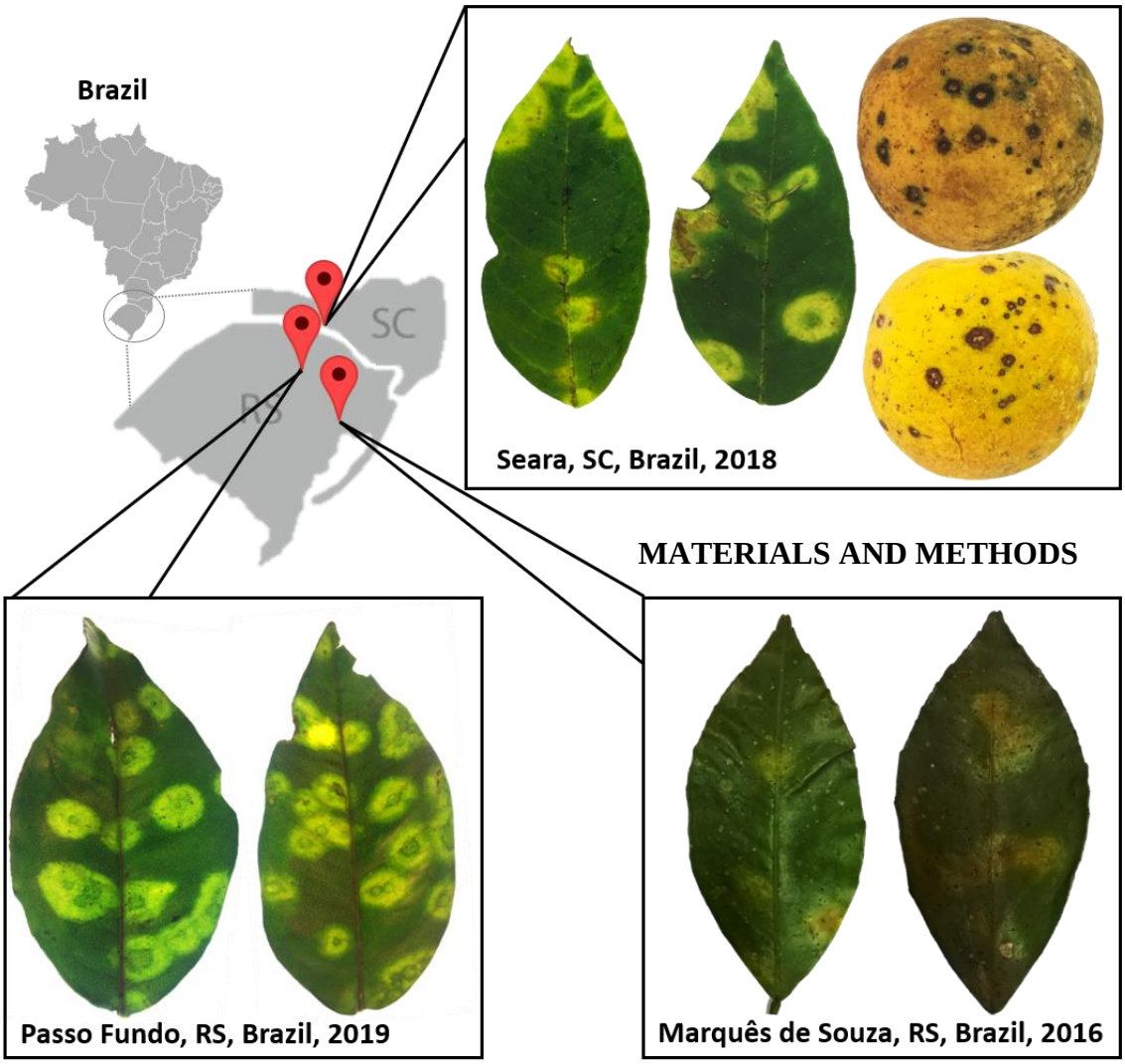

Figure 1- Chlorotic and necrotic symptoms in leaves and fruits of sweet orange (*Citrus sinensis*) collected in Seara (2018), state of Santa Catarina (SC), and Marquês de Souza (2016) and Passo Fundo (2019), state of Rio Grande do Sul (RS).

6.2 MATERIALS AND METHODS

6.2.1 Plant material and *Brevipalpus* mites

Sweet orange leaves exhibiting bright chlorotic lesions and rare necrosis, and fruits with necrotic symptoms, were identified in three municipalities of the Southern region of Brazil: Marquês de Souza (-29.207780° and -52.235307°) and Passo Fundo (-28.256698° and -52.483400°), state of Rio Grande do Sul, and Seara, state of Santa Catarina (-27.154776° and -52.305654°) (Figure 1). *Brevipalpus* mites found in the samples collected in the three municipalities were identified in the Laboratory of Electron Microscopy applied to Agricultural Research (NAP/MEPA) (ESALQ/USP, Piracicaba, SP, Brazil).

6.2.2 *Brevipalpus* mites identification

About 54 females of *Brevipalpus* spp. found in sweet orange trees collected in Marquês

de Souza/RS, Passo Fundo/RS and Seara/SC were analyzed by scanning electron microscopy (SEM) or mounted for light microscopy (LM). The protocol for the identification of mites was as previously described (Chabi-Jesus et al., 2018) and the taxonomic characteristics were evaluated following the morphological criteria established for the *B. phoenicis* sensu lato group (Beard et al., 2015).

6.2.3 Attempts to identify the causal agent

Ultrathin sections of symptomatic leaves of *Citrus sinensis* collected from Marquês de Souza, RS and Seara, SC were and analyzed by transmission electron microscopy (TEM), as previously described (Chabi-Jesus et al., 2018). Around 100mg of symptomatic plant tissue from each sample was macerated in the presence of liquid nitrogen and used for total RNA extraction using the Trizol protocol (Thermo Fisher Scientific, Madison, WI, USA). cDNAs were generated with RevertAid H Minus First-Strand cDNA Synthesis Kit (Thermo Scientific, Madison, WI, USA). The presence of CL-associated viruses was determined by PCR using cDNA solutions (3 µL), GoTaq G2 Master Mix Green kit (Promega, Madison, WI, USA), and specific primer pairs to detect all CL-associated viruses characterized so far (Table 1) (Kondo et al., 2006; Ramalho et al., 2014; Roy et al., 2014; Ramos-González et al., 2017; Chabi-Jesus et al., 2018) (Melzer et al., 2013; Roy et al., 2013b; Ramos-González et al., 2016).

Table 1. Primers list used for the detection viruses associated with citrus leprosis disease by RT-PCR

BTV		**Region**	**Sequence (5'-3')**	**Size (bp)**	**Reference**
genus	virus				
Dichorhavirus	**OFV**	*N*	F: TGTCATAGCCGACATAAACACC R: TGTAGAGCTTGCGAGATACAGG	326	(Kubo et al., 2009)
	CiLV-N	*N*	F: CCGTACCCATTGTGAAAATA R: GAACCCCTTTGAGGAATG	420	(Ramos-González et al., 2017b)
	OFV+CiLV-N	*L*	F2: CAASTGTCATGCCTGCATGG R2: TTGATRCATGATGCRAGRCTGTATG	362	
	CiCSV	*G*	8F: CTGTTTTGCCCATGCTAC 8R: CCTCCTCTTCTAGCGTCAT	500	(Chabi-Jesus et al., 2018)
	CoRSV	*L*	F: GGACCATGAGACAGGAGGTG R: CTCTGCCAGTCCTCAATGTG	394	(Kitajima et al., 2011)
	ClCSV	*L*	PLF: AGTGTACCGCCTCACAGAAG PLR: CGGGGTCTTGTTGTTCATAG		(Kubo et al., 2011)
Cilevirus	**CiLV-C**	*mp*	F: GCGTATTGGCGTTGGATTTCTGAC R: TGTATACCAAGCCGCCTGTGAACT	339	(Locali et al., 2003)
	CiLV-C2	*p29*	F: ATGAGTAACATTGTGTCGTTTTCGTTGT R: TCACTCTTCCTGTTCATCAACCTGTT	795	(Roy et al., 2013a)

6.2.4 High throughput sequencing and validation of genomic sequences

RNA extracts from samples collected in Marquês de Souza (MSa) and Seara (Ser) were used to set up libraries for the mRNA sequencing. Ribosomal RNA depletion, library construction, and Illumina sequencing were performed Laboratory of Animal Biotechnology (ESALQ/USP, Piracicaba, SP, Brazil). Reads of 80-90 nucleotide (k-mer 33-43-55) were assembled with SPAdes (Bankevich et al., 2012). Viral contigs were identified using the Basic Local Alignment Search Tool (BLASTx and BLASTn). Based on the identity and length of the contigs, the virus sequences were selected for assembly mapping to reference genomes with Bowtie2 (Langmead and Salzberg, 2012). After obtaining the *in silico* genomes, 25 primer pairs were designed along the genome (Supplementary Table 1, Annex I) with Geneious software (Kearse et al., 2012), aiming to validate the sequences and obtain their extremities. For validation of the genomic sequence, cDNA from both samples were used as templates for PCR amplification with the following amplification protocol: 94°C [3 min], (94°C [30 sec], 54°C [30 sec], 72°C [1 min and 20 sec]) × 35 cycles, 72°C [5 min], 4°C [10 min]. The fragments obtained by PCR were purified by Wizard® SV Gel and PCR Clean-Up System (Promega, Madison, WI, USA) and sequenced by the Sanger method. The 3 'and 5' ends of the genome of each isolate were obtained using the RACE 5'/3' method (Clontech Laboratories, Mountain View, CA, USA). The generated fragments were ligated in pGEM-T-easy vector (Promega, Madison, WI, USA), cloned using *Escherichia coli* DH10B and about five clones were used for the sequencing of each end. All sequences were analyzed in the Geneious software (Kearse et al., 2012). Similarity plots among genome sequences obtained in this study and those of dichorhaviruses available in the NCBI were generated using Simplot version 3.5.1 (LOLE et al., 1999).

6.2.5 Detection of recombination events

Recombination events were assessed using seven methods (RDP, GENECONV, Bootscan, Maxchi, Chimaera, SiScan, and Topal) implemented in the RDP version 5.5 (Martin et al., 2015). First, sequences were aligned using the MUSCLE software, implemented in Geneious software (Kearse et al., 2012). Recombination events detected by more than three programs implemented in the RDP version 5.5 were considered as presumed recombinants.

6.2.6 Phylogenetic analysis and detection of reassortment events

Alignments were performed using MUSCLE programs, implemented in the MEGA version 7.0.21 (Kumar et al., 2016). All dichorhavirus sequences available at the NCBI were retrieved

and incorporated in this analysis. The best models for nucleotide or amino acid substitutions, determined according to likelihood ratio tests in MEGA version 7.0.21 (Kumar et al., 2016), were as follow: GRT+G+I for RNA1 and RNA2, and JTT+G+I and LG+G+F for the amino acid sequences alignments of N protein and L protein, respectively. Phylogenetic trees were estimated by Bayesian inference using a variant of Markov Chains Monte MCM method (MCMC), with 6 million generations with MrBayes implemented in Geneious program (Kearse et al., 2012). The protein sequences of sonchus yellow net betanucleorhabdovirus (SYNV; GenBank accession number: NC001615.3) was used as an outgroup in the trees from protein sequences of dichorhaviruses. The trees were viewed and edited in iTOL (Letunic and Bork, 2007). From the topological comparison of the phylogenetic trees generated with sequences present in RNA1 and RNA2 reassortments events were estimated.

6.3 RESULTS AND DISCUSSION

Chlorotic and necrotic lesions observed in leaves and fruits of sweet orange plants collected in the states of Santa Catarina (SC) and Rio Grande do Sul (RS), Brazil, resembled typical symptoms of CL disease (Figure 1). Bright chlorotic lesions were found predominantly in the leaves, similar to what was seen for CiCSV (Chabi-Jesus et al., 2018). The transmission electron microscope (TEM) analyses of ultrathin sections of sweet orange symptomatic leaves collected in Marquês de Souza/RS and Seara/SC indicated the presence of bacilliform particles of ca. ~ 40 × 100 nm clustered in translucent "spoke wheel" inclusions in the parenchymal cells of the leaflet lesions analyzed (Figure 2), as observed in other dichorhaviruses infections (Dietzgen et al., 2018). However, molecular tests were negative for the detection of all known dichorhaviruses (Figure 2) and cileviruses (data not shown).

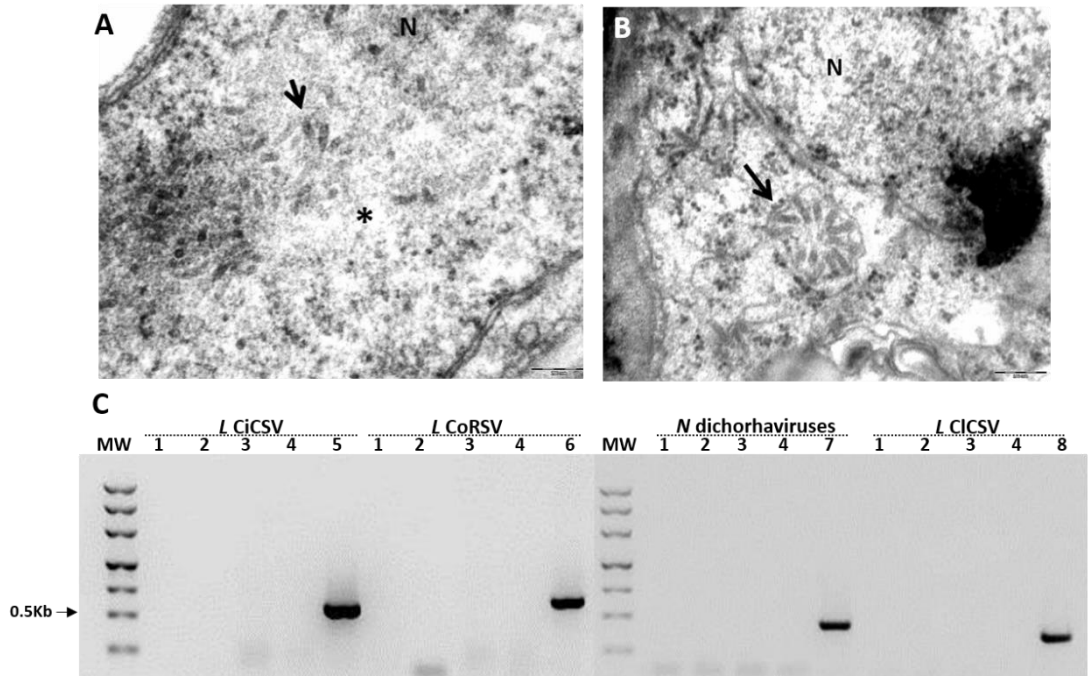

Figure 2- Transmission electron microscopy (TEM) and RT-PCR results from sweet orange tissues collected in small citrus orchards in the Brazilian Southern region exhibiting symptoms of citrus leprosis disease. A) Micrograph of a section of a leaf collected in Seara, state of Santa Catarina (SC), showing a group of particles arranged as spokewheel inclusions (arrow) present in the nucleus (N) of a palisade parenchyma cell. B) Spokewheel inclusion (arrow) associated with the endoplasmic reticulum near the nucleus (N) in a section of a leaf collected in Marquês de Souza, state of Rio Grande do Sul (RS). C) 1% agarose gel electrophoresis of RT-PCR products for the detection of dichorhaviruses. MW: Molecular weight marker, M1181 Ladder (Sinapse Biotechnology). Lane 1: Reverse-transcription blank; 2-4: Chlorotic lesion from sweet orange leaves collected in: 2. Seara, SC; 3. Marquês de Souza, RS; 4. Passo Fundo, RS; 5-8: Control plants infected with: 5. CiCSV from Teresina, PI; 6. CoRSV from Limeira, SP; 7. CiLV-N from Ibiúna, SP; 8. ClCSVfrom Piracicaba, SP.

Along with the cytopathological effects characteristics of dichorhaviruses, morphoanatomical examination of *Brevipalpus* mites found in sweet orange samples from Marquês de Souza/ RS, Passo Fundo/RS and Seara/SC led to their classification as members of the *B. phoenicis* sensu strictu species (Beard et al., 2015) (Figure 3). In the sweet orange trees collected in Marquês de Souza and Seara it was only possible to identify four specimens of *Brevipalpus*, all identified as *B. phoenicis* s.s. However, from the tree collected in Passo Fundo/RS it was possible to characterize 50 specimens of *B. phoenicis* s.s. Although transmission has not been confirmed, the constant association of these viruses with *B. phoenicis* s.s. suggests transmission by that vector. *B. phoenicis* s.s. persistently transmits CiLV-N, the first citrus dichorhavirus identified in Brazil (Ramos-González et al., 2017a). In addition to the *Brevipalpus* species, citrus plants infected with CiLV-N and the plants used in this work were

found in backyards, located in regions of mild temperatures (annual average temperature <19 ° C) (Ramos-González et al., 2017a; Freitas-Astúa et al., 2018).

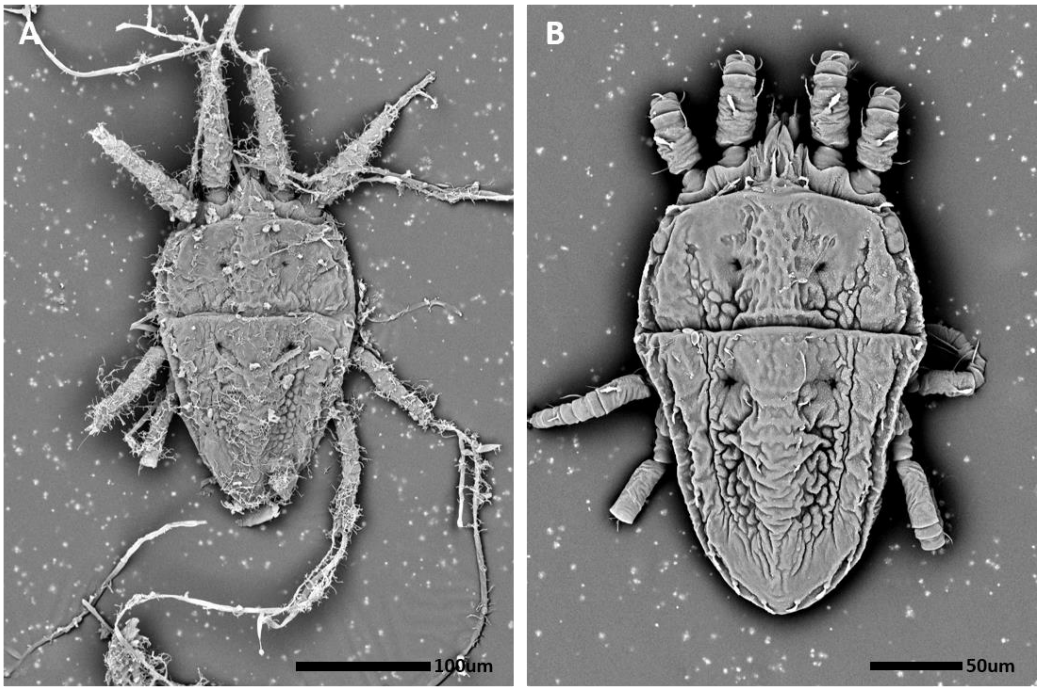

Figure 3- Microphotographs of *Brevipalpus phoenicis* sensu stricto mites found in leaves and fruits of sweet orange (*Citrus sinensis*) showing symptoms associated with citrus leprosis disease, collected in Marquês de Souza/RS (A) and Seara/SC (B). Morphological characteristics evaluated were: number of dorsolateral setae, number of solenidia on the tarsus of leg II, palp femorogenu setae, reticulation patterns of prodorsum, ophistosoma. In the venter it was observed the ventral and genital shields reticulations.

Symptomatic sweet orange samples collected in Marquês de Souza/RS (MSa) and Seara/SC (Ser) were submitted to HTS technology, RACE, and validation by Sanger sequencing. Both viral isolates, named MSa and Ser, respectively, show ss(-)RNA genomic structure, in which RNA1 has five ORFs: *N-P-MP-M-G,* and RNA2 has a single ORF: *L* (*RdRP*). This organization is typical of members of the genus *Dichorhavirus* (Dietzgen et al., 2014, 2018), which corroborates the results observed through TEM. Globally, the genomes of the two isolates comprise approximately 12,600 nt divided into 6,648nt in RNA1 and 6,012nt in RNA2. Nucleotide identity values between the two isolates were superior to 98.8% for both RNA1 and RNA2 (Figure 4, Supplementary Table 1, Annex I). Comparisons with other dichorhaviruses showed identities varying between 57-72% (Supplementary Table 1, Annex I). The highest identity values, of 64-74% along the genome sequence, were observed when comparing the new dichorhavirus with CiLV-N (Figure 4).

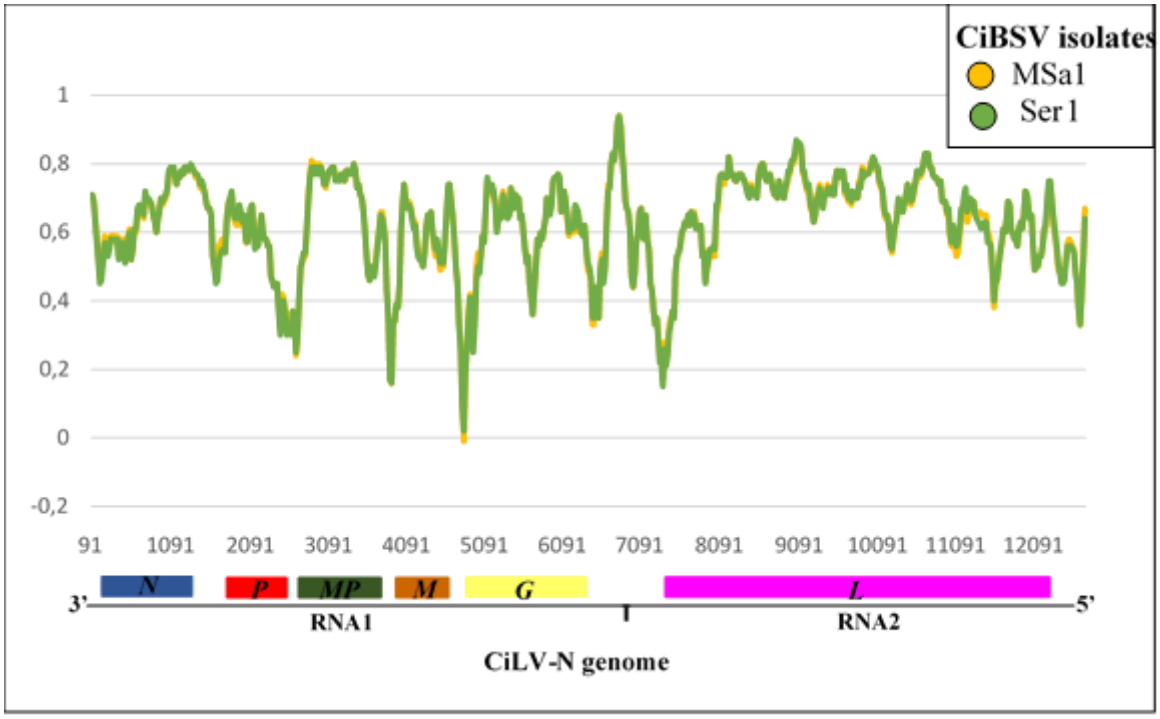

Figure 4. Similarity plots of the nucleotide sequences of RNA1 and RNA2 of CiBSV isolates calculated by SimPlot version 3.5.1. The full length of the genome nucleotide sequences of CiBSV_MSa1 and CiBSV_Ser1 isolates sequenced in this study were compared with CiLV-N. The vertical axis indicates the nucleotide identities, expressed as percentages, and the horizontal axis indicates the nucleotide positions of RNA1 and RNA2 of CiLV-N.

From the deduced amino acid sequences (aa), the percentage identity between the MSa and Ser isolates ranged from 98.9 to 100% (Supplementary Table 1, Annex I). When comparing the amino acid deduced sequences of the MSa isolate with those of other dichorhaviruses, the identity values range from 71-82% with CiLV-N Ibi (GenBank access number: KX982179 and KX982178), 33-62% with OFV (NC_009609 and NC_009608), 38-64% with CoRSV (NC_038756 and NC_038755), 36-64% with ClCSV (NC_043648 and NC_043649) and 37-64% with CiCSV (KY700686 and KY700685) (Supplementary Table 1, Annex I). The results of nucleotide and deduced amino acid identities, and the genomic structure of the two isolates characterized in this work suggest that they are new members of the genus *Dichorhavirus* (ICTV, 2018). According to the dichorhavirus species demarcation criteria accepted by the International Committee on Taxonomy of Viruses (ICTV), members of the same species are those who have more than 80% nucleotide identity for RNA1 and *L* gene (Dietzgen et al., 2018). Since the identity of these viruses compared to the other dichorhavirus is below the limit, they should be considered members of a new tentative species, named) citrus bright spot virus (CiBSV).

Recombination events were not found in the CiBSV_MSa1 and CiBSV_Ser1 genome sequences; thus, both were used in phylogenetic analyses. The phylogenetic reconstruction using Bayesian inference was based on complete sequences and on N and L proteins of the definitive and tentative members of genus *Dichorhavirus* (Figure 5). In all trees, the CiBSV isolates are grouped with CiLV-N. The former is associated with the presence of *B. phoenicis* s.s. (Figure 3), while the latter is proven to be transmitted by mites of that species (Ramos-González et al., 2017). These results strengthens the hypothesis of dichorhavirus sub-clade grouping according to the vector mite species (Chabi-Jesus et al., 2018). The "CoRSV group" is composed by CoRSV, transmitted by *B. papayensis* and *B. yothersi*, CiCSV, transmitted by *B. yothersi* and *B.* aff. *yothersi*, and ClCSV by *B. yothersi* (Chabi-Jesus et al., 2018; Nunes et al., 2018; Ramos-González et al., 2018). OFV stands alone in a sub-clade and is the only dichorhavirus reported so far to be vectored by *B. californicus* (Kondo et al., 2003).

Future studies will be necessary to confirm the transmission of CiBSV by *B. phoenicis* s.s., and also the sub-clade separation of dichorhaviruses correlated with the vector. Nevertheless, the presence of this species in the evaluated plants associated with phylogenetic and vector relationships support the possibility that CiBSV is transmitted by mites of this species. Overall, considering both phylogenies based on the complete genome and proteins (N and L), the phylogenetic groups are well defined (Figure 5). The only group formed by viruses with more than one vector species is the CoRSV group; however, *B. yothersi* is the common vector for members of all three virus species, even though other mites may be able to transmit them as well. We have evidence to support that there are specific relationships between dichorhaviruses and *Brevipalpus* mite species. The ability of the viruses to replicate within and be transmitted by different vectors likely reflects the phylogenetic relationships between the dichorhaviruses.

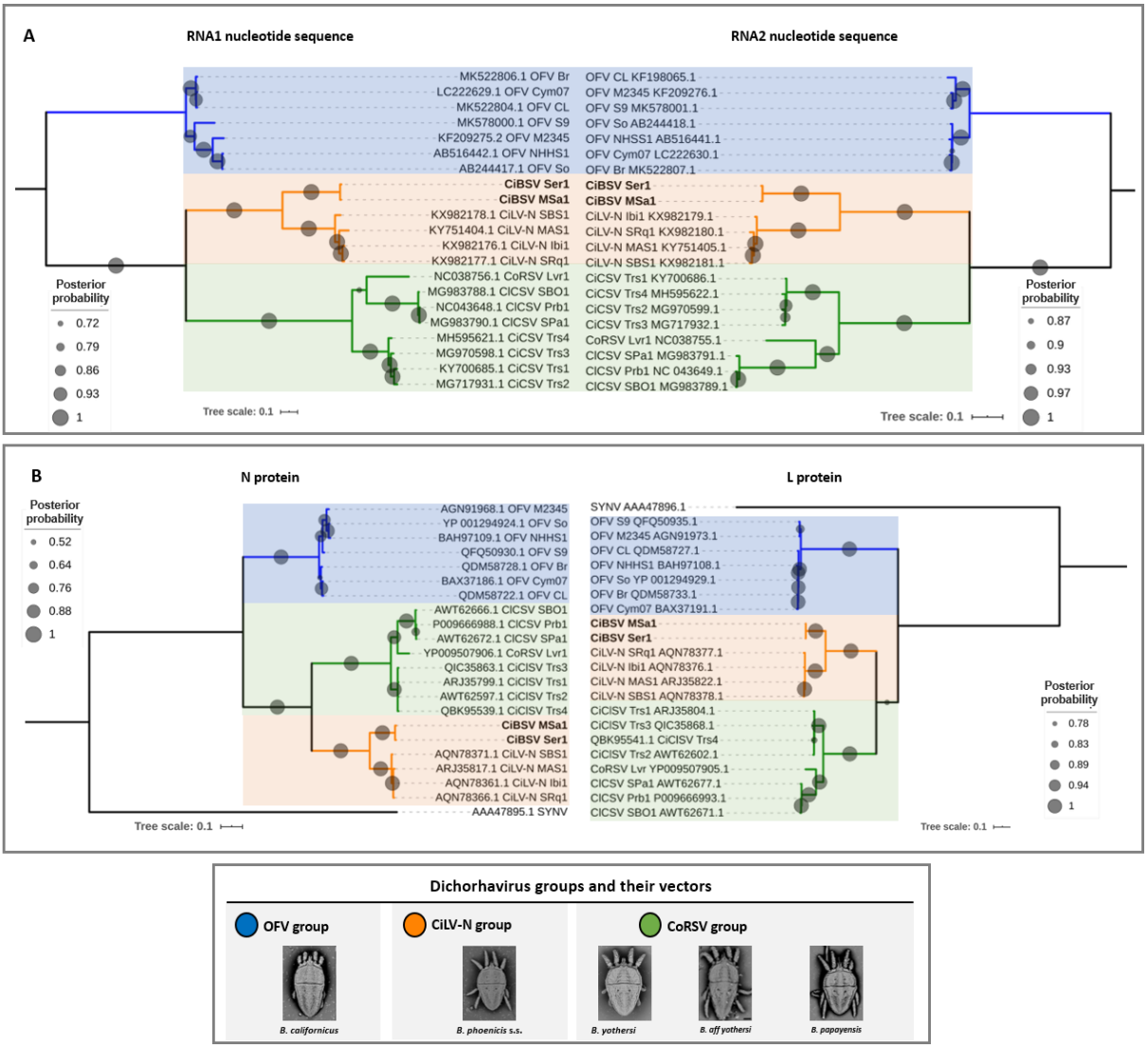

Figure 5- Phylogenetic reconstruction from members of the genus *Dichorhavirus* and CiBSV isolates (bold). The trees were based on complete sequence of RNA1 and RNA2 (A), and amino acid sequence of N and L proteins (B). The phylogenetic trees were generated with 2,000,000 generations and SYNV (*Sonchus yellow* net virus) was used as an outgroup in the trees from amino acid sequences. The color of nodes are based on the dichorhavirus group: OFV (blue; transmitted by *Brevipalpus californicus*), CiLV-N (orange; transmitted by *B. phoenicis* s.s.) and CoRSV (green; transmitted by *B. papayensis*, *B. yothersi* and aff. *yothersi*).

In addition to the association between dichorhavirus phylogeny and the ability of *Brevipalpus* spp. to vector them, it has been suggested that the distribution of these viruses is closely related to the distribution of mites (Ramos-González et al., 2017; Freitas-Astúa et al., 2018). The dichorhavirus vectors associated with citrus leprosis are hardly found in commercial citrus orchards in Brazil (Ramos-González et al., 2017a; Chabi-Jesus et al., 2018; Freitas-Astúa et al., 2018). The vector species of OFV, *B. californicus*, has only one report on citrus plants in Brazil (Bobot et al., 2011). In addition, *B. phoenicis* s.s., vector of CiLV-N and probably of CiBSV, is only found in non-commercial citrus orchards with high altitudes and mild

temperatures (Ramos-González et al., 2017b). *B. yothersi* is widely distributed from Mexico to Argentina (Sánchez-Velázquez et al., 2015; Andrade et al., 2018). The reason for the predominance of *B. yothersi* species in these orchards is not known; however, this differential distribution of *Brevipalpus* species in Brazil may be associated with (*i*) climatic conditions, (*ii*) successful in colonizing different citrus species and/or (*iii*) different levels of susceptibility to chemical products (Sánchez-Velázquez et al., 2015; Salinas-Vargas et al., 2016; Amaral et al., 2018; Bassanezi et al., 2019). The behavior of *Brevipalpus* genetic diversity in face of climatic factors and resistance/susceptibility to acaricides is largely unknown (Omoto, 1998; Navia et al., 2013; Salinas-Vargas et al., 2016). *B. yothersi* is the mite species that vectors the main BTV that causes citrus leprosis disease in Brazil, the citrus leprosis virus C (CiLV-C; ss(+) RNA genome, genus *Cilevirus*) (Locali-Fabris et al., 2006; Ramos-González et al., 2016). Additionally, *B. yothersi* is also associated with the transmission of the dichorhavirus CiCSV, so far found only in gardens of Teresina. Piauí (Chabi-Jesus et al., 2018, 2019). Although, currently, dichorhaviruses are not economically important for the citrus producing regions in Brazil, here we report the third dichorhavirus naturally infecting sweet orange plants in the country. Since other viruses of the same genus were recently characterized in Brazil, it is possible to conclude that a high diversity of dichorhaviruses occurs in the country, which poses potential risks of invasion and saturation in crops and ornamental plants.

6.4 CONCLUSIONS

In this work, we identified distinct viruses associated with citrus leprosis disease in sweet orange trees collected in two Brazilian states. According to the symptoms observed in the infected plants, the morphology of the virions, genomic structure, and the nucleotide identity, the two isolates sequenced were considered as members of a tentative new species of the genus *Dichorhavirus*, and the name citrus bright spot virus is suggested. This manuscript reports the first dichorhavirus associated with citrus leprosis in Southern Brazil.

REFERENCES

Amaral, I., de Moraes, G. J., Melville, C. C., and Andrade, D. J. (2018). Factors affecting prevailing population levels of *Brevipalpus yothersi* (Acari: Tenuipalpidae) in citrus areas affected by citrus leprosis in the State of Sao Paulo, Brazil. *Exp. Appl. Acarol.* 74, 395–402. doi:10.1007/s10493-018-0239-x.

Amarasinghe, G. K., Ayllón, M. A., Bào, Y., Basler, C. F., Bavari, S., Blasdell, K. R., et al. (2019). Taxonomy of the order *Mononegavirales*: update 2019. *Arch. Virol.* 164, 1967–1980. doi:10.1007/s00705-019-04247-4.

Andrade, D. J., Lorençon, J. R., Siqueira, D. S., Novelli, V. M., and Bassanezi, R. B. (2018). Space–time variability of citrus leprosis as strategic planning for crop management. *Pest Manag. Sci.* 74, 1798–1803. doi:10.1002/ps.4877.

Bankevich, A., Nurk, S., Antipov, D., Gurevich, A. A., Dvorkin, M., Kulikov, A. S., et al. (2012). SPAdes: A new genome assembly algorithm and its applications to single-cell sequencing. *J. Comput. Biol.* 19, 455–477. doi:10.1089/cmb.2012.0021.

Bassanezi, R. B., Czermainski, A. B. C., Laranjeira, F. F., Moreira, A. S., Ribeiro, P. J., Krainski, E. T., et al. (2019). Spatial patterns of the Citrus leprosis virus and its associated mite vector in systems without intervention. *Plant Pathol.* doi:10.1111/ppa.12930.

Beard, J. J., Ochoa, R., Braswell, W. E., and Bauchan, G. R. (2015). *Brevipalpus phoenicis* (Geijskes) species complex (Acari: Tenuipalpidae)-a closer look. *Zootaxa* 3944, 1–67. Available at: http://www.ncbi.nlm.nih.gov/pubmed/25947538 [Accessed June 30, 2015].

Bobot, T. da E., Franklin, E., Navia, D., Gasnier, T. R. J., Lofego, A. C., and Oliveira, B. M. de (2011). Mites (Arachnida, Acari) on *Citrus sinensis* L. Osbeck orange trees in the state of Amazonas, Northern Brazil. *Acta Amaz.* 41, 557–566. doi:10.1590/S0044-59672011000400013.

Chabi-Jesus, C., Ramos-González, P. L., Guerra-Peraza, O., Kitajima, E. W., Harakava, R., Beserra Jr., J. E. A., et al. (2018). Identification and characterization of citrus chlorotic spot virus, a new dichorhavirus associated with citrus leprosis-like symptoms. *Plant Dis.* 102, 1588–1598. doi:10.1094/PDIS-09-17-1425-RE.

Chabi-Jesus, C., Ramos-González, P. L., Tassi, A. D., Barguil, B. M., Beserra Junior, J. E. A., Harakava, R., et al. (2019). First report of citrus chlorotic spot virus infecting the succulent plant *Agave desmettiana* . *Plant Dis.* 103, 1438–1438. doi:10.1094/pdis-09-18-1617-pdn.

Cook, G., Kirkman, W., Clase, R., Steyn, C., Basson, E., Fourie, P. H., et al. (2019). Orchid fleck virus associated with the first case of Citrus Leprosis-N in South Africa. *Plant Pathol.* 155, 1373–1379.

Cruz-Jaramillo, J. L., Ruiz-Medrano, R., Rojas-Morales, L., López-Buenfil, J. A., Morales-Galván, O., Chavarín-Palacio, C., et al. (2014). Characterization of a proposed dichorhavirus associated with the citrus leprosis disease and analysis of the host response. *Viruses* 6, 2602–22. doi:10.3390/v6072602.

Dietzgen, R. G., Kondo, H., Goodin, M. M., Kurath, G., and Vasilakis, N. (2017). The family *Rhabdoviridae*: mono- and bipartite negative-sense RNA viruses with diverse genome organization and common evolutionary origins. *Virus Res.* 227, 158–170. doi:10.1016/j.virusres.2016.10.010.

Dietzgen, R. G., Kuhn, J. H., Clawson, A. N., Freitas-Astúa, J., Goodin, M. M., Kitajima, E. W., et al. (2014). Dichorhavirus: a proposed new genus for *Brevipalpus* mite-transmitted, nuclear, bacilliform, bipartite, negative-strand RNA plant viruses. *Arch. Virol.* 159, 607–19. doi:10.1007/s00705-013-1834-0.

Dietzgen, R. G. R. G., Freitas-Astúa, J., Chabi-Jesus, C., Ramos-González, P. L. P. L., Goodin, M. M. M. M., Kondo, H., et al. (2018). Dichorhaviruses in their host plants and mite vectors. *Adv. Virus Res.* 102, 119–148. doi:10.1016/bs.aivir.2018.06.001.

Freitas-Astúa, J., Ramos-González, P. L., Arena, G. D., Tassi, A. D., and Kitajima, E. W. (2018). *Brevipalpus*-transmitted viruses: parallelism beyond a common vector or convergent evolution of distantly related pathogens? *Curr. Opin. Virol.* 33, 66–73. doi:10.1016/j.coviro.2018.07.010.

García-Escamilla, P., Duran-Trujillo, Y., Otero-Colina, G., Valdovinos-Ponce, G., Santillán-Galicia, M. T., Ortiz-García, C. F., et al. (2017). Transmission of viruses associated with cytoplasmic and nuclear leprosis symptoms by *Brevipalpus yothersi* and *B. californicus*. *Trop. Plant Pathol.* 43, 69–77. doi:10.1007/s40858-017-0195-8.

ICTV (2018). Available at: https://talk.ictvonline.org/ictv-reports/ictv_online_report/negative-sense-rna-viruses/mononegavirales/w/rhabdoviridae/791/genus-dichorhavirus [Accessed September 30, 2020].

Kearse, M., Moir, R., Wilson, A., Stones-havas, S., Cheung, M., Sturrock, S., et al. (2012). Geneious Basic : An integrated and extendable desktop software platform for the organization and analysis of sequence data. *Bioinformatics* 28, 1647–1649. doi:10.1093/bioinformatics/bts199.

Kitajima, E. W., Chagas, C. M., Braghini, M. T., Fazuoli, L. C., Locali-Fabris, E. C., and Salaroli, R. B. (2011). Natural infection of several Coffea species and hybrids and *Psilanthus ebracteolatus* by the coffee ringspot virus (CoRSV). *Sci. Agric.* 68, 503–507. doi:10.1590/S0103-90162011000400017.

Kitajima, E. W., Chagas, C. M., and Rodrigues, J. C. V (2003). *Brevipalpus*-transmitted plant virus and virus-like diseases: cytopathology and some recent cases. *Exp. Appl. Acarol.* 30, 135–60.

Kitajima, E. W., Kubo, K. S., Ferreira, P. de T. O., Alcântara, B. K. de, Boari, A. J., Gomes, R. T., et al. (2008). Chlorotic spots on Clerodendrum, a disease caused by a nuclear type of *Brevipalpus* (Acari:Tenuipalpidae) transmitted virus. *Sci. Agric.* 65, 36–49. doi:10.1590/S0103-90162008000100006.

Kitajima, E. W., Müller, G. W., Costa, A. S., and Yuki, W. (1972). Short, rod-like particles associated with Citrus leprosis. *Virology* 50, 254–8.

Kitajima, E. W., Rodrigues, J. C. V., and Freitas-Astua, J. (2010). An annotated list of ornamentals naturally found infected by *Brevipalpus* mite-transmitted viruses. *Sci. Agric.* 67, 348–371. doi:10.1590/S0103-90162010000300014.

Kondo, H., Hirota, K., Maruyama, K., Andika, I. B., and Suzuki, N. (2017). A possible occurrence of genome reassortment among bipartite rhabdoviruses. *Virology* 508, 18–25. doi:10.1016/j.virol.2017.04.027.

kondo, H., Maeda, T., and Inouye, N. (1995). Host range and some properties of orchid fleck virus isolated from oriental Cymbidium in Japan. *Japanese with English Summ. Bull Res Inst Bioresour Okayama Univ* 3, 151–161. Available at: https://agris.fao.org/agris-search/search.do?recordID=JP9602257 [Accessed September 30, 2020].

Kondo, H., Maeda, T., Shirako, Y., and Tamada, T. (2006). Orchid fleck virus is a rhabdovirus with an unusual bipartite genome. *J. Gen. Virol.* 87, 2413–2421. doi:10.1099/vir.0.81811-0.

Kondo, H., Maeda, T., and Tamada, T. (2003). Orchid fleck virus: *Brevipalpus californicus* mite transmission, biological properties and genome structure. *Exp. Appl. Acarol.* 30, 215–223. Available at: http://www.ncbi.nlm.nih.gov/pubmed/14756418 [Accessed July 25, 2016].

Kubo, K. S., Freitas-Astúa, J., Machado, M. A., and Kitajima, E. W. (2009). Orchid fleck symptoms may be caused naturally by two different viruses transmitted by *Brevipalpus*. *J. Gen. Plant Pathol.* 75, 250–255. doi:10.1007/s10327-009-0167-z.

Kubo, K. S., Novelli, V. M., Bastianel, M., Locali-Fabris, E. C., Antonioli-Luizon, R.,

Machado, M. A., et al. (2011). Detection of *Brevipalpus*-transmitted viruses in their mite vectors by RT–PCR. *Exp. Appl. Acarol.* 54, 33–39. doi:10.1007/s10493-011-9425-9.

Kumar, S., Stecher, G., and Tamura, K. (2016). MEGA7: Molecular evolutionary genetics analysis version 7.0 for bigger datasets. *Mol. Biol. Evol.* 33, 1870–1874. doi:10.1093/molbev/msw054.

Kuzmin, I. V., Novella, I. S., Dietzgen, R. G., Padhi, A., and Rupprecht, C. E. (2009). The rhabdoviruses: Biodiversity, phylogenetics, and evolution. *Infect. Genet. Evol.* 9, 541–553. doi:10.1016/j.meegid.2009.02.005.

Langmead, B., and Salzberg, S. L. (2012). Fast gapped-read alignment with Bowtie 2. *Nat. Methods* 9, 357–359. doi:10.1038/nmeth.1923.

Letunic, I., and Bork, P. (2007). Interactive Tree Of Life (iTOL): An online tool for phylogenetic tree display and annotation. *Bioinformatics* 23, 127–128. doi:10.1093/bioinformatics/btl529.

Locali-Fabris, E. C., Freitas-Astúa, J., Souza, A. A., Takita, M. A., Astúa-Monge, G., Antonioli-Luizon, R., et al. (2006). Complete nucleotide sequence, genomic organization and phylogenetic analysis of citrus leprosis virus cytoplasmic type. *J. Gen. Virol.* 87, 2721–9. doi:10.1099/vir.0.82038-0.

Locali, E. C., Freitas-Astua, J., de Souza, A. A., Takita, M. A., Astua-Monge, G., Antonioli, R., et al. (2003). Development of a molecular tool for the diagnosis of leprosis, a major threat to citrus production in the Americas. *Plant Dis.* 87, 1317–1321. doi:10.1094/PDIS.2003.87.11.1317.

LOLE, K. S., BOLLINGER, R. C., PARANJAPE, R. S., GADKARI, D., KULKARNI, S. S., NOVAK, N. G., et al. (1999). Full-length human immunodeficiency virus type 1 genomes from subtype C-infected seroconverters in India, with evidence of intersubtype recombination.pdf. *J. Virol.* 73, 152–160.

Martin, D. P., Murrell, B., Golden, M., Khoosal, A., and Muhire, B. (2015). RDP4: Detection and analysis of recombination patterns in virus genomes. *Virus Evol.* 1, vev003–vev003. doi:10.1093/ve/vev003.

Melzer, M. J., Simbajon, N., Carillo, J., Borth, W. B., Freitas-Astúa, J., Kitajima, E. W., et al. (2013). A cilevirus infects ornamental hibiscus in Hawaii. *Arch. Virol.* doi:10.1007/s00705-013-1745-0.

Navia, D., Mendonça, R. S., Ferragut, F., Miranda, L. C., Trincado, R. C., Michaux, J., et al. (2013). Cryptic diversity in *Brevipalpus* mites (Tenuipalpidae). *Zool. Scr.* 42, 406–426. doi:10.1111/zsc.12013.

Nunes, M. A., de Carvalho Mineiro, J. L., Rogerio, L. A., Ferreira, L. M., Tassi, A., Novelli, V. M., et al. (2018). First Report of *Brevipalpus papayensis* as vector of *Coffee ringspot virus* and *Citrus leprosis virus C*. *Plant Dis.* 102, 1046–1046. doi:10.1094/PDIS-07-17-1000-PDN.

Omoto, C. (1998). Acaricide resistance management of leprosis mite (*Brevipalpus phoenicis*) in Brazilian Citrus. *Pestic. Sci.* 52, 189–191.

Ramalho, T. O., Figueira, A. R., Sotero, A. J., Wang, R., Geraldino Duarte, P. S., Farman, M., et al. (2014). Characterization of Coffee ringspot virus-Lavras: a model for an emerging threat to coffee production and quality. *Virology* 464–465, 385–96. doi:10.1016/j.virol.2014.07.031.

Ramalho, T. O., Figueira, A. R., Wang, R., Jones, O., Harris, L. E., Goodin, M. M., et al. (2015). Detection and survey of coffee ringspot virus in Brazil. *Arch. Virol.* 161, 335–343. doi:10.1007/s00705-015-2663-0.

Ramos-González, P. L., Chabi-Jesus, C., Guerra-Peraza, O., Breton, M. C., Arena, G. D. G. D. G. D., Nunes, M. A. M. A., et al. (2016). Phylogenetic and molecular variability studies reveal a new genetic clade of Citrus leprosis virus C. *Viruses* 8, 153. doi:10.3390/v8060153.

Ramos-González, P. L., Chabi-Jesus, C., Guerra-Peraza, O., Tassi, A. D., Kitajima, E. W., Harakava, R., et al. (2017a). Citrus leprosis virus N: a new dichorhavirus causing citrus leprosis disease. *Phytopathology*, 1–48. doi:10.1094/PHYTO-02-17-0042-R.

Ramos-González, P. L. P. L., Chabi-Jesus, C., Banguela-Castillo, A., Tassi, A. D. A. D., Rodrigues, M. C. M. da C., Kitajima, E. W. E. W., et al. (2018). Unveiling the complete genome sequence of clerodendrum chlorotic spot virus, a putative dichorhavirus infecting ornamental plants. *Arch. Virol.* 163, 2519–2524. doi:10.1007/s00705-018-3857-z.

Ramos-González, P. L. P. L., Chabi-Jesus, C., Guerra-Peraza, O., Tassi, A. D. A. D., Kitajima, E. W. E. W., Harakava, R., et al. (2017b). Citrus leprosis virus N: A new dichorhavirus causing Citrus leprosis disease. *Phytopathology* 107, 963–976. doi:10.1094/PHYTO-02-17-0042-R.

Roy, A., Choudhary, N., Guillermo, L. M., Shao, J., Govindarajulu, A., Achor, D., et al. (2013a). A novel virus of the genus *Cilevirus* causing symptoms similar to citrus leprosis. *Phytopathology* 103, 488–500. doi:10.1094/PHYTO-07-12-0177-R.

Roy, A., Leon, M. G., Stone, A. L., Schneider, W. L., Hartung, J., and Brlansky, R. H. (2014). First report of citrus leprosis virus nuclear type in sweet orange in Colombia. *Plant Dis.* 98, 1162. doi:10.1094/PDIS-02-14-0117-PDN.

Roy, A., Shao, J., Hartung, J. S., Schneider, W., and Brlansky, R. (2013b). A case study on discovery of novel citrus leprosis virus cytoplasmic type 2 utilizing small rna libraries by next generation sequencing and bioinformatic analyses. *J. Datamining Genomics Proteomics* 4.

Salinas-Vargas, D., Santillán-Galicia, M. T., Guzmán-Franco, A. W., Hernández-López, A., Ortega-Arenas, L. D., and Mora-Aguilera, G. (2016). Analysis of genetic variation in *Brevipalpus yothersi* (Acari: Tenuipalpidae) populations from four species of citrus host plants. *PLoS One* 11, 1–11. doi:10.1371/journal.pone.0164552.

Sánchez-Velázquez, E. J., Santillán-Galicia, M. T., Novelli, V. M., Nunes, M. A., Mora-Aguilera, G., Valdez-Carrasco, J. M., et al. (2015). Diversity and genetic variation among *Brevipalpus* populations from Brazil and Mexico. *PLoS One* 10, e0133861. doi:10.1371/journal.pone.0133861.

Walker, P. J. P., Firth, C., Widen, S. S. G., Blasdell, K. R. K., Guzman, H., Wood, T. T. G., et al. (2015). Evolution of genome size and complexity in the *Rhabdoviridae*. *PLOS Pathog.* 11, e1004664. doi:10.1371/journal.ppat.1004664.

Whitfield, A. E., Huot, O. B., Martin, K. M., Kondo, H., and Dietzgen, R. G. (2018). Plant rhabdoviruses—their origins and vector interactions. *Curr. Opin. Virol.* 33, 198–207. doi:10.1016/j.coviro.2018.11.002.

ANNEX I

Supplementary Table 1- Percentage of deduced nucleotide (nt) and amino acid (aa) identity between CiBSV isolates and other members of the genus *Dichorhavirus*.

CiBSV_MSa1	**CiBSV_Ser1**		**CiLV-N Ibi**		**OFV**		**CoRSV**		**ClCSV**		**CiCSV**	
	nt	**aa**	**nt**	**aa**	**nt**	**aa**	**nt**	**aa**	**nt**	**aa**	**nt**	**aa**
RNA1	98.8	-	70.2	-	53.4	-	56.1	-	56.6	-	56.3	-
N	98.8	99.3	73.3	80.6	57.1	48.7	60.7	57.4	61.0	56.8	60.2	57.5
P	99.3	100	71.2	74.6	51.4	33.8	57.6	46.9	59.4	46.9	56.5	44.8
MP	98.8	99.4	78.7	85.5	64.4	62.8	65.8	62.5	64.6	63.6	65.9	62.2
M	99.1	100	64.9	71.7	52.7	39.2	57.7	49.2	57.5	45.9	59.4	49.2
G	99.1	98.9	70.6	74.1	50.0	33.1	51.9	38.9	52.7	36.5	52.1	37.8
RNA2	99.1	-	73.9	-	59.8	-	62.5	-	62.7	-	62.5	-
L	99.2	99.9	74.2	82.6	60.9	56.9	63.4	64.5	63.8	64.2	64.0	64.3

Supplementary Table 2- List of primers used for validation and obtaining the 3 'and 5' extremes of the CiBSV genomes, based on CiBSV_MSa1 sequence.

Primer Sequences (5′−3′)	**Direction**	**Target Region**	**Size (bp)**
RNA1			
CAGTCACTATAGATTACTCAGCAG	F:	265-288	945
CTCTGCTGTACCTCCAGAAT	R:	1190-1209	
AAACATACATGGACCACTCA	F:	977-996	938
TCATAGGTGGTGTTATTCCA	R:	1895-1914	
AGCATGATCGGTACATCAA	F:	1770-1788	706
AGTTCAGGCATGGCTTCT	R:	2458-2475	
AAGCATTCTCCAGGAAGAC	F:	2227-2245	942
GTTGGTGACAGCCTTGTT	R:	3151-3168	
CAACAAGACACTCCAAACTG	F:	2901-2920	882
ATATATGTGAACTTCTTGTCACC	R:	3760-3782	
TTCAAGGGTTCACAGATATAGA	F:	3533-3554	937
CGACAGTGGCACTTATTTC	R:	4451-4469	
AGAGGTGGCCAAATTCTC	F:	4222-4239	945
CTGCATCTGTTGTACTGGAG	R:	5147-5166	
ATGAGTATAGTCCCCAACACAG	F:	4917-4938	930
GAGGATGATGGTGCTGAC	R:	5829-5846	
GGAGAGTCTTCTAGCAAAACAG	F:	5598-5619	852
CTCCATAAGGCTTGCACTA	R:	6431-6449	
RNA2			
TCTCTTCTTGATTCTTCTTTCA	F:	201-222	926
CCTGTCACCTCATCTACCAT	R:	1107-1126	
CAATATGATTGTGTACAACAGG	F:	884-905	940
GATGGTAAAGTACAGCCTCA	R:	1804-1823	
TCAGAACTAATACAGATGATCAGG	F:	1581-1604	940
ATGTTACATTGTTAAAATACATCATCT	R:	2494-2520	
ATGAAGGTGGACCTTGTG	F:	2271-2288	931
TATCACCGGAGCAGAGAC	R:	3184-3201	
AAGGAGCCCAAATACCTG	F:	2952-2969	940
GTATCGAGTATGCAATGTTTG	R:	3871-3891	
GCCTACGGAGAGGAAGAT	F:	3654-3671	938
GGGTCTACTGAGCTGTATATGA	R:	4570-4591	
GCTGATTACTTAAGCATGGA	F:	4341-4360	935
GAGCCACATCTCTCGTACA	R:	5257-5275	
TATGGCGGAACTTCTATATG	F:	5038-5057	780
TTAGCAATATGAACCCCATC	R:	5798-5817	
RACE 5'/3' universal primer Clontech®[3]			
TAATACGACTCACTATAGGGCAAGCAGTGGTATCAACGCAGAGT	*Long*	-	-
CTAATACGACTCACTATAGGGC	*Short*	-	-
RNA1 5' RACE			

GATTACGCCAAGCTTCGTTAGCAGCTGCAGCCCTGGAGTC	F *Long*	612-636	636
TGCTACTCCTACCATCAC	F *Short*	543-560	560
RNA1 3' RACE			
GATTACGCCAAGCTTTGACACCTCTTGCATACCGAGCCTTTCC	F *Long*	5939-5966	718
TCAATGTTGAGGTCAGTAG	F *Short*	6210-6228	447
RNA2 5' RACE			
GATTACGCCAAGCTTGTCGAGTCATCGTTGCGATAGAGTTCCT GGATG	F *Long*	485-517	517
TGCCAGCAGTTTACATG	F *Short*	409-425	425
RNA2 3' RACE			
GATTACGCCAAGCTTCTGTCCCTGGCCATAGCACTTTTCCACTC	F *Long*	5460-5488	552
TGTGAGGAGCCTGTTC	F *Short*	5534-5549	478

7 FINAL CONSIDERATIONS

- Citrus leprosis (CL) is a multietiological viral disease with a slow spread rate, but an increasing incidence, which is likely associated with the inefficient control of the *Brevipalpus* mite populations acting as vectors. The cilevirus CiLV-C is the prevalent CL causal agent in Latin America. The population of this virus is subdivided into three lineages: CRD, SJP, and ASU whose members share ≈ 85% nucleotide sequence identity between their genomes and show signs of recombination processes. Members of the clade CRD were identified in citrus orchards from Mexico to Argentina in the period 1932 – 2019, while those of the clade SJP were detected only in orchards of the citrus belt of São Paulo and Minas Gerais after 2015. In this region, viruses of the clade SJP are more frequently detected than those of the clade CRD and they often occur in mixed infection. Statistical tests and phylogeny analyses of the CiLV-C population showed that CRD and SJP are genetically distinct subpopulations ($Fst \geq 0.93$), with low genetic diversity ($\pi = 0.01$) and under high negative selection pressure ($\omega \leq 0.3$). Clade ASU, with only one member, represents an unprecedented diversity inside the CiLV-C population, but the current existence of viruses of this lineage is unknown. CiLV-C lineages likely arose from their most recent common ancestor (MRCA) in ≈ 500 A.D. One of that clades lately gave rise to both the clade ASU and the ancestral viruses of the current clade CRD. Subsequently, the diversification of clades CRD and SJP probably occurred around 1870 – 1900 A.D., a process which seems to be associated with the beginning of the intensive citriculture. Accordingly, the main CiLV-C lineages likely originated in a native ecosystem of South America and later spread along with the citriculture development. Citrus act as non-permissive hosts where CiLV-C subpopulations undergo high selection pressure likely ensuing from continuous bottlenecks, and where haplotypes are stochastically fixed. The reason for the heterogeneous distribution of CiLV-C subpopulations is still unknown.
- Although geographically restricted and less frequently found, CL of the nuclear type has proved to be caused by highly diverse viruses, which further supports the hypothesis that South America is the center of origin and diversification of BTVs. Citrus leprosis virus N (CiLV-N), citrus bright spot virus (CiBSV), and citrus chlorotic spot virus (CiCSV) are three new dichorhavirus species. Overall, the symptoms caused by these viruses vary from chlorotic lesions with necrotic centers in the infections by CiLV-N, to pale or bright chlorotic and less restricted lesions on leaves of plants infected by CiCSV and CiBSV, respectively. CiLV-N, first detected by TEM in the early 1970s in Brazil, is transmitted by *B. phoenicis* s.s. CiLV-N isolates have been molecularly detected in non-commercial citrus orchards in four regions of the state

of São Paulo and one region of thestate of Parana, in Curitiba. In general, these regions are located at high altitudes and show an average annual temperature of ≈ 18ºC. CiBSV, identified in two municipalities in the state of Rio Grande do Sul and in one municipality in Santa Catarina, seems to be transmitted by *B. phoenicis* s.s. On the other hand, CiCSV was found in Teresina, Piauí, a region placed at the sea level with an average temperature above 27°C. The virus was found naturally infecting sweet orange, beach hibiscus (*Taliparitì tiliaceum* syn. *Hibiscus tiliaceus*), and agave plants (*Agave desmettiana*), which represents the first report of a BTV infecting a succulent plant. Transmission of CiCSV is associated with *B. yothersi* and/or *B.* aff. *yothersi*. Mites provisionally identified as *B.* aff. *yothersi* might represent a new species in the genus and their role as viral vectors need to be further examined. Inclusion of CiLV-N, CiCSV, CiBSV in phylogenetic analyses helped to define three groups of dichorhaviruses whose array seems to follows a close association with the mite vector, *i.e*. group orchid fleck virus (OFV) is transmitted by *B. californicus*, group CiLV-N, which also include CiBSV, is associated with *B. phoenicis* s.s., and group coffee ring spot virus (CoRSV), also comprising CiCSV and ClCSV, is transmitted by *B. papayensis* and/or *B. yothersi*. Specific dichorhavirus-mite association might determine the virus distribution as observed with other rhabdoviruses.

- Data generated in this work and the analyses carried out have largely expanded and improved the knowledge not only about CL associated viruses but also the viral genera encompassing them. In particular, the work indicates the existence of a larger diversity of citrus-infecting BTVs and alert about spillover events involving BTVs in the past, and their potential occurrence in the future. In strictly practical terms, molecular data have impacted the number of viral targets and the specificity of tests whereby they can be detected, which will allow a better understanding of the viral epidemiology, and the design of more reliable disease control strategies. Finally, the work provides a framework and technical know-how paving future efforts to tackle similar problems faced by the Brazilian agriculture.